PSS®E models for load and distributed PV in the NEM

November 2022

Model development and validation

Important notice

Purpose

This publication provides information on the development and validation of AEMO's power system models for distributed PV and load in PSS®E. It is generally based on information available to AEMO up to February 2022 unless otherwise indicated.

Disclaimer

AEMO has made reasonable efforts to ensure the quality of the information in this report but cannot guarantee that information, forecasts and assumptions are accurate, complete or appropriate for your circumstances. Any views expressed in this report are those of AEMO unless otherwise stated, and may be based on information given to AEMO by other persons. This document or the information in it may be subsequently updated or amended. This document does not constitute legal or business advice, and should not be relied on as a substitute for obtaining detailed advice about the National Electricity Law, the National Electricity Rules, or any other applicable laws, procedures or policies.

Accordingly, to the maximum extent permitted by law, AEMO and its officers, employees and consultants involved in the preparation of this document:

- make no representation or warranty, express or implied, as to the currency, accuracy, reliability or completeness of the information in this document; and
- are not liable (whether by reason of negligence or otherwise) for any statements or representations in this document, or any omissions from it, or for any use or reliance on the information in it.

Copyright

© 2022 Australian Energy Market Operator Limited. The material in this publication may be used in accordance with the copyright permissions on AEMO's website.

Version control

Version	Release date	Changes
Draft	11/3/2022	First sharing of draft with Network Service Providers
Release	21/10/2022	Release of report to Network Service Providers
Release	23/11/2022	Public release of report

AEMO acknowledges the Traditional Owners of country throughout Australia and recognises their continuing connection to land, waters and culture. We pay respect to Elders past and present.

Executive summary

AEMO and network service providers (NSPs) use power system models to assess power system performance under different conditions. The results from these studies inform operational and planning decisions, assisting AEMO to fulfill its responsibilities to maintain a secure power system.

Significant quantities of distributed PV (DPV) are now installed in the National Electricity Market (NEM). DPV can demonstrate complex behaviours during power system disturbances. Therefore, for studies to be accurate, DPV must be accurately represented in AEMO's power system models.

Furthermore, the "ZIP" load models in use by AEMO, NSPs and others were last modified and validated in 1999, and the end-use load composition has changed considerably since that time. More sophisticated aggregate load models are now available, having been pioneered in other jurisdictions to better represent a range of power system phenomena.

This report presents the combined development and validation of two models to represent load and DPV in PSSE®E studies of the NEM: a composite load model (CMLD) and DPV model (DERAEMO1). AEMO is also in the process of developing similar models in other platforms (PSCAD and PowerFactory), which will be reported on separately.

This report summarises several years of model development work (since 2018), incorporating many different and complex datasets. The model development, tuning and validation process is summarised below.

DPV model development process

International review identified state-of-the-art best practice models for representing aggregate DPV lumped at the bus. A collaborative development process in the USA led by the Western Electricity Coordinating Council (WECC) resulted in the release of the 'DER_A' model specification in 2018, developed to represent the aggregate behaviour of DERs in RMS type power system simulation packages. AEMO developed user-written adjustments to the DER_A model to better represent DPV tripping behaviour in Australia which could not be captured by the standard DER_A model (including multi-stage frequency tripping and RoCoF tripping).

The DPV model is inserted into the PSSE snapshot at each PSSE bus individually, based on the estimated quantity of DPV at each bus, and includes a representation of graduated voltage tripping behaviour (a proportion of the DPV at each bus will enter momentary cessation and a proportion will trip as a function of the minimum voltage experienced at each bus), and various control behaviours (frequency-watt).

AEMO developed a set of parameters suitable for simulating DERs in the NEM, informed by the processes outlined by the North American Electric Reliability Corporation (NERC)[1,2]. The parameters for the DPV model were developed using a "bottom-up" approach from a range of data sources, including those summarised in

[1] NERC (Dec 2016) Reliability Guideline: Modelling DER in Dynamic Load Models, at https://www.nerc.com/comm/PC_Reliability_Guidelines_DL/Reliability_Guideline_-_Modeling_DER_in_Dynamic_Load_Models_-_FINAL.pdf.

[2] NERC (Sept 2017) Reliability Guideline: Distributed Energy Resource Modelling, at https://www.nerc.com/comm/PC_Reliability_Guidelines_DL/Reliability_Guideline_-_DER_Modeling_Parameters_-_2017-08-18_-_FINAL.pdf.

Table 1. DER model parameters are varied by region and date, depending on the composition of inverters on the various Australian Standards.

Table 1 Datasets used to develop input parameters for the DPV model

Dataset	Source	Application
Installed capacity of DPV at each transmission bus	Datasets provided by NSPs	Allowed mapping of installed DPV capacity to PSS®E buses
The proportion of inverters installed under each Australian Standard (AS/NZS4777.3:2005 and AS/NZS4777.2:2015) at each point in time.	Datasets provided by the APVI and the Clean Energy Regulator	Informed the proportion of inverters operating under each Australian Standard.
Australian Standards (AS/NZS4777.3:2005 and AS/NZS4777.2:2015)	Standards Australia[3]	Informed the behaviour of inverters installed under each standard.
Bench testing of a sample of 24 inverters, conducted by UNSW Sydney.	Bench testing conducted by UNSW Sydney[4]	Informed parameters such as trip delay timers and voltage tripping parameters.
Surveys of inverter manufacturers on frequency trip settings for older inverters	AEMO conducted surveys[5]	Informed staged frequency trip settings
Distribution Network Service Provider (DNSP) prescribed volt-var response model settings and the dates when these were introduced or changed.	DNSP advice and documentation	Informed model settings for volt-var response. This functionality has been disabled for this model revision (refer to Section 2.3.7 for more information).
Observations from field measurements of a sample of thousands of individual DPV inverters during disturbances	Analysis of datasets provided by Solar Analytics (at 60s/30s/5s resolutions)[6].	The proportion of inverters disconnecting in each disturbance was determined (based on observation of generation from the inverter dropping to close to zero immediately following a disturbance), as well as assessment of compliance rates with response modes such as frequency-watt, defined in Australian Standards.

The DPV model was then tuned and validated in conjunction with the load model as described below.

Load model development process

International review identified the state-of-the-art best practice model for representing aggregate load lumped at the transmission or sub-transmission bus[7]. The dynamic load model "CMLD" developed by WECC was selected[8,9].

[3] Standards Australia, https://www.standards.org.au/.

[4] Addressing Barriers to Efficient Renewable Integration, at https://research.unsw.edu.au/projects/addressing-barriers-efficient-renewable-integration, and http://pvinverters.ee.unsw.edu.au/.

[5] AEMO (April 2016) Response of existing PV inverters to frequency disturbances, at https://aemo.com.au/-/media/files/electricity/nem/security_and_reliability/reports/response-of-existing-pv-inverters-to-frequency-disturbances-v20.pdf.

[6] AEMO (May 2021) Behaviour of distributed resources during power system disturbances, at https://aemo.com.au/-/media/files/initiatives/der/2021/capstone-report.pdf?la=en&hash=BF184AC51804652E268B3117EC12327A.

[7] PEACE Consulting (June 2019) Developing Dynamic Load Models for the Australian Eastern Interconnected System, at https://aemo.com.au/-/media/files/initiatives/der/2020/aemo-load-modeling-062819-final.pdf?la=en.

[8] WECC. 2015. Composite Load Model Specifications, at http://home.engineering.iastate.edu/~jdm/ee554/WECC%20Composite%20Load%20Model%20Specifications%2001-27-2015.pdf.

[9] NERC. 2016. Technical Reference Document - Dynamic Load Modelling, at https://www.nerc.com/comm/PC/LoadModelingTaskForceDL/Dynamic%20Load%20Modeling%20Tech%20Ref%202016-11-14%20-%20FINAL.PDF.

The CMLD aggregates dynamic and static power system loads and lumps them at the distribution bus level. The model consists of six load components, including four different motor types, power electronics load, and static load, as shown in **Figure 1**[10].

Figure 1 The composite load model (CMLD) structure

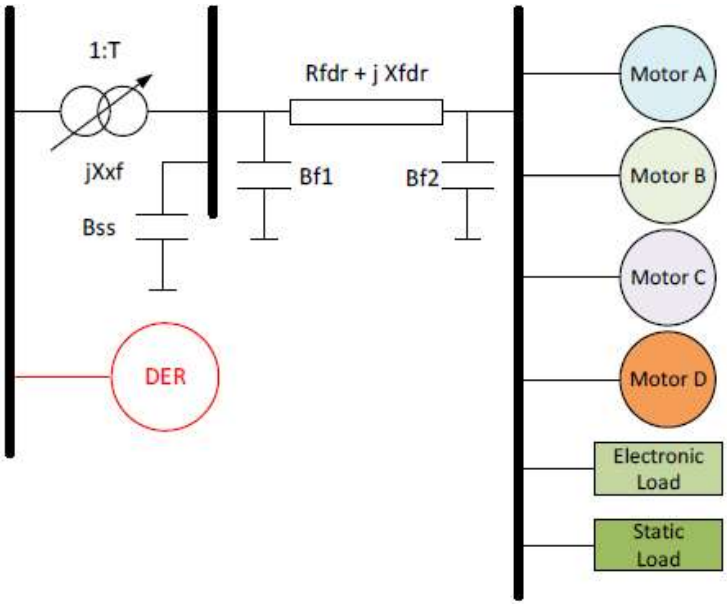

AEMO then developed a set of parameters suitable for simulating load in the NEM, informed by the processes outlined by NERC[11]. The NEM region specific parameters for the CMLD model were developed using a "bottom-up" approach from a range of data sources, as summarised in **Table 2**. CMLD load composition parameters are varied by region, time of day and season.

Table 2 Datasets used to develop input parameters for the CMLD model

Dataset	Source	Application
Breakdown of total load into residential, commercial, and industrial	AEMO Electricity Statement of Opportunities[12]	Informed load composition by region, time of day and season
Detailed appliance specific breakdown of residential customer load.	Australian Government Residential Baseline Study[13]	Informed residential load composition by region, time of day and season
Estimate of commercial end-use load composition, by region, sector, season, and weekday/weekend.	Delta Q (consultant) was engaged by AEMO[14]	Informed commercial load composition by region, time of day and season. Delta Q created average daily load profiles (24 hr period).

[10] Power and Energy, Analysis, Consulting and Education (PEACE®). 2019. Developing Dynamic Load Models for the Australian Eastern Interconnected System, at https://aemo.com.au/-/media/files/initiatives/der/2020/aemo-load-modeling-062819-final.pdf?la=en.

[11] NERC (Dec 2016) Technical Reference Document: Dynamic Load Modelling, at https://www.nerc.com/comm/PC/LoadModelingTaskForceDL/Dynamic%20Load%20Modeling%20Tech%20Ref%202016-11-14%20-%20FINAL.PDF.

[12] AEMO, at https://aemo.com.au/en/energy-systems/electricity/national-electricity-market-nem/nem-forecasting-and-planning/forecasting-and-reliability/nem-electricity-statement-of-opportunities-esoo.

[13] Australian Government (26 October 2015) Report: Residential Baseline study for Australia 2000 – 2030, at https://www.energyrating.gov.au/document/report-residential-baseline-study-australia-2000-2030.

[14] Delta Q (22 April 2020) AEMO Commercial Load Model, at https://aemo.com.au/-/media/files/initiatives/der/2020/2020-06-26-deltaq-final-report-aemo-commercial-load-model-user-guide-revb.pdf?la=en.

Dataset	Source	Application
Individual sector specific categories for the largest ~100 industrial load customers,	AEMO datasets	Informed industrial load composition by region. Large industrial customers were assumed to have relatively constant load levels by time of day and season.
Rules of Association, allocating end use load types to the equivalent CMLD model components	International literature (Lawrence Berkeley National Laboratory (LBNL) New England study), adjusted with advice from NSPs and international consultants.	Informed load composition by region, time of day and season
Proportion of NEM load attributable to Motor D by time of day, season, and region (residential and commercial single phase motor compressors, such as air conditioning and refrigeration)	Energy Efficient Strategies (consultant) was engaged by AEMO[A]	Informed load composition by region, time of day and season
Parameters defining motor behaviours during disturbances, including comparison with international motor standards.	International literature	Informed behaviour of various model components when exposed to various power system disturbance conditions
Bench testing of 14 single phase commercial and residential devices (mostly refrigerators)	Energy Efficient Strategies (consultant) was engaged by AEMO[B]	Informed select Motor D parameters.

A. Energy Efficient Strategies (31 July 2020) Single Phase Induction Motor Loads on the NEM from Refrigeration and Air Conditioners, at https://aemo.com.au/-/media/files/initiatives/der/2020/2020-08-05-ees-ac-load-composition.pdf?la=en.
B. Energy Efficient Strategies (26 June 2020) Results of low voltage stall measurements on single phase induction motors and inverter systems, at https://aemo.com.au/-/media/files/initiatives/der/2020/2020-08-05-ees-results-of-stall-measurements-on-motor-d-and-inverter-systems.pdf?la=en.

Model tuning and validation

Historical disturbances observed in the NEM between 2017 and 2021 were selected for model validation studies. Twelve severe voltage disturbances and three severe frequency disturbances were selected, occurring in different NEM regions at different times of the day. PSS®E snapshots were prepared for each disturbance to represent the event as accurately as possible.

The CMLD and DPV models were validated against each disturbance, comparing model outcomes with the following:

- High Speed Monitoring (HSM) at as many locations as possible in the transmission and distribution networks, to validate the dynamic and steady-state effects of load and DPV seen at a bus, during and following disturbances.
- SCADA measurements, providing an estimate of net change in total load in a region following a disturbance.
- Field measurements from a sample of thousands of DPV inverters (provided by Solar Analytics), analysed statistically to give an indication of the behaviour of DPV in the region. This was used to validate the proportion of DPV tripping, and the proportion of DPV performing over-frequency curtailment.

A small subset of parameters was tuned to provide the best match against the HSM data and observed net changes in DPV and load simultaneously across all events. Tuned parameters include:

- The voltage trip parameters in the DPV model.
- The frequency trip parameters in the DPV model.
- The tripping parameters for the motor, static and power electronic loads in the CMLD model.

- Distribution circuit parameters for the CMLD model
- Separate trip fractions for the power electronics loads in the QLD region to account for the effect of LNG loads.

Metrics were developed to track the performance of the final CMLD and DPV models through various versions, ensuring tuning was producing ongoing improvements in overall accuracy and precision of the models across all the validation cases.

Model performance

The performance of the CMLD+DPV model is compared against the existing ZIP load model as follows:

✓✓	CMLD+DPV models align with observed data *significantly better* than the ZIP model
✓	CMLD+DPV models align with observed data *at least as well* as the ZIP model
X	CMLD+DPV models align with observed data *less well* than the ZIP model

The overall performance of the CMLD+DPV models is also assessed directly against the HSM data as follows:

Green	CMLD+DPV provides a *good match* to observed data
Yellow	CMLD+DPV provides a *fair match* to observed data
Red	CMLD+DPV provides a *poor match* to observed data

Table 3 summarises the model performance for voltage disturbances, and Table 4 summarises model performance for frequency disturbances.

Table 3 Voltage events – comparing CMLD+DPV model performance against HSM and existing ZIP model

		Events with minimal DPV generation (CMLD)					Events with significant DPV generation (CMLD+DPV)						
		8/03/18	11/04/18	18/02/19	17/04/19	22/02/21	3/03/17	18/01/18	9/10/18	3/03/19	26/11/19	24/01/21	12/03/21
Voltages	Voltage overshoot	✓	X	✓	✓✓	✓✓	X	X	✓✓	✓	✓✓	✓	✓
	Voltage recovery rate	X	✓✓	✓	✓✓	✓✓	✓✓	✓✓	✓	✓	✓✓	✓✓	✓✓
	Steady state post disturbance	✓	✓	✓	✓	✓	✓	✓✓	✓	✓	✓	✓	✓
Active Power	During dynamic state	✓	✓	✓	✓	✓✓	✓	✓✓	✓✓	✓	✓	✓	✓
	Steady state post disturbance	✓✓	✓✓	✓	✓✓	✓✓	✓	✓✓	✓	✓	✓	✓✓	✓✓
Reactive Power	During dynamic state	✓✓	✓✓	✓	✓	✓✓	-	✓✓	✓✓	✓	✓✓	✓	✓
	Steady state post disturbance	✓	✓	✓	✓	✓✓	-	✓✓	✓	✓	✓	✓✓	✓

Table 4 Frequency disturbances – CMLD+DPV model performance

		25/08/2018				16/11/2019	31/01/2020	
		SA	QLD	VIC	NSW	SA	SA	VIC
Frequency	During dynamic state	✓✓	✓	✓	✓	✓✓	✓✓	✓
	Steady-state post disturbance	✓	✗	✓	✓	✓✓	✓✓	✓✓

These results show that the CMLD+DPV model provides a significantly better or equally good alignment with HSM data compared with the existing ZIP load model for almost all properties and validation cases studied. These models therefore appear provide an improvement over the existing ZIP model for representing dynamic load and DPV behaviour.

Some cases do remain where neither model provides a good representation of power system behaviour. This can form a focus for improvement in subsequent model revisions.

Explicitly examining the CMLD+DPV representations of load and DPV tripping and curtailment in response to disturbances, **Figure 2** shows the model performance for voltage disturbances, and **Figure 3** shows the model performance for frequency disturbances. The blue bars indicate load loss estimated by the CMLD model, yellow bars indicate DPV loss estimated by the DPV model, and red bars indicate total net contingency sizes predicted by the combination of both models. The estimated actual values (target values) are indicated with dots and error bars. The models distinguish well between cases with minimal load/DPV loss, and cases with significant load and DPV loss. In most cases, target values are achieved to within the uncertainty range of the actuals estimates. The models sometimes over-predict and sometimes under-predict, and have been tuned to achieve the middle of the range and give the best central estimate.

Figure 2 Voltage disturbances: Model performance for load/DPV loss

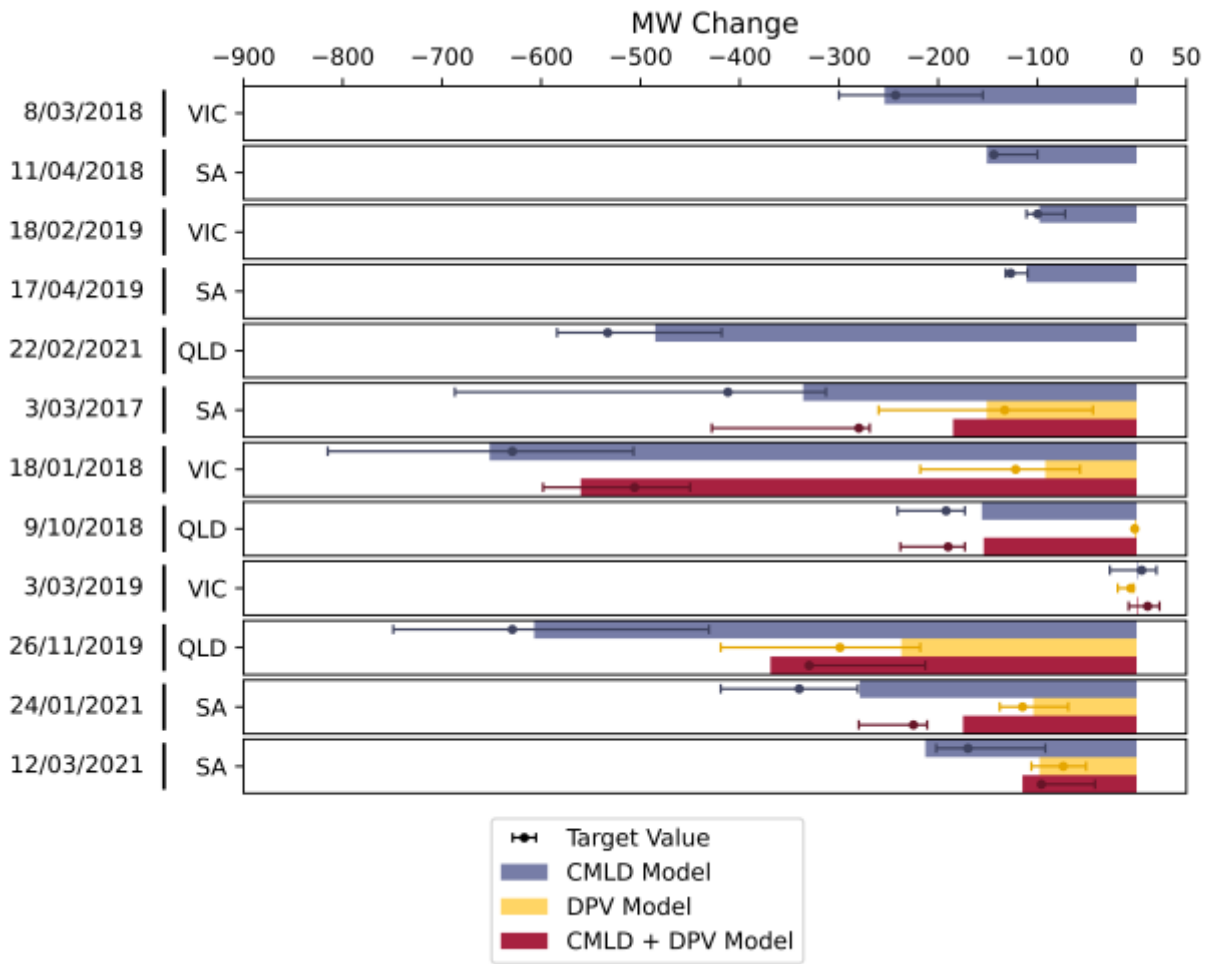

Figure 3 Frequency disturbances: Model performance for DPV/load change

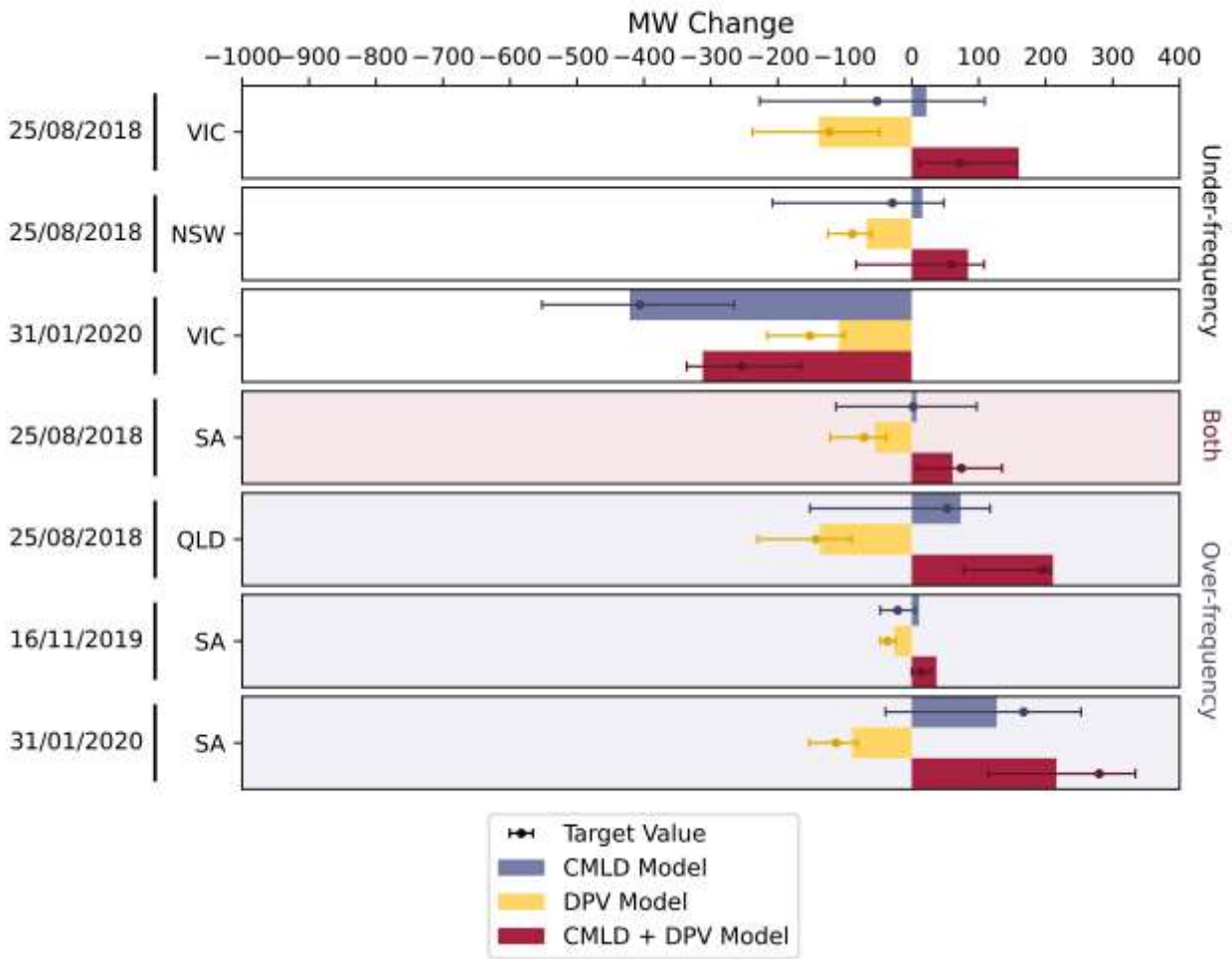

The maximum errors observed for DPV/load change across all validation cases are summarised in **Table 5**. The models accurately capture cases where very little DPV or load tripping was observed. **The CMLD+DPV models provide a considerable improvement in the representation of DPV and load tripping behaviour compared with the existing ZIP model, which cannot represent any level of DPV and load tripping at all.**

Table 5 Uncertainty ranges for CMLD+DPV representation of load and DPV change in disturbances

	CMLD	DPV	CMLD+DPV
Voltage disturbances	-19% / +25%	-25% / +33%	-34% / +20%
Under-frequency disturbances	-92 / +14 MW	-44 / +16 MW	-107 / +58 MW
Over-frequency disturbances	-33 / +40 MW	-24 / -6 MW	-23 / +64 MW

Next steps

Once confirmed with suitable due diligence processes, including review by NSPs, AEMO intends for these models to be applied operationally and in planning studies for re-assessment of network stability limits, frequency control requirements, system strength requirements, inertia requirements, and other elements of power system operation

and planning. The application of these models aims to ensure that DPV and load behaviour is accounted for in power system operation with the best possible models and information available, and AEMO fulfills responsibilities to operate the power system within a secure technical envelope. The re-assessment of these power system requirements is expected to rollout progressively during 2022 and 2023, with an initial focus on areas where the changes are most significant. AEMO will collaborate with NSPs on identifying priority areas.

While it has been demonstrated that the CMLD+DPV models provide a significantly better or equally good alignment with HSM data compared with the existing ZIP load model, AEMO expects that appropriate engineering judgement be used in the application of these models. In some circumstances, particularly where distributed PV shake-off is not a significant factor, the use of the ZIP load model may remain the most appropriate and offer shorter simulation times.

The development of the models presented in this report represents only the first step in continuing improvement in the DER and load models utilised by AEMO, NSPs, and others. As the power system evolves, constant updates and improvements to these models are required. New data sources and evidence will also continue to become available, allowing further improvements. AEMO anticipates an ongoing program of work, in collaboration with NSPs and other stakeholders, continuing to improve these models and account for ongoing system changes. AEMO invites and encourages stakeholder collaboration in this continual improvement process.

Contents

1	Introduction	22
2	Distributed PV model development process	24
2.1	Developing a DPV model	24
2.2	Adapting DER_A as a user-written model (DERAEMO1)	25
2.3	Parameter selection	29
3	CMLD model development process	51
3.1	Developing a Composite Load Model	51
3.2	Approach overview	52
3.3	Load composition parameters	53
3.4	Load behaviour parameters	56
4	Consolidated model development process	65
4.1	The CMLD and DPV model	65
4.2	The CMLD and DPV model in a power system network	66
4.3	Selection of events for model validation	70
4.4	Data collection	72
4.5	Assessing model performance	73
5	Validation: voltage disturbances without DPV	78
5.1	8 March 2018 – Victoria	78
5.2	11 April 2018 – South Australia	83
5.3	18 February 2019 – Victoria	88
5.4	17 April 2019 – South Australia	92
5.5	22 February 2021 - Queensland	97
6	Validation: voltage disturbances with DPV	103
6.1	3 March 2017 – South Australia	103
6.2	18 January 2018 – Victoria	109
6.3	9 October 2018 – Queensland	115
6.4	3 March 2019 – Victoria	121
6.5	26 November 2019 – Queensland	126
6.6	24 January 2021 – South Australia	134
6.7	12 March 2021 – South Australia	142
7	Validation: frequency disturbances	148
7.1	25 August 2018 – South Australia	148
7.2	25 August 2018 – Queensland	158
7.3	25 August 2018 – Victoria	166
7.4	25 August 2018 – New South Wales	174

7.5 16 November 2019 – South Australia 182
7.6 31 January 2020 – South Australia 190
7.7 31 January 2020 – Victoria 198
8 Summary of combined model performance 207
8.1 Performance for voltage disturbances 207
8.2 Performance for frequency disturbances 214
9 Further improvements to load and DER models 220
9.1 EMT model development (underway) 220
9.2 Future improvements to the DPV model 221
9.3 Future improvements to the CMLD model 222
9.4 Under frequency load shedding 224
9.5 Future improvements to general PSS®E models 225
9.6 Model deployment process 225
9.7 Addressing peak reactive/active power representations 225
A1. DPV model parameters 229
A2. CMLD Model Parameters 233
A3. Validation of the DPV user written model for PSS®E 242
A3.1 Active/Reactive Power Control 242
A3.2 Current/output control 243
A3.3 Tripping logic 244

Tables

Table 1 Datasets used to develop input parameters for the DPV model 4
Table 2 Datasets used to develop input parameters for the CMLD model 5
Table 3 Voltage events – comparing CMLD+DPV model performance against HSM and existing ZIP model 7
Table 4 Frequency disturbances – CMLD+DPV model performance 8
Table 5 Uncertainty ranges for CMLD+DPV representation of load and DPV change in disturbances 10
Table 6 Data sources used in the development of DPV model parameters 29
Table 7 DPV standards and NSP requirements categorised by installation date 33
Table 8 Categories of inverter behaviour 34
Table 9 120 ms voltage notch/sag tests – 2015 inverters 36
Table 10 120 ms voltage sag tests – 2005 inverters 37
Table 11 Trendline parameters from bench test results 40
Table 12 Parameters determined from inverter bench testing 43

Table 13	UNSW Inverter testing – source data used to determine DERAEMO1 Parameters	44
Table 14	Additional DPV frequency disconnection assumptions applied in DERAEMO1	49
Table 15	Components of the CMLD Model	52
Table 16	Data sources used to inform load composition parameters in the CMLD model	54
Table 17	CMLD motor type classification and general specifications	60
Table 18	CMLD motor parameters adopted	60
Table 19	Summary of findings from Motor D testing	63
Table 20	Motor trip temperature calculation	64
Table 21	Voltage events used for validation studies	71
Table 22	Frequency events used for validation studies	71
Table 23	Event summary – 8 March 2018	78
Table 24	Simulation event summary – 8 March 2018	79
Table 25	Assessment of model performance – 8 March 2018	83
Table 26	Event summary – 11 April 2018	83
Table 27	Simulation event summary – 11 April 2018	84
Table 28	Assessment of model performance – 11 April 2018	87
Table 29	Event summary – 18 February 2019	88
Table 30	Simulation event summary – 18 February 2019	89
Table 31	Assessment of model performance – 18 February 2019	92
Table 32	Event summary – 17 April 2019	92
Table 33	Simulation event summary – 17 April 2019	93
Table 34	Assessment of model performance – 17 April 2019	97
Table 35	Event summary – 22 February 2021	97
Table 36	Simulation event summary – 22 February 2021	98
Table 37	Assessment of model performance – 22 February 2021	101
Table 38	Event summary – 3 March 2017	103
Table 39	Simulation event summary – 3 March 2017	104
Table 40	Summary of change in demand and distributed PV – 3 March 2017	107
Table 41	Assessment of model performance – 3 March 2017	108
Table 42	Event summary – 18 January 2018	109
Table 43	Simulation event summary – 18 January 2018	110
Table 44	Summary of change in demand and distributed PV – 18 January 2018	114
Table 45	Assessment of model performance – 18 January 2018	114
Table 46	Event summary – 9 October 2018	115
Table 47	Simulation event summary – 9 October 2018	116
Table 48	Summary of change in demand and distributed PV – 9 October 2018	119
Table 49	Assessment of model performance – 9 October 2018	120
Table 50	Event summary – 3 March 2019	121

Table 51	Simulation event summary – 3 March 2019	122
Table 52	Summary of change in demand and distributed PV – 3 March 2019	125
Table 53	Assessment of model performance – 3 March 2019	126
Table 54	Event summary – 26 November 2019	126
Table 55	Simulation event summary – 26 November 2019	128
Table 56	Summary of change in demand and distributed PV – 26 November 2019	132
Table 57	Assessment of model performance – 26 November 2019	133
Table 58	Event summary – 24 January 2021	134
Table 59	Simulation event summary – 24 January 2021	135
Table 60	Summary of change in demand and distributed PV – 24 January 2021	140
Table 61	Assessment of model performance – 24 January 2021	141
Table 62	Event summary – 12 March 2021	142
Table 63	Simulation event summary – 12 March 2021	143
Table 64	Summary of change in demand and distributed PV – 12 March 2021	146
Table 65	Assessment of model performance – 12 March 2021	147
Table 66	Event summary – 25 August 2018 – South Australia	148
Table 67	Simulation event summary – 25 August 2018	149
Table 68	Summary of distributed PV behaviour – 25 August 2018 (SA)	153
Table 69	Summary of change in demand and distributed PV – 25 August 2018 (SA)	156
Table 70	Assessment of model performance – 25 August 2018 (SA)	157
Table 71	Event summary – 25 August 2018 (QLD)	158
Table 72	Summary of distributed PV behaviour – 25 August 2018 (QLD)	161
Table 73	Summary of change in demand and distributed PV – 25 August 2018 (QLD)	164
Table 74	Assessment of model performance – 25 August 2018 (QLD)	164
Table 75	Event summary – 25 August 2018 – Victoria	166
Table 76	Summary of distributed PV behaviour – 25 August 2018 (VIC)	170
Table 77	Summary of change in demand and distributed PV – 25 August 2018 (VIC)	172
Table 78	Assessment of model performance – 25 August 2018 (VIC)	173
Table 79	Event summary – 25 August 2018 – (NSW)	174
Table 80	Summary of distributed PV behaviour – 25 August 2018 (NSW)	178
Table 81	Summary of change in demand and distributed PV – 25 August 2018 (NSW)	180
Table 82	Assessment of model performance – 25 August 2018 (NSW)	181
Table 83	Event summary – 16 November 2019	182
Table 84	Simulation event summary – 16 November 2019	182
Table 85	Summary of distributed PV behaviour – 16 November 2019 (SA)	186
Table 86	Summary of change in demand and distributed PV – 16 November 2019	188
Table 87	Assessment of model performance – 16 November 2019	189
Table 88	Event summary – 31 January 2020 – South Australia	190

Table 89 Simulation event summary – 31 January 2020 190
Table 90 Summary of distributed PV behaviour – 31 January 2020 (SA) 194
Table 91 Summary of change in demand and distributed PV – 31 January 2020 (SA) 196
Table 92 Assessment of model performance – 31 January 2020 (SA) 197
Table 93 Event summary – 31 January 2020 198
Table 94 Summary of distributed PV behaviour – 31 January 2020 (VIC) 202
Table 95 Summary of change in demand and distributed PV – 31 January 2020 (VIC) 204
Table 96 Assessment of model performance – 31 January 2020 (VIC) 205
Table 97 Voltage events – comparing CMLD+DPV model performance against HSM and existing ZIP model 208
Table 98 DPV model performance for voltage disturbances – events with significant DPV 209
Table 99 CMLD performance for load loss for voltage events with minimal DPV generation 210
Table 100 CMLD performance for load loss for voltage events with significant DPV generation 210
Table 101 Error observed for CMLD and DPV models in voltage disturbances 214
Table 102 Dynamic behaviour for frequency events – comparing CMLD+DPV vs existing ZIP model and HSM 214
Table 103 DPV model performance for DPV loss in under-frequency disturbances 215
Table 104 DPV model performance for DPV curtailment and disconnection in over-frequency disturbances 216
Table 105 CMLD model performance for underlying load behaviour in under-frequency disturbances (excluding UFLS trip) 217
Table 106 CMLD model performance for underlying load behaviour in over-frequency disturbances (excluding UFLS trip) 217
Table 107 CMLD and DPV model performance for under-frequency disturbances (excluding UFLS trip) 218
Table 108 CMLD and DPV model performance for over-frequency disturbances (excluding UFLS trip) 218
Table 109 Error range observed for CMLD+DPV in frequency disturbances (excluding UFLS trip) 218
Table 110 Pathways for continuing improvement to the DPV model 221
Table 111 Pathways for continuing improvement to load models 222
Table 112 DPV model parameters for each inverter standard including DNSP volt-VAR requirements 229
Table 113 Sample parameters for NSW load connected at the HV bus in PSS®E with commentary 233

Figures

Figure 1 The composite load model (CMLD) structure 5
Figure 2 Voltage disturbances: Model performance for load/DPV loss 9
Figure 3 Frequency disturbances: Model performance for DPV/load change 10

Figure 4	The DER_A model	25
Figure 5	A high-level overview of the DERAEMO1 model	26
Figure 6	The implementation of the DER model	27
Figure 7	DERAEMO1 Example over-voltage tripping adjustment	28
Figure 8	How various data sources have been integrated into the DERAEMO1 model	31
Figure 9	Mapping process employed to link a Connection Point ID to a PSS®E bus number	32
Figure 10	Example of disconnect behaviour (voltage notch test, inverter 21)	35
Figure 11	Example of ride-through with momentary cessation (voltage notch test, inverter 6)	35
Figure 12	Example of ride-through without momentary cessation (voltage notch test, inverter 22)	36
Figure 13	Transfer function used to map a minimum voltage to a reduction in DPV output	38
Figure 14	Voltage sag/notch test results (2015 standard inverters)	40
Figure 15	Finalised Vrfrac block parameters	42
Figure 16	11 kV feeder 2P fault 12/04/2018 10:09:51 (Voltages)	45
Figure 17	11kV feeder 2P fault 12/04/2018 10:09:51 (Active/Reactive Power)	45
Figure 18	The proportion of disconnections depending on the minimum or maximum frequency reached during frequency excursion	49
Figure 19	The CMLD model structure	51
Figure 20	Illustration of bottom-up development of CMLD model composition (example for South Australia for Sunday 24 January 2021, 4:30-5:00 pm)	54
Figure 21	Torque characteristics in electrical induction motors	58
Figure 22	Minimum breakdown torque	58
Figure 23	Minimum locked rotor torque	59
Figure 24	Minimum pull up torque	59
Figure 25	Motor A torque speed curve	61
Figure 26	Motor B & C torque speed curve	62
Figure 27	Load model response to an under-frequency ramp (50 Hz to 48Hz and back)	63
Figure 28	The combined CMLD and DPV model structure	65
Figure 29	NEM network topology	66
Figure 30	A simplified NEM network topology (valid when analysing the effect of a change in the network)	68
Figure 31	Diagram showing how to analyse a change in the various quantities	70
Figure 32	Map – 8 March 2018	78
Figure 33	Voltage – 8 March 2018 – 500 kV Loy Yang Power Station (LYPS)	80
Figure 34	Voltage – 8 March 2018 – 22 kV Bendigo Terminal Station (BETS)	80
Figure 35	Active/reactive power – 8 March 2018	81
Figure 36	Operational demand measurements (SCADA) – Victoria Total – 8 March 2018	82
Figure 37	Map – 11 April 2018	84
Figure 38	Voltage – 11 April 2018 – Para West Bus 275 kV	85
Figure 39	Active/reactive power – 11 April 2018	86

Figure 40 Operational demand measurements (SCADA) – South Australia total – 11 April 2018 86
Figure 41 Map – 18 February 2019 88
Figure 42 Voltage – 18 February 2019 – Tarrone Terminal Station (TRTS) 132 kV 89
Figure 43 Voltage – 18 February 2019 – South Morang Terminal Station (SMTS) 330 kV 90
Figure 44 Active/reactive power – 18 February 2019 90
Figure 45 Operational demand measurements (SCADA) – Victoria total – 18 February 2019 91
Figure 46 Map – 17 April 2019 93
Figure 47 Voltage – 17 April 2019 – 275 kV Torrens Island Power Station A (TIPS A) 94
Figure 48 Voltage – 17 April 2019 – 275 kV South East Bus 94
Figure 49 Active power – 17 April 2019 – Torrens Island Power Station A (TIPS A) to Kilburn 95
Figure 50 Active power – 17 April 2019 – 275 kV South East to Heywood Feeder (HYTS) 2 95
Figure 51 Active/reactive power – 17 April 2019 96
Figure 52 Operational demand measurements (SCADA) – South Australia total – 17 April 2019 96
Figure 53 Map – 22 February 2021 98
Figure 54 Voltage – 22 February 2021 – 275 kV South Pine H002 bus 99
Figure 55 Voltage – 22 February 2021 – 275 kV Swanbank E H051 bus 99
Figure 56 Active/reactive power – 22 February 2021 – South Pine 275 kV bus feeder to 275/110 kV H2 Transformer 100
Figure 57 Active/reactive power – 22 February 2021 – 275 kV Swanbank (SBK2) to Greenbank H051 Feeder 805 100
Figure 58 Operational demand measurements (SCADA) – Queensland total – 22 February 2021 101
Figure 59 Map – 3 March 2017 104
Figure 60 Voltage – 3 March 2017 – 275 kV Torrens Island Power Station (TIPS) B bus 105
Figure 61 Active power – 3 March 2017 – 275 kV Torrens Island Power Station (TIPS) B Generator 1 Feeder 106
Figure 62 DPV measurements – South Australia total – 3 March 2017 106
Figure 63 Operational demand measurements (SCADA) – 3 March 2017 107
Figure 64 Map – 18 January 2018 110
Figure 65 Voltage – 18 January 2018 – 220 kV Rowville Terminal Station (ROTS) 111
Figure 66 Voltage – 18 January 2018 – 66 kV Cranbourne Terminal Station 111
Figure 67 Active/reactive power – 18 January 2018 112
Figure 68 DPV measurements – Victoria total – 18 January 2018 113
Figure 69 Operational demand measurements (SCADA) – Victoria total – 18 January 2018 113
Figure 70 Map – 9 October 2018 116
Figure 71 Voltage – 9 October 2018 – 275 kV Braemar bus 117
Figure 72 Active/reactive power plots – 9 October 2018 118
Figure 73 DPV measurements (Solar Analytics) – Queensland total – 9 October 2018 118
Figure 74 Operational demand measurements (SCADA) – 9 October 2018 119
Figure 75 Map – 3 March 2019 121

Figure 76 Voltage – 3 March 2019 – 500 kV Hazelwood Terminal Station (HWTS) bus 123
Figure 77 Voltage – 3 March 2019 – 500 kV Hazelwood Terminal Station (HWTS) bus (15 s duration) 123
Figure 78 Active/reactive power – 3 March 2019 – 500 kV Hazelwood to 500kV South Morang Feeder 1 (HWTS_SMTS1) 124
Figure 79 DPV measurements (Solar Analytics) – Victoria total – 3 March 2019 124
Figure 80 Operational demand measurements (SCADA) – 3 March 2019 125
Figure 81 Map – 26 November 2019 127
Figure 82 Voltage – 26 November 2019 – 275 kV Greenbank Bus 128
Figure 83 Active/reactive power – 26 November 2019 – 275 kV Greenbank (GBK) to Mudgeeraba Line 1 129
Figure 84 Active/reactive power – 26 November 2019 130
Figure 85 DPV measurements (Solar Analytics) – Queensland total – 26 November 2019 131
Figure 86 Operational demand measurements (SCADA) – 26 November 2019 132
Figure 87 Map – 24 January 2021 135
Figure 88 Voltage – 24 January 2021 – 275 kV Para bus (Third fault – Cherry Gardens – Mount Barker South trip) 136
Figure 89 Active power – 275 kV TIPS B to City West Feeder – 24 January 2021 137
Figure 90 Reactive power – 275 kV TIPS B to City West Feeder – 24 January 2021 137
Figure 91 Active power – 275 kV Robertstown to Tungkillo Feeder 1 – 24 January 2021 138
Figure 92 Reactive power – 275 kV Robertstown to Tungkillo Feeder 1 – 24 January 2021 139
Figure 93 DPV measurements (Solar Analytics) – South Australia total – 24 January 2021 139
Figure 94 Operational demand measurements (SCADA) – 24 January 2021 140
Figure 95 Map – 12 March 2021 143
Figure 96 Voltage – 12 March 2021 – Torrens Island A bus 144
Figure 97 Active/reactive power plots – 12 March 2021 – Torrens Island Power Station (TIPS) A to Kilburn Line 1 275 kV 145
Figure 98 DPV measurements (Solar Analytics) – South Australia Total – 12 March 2021 145
Figure 99 Operational demand measurements (SCADA) – South Australia total – 12 March 2021 146
Figure 100 Frequency – 25 August 2018 – 275 kV Para bus (SA) 151
Figure 101 Voltage – 25 August 2018 – Para bus (SA) 151
Figure 102 Active/reactive power – 25 August 2018 (SA) – 275 kV Para to TIPS A Feeder 152
Figure 103 DPV measurement (Solar Analytics) – 25 August 2018 – (SA) 153
Figure 104 Active power responses of the CMLD load components – 25 August 2018 (SA) 155
Figure 105 Operational demand measurements (SCADA) – 25 August 2018 (SA) 156
Figure 106 Frequency – 25 August 2018 (QLD) 159
Figure 107 Voltage – 25 August 2018 (QLD) – 275 kV Braemar bus 160
Figure 108 Active/reactive power – 25 August 2018 (QLD) – 275 kV Greenbank to Molendinar 8824 Feeder 160
Figure 109 DPV measurement (Solar Analytics) – 25 August 2018 (QLD) 161

Figure 110 Active power responses of the CMLD load components – 25 August 2018 (QLD) 163
Figure 111 Operational demand measurements (SCADA) – 25 August 2018 (QLD) 164
Figure 112 Frequency – 25 August 2018 (VIC) 167
Figure 113 Voltage – 25 August 2018 – Rowville Terminal Station (ROTS) bus (VIC) 168
Figure 114 Active/reactive power – 25 August 2018 (VIC) – 500/220 kV Rowville (ROTS) Transformer A1 Feeder 169
Figure 115 DPV generation (estimated from Solar Analytics data) – 25 August 2018 (VIC) 169
Figure 116 Active power responses of the CMLD load components – 25 August 2018 (VIC) 171
Figure 117 Operational demand measurements (SCADA) – 25 August 2018 (VIC) 172
Figure 118 Frequency – 25 August 2018 (NSW) 175
Figure 119 Voltage – 25 August 2018 – 330 kV Liddell Power Station G1 Feeder 176
Figure 120 Voltage – 25 August 2018 – 500 kV Eraring Power Station bus (NSW) 176
Figure 121 Active/reactive power – 25 August 2018 (NSW) – 330/22 kV Liddell Power Station G2 Feeder 177
Figure 122 Active/reactive power – 25 August 2018 (NSW) – 500/23 kV Eraring Generator 3 Feeder 177
Figure 123 DPV measurement (Solar Analytics) – 25 August 2018 (NSW) 178
Figure 124 Active power responses of the CMLD load components – 25 August 2018 (NSW) 179
Figure 125 Operational demand measurements (SCADA) – 25 August 2018 (NSW) 180
Figure 126 Frequency – 16 November 2019 – 275 kV Pelican Point Switching Station 184
Figure 127 Voltage – Pelican Point Switching Station – 16 November 2019 (SA) 185
Figure 128 Active/reactive power – 16 November 2019 (SA) – 275 kV Pelican Point GT12 Feeder 185
Figure 129 DPV measurements (Solar Analytics) – South Australia Total – 16 November 2019 186
Figure 130 Active power responses of the CMLD load components – 16 November 2019 (SA) 187
Figure 131 Operational demand measurements (SCADA) – 16 November 2019 188
Figure 132 Frequency – 31 January 2020 – 275kV Para bus (SA) 192
Figure 133 Voltage – 31 January 2020 – 275 kV Para bus (SA) 193
Figure 134 Active/reactive power – 31 January 2020 - 275 kV Pelican Point to Lefevre Feeder 193
Figure 135 DPV measurements (Solar Analytics) – 31 January 2020 (SA) 194
Figure 136 Active power responses of the CMLD load components – 31 January 2020 (SA) 195
Figure 137 Operational demand measurements (SCADA) – South Australia Total – 31 January 2020 196
Figure 138 Frequency – 31 January 2020 (VIC) 199
Figure 139 Voltage – 31 January 2020 (VIC) – 220 kV Rowville bus 200
Figure 140 Active/reactive power – 31 January 2020 (VIC) – 500/220 kV Rowville Transformer 1 Feeder 201
Figure 141 DPV measurements (Solar Analytics) – 31 January 2020 (VIC) 201
Figure 142 Active power responses of the CMLD load components – 31 January 2020 (VIC) 203
Figure 143 Operational demand measurements (SCADA) – Victoria Total – 31 January 2020 204
Figure 144 Model performance for load/DPV loss across voltage disturbances 212
Figure 145 Model performance for load/DPV loss across voltage disturbances 213

Figure 146 Model performance for load/DPV change for frequency disturbances (actual MW change) 219

Figure 147 Active/Reactive Power – 18 January 2018 – 66kV Cranbourne Terminal Station (CBTS) Transformer B1 Feeder 226

Figure 148 Comparison of PSS®E CMLD model results with/without smoothing constant – Reactive Power on Torrens A to Northfield line (11 April 2018) 228

Figure 149 DPV model active/reactive power control block diagram 243

Figure 150 DER_A/DPV model current control block diagram 244

Figure 151 DPV model tripping block diagram 245

1 Introduction

AEMO and network service providers (NSPs) use power system models to assess power system performance under different conditions. The results from these studies inform operational and planning decisions, allowing AEMO to fulfil its responsibilities to maintain a secure power system.

AEMO applies power system models across a variety of platforms including:

- PSS®E (a Root Mean Square [RMS] studies platform).
- PSCAD (an Electro-Magnetic Transient [EMT] studies platform).
- PowerFactory (which can perform either RMS or EMT studies).

It is important that the models used in these studies accurately represent the power system to inform the secure operation of the power system.

There are now significant quantities of distributed PV (DPV) installed in the National Electricity Market (NEM). Previous investigations have shown that DPV can produce complex behaviours during power system disturbances. Therefore, it is important that it is accurately represented in AEMO's power system models.

AEMO's load models were last tuned and validated in 1999, and the end-use load composition has changed considerably since that time. More sophisticated aggregate load models are now available, having been pioneered in other jurisdictions to better represent a range of power system phenomena. As part of this work, AEMO has developed and validated new load models, with parameters based on the load composition and behaviour in NEM regions, in line with international best practice methodologies.

This report focuses on the combined development and validation of the composite load (CMLD) and DPV (DERAEMO1) models in PSS®E. AEMO is also developing similar models in PSCAD and PowerFactory, which will be reported on separately.

By investing in ongoing DPV and CMLD model development, AEMO seeks to fulfil its responsibilities to accurately assess the technical envelope of the power system and maintain power system security now and into the future.

Prior to this work, AEMO (and other stakeholders in the NEM) used a simple ZIP model (polynomial static load model) for all RMS and EMT studies, and DPV was represented as negative load.

It is important that the DPV model developed through this work is used in conjunction with the CMLD model to represent the interactive behaviour of load and DPV accurately. If the DPV model is used with older load models (such as the ZIP model), it will not accurately capture power system behaviour.

Structure of this report

This report is structured as follows.

- Section 2 discusses the development of the DPV model and the selection of the associated parameters.
- Section 3 discusses the development of input assumptions and parameters of the CMLD model.
- Section 4 describes the process followed to fine tune the parameters for both models.

- Section 5 presents the results of validation studies for the CMLD model for voltage disturbances. These studies focus on historical events where voltage disturbances occurred with little DPV generation.
- Section 6 presents the results of validation studies for the CMLD and DERAEMO1 models for voltage disturbances. These studies focus on historical events where voltage disturbances occurred, and there was some level of DPV generation.
- Section 7 presents the results of validation studies for the CMLD and DERAEMO1 models for frequency disturbances. These studies focus on historical events where frequency disturbances occurred, and there was some level of DPV generation.
- Section 8 summarises the combined model performance.
- Section 9 discusses potential future improvements to the models.
- Appendix A1 summarises the recommended parameters of the DERAEMO1 model for studies in the NEM.
- Appendix A2 summarises the recommended parameters of the CMLD model for studies in the NEM.
- Appendix A3 presents the validation simulations used to verify the correct operation of the additional features of the user-written DERAEMO1 model.

2 Distributed PV model development process

2.1 Developing a DPV model

AEMO undertook the following stages to develop a DPV model for the NEM:

1. **International best-practice review.**
   - AEMO conducted an international review to identify best practice approaches to modelling DPV for power system studies. This review identified that a collaborative development process in the USA, led by the Western Electricity Coordinating Council (WECC), had resulted in the release of the 'DER_A' model specification in 2018[15]. The DER_A model was developed to represent the aggregate behaviour of DPV and battery energy storage resources in RMS type power system simulation packages. Since its release, the DER_A model has been implemented in the standard model libraries for several RMS power system software vendors (including Siemens PSS®E, General Electric PSLFTM, DIgSILENT's PowerFactory, and PowerWorld Simulator).
2. **Adaptation (user-written model) to add new features.**
   - AEMO identified that the DER_A model did not represent several characteristics of DPV behaviour that are known to occur in the NEM. These characteristics include staged frequency tripping and rate of change of frequency (RoCoF) triggered tripping. Therefore, AEMO developed a modified model version (termed "DERAEMO1") that represents these characteristics. The DPV model has been implemented as a user-written model in PSS®E. This is summarised in Section 2.2.
3. **Parameter development.**
   - AEMO worked with assistance from Power and Energy, Analysis, Consulting and Education (PEACE®) to develop a set of parameters suitable for DPV inverters in the NEM, utilising the initial framework[16] and parameterisation[17] outlined by the North American Electric Reliability Corporation (NERC), and cross-checked the validity of the parameters against the verification report[18] that was released late in the validation process. Bench testing conducted by the University of New South Wales (UNSW) as part of an Australian Renewable Energy Agency (ARENA)-funded collaboration provided essential input data to this parameter development process[19]. This is summarised in Section 2.3.

[15] Power and Energy, Analysis, Consulting and Education (PEACE®). Proposal for DER_A model, June 2019, at https://www.wecc.org/Reliability/DER_A_Final_061919.pdf.

[16] NERC. Reliability Guideline – Distributed Energy Resource Modelling, September 2017, at https://www.nerc.com/comm/PC_Reliability_Guidelines_DL/Reliability_Guideline_-_DER_Modeling_Parameters_-_2017-08-18_-_FINAL.pdf.

[17] NERC. Reliability Guideline – Parameterization of the DER_A model, September 2019, at https://www.nerc.com/comm/PC_Reliability_Guidelines_DL/Reliability_Guideline_DER_A_Parameterization.pdf.

[18] NERC. Reliability Guideline – Model Verification of Aggregate DER Models used in Planning Studies, March 2021, at https://www.nerc.com/comm/RSTC_Reliability_Guidelines/Reliability_Guideline%20_DER_Model_Verification_of_Aggregate_DER_Models_used_in_Planning_Studies.pdf.

[19] UNSW. Addressing Barriers to Efficient Renewable Integration, at https://research.unsw.edu.au/projects/addressing-barriers-efficient-renewable-integration.

4. **Validation studies.**
   - DPV models were added into system-wide snapshots of historical disturbances to test and tune the model performance against the observed power system behaviour. This is summarised in Sections 5, 6 and 7.

2.2 Adapting DER_A as a user-written model (DERAEMO1)

2.2.1 The DER_A model

The DER_A model developed by WECC is illustrated in **Figure 4**[20]. AEMO has applied the model to represent the behaviour of aggregate distributed PV connected in the low voltage network based on conditions experienced at the upstream transmission or sub-transmission bus (to the level represented in typical PSS®E snapshots of the NEM).

Figure 4 The DER_A model

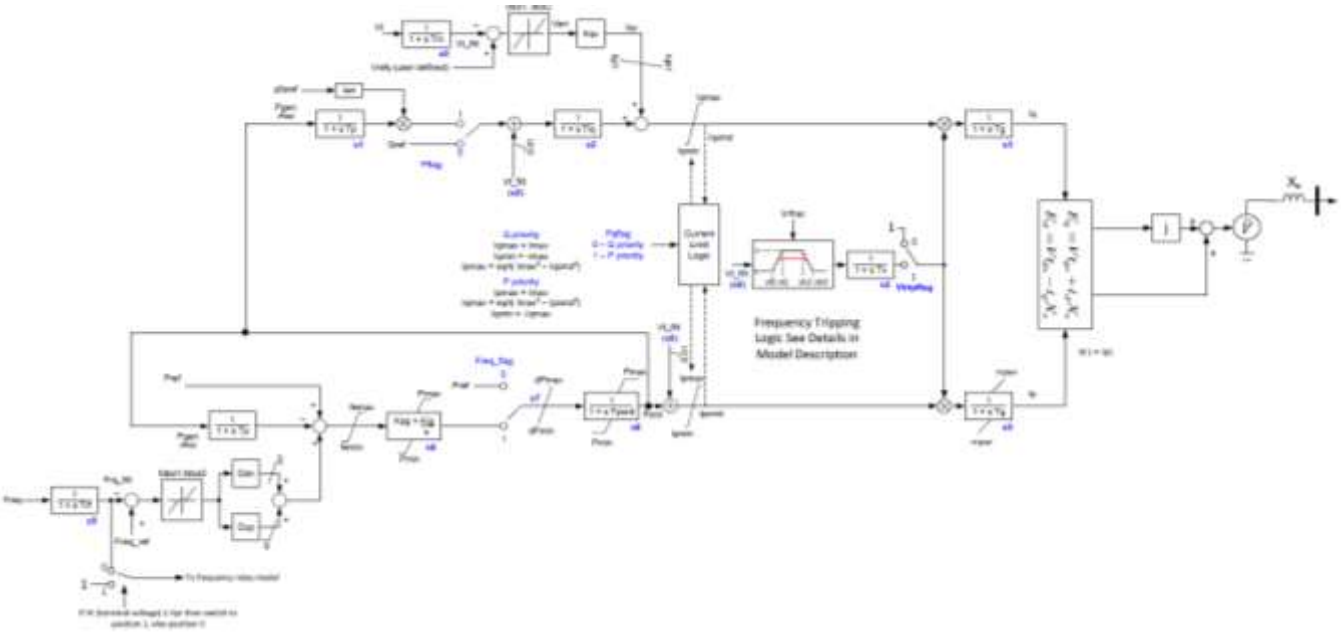

The model includes representations of the following behaviours:

- Constant power factor and constant reactive power control modes (allows voltage control to be active along with PF/Q control, depending on whether voltage is within the deadband or not).
- Proportional reactive power-voltage control mode with reactive power gain, limits, and deadband.
- Active power-frequency control with asymmetric droop gain and deadband.
- Representation of a fraction of resources tripping or entering momentary cessation at low and high voltage, including a four-point piece-wise linear gain (partial tripping includes a timer feature as well).
- Representation of a fraction of DER that restore output following an under voltage or over voltage.

[20] Pouyan Pourbeik, PEACE (11 September 2018) Proposal for DER_A Model.

- Active power ramp rate limits during return to service after trip or enter service following a fault or during frequency response.
- Selectable active-reactive current (PQ) priority options.

2.2.2 The DERAEMO1 model

The DERAEMO1 model, which AEMO adapted from the DER_A model developed by WECC, includes the following features that are additional to the DER_A model:

- Partial power reduction following an under-frequency or over-frequency event, representing DPV tripping due to frequency over 26 independent stages (13 for over-frequency and 13 for under-frequency).
- Partial power reduction following a low or high RoCoF, representing fractional DPV tripping over three independent stages.
- Asymmetric reactive power-voltage control[21].
- Flexible voltage reference such that the under-voltage and over-voltage DPV tripping behaviour scales independently of the initial transmission bus voltage.

The block diagram for the DERAEMO1 model is broken into three segments:

- Active/reactive power control.
- Current/output control.
- Tripping logic.

Figure 5 shows a high-level overview of the DERAEMO1 model implementation. The details of these blocks are described further in Appendix A3.

Figure 5 A high-level overview of the DERAEMO1 model

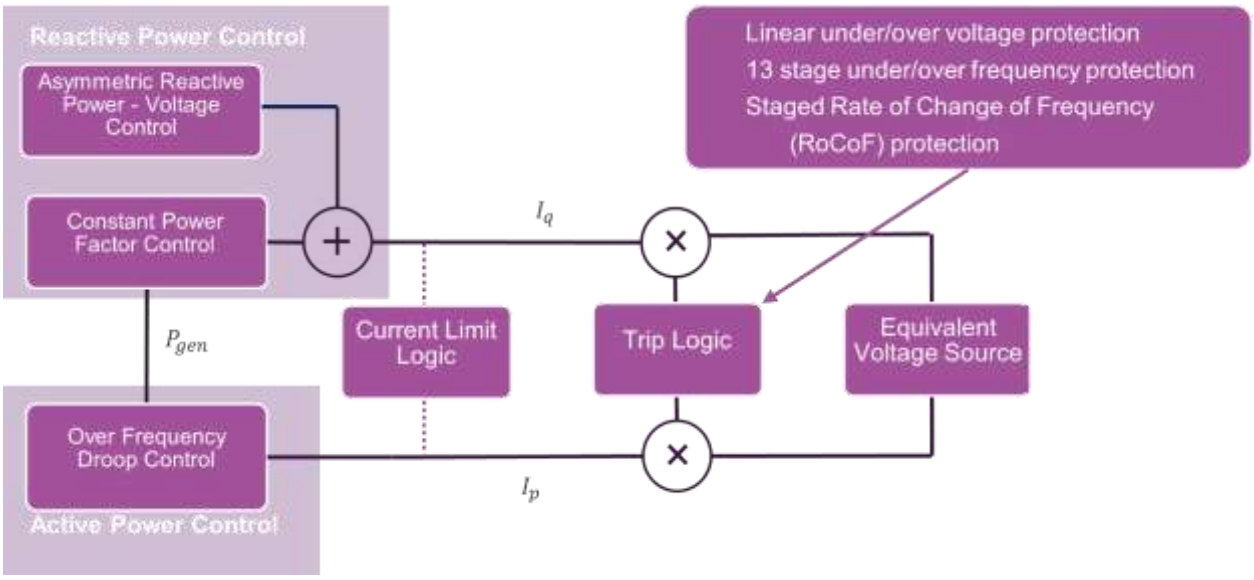

[21] Asymmetry refers to separate proportional gains in response to under or over-voltage conditions.

2.2.3 Implementation of the DERAEMO1 model at the transmission bus

A single instance of the DERAEMO1 model is connected to each transmission bus, as shown in **Figure 6**. This single model represents the aggregate behaviour of all DPV connected downstream of that transmission bus, which includes a proportion of DPV installed under different standards (and therefore demonstrating different behaviours). Each of the 134 parameters in the DERAEMO1 model is therefore calibrated as necessary to represent the total aggregate behaviour of the DPV connected downstream of that bus, depending on the composition of DPV installed.

Figure 6 The implementation of the DER model

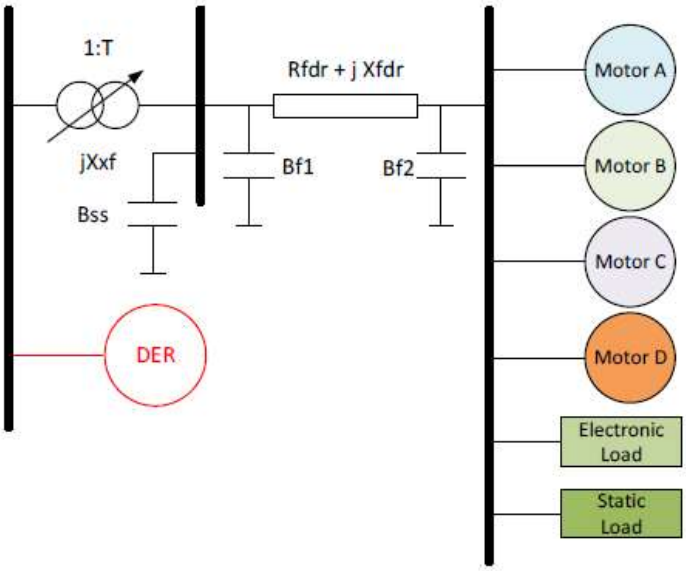

2.2.4 Adjusting the voltage reference

PSS®E snapshots downloaded from OPDMS may have transmission bus voltages outside of the normal operating voltage range, which may not reflect the actual transmission bus voltage. Furthermore, a transmission bus voltage outside of the normal range may not provide an accurate reflection of the relative bus voltage at the distribution level where distributed PV systems are connected. When the initial bus voltage is excessively high or excessively low pre-disturbance, this can make the modelled DPV more sensitive to voltage disturbances than is likely in reality.

To account for this, the DERAEMO1 model normalises the voltage reference to the tripping logic around the 1 pu level. This means that the point at which voltage tripping occurs is not a fixed setpoint, but rather a relative setpoint from the initial bus voltage. The reference voltage at which tripping will occur is adjusted by the difference between the pre-disturbance voltage, and 1pu:

$$vref_{tripping} = 1 + vt - vt_{initial}$$

For example, as illustrated in Figure 7, if the pre-disturbance bus voltage is 1.05 pu, there is little headroom before over-voltage tripping will begin to occur at vh1 (1.13 pu). To account for this, the voltage tripping logic in the DERAEMO1 model subtracts 0.05 pu from the voltage reference which increases the headroom. Without the voltage reference adjustment, a 0.10 pu increase in bus voltage would cause 40% of the modelled DPV to

disconnect, which is likely an overestimation of the tripping behaviour. The same logic is also applied to the under-voltage tripping but is less noticeable as the tripping setpoints are wider and further away from the nominal bus voltage.

Figure 7 DERAEMO1 Example over-voltage tripping adjustment

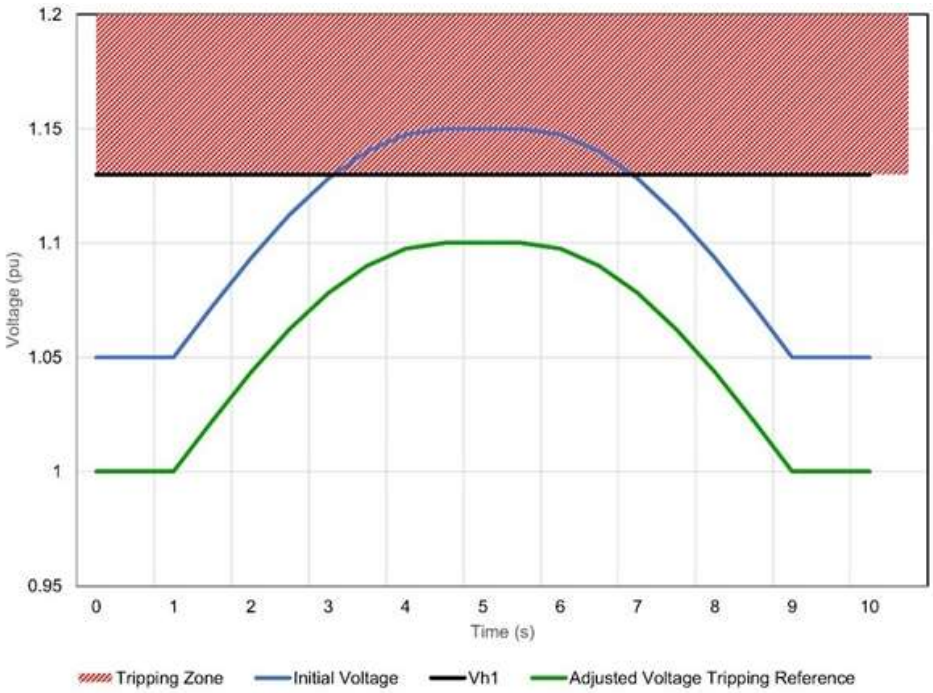

This adjustment is important to reduce the likelihood of over-representing DPV disconnection in cases where the pre-disturbance bus voltage is far above 1 pu. During very lightly loaded periods, the distribution bus voltage may actually be closer to 1.1 pu, and this adjustment reduces the severity of the DPV disconnection that could occur if distribution voltages are already high and close to the range where DPV may trip on the sensitive over-voltage protection settings defined in AS/NZS4777.2.

2.2.5 Model testing

The model's performance was validated to confirm that the additional model functions operated as expected, confirming correct behaviours for fault ride-through, under- and over-frequency trip, over-frequency droop response, under- and over-voltage, and high RoCoF (see Appendix A3).

2.2.6 Model limitations

Some DPV inverters have been observed to disconnect in response to phase angle jumps. UNSW has verified this in bench tests of inverters[22].

Unfortunately, this behaviour cannot be accurately represented in an RMS-based simulation platform such as PSS®E. However, AEMO is working towards including a representation of phase angle trip logic in PSCAD models

[22] UNSW. Addressing Barriers to Efficient Renewable Integration – Milestone Report 2, July 2019, at https://drive.google.com/viewerng/viewer?url=https://raw.githubusercontent.com/kndirangu1/Data/master/Papers/Milestone+Report+2+V3.pdf.

of DPV. The EMT-type DERAEMO1 model, in addition to the features described in this document, includes fractional four-stage voltage phase-angle jump tripping. This allows disconnection of DPV based on voltage phase-angle jump. The EMT DERAEMO1 model is currently being validated and is outside of the scope of this document.

2.3 Parameter selection

The NERC has provided guidance to system operators in the USA on how to collect data and develop parameters for the DER_A model[23]. AEMO used these guidelines to inform the development of the DERAEMO1 model parameters.

Parameters were developed individually for each NEM region. Parameters also account for the different proportions of DPV installed under different inverter connection standards (AS 4777.3:2005, AS/NZS4777.2:2015 and AS/NZS4777.2:2020). The parameters have been selected to represent the trip settings, deadbands, response times, and other behaviours of the DPV in that region for a given point in time.

2.3.1 Data sources

The primary data sources used during the development of DERAEMO1 parameters are summarised in **Table 6**. **Figure 8** outlines how the different data sources informed parameters in the DERAEMO1 model. Further detail on each part is provided in the sections indicated in Table 6.

Table 6 Data sources used in the development of DPV model parameters

Data source	Details	Purpose	Section
Installed capacity of DPV at each bus in the PSS®E model	The installed capacity of DPV at each transmission or sub-transmission bus represented in the PSS®E model was determined based on data provided by NSPs and from the DER Register[A].	This is necessary to allocate the proportion of DPV in the region installed downstream of each transmission or sub-transmission bus (to the level represented in the PSS®E snapshot) as accurately as possible.	2.3.2
Installed capacity of DPV in the region over time by postcode, from the Australian Photovoltaic Institute (APVI)[B]	The APVI provides data on the total installed capacity of DPV in each NEM region, split by postcode and installation date.	This data helped estimate the breakdown of inverters installed under the AS 4777.3: 2005 and AS/NZS4777.2: 2015 standards in each region, and was also used to refine the estimates of the amount of DPV installed in each geographic area. It was assumed that all systems installed before 9 October 2016 were installed under AS 4777.3:2005, and all systems installed after this date were installed under AS/NZS4777.2:2015.	2.3.2
Clean Energy Regulator (CER) database	The CER maintains a database of distributed energy resources installed in the NEM, including install date, inverter manufacturer, capacity, and applicable Australian Standards.	This data was used to confirm the proportion of NEM inverters applicable under each standard for a given date. This information was also used in conjunction with UNSW inverter bench tests to determine the percentage of installed inverters across the NEM represented by individual inverter products from particular manufacturers with known behaviours[C].	2.3.2

[23] NERC. Reliability Guideline – Parameterization of the DER_A model, September 2019, at https://www.nerc.com/comm/PC_Reliability_Guidelines_DL/Reliability_Guideline_DER_A_Parameterization.pdf.

Data source	Details	Purpose	Section
Inverter bench testing	At the time of parameter derivation, UNSW had conducted experimental 'bench tests' on 24 single-phase (1P) DPV inverters[D] (representing ~19% of the NEM installed capacity) to determine behaviour under various conditions[E].	These tests informed a wide range of model parameters that dictate the behaviour of inverters when they experience various conditions, as outlined in more detail in the following sections.	2.3.4
Survey of frequency trip settings	AEMO conducted a survey[F] requesting information from inverter manufacturers on default under and over-frequency trip settings for inverters installed under AS 4777.3:2005.	AEMO determined the proportion of DPV installed capacity associated with each manufacturer and model number known to have particular frequency trip settings using the CER database (see above). AEMO then determined the percentage of inverters that will trip at various under and over-frequency trip settings.	2.3.8
Australian Standards	Australian standards (AS 4777.3:2005, AS/NZS4777.2:2015 and AS/NZS4777.2:2020) specify inverter behaviour requirements for the periods when each standard is applied.	The specifications in Australian standards informed select parameters that dictate inverter behaviour when experiencing various conditions.	2.3.7
Field measurements of individual DPV devices during disturbances	Five second and 60 second Solar Analytics[G] datasets were collected for each of the daytime disturbances in this report. These data sets consist of field measurements from thousands of individual DPV devices across NEM regions.	This sample of inverters was used to estimate the proportion of DPV disconnecting and/or curtailing or demonstrating other complex behaviours during historical power system disturbances. The proportion of DPV disconnecting in the model was calibrated against these historical observations during the model validation process.	2.3.6
High Speed Monitoring (HSM) data in the transmission network	HSM data was collected from transmission monitors for historical disturbances. As of August 2021, AEMO has access to 138 monitors in 61 locations across the NEM. For events where AEMOs HSM data was not attainable or inadequate, AEMO requested additional data from NSPs.	This was used in validation studies. DER and CMLD model parameters were tuned to best match the observed high speed time series profiles for voltage, active power, reactive power, and frequency at locations close to the disturbance. More distant locations were also checked to confirm alignment.	5, 6, 7
High Speed Monitoring (HSM) data in the distribution network	HSM data was provided by Energy Queensland from selected feeders.	This was used to calibrate the DER and load model responses in "playback" studies, aiming to represent the load and DPV on the single radial feeder for a given frequency or voltage disturbance.	2.3.5
Supervisory Control and Data Acquisition (SCADA) monitoring data	SCADA data was collected at four second resolution.	AEMO used regional measurements of total power system load to estimate load loss, for calibration of the models. SCADA data was also used to confirm a system snapshot had the correct generator and battery energy storage P and Q setpoints, and whether capacitor banks and shunts were in/out of service.	-

A. AEMO. DER Register, at https://aemo.com.au/en/energy-systems/electricity/der-register.
B. Australian PV Institute. PV Postcode Data, at https://pv-map.apvi.org.au/postcode.
C. Data from the CER was analysed and visualised by the Australian PV Institute (APVI), which was used to estimate the NEM installed capacity on a per-region basis. Available at https://pv-map.apvi.org.au/analyses.
D. Bench testing and NEM installed capacity data for a further 4 inverters was made available after the initial parameters were derived. The voltage trip parameters (vrfrac, vl0, vl1) were refreshed to include the updated sample.
E. UNSW. Addressing Barriers to Efficient Renewable Integration – Bench Testing of Rooftop PV Inverters, at http://pvinverters.ee.unsw.edu.au/.
F. AEMO. Response of Existing PV Inverters to Frequency Disturbances, April 2016, at https://aemo.com.au/-/media/files/electricity/nem/security_and_reliability/reports/response-of-existing-pv-inverters-to-frequency-disturbances-v20.pdf.
G. Solar Analytics are a company who specialise in energy monitoring solutions. Refer to their website for more information - https://www.solaranalytics.com/au/.

Figure 8 How various data sources have been integrated into the DERAEMO1 model

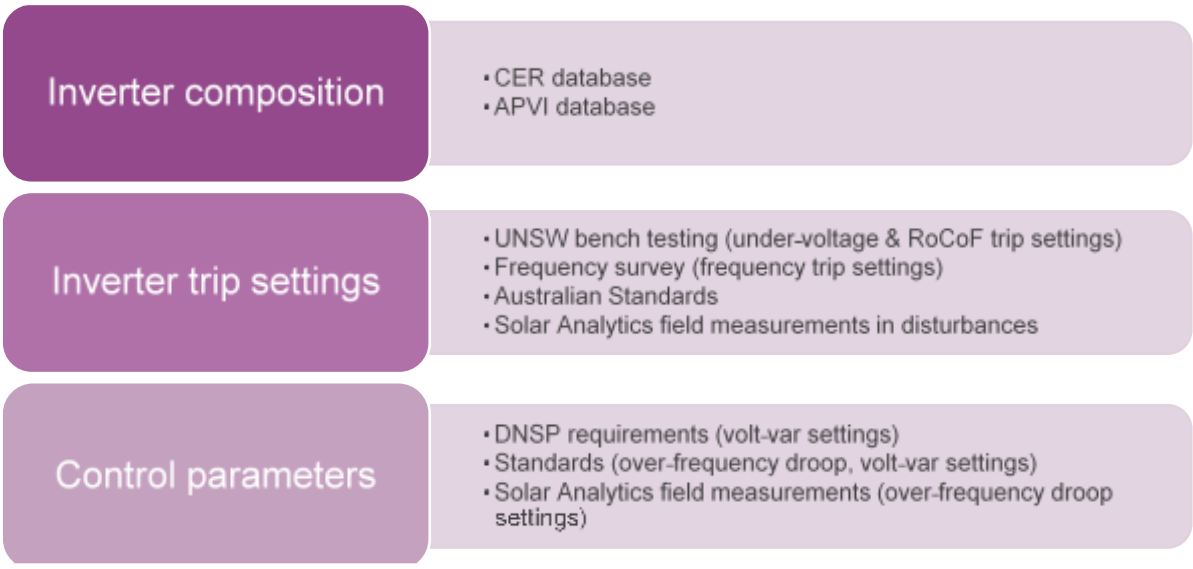

2.3.2 Capacity of DPV installed at each bus

AEMO used data from DNSPs and the Clean Energy Regulator (CER) to estimate the amount of DPV at each connection point[24] (CP).

The CER dataset provided the installed DPV capacity and installation date grouped by postcode. AEMO translated this data to a connection point ID (CPID) within the vicinity of each postcode. To cross-reference, DNSPs provided installed DPV capacity (grouped by CP) [25].

Where possible, the DNSP CPs were converted to a PSS®E bus number. Where data was lacking, or more than one bus was attributed to a CP, the CP was converted to a National Meter Identifier (NMI)[26] or Transmission Node Identity (TNI)[27]. The NMI and TNI data was then converted to a PSS®E bus number (as shown in **Figure 9**).

Figure 9 shows the process AEMO followed to convert a CPID to a PSS®E bus number by assessing whether the CPID can be matched to a bus number directly, an NMI, a TNI to NMI, a TNI, or if the map does not exist and no other information is known, it is disregarded.

[24] A connection point is the physical point at which the assets owned by a TNSP meet the assets owned by a DNSP. These may also be known as Bulk Supply Points (BSPs), terminal stations, exit points, or Transmission Node Identifiers (TNIs).

[25] AEMO. Connection Point Forecasting Methodology, July 2016, at https://www.aemo.com.au/-/media/files/electricity/nem/planning_and_forecasting/tcpf/2016/aemo-transmission-connection-point-forecasting-methodology.pdf.

[26] A unique identifier for connection points and associated metering points used for customer registration and transfer, change control and data transfer.

[27] Identifier of connection points across the NEM.

Figure 9 Mapping process employed to link a Connection Point ID to a PSS®E bus number

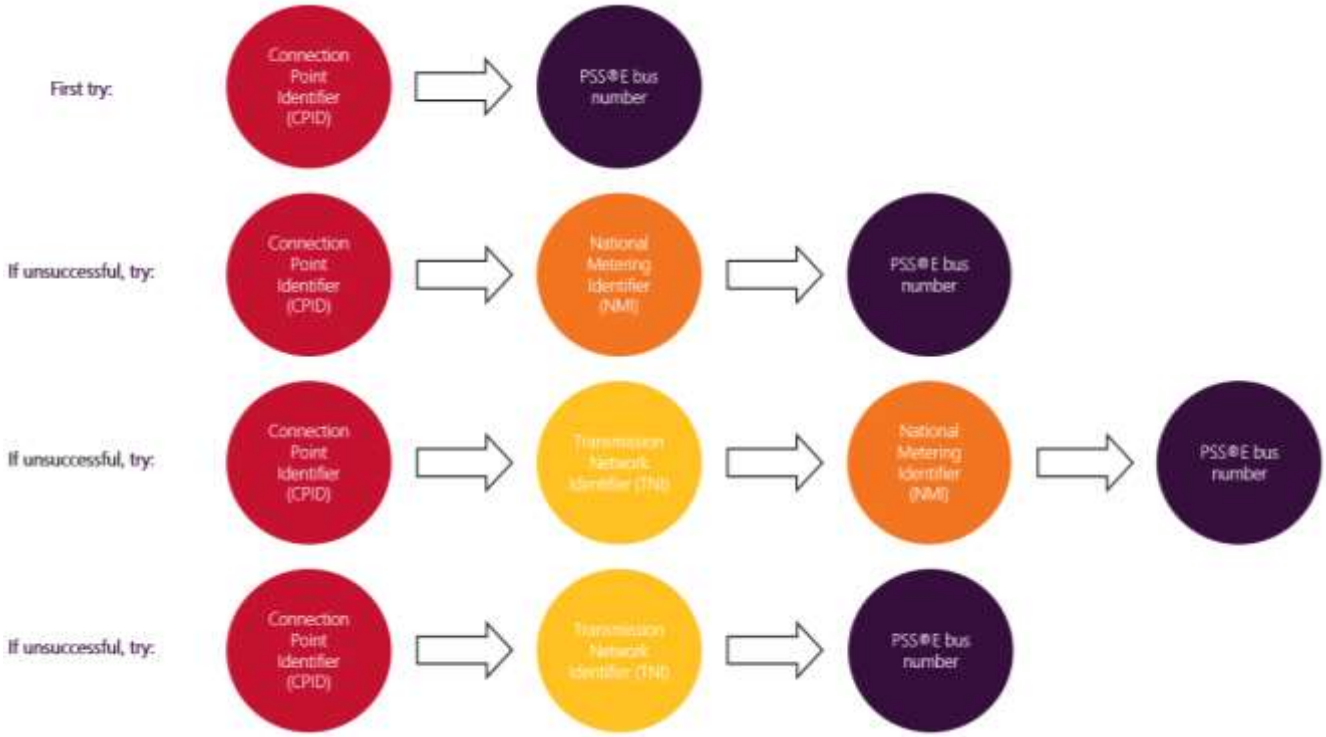

In this manner, ~86% of NEM installed DPV capacity was converted from CPID to an equivalent PSS®E bus number. The remaining ~14% was accounted for by scaling the installed capacity of DPV at all the PSS®E buses with known DPV to match the total DPV installed capacity for the region from the CER.

This approach provided an estimate of the proportion of DPV in the region allocated to each PSS®E bus, which was scaled by the total installed capacity of DPV in a region in a particular snapshot in time.

This approach has some inherent error, because the proportion of the region's total DPV attributed to each CP may change over time as more capacity is installed. As this is expected to be a slow change, AEMO intends to update the maps from time to time to correct any long-term shifts in DPV distribution throughout each region.

2.3.3 Approach for calculating aggregate parameters

The 134 parameters in the DERAEMO1 model are listed in full in Appendix A1. The value assigned to each parameter was calculated individually for sub-groups of DPV, based on:

- Region (QLD, NSW, VIC, SA or TAS).
- The proportion of DPV in the region installed under each standard/NSP requirement at the point in time represented by the PSS®E snapshot.

A single parameter set was used for the DERAEMO1 model for each region at each transmission bus in a particular region.

For some parameters, a static value was be applied. For other parameters, a weighted average was applied to weight the parameter between the standards, based on the varying proportion of inverters applicable to each

inverter standard or requirement in each region. The relevant grid connection standards and NSP requirements used for this weighted average are summarised in **Table 7**.

Table 7 DPV standards and NSP requirements categorised by installation date

Installation date	Assumed standard/NSP requirements
Prior to 9 Oct 2016	AS4777.3:2005 ("the 2005 standard")[A]
After 9 Oct 2016	AS/NZS4777.2:2015 ("the 2015 standard")[B]
Volt-var response considered from the following dates: • **SA from 1 December 2017** • **NSW from 1 December 2018** • **QLD from 1 December 2019** • **VIC from 1 December 2019** • **TAS from 1 January 2021**	AS/NZS4777.2:2015 with volt-var response enabled (volt-var response has been disabled for this release, refer to Section 2.3.7)
South Australia after 1 August 2020	AS/NZS4777.2:2015 with the South Australian Voltage Ride-through (VDRT) requirement[C] applied (these inverters are assumed to have identical disturbance ride-through characteristics to other AS/NZS4777.2:2015 inverters installed prior to this date, based on observations during field disturbances[D,E])
After 31 December 2021	AS/NZS4777.2:2020 ("the 2020 standard")[F]

A. Standards Australia. AS 4777.3-2005 - Grid connection of energy systems via inverters, Part 3: Grid protection requirements, May 2005, at https://www.techstreet.com/sa/standards/as-4777-3-2005?product_id=2070567.
B. Standards Australia. AS/NZS 4777.2-2005 - Grid connection of energy systems via inverters, Part 2: Inverter requirements, September 2015, at https://www.techstreet.com/sa/standards/as-nzs-4777-2-2015?product_id=2067373.
C. AEMO. Short Duration Undervoltage Disturbance Ride-Through Test Procedure, February 2021, at https://aemo.com.au/en/initiatives/major-programs/nem-distributed-energy-resources-der-program/standards-and-connections/vdrt-test-procedure.
D. AEMO (November 2021) Final Report – Trip of Torrens Island A and B West 275kV busbars on 12 March 2021, Section A3, https://aemo.com.au/-/media/files/electricity/nem/market_notices_and_events/power_system_incident_reports/2021/final-report-torrens-island-275-kv-west-busbar-trip.pdf?la=en.
E. AEMO (June 2021) Trip of Multiple Cherry Gardens Lines on 24 January 2021, Section A3, https://aemo.com.au/-/media/files/electricity/nem/market_notices_and_events/power_system_incident_reports/2021/trip-of-multiple-cherry-gardens.pdf?la=en.
F. Standards Australia. 2020. AS/NZS 4777.2:2020 - Grid connection of energy systems via inverters, Part 2: Inverter requirements, at https://www.techstreet.com/sa/standards/as-nzs-4777-2-2020?product_id=2202786.

Weighted averages were calculated for the following "fraction" parameters:

- The 13 under-frequency trip fractions (frac_fl1 to frac_fl13).
- The 13 over-frequency trip fractions (frac_fh1 to frac_fh13).
- The three RoCoF trip fractions (frac_RoCoF_1 to frac_RoCoF_3).
- Under/over-voltage reconnection fraction (vrfrac).

These parameters gave the percentage of the DPV fleet that will trip or show other behaviours following a disturbance beyond a defined threshold. Calculating these parameters as a weighted average based on the proportion of inverters installed under each standard with known behaviours therefore provides a precise reflection of the percentage of the fleet that will demonstrate the behaviour indicated.

Weighted averages were also applied for the following parameters, representing an estimated average of fleet behaviour:

- Under-voltage trip delays (tvl0, tvl1).
- Over-voltage trip delays (tvh0, tvh1).
- Over-voltage trip setpoints (vh0, vh1).

- Under-voltage trip setpoint (vl0).
- Over-frequency curtailment droop gain (Ddn).
- Maximum converter current (Imax).

For this second set of parameters, the blending approach does introduce some limitations in the ability of the model to fully represent the complex suite of behaviours from the DPV fleet but was considered a reasonable compromise that sufficiently represents behaviour to the level of uncertainty in the input datasets.

The remaining parameters shared the same value across all categories and were not expected to change over time or between standards, so a static value was applied.

2.3.4 Parameters informed by inverter bench testing

Many model parameters were directly informed by inverter bench testing conducted by UNSW Sydney under an ARENA funded project[28]. At the start of this model development process, twenty four inverters had been tested, and used to inform the model parameters[29]. NEM installed capacity data indicates that this sample constitutes ~19% of inverters installed in the NEM. The behaviour of this sample was assumed to be representative of NEM DPV installed capacity. As data became available for more inverters during this project, the voltage trip parameters (vrfrac, vl0, vl1) were refreshed to include the new data.

In total, nine inverters installed under the 2005 standard and 21 inverters installed under the 2015 standard were tested[30].

Categorising inverter behaviours

The findings from the voltage notch/sag tests (a step down in voltage to varying levels, for a varying duration) were used to inform the voltage trip parameters (vrfrac, vl0, vl1). The voltage notch tests (a step down in voltage from 230 V to 50 V, for a duration of 0.1s) were also used to inform the voltage trip time parameter (tvl1). The voltage ramp tests (a ramp down in voltage from 230 V to 160 V, for a duration of 10s) were used to inform the voltage trip time parameter (tvl0).

Three categories of inverter behaviour were defined for assessing an inverter's performance during these tests, as summarised in **Table 8**.

Table 8 Categories of inverter behaviour

Category	State after fault	Inverter behaviour during test
1 - Disconnects	Disconnected	Disconnects after a short delay (~30 ms)
2 – Ride-through with momentary cessation	Connected	Does not disconnect but momentarily ceases current injection during the sag
3 – Ride-through without momentary cessation	Connected	Does not disconnect and continues to output current during the sag

[28] UNSW. Addressing Barriers to Efficient Renewable Integration – Bench Testing of Rooftop PV Inverters, at http://pvinverters.ee.unsw.edu.au/.

[29] Results from the bench-testing of Inverter 11 were not used to inform parameters, as the device tested was found to malfunction during operation.

[30] Out of the sample of 24 inverters for which NEM installed capacity data was initially available, 2 inverters featured the ability to switch between compliance with the 2005 standard or the 2015 standard. These inverters were tested under both standards, the results of which were treated as separate inverters.

Category 1 – Disconnects

A representative example of an inverter demonstrating disconnection behaviour during the voltage notch test is given in **Figure 10**. During the voltage dip's falling edge, the output current remains almost constant, which is the expected behaviour of a current-controlled inverter. After a delay of 20 ms, the inverter's output current falls to 0. When the voltage recovers to its nominal value, the inverter's current remains at 0 and the DER inverter is considered to have disconnected from the network.

Figure 10 Example of disconnect behaviour (voltage notch test, inverter 21)

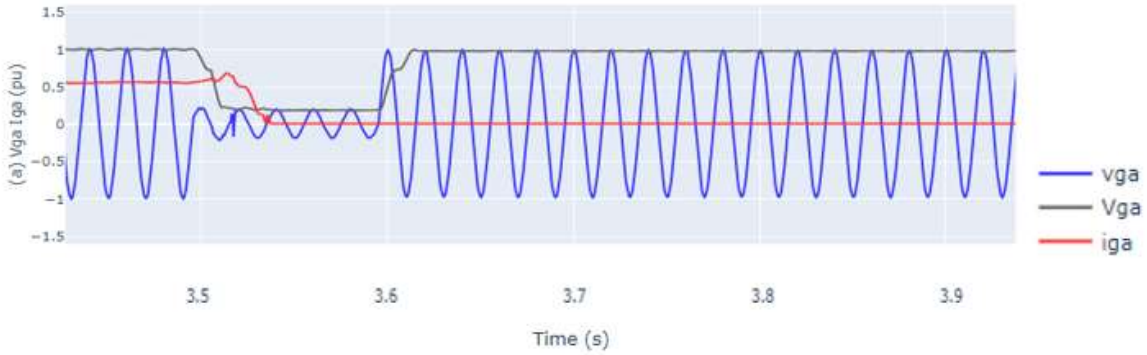

Category 2 – Ride-through with momentary cessation

A representative example of an inverter demonstrating ride-through with momentary cessation during the voltage notch test is given in **Figure 11**. After a delay of 30 ms, the DPV inverter's output current reduces to 0. When the voltage recovers, the output current returns to its nominal value after a short delay. This behaviour, where the inverter momentarily reduces its output to zero, is referred as momentary cessation[31].

Figure 11 Example of ride-through with momentary cessation (voltage notch test, inverter 6)

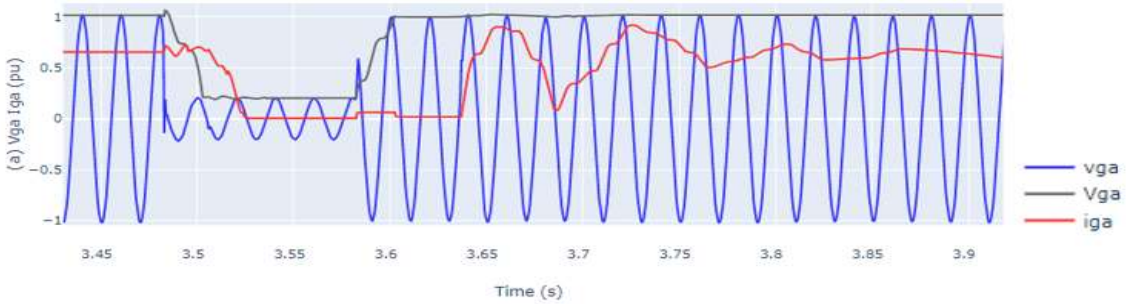

Category 3 – Ride-through without momentary cessation

A representative example of an inverter demonstrating ride-through behaviour without momentary cessation is given in **Figure 12**. This inverter does not reduce its output current to zero during the voltage notch test. During the falling edge of the voltage notch, the inverter's output voltage (V_{ga}), the current (i_{ga}) increases slightly and is

[31] IEEE Std 1547-2018, "IEEE Standard for Interconnection and Interoperability of Distributed Energy Resources with Associated Electric Power Systems Interfaces".

maintained close to its nominal value (~1.1 pu) during the fault. When the voltage recovers, the current returns gradually to its initial pre-fault value.

Figure 12 Example of ride-through without momentary cessation (voltage notch test, inverter 22)

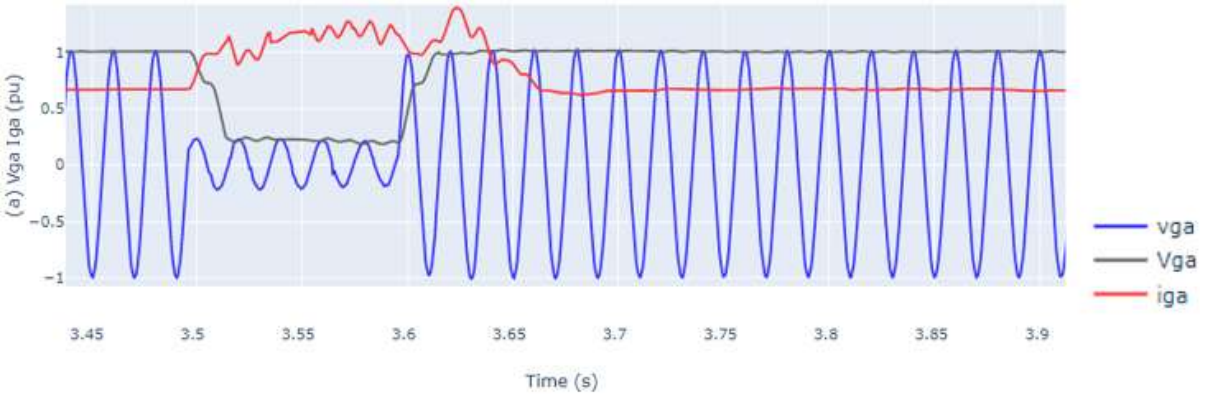

Voltage notch/sag tests

Findings from the voltage notch/sag tests were used to inform the voltage trip parameters (vrfrac, vl0, vl1). **Table 9** and **Table 10** show the behaviour of inverters from different manufacturers, categorised as either ride-through (RT) or disconnect (DC) for faults of varying depths (all tests presented in this table were for a voltage notch/sag of 120 ms duration). The percentage inverters disconnecting at each depth of voltage notch/sag can be estimated from these samples, as shown in the bottom row of each table.

Table 9 120 ms voltage notch/sag tests – 2015 inverters

Inverter #	10% sag (0.9 pu)	20% sag (0.8 pu)	30% sag (0.7 pu)	40% sag (0.6 pu)	50% sag (0.5 pu)	60% sag (0.4 pu)	70% sag (0.3 pu)	80% sag (0.2 pu)
Inverter 1	RT	RT	RT	RT	RT	RT	RT	RT
Inverter 2	RT	RT	RT	RT	RT	DC[A]	RT	DC
Inverter 3	RT	RT	RT	RT	RT	RT	RT	RT
Inverter 4	RT	DC	DC	DC	DC	DC	DC	DC
Inverter 5	RT	RT	RT	RT	RT	RT	RT	RT
Inverter 6	RT	RT	RT	RT	RT	RT	RT	RT
Inverter 7	RT	RT	RT	RT	RT	RT	RT	RT
Inverter 10	DC	DC	DC	DC	DC	DC	DC	DC
Inverter 12	DC	DC	DC	DC	DC	DC	DC	DC
Inverter 13	RT	RT	RT	RT	RT	RT	RT	RT
Inverter 16	RT	RT	DC	DC	DC	DC	DC	DC
Inverter 17	RT	RT	RT	RT	RT	RT	RT	RT
Inverter 19	RT	RT	RT	RT	RT	RT	RT	RT
Inverter 20	RT	RT	RT	RT	RT	DC	DC	DC
Inverter 22	RT	RT	RT	RT	RT	RT	RT	RT
Inverter 23	RT	RT	RT	RT	RT	RT	RT	RT

Inverter #	10% sag (0.9 pu)	20% sag (0.8 pu)	30% sag (0.7 pu)	40% sag (0.6 pu)	50% sag (0.5 pu)	60% sag (0.4 pu)	70% sag (0.3 pu)	80% sag (0.2 pu)
Inverter 25	RT	RT	RT	RT	RT	RT	RT	RT
Inverter 26	DC	DC	DC	DC	DC	DC	DC	DC
Inverter 27	RT	RT	RT	RT	RT	RT	RT	DC
Inverter 28	RT	RT	RT	RT	RT	DC	DC	DC
% that ride-through	85%	80%	75%	75%	75%	60%	65%	55%
Average (2015 standard)	71%							

A. This inverter failed the test as it tripped on over current. It is assumed that this behaviour would be replicated in the field and therefore this inverter would fail to reconnect on a 60% voltage sag for 120 ms.

Table 10 120 ms voltage sag tests – 2005 inverters

Inverter #	10% sag (0.9 pu)	20% sag (0.8 pu)	30% sag (0.7 pu)	40% sag (0.6 pu)	50% sag (0.5 pu)	60% sag (0.4 pu)	70% sag (0.3 pu)	80% sag (0.2 pu)
Inverter 1	RT	RT	RT	RT	RT	RT	RT	RT
Inverter 6	RT	RT	RT	RT	RT	RT	RT	RT
Inverter 8	RT	RT	RT	RT	RT	DC	DC	DC
Inverter 9	RT	RT	RT	RT	RT	RT	RT	RT
Inverter 14	RT	RT	RT	RT	RT	RT	RT	RT
Inverter 15	DC	DC	DC	DC	DC	DC	DC	DC
Inverter 18	DC	DC	DC	DC	DC	DC	DC	DC
Inverter 21	DC	DC	DC	DC	DC	DC	DC	DC
Inverter 24	RT	RT	RT	RT	RT	RT	RT	RT
% that ride-through	67%	67%	67%	67%	67%	56%	56%	56%
Average (2005 standard)	63%							

The way these voltage notch/sag tests informed the voltage trip parameters is outlined in the following section.

Voltage trip parameters (Vrfrac, Vl1 and Vl0)

Vrfrac block logic

The original DER_A model design, developed by WECC[32], allows for emulation of partial tripping of the aggregated model, given that the model is intended to represent the aggregated distributed resources connected downstream of a bus. The model includes several timers (tvl1, tvl0) to emulate different groups of distributed inverters disconnecting under low voltage scenarios. This is useful, for example, when some older legacy technology may disconnect for a mild voltage dip, while modern inverters that comply with newer standards may not disconnect unless the voltage drops significantly for a longer duration. The WECC documentation also notes that the design of the vrfrac block can represent the gradient of voltage along a feeder; in this case, inverters

[32] Power and Energy, Analysis, Consulting and Education (PEACE®). Proposal for DER_A model, June 2019, at https://www.wecc.org/Reliability/DER_A_Final_061919.pdf.

along the feeder experience a different depth of voltage notch/sag such that some may disconnect while others do not at the same bus.

This functionality is unchanged in the AEMO DPV model. It is used to emulate the varying performance characteristics of the aggregate fleet of inverters, as well as to replicate the proportions of inverters observed to disconnect in field measurements in historical disturbances (based on the varying voltages observed at each bus across the network in each disturbance).

Figure 13 (adapted from WECC documentation[33]) explains the behaviour of the voltage trip component of the DPV model (referred to as the vrfrac block). As in the WECC DER_A model, the DPV model uses the vrfrac block to scale the aggregate power output of the generator. The y-axis in Figure 13 can be called the "vrfrac multiplier" and is the output of the vrfrac block.

The output of the vrfrac block is low-pass filtered with a time constant (Tv) that emulates a delayed inverter response and then multiplied by the output active and reactive currents (i_p,i_q) to scale the net output active and reactive power of the DPV model. This block can represent a proportion of inverters demonstrating momentary cessation behaviour (reducing active and reactive power injection during a fault), as well as representing the proportion of inverters that recover (do not disconnect) following fault recovery. AEMO's focus for developing DPV parameters has been to replicate DPV disconnection behaviour post fault as accurately as possible; future revisions of the model could also more explicitly consider the representation of momentary cessation behaviour.

Figure 13 Transfer function used to map a minimum voltage to a reduction in DPV output

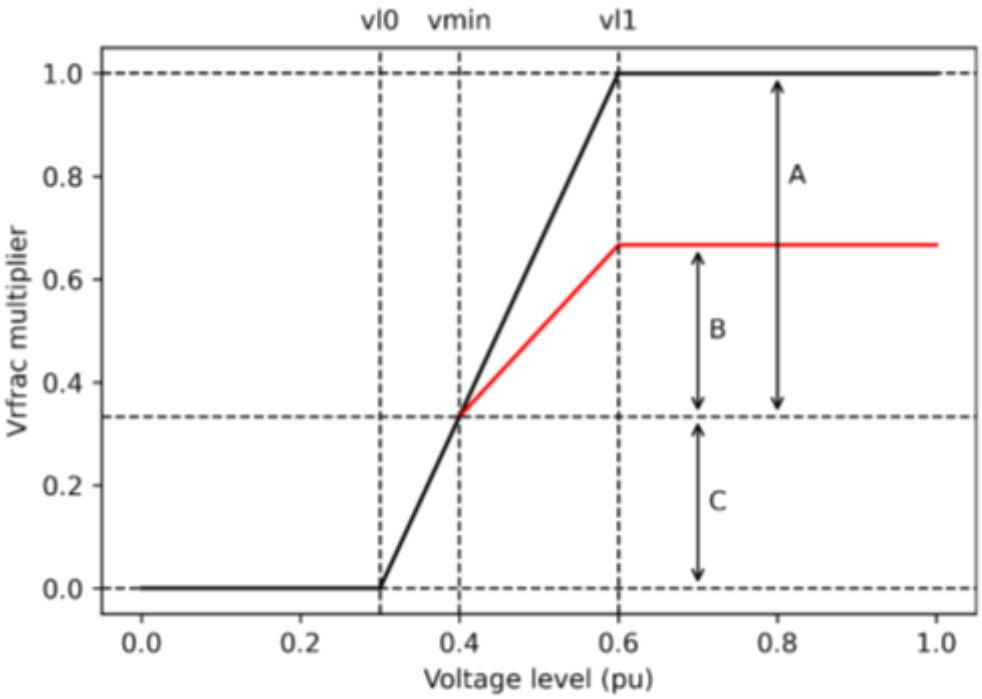

[33] Power and Energy, Analysis, Consulting and Education (PEACE®). Proposal for DER_A model, June 2019, at https://www.wecc.org/Reliability/DER_A_Final_061919.pdf.

The following parameters, shown in Figure 13, are inputs to the DPV model and together define the proportion of inverters that recover (not disconnect) following a voltage notch/sag:

- vl1 – the voltage at which inverters begin to disconnect (if voltage at a bus is below this level for more than tvl1)
- vl0 – (together with vl1) defines the gradient of the voltage tripping profile and defines the voltage below which all inverters at a bus disconnect if the tvl0 timer is exceeded (if voltage stays below vl0 for greater than tvl0, the output of the block will always remain at zero).
- Vrfrac – gives the fraction of inverters at a bus that recover (do not disconnect) following the voltage notch/sag, defined as:

$$vrfrac = \frac{B}{A} \quad (1)$$

To read Figure 13, assume that the pre-fault voltage is 1.0 pu and the proportion of inverters connected is 1.0. The voltage reduces to the minimum voltage (vmin) as the fault occurs. This can be visually represented by following the black line.

After the minimum voltage occurs, the recovery begins. If vl1 has not been exceeded for the time out value tvl1 (low voltage cut out timer), the recovery follows the black curve back to the original starting position. In this scenario, all the DPV recovers, and no inverters have disconnected.

In contrast, the model follows the red curve if voltage is below vl1 for more than the tvl1 timer. The diagram indicates that this results in a proportion of DPV inverters disconnecting following the disturbance (a lower proportion of inverters remaining connected post-disturbance).

Determining vrfrac block parameters from bench testing

In the DPV model, vl1 was set to 0.9 pu. This is because some inverters were observed to start to disconnect in voltage notch tests for voltage sags at 0.9 pu or deeper (as shown in Table 9 and Table 10).

Having selected a value for vl1, vrfrac and vl0 are co-dependent parameters that determine the proportion of inverters that recover following a voltage sag.

Referring to Figure 13, the output of the vrfrac block after voltage has recovered following a voltage sag where tvl1 is exceeded can be represented as:

$$vrfrac\ multiplier = B + C \quad (1)$$

Also from the diagram:

$$B = vrfrac \times A$$

$$C = 1 - A$$

A is simply the proportional distance traversed travelled down the black line, which can be written as:

$$A = \frac{vl1 - vmin}{vl1 - vl0}$$

Incorporating this into equation (1) yields:

$$vrfrac\ multiplier = vrfrac \times \frac{vl1 - vmin}{vl1 - vl0} + \frac{vmin - vl0}{vl1 - vl0}$$

Which can be refactored into a linear expression, such that:

$$vrfrac\ multiplier = m \times vmin + d$$

Where:

$$m = \frac{1 - vrfrac}{vl1 - vl0}$$

$$d = \frac{vrfrac \times vl1 - vl0}{vl1 - vl0}$$

This was used to estimate values of vl0 from estimates of vrfrac, based on the UNSW bench tests, as outlined below.

Figure 14 shows the proportion of the UNSW bench testing sample that exhibited ride-through behaviour for voltage sag/notch tests of varying depth, as summarised in **Table 9** and **Table 10**. The results are shown only for inverters under the 2015 standard, but a similar process was undertaken for inverters under the 2005 standard. The dotted line shows the trendline of best fit to the bench test data (constrained so that at vl1 = 0.9 pu, 100% of inverters ride-through, based on observations from the bench testing).

Figure 14 Voltage sag/notch test results (2015 standard inverters)

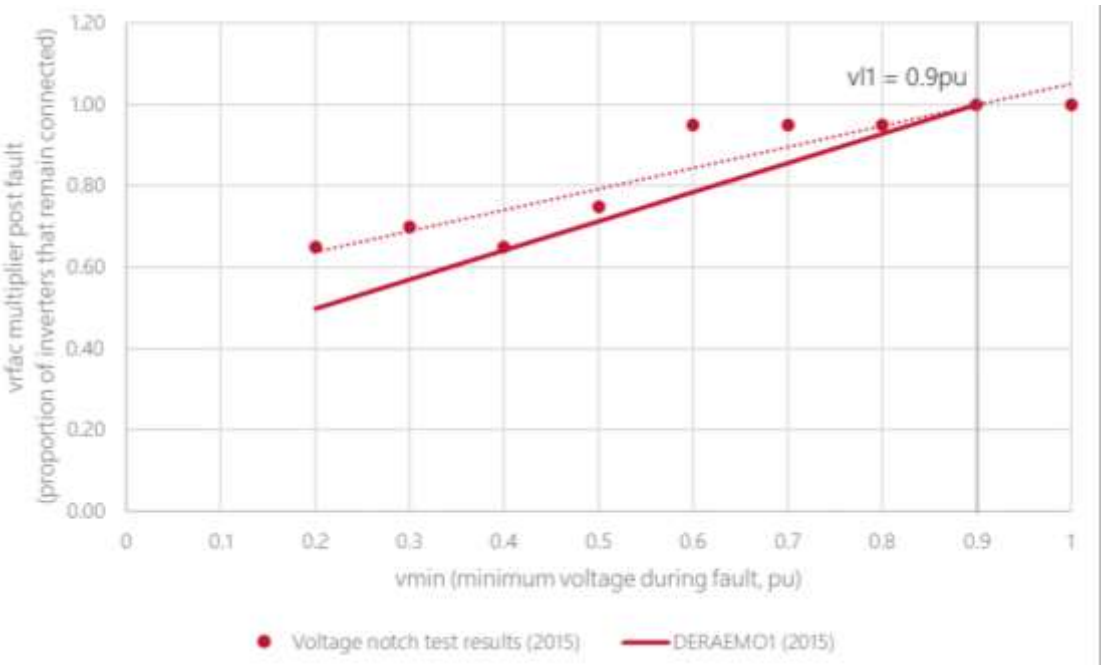

Table 11 Trendline parameters from bench test results

	2015 bench tests trendline	2005 bench tests trendline
m (gradient)	0.60	1.56
d (intercept)	0.44	-0.40

To determine initial values, vrfrac was set to the average proportion of inverters that rides through, averaged across all voltage bench tests:

AS/NZS4777.2:2015 inverters: vrfrac = 71%

AS/NZS4777.3:2005 inverters: vrfrac = 63%

An initial starting point value for vl0 was then calculated based on the fitted trendlines from the voltage notch tests (Table 11 and Figure 14), based on vl1 = 0.9 pu and the following relationship:

$$vl0 = vl1 - \frac{1 - vrfrac}{m} \quad (2)$$

However, validation studies in historical disturbances (as outlined in Section 6) indicated that these initial estimates for vl0 and vrfrac (for inverters installed under both the 2005 and 2015 standards) resulted in underestimation of DPV loss. Whilst keeping the vrfrac parameter constant, vl0 was tuned based on field measurements to determine the final set of DPV model parameters. An increased value of vl0 produced DPV loss estimates that were closer to field measurements; this may be because the inverters tested are not a sufficiently representative sample. In future model revisions, with further bench testing data available from a larger sample, it may be possible to more accurately estimate these parameters based on test results, suitably matching with field measurements.

Figure 15 illustrates the final parameters selected for the vrfrac block, for each of the 2005 and 2015 inverters. In the final model, weighted average blended values are applied for each parameter, depending on the relative installed capacities of 2005 and 2015 installed at the time of the disturbance.

Consider the behaviour of the 2005 inverters illustrated in Figure 15. Before the fault, the voltage is assumed to be 1.0 pu, and the vrfrac multiplier is 1 (indicating all inverters are connected). When a disturbance occurs, the voltage decreases linearly down to vmin (0.6 pu in the purple example). As shown, a vmin value of 0.6 pu is below vl0, resulting in Vrfrac proportion ($vrfrac\ multiplier = vrfrac = 0.62$) remaining connected at the end of the disturbance (as long as tvl0 is not exceeded, causing the output of the model to always remain at zero). In contrast, for the 2015 inverters a vmin of 0.6 pu does not fall below vl0, so a higher proportion of inverters remain connected post-disturbance ($y = 0.78$), when compared with inverters installed under the 2005 standard.

Figure 15 Finalised Vrfrac block parameters

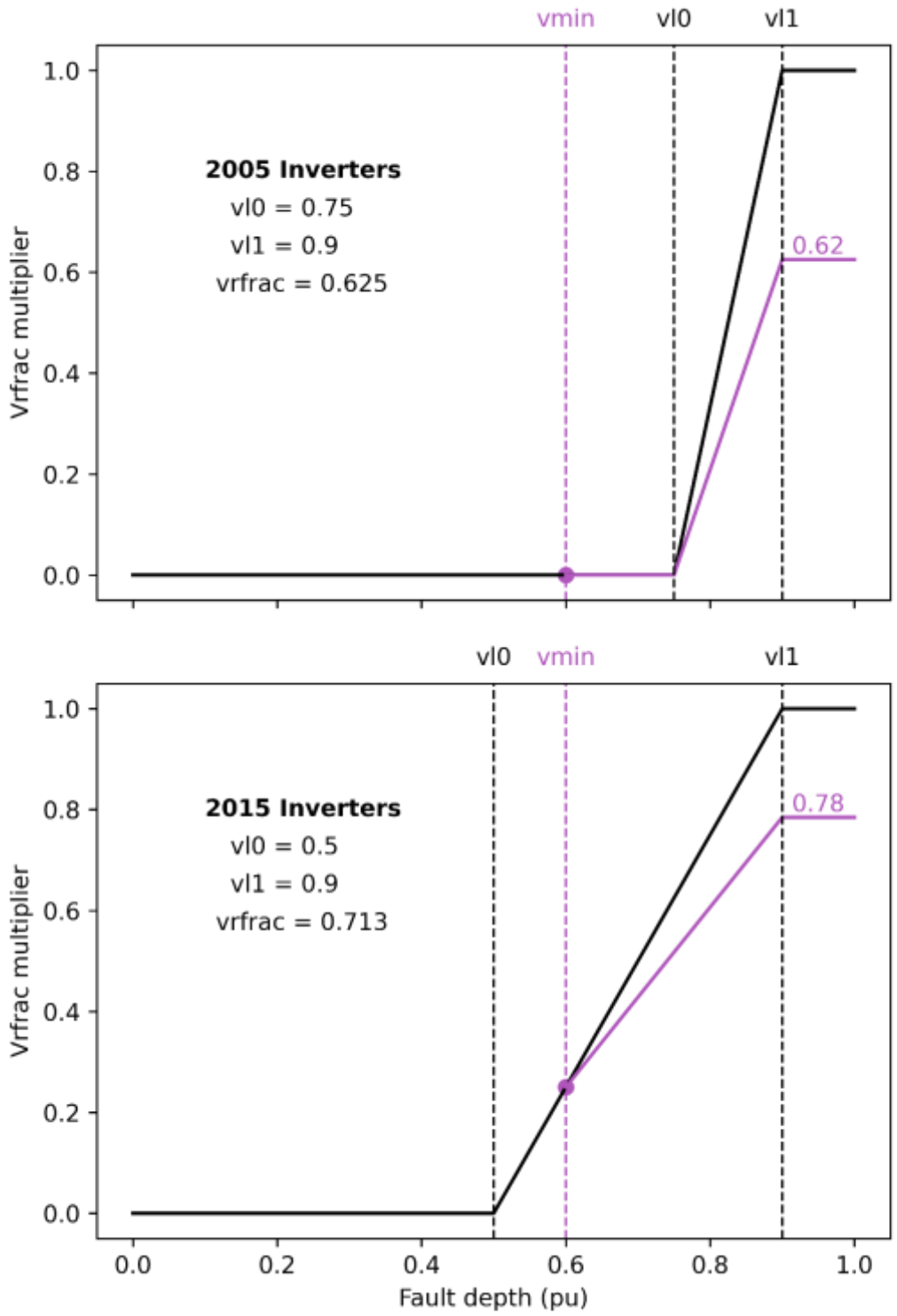

Parameters directly informed by inverter bench testing

Table 12 summarises these and other parameters that were directly informed by inverter bench testing.

Table 12 Parameters determined from inverter bench testing

Parameter	Description	Average value		UNSW test used[A]
		2005 standard	2015 standard	
Imax	Maximum converter current	1.19 pu	1.2 pu	Voltage Ramp 230 V to 160 V 10 s or Voltage Notch 230 V to 50 V 0.1 s [B]
vl1	Second breakpoint for low voltage cut-out	0.9 pu		Voltage Sag tests from 0.9 pu for 120 ms to 0.2 pu for 120 ms
tvl1	Low voltage cut-out timer corresponding to voltage vl1	0.027 s	0.037 s	Voltage Notch 230 V to 50V 0.1 s
tvl0	Low voltage cut-out timer corresponding to voltage vl0	1.58 s	1.77 s	Voltage Ramp 230 V to 160 V 10 s
tvh1	High voltage cut-out timer corresponding to voltage vh1	1.94 s	1.87 s	Voltage Step 230 V to 260 V [C]
tvh0	High voltage cut-out timer corresponding to voltage vh0	0.88 s	0.16 s	Voltage Notch 230 V to 270 V 7 s
vrfrac	Fraction of inverters that recover their output following a fault	0.625	0.713	Voltage Sag tests from 0.9 pu for 120 ms to 0.2 pu for 120 ms
tfl13	Low frequency cut-out timer corresponding to frequency fl13 (47 Hz)	- [D]	1.65 s	Frequency Step 50 Hz to 45 Hz
tfh13	High frequency cut-out timer corresponding to frequency fh13 (53 Hz)	- [D]	0.15 s	Frequency Step 50 Hz to 55 Hz
Frac_RoCoF_1	Fraction for RoCoF trip 1	2 of the 24 inverters tested tripped under high RoCoF. RoCoF trip fractions are based on installed capacity of these manufacturer's inverters for each region.		Frequency Ramp (0.4 Hz/s)
Frac_RoCoF_2	Fraction for RoCoF trip 2			Frequency Ramp (1 Hz/s)
Frac_RoCoF_3	Fraction for RoCoF trip 3			Frequency Ramp (4 Hz/s)
tRoCoF_1	Pick up time for RoCoF trip 1	1.41 s		Frequency Ramp (0.4 Hz/s)
tRoCoF_2	Pick up time for RoCoF trip 2	0.83 s		Frequency Ramp (1 Hz/s)
tRoCoF_3	Pick up time for RoCoF trip 3	0.29 s		Frequency Ramp (4 Hz/s)

A. UNSW, Bench Testing of Rooftop PV Inverters, http://pvinverters.ee.unsw.edu.au/.
B. Where a voltage notch test resulted in momentary cessation or complete disconnection, the voltage ramp test was considered appropriate. Similarly, where a voltage ramp test resulted in a current reduction or complete disconnection, the voltage notch test was considered appropriate.
C. The tvh1 parameter for Inverter 24 could not be determined as the results of the Voltage Step 230 V to 260 V test for Inverter 24 were not available at the time of parameter derivation.
D. During initial parameter determination, results from the 2016 DPV Frequency Trip Survey conducted by AEMO were used to inform over/under-frequency trip parameters for inverters installed under the 2005 standard. Further data from bench-testing conducted by UNSW subsequently indicated that all inverters on both the 2005 and 2015 standards tripped before 47 Hz / 53Hz (the 13th under/over-frequency setpoints). This parameter was therefore set to zero for inverters installed under the 2005 standard. Report containing survey findings available at https://aemo.com.au/-/media/files/initiatives/der/2021/capstone-report.pdf.

The source data used to determine the parameters in Table 12 is shown in **Table 13**. The complete test results can be viewed on UNSW's website[34].

[34] See UNSW. Addressing Barriers to Efficient Renewable Integration – Bench Testing of Rooftop PV Inverters, at http://pvinverters.ee.unsw.edu.au/.

Table 13 UNSW Inverter testing – source data used to determine DERAEMO1 Parameters

Inverter #	Standard	Imax	Trip Time (s)								
			tvl1	tvl0	tvh1	tvh0	tfl13	tfh13	tRoCoF_1	tRoCoF_2	tRoCoF_3
Inverter 1	2015	1.09	0.030	1.77	N/A	0.17	1.83	0.04	N/A	N/A	N/A
Inverter 1	2005	1.00	0.022	2.53	1.96	0.02	1.86	1.86	N/A	N/A	N/A
Inverter 2	2015	1.33	0.100	2.14	N/A	0.21	1.84	0.03	N/A	N/A	N/A
Inverter 3	2015	1.22	N/A	2.41	1.95	0.14	1.45	0.17	N/A	N/A	N/A
Inverter 4	2015	1.00	0.020	1.10	N/A	N/A	N/A	0.09	N/A	N/A	N/A
Inverter 5	2015	1.29	N/A	2.00	1.83	0.17	1.41	0.14	1.41	0.43	0.21
Inverter 6	2015	1.22	N/A	1.87	1.98	0.18	1.84	0.04	N/A	N/A	N/A
Inverter 6	2005	1.15	0.030	2.11	1.95	1.97	1.82	1.82	N/A	N/A	N/A
Inverter 7	2015	1.30	N/A	1.64	N/A	0.17	1.94	0.14	N/A	N/A	N/A
Inverter 8	2005	1.09	0.040	2.10	N/A	1.86	1.54	0.52	N/A	N/A	N/A
Inverter 9	2005	1.50	N/A	0.75	1.68	0.20	1.61	0.18	N/A	N/A	N/A
Inverter 10	2015	1.10	0.010	0.39	N/A	N/A	1.63	0.11	N/A	N/A	N/A
Inverter 12	2015	1.02	0.040	0.93	N/A	N/A	1.54	0.06	N/A	N/A	N/A
Inverter 13	2015	1.30	N/A	1.90	1.95	0.15	1.42	0.15	N/A	N/A	N/A
Inverter 14	2005	1.15	N/A	2.11	3.32	0.03	1.85	0.29	N/A	1.22	0.37
Inverter 15	2005	1.04	0.020	N/A	1.58	0.12	1.54	0.06	N/A	N/A	N/A
Inverter 16	2015	1.20	N/A	1.34	N/A	N/A	1.15	0.95	N/A	N/A	N/A
Inverter 17	2015	1.30	N/A	1.67	1.67	0.18	1.67	0.10	N/A	N/A	N/A
Inverter 18	2005	1.10	0.030	0.19	1.56	N/A	1.59	0.08	N/A	N/A	N/A
Inverter 19	2015	1.15	N/A	1.85	N/A	0.15	1.94	0.15	N/A	N/A	N/A
Inverter 20	2015	1.03	0.024	3.04	N/A	0.17	1.61	0.08	N/A	N/A	N/A
Inverter 21	2005	1.12	0.020	0.28	1.56	N/A	1.59	0.07	N/A	N/A	N/A
Inverter 22	2015	1.60	N/A	1.92	N/A	0.18	1.94	0.14	N/A	N/A	N/A
Inverter 23	2015	1.11	N/A	1.35	N/A	0.05	1.51	0.04	N/A	N/A	N/A
Inverter 24	2005	1.53	N/A	2.60	N/A	1.96	1.80	N/A	N/A	N/A	N/A
Average – AS/NZS477.3: 2005		1.19	0.027	1.58	1.94	0.88	1.69	1.20	N/A	1.22	0.37
Average – AS/NZS4777.2: 2015		1.20	0.037	1.77	1.87	0.16	1.65	0.15	1.41	0.43	0.21

Notes: N/A means the inverter did not trip in the relevant test. For cut-out timers, only inverters that did trip were considered. All inverters that reduced power output by >95% were considered to have tripped. For the voltage sag tests, inverters that did not reduce power output to zero for the duration of the fault are considered not to have tripped. If trip time was greater than 4s, the inverters was considered to have not tripped, and was not used to inform trip delay times.

2.3.5 Validation against Energy Queensland HSM data

Energy Queensland provided high speed data at the 11 kV level from faults observed in its distribution network. This was used to confirm the speed of disconnection of inverters, confirming parameters determined from the UNSW inverter bench testing.

Two events were analysed: one during a high DPV generation period, and one during a low DPV generation period. Energy Queensland data indicated that at the time of the disturbance, 58% of residential homes on this

residential feeder had DPV systems installed. There was 2.6 MW of PV installed at the time of the fault, of which 0.7 MW was installed after October 2016 under AS/NZS4777.2:2015.

A 2P fault on the feeder is shown in **Figure 16** and **Figure 17**. This illustrates a typical combined load and DPV response for a period with a medium PV capacity factor (~31% at the time of this fault, estimated based on AEMO's ASEFS2 solar forecasting system[35]). The post-fault active power increased by 100 kW (35.7%), which indicates disconnection of DPV.

Figure 16 11 kV feeder 2P fault 12/04/2018 10:09:51 (Voltages)

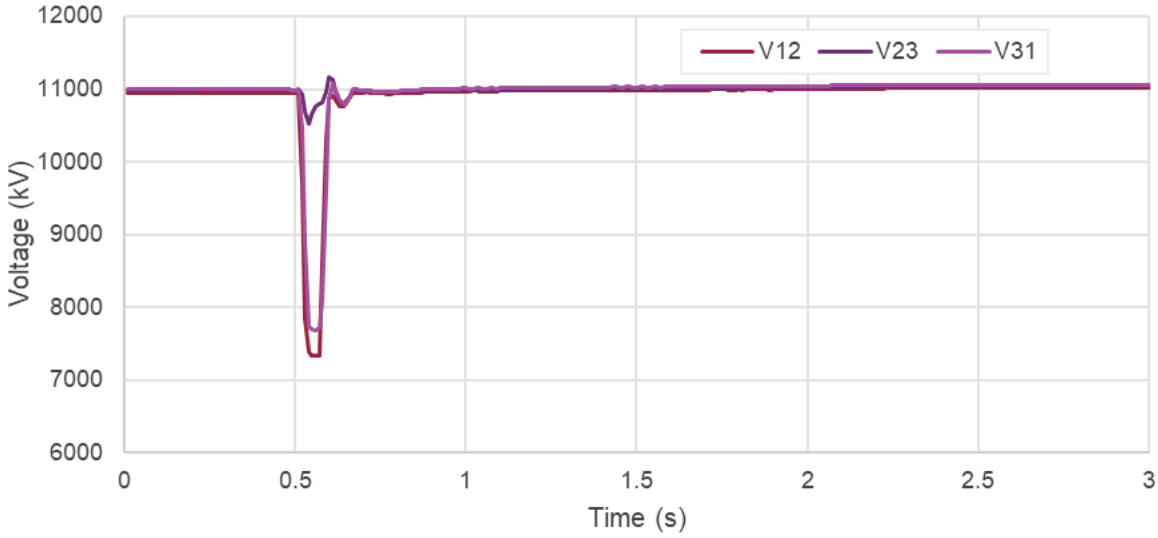

Figure 17 11kV feeder 2P fault 12/04/2018 10:09:51 (Active/Reactive Power)

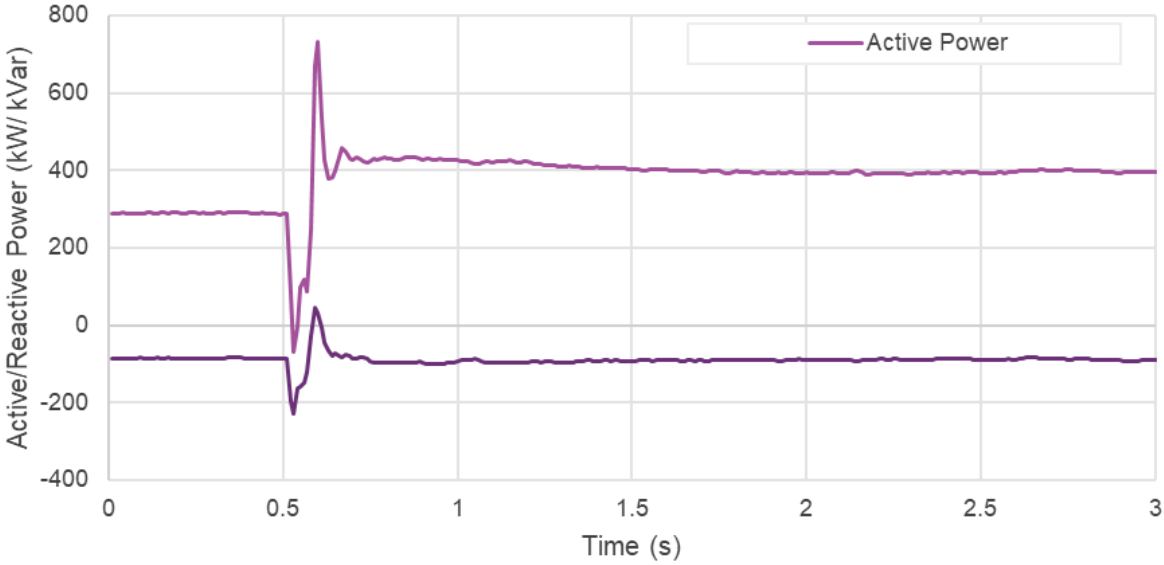

[35] AEMO, Australian Solar Energy Forecasting System, https://aemo.com.au/en/energy-systems/electricity/national-electricity-market-nem/nem-forecasting-and-planning/operational-forecasting/solar-and-wind-energy-forecasting/australian-solar-energy-forecasting-system.

The fast disconnection behaviour demonstrated in this figure validates the findings from the UNSW inverter bench test results. From the UNSW study results, the DER disconnection parameter tvl1 was selected to be 27 ms for 2005 inverters and 37 ms for the 2015 inverters. Based on this real-life case study, DPV disconnection is observed to occur within his timeframe.

2.3.6 Parameters informed by observed DPV behaviour during historical disturbances

A number of model parameters were informed by field measurements from thousands of distributed PV devices in the NEM, based on datasets provided to AEMO by Solar Analytics. The analysis of these datasets is described in AEMO's report "Behaviour of distributed resources during power system disturbances"[36].

vl0 (pu): Undervoltage trip gradient thresholds

As discussed in Section 2.3.4, the parameters vl1 and vl0 define the under-voltage trip function for the DPV model. These define the fraction of DPV that recovers (does not disconnect) after an under-voltage event, based on the depth of the voltage sag. The vl0 parameter was tuned to reflect the observed DPV disconnection for the disturbance events, and validated against disconnection estimates based on data from Solar Analytics.

Ddn (pu): reciprocal of droop for over-frequency conditions

Ddn is the over-frequency control gain which defines the controlled over-frequency curtailment of the DPV model. Over-frequency curtailment is a requirement for inverters installed after AS/NZS4777.2:2015. However, during several over-frequency events AEMO has observed that many inverters do not deliver the over-frequency curtailment requirement[37,38,39]. On average across these disturbances, AEMO identified that only 30% to 50% of the 2015 systems correctly provided over-frequency droop response as specified in the 2015 standard. A further 30% to 50% of DPV systems did not provide the required frequency response, and instead continued to generate uninterrupted without reducing output. By tuning the Ddn parameter, the over-frequency curtailment gain has been calculated as per the requirements in the 2015 standard (28.6), multiplied by 35% (giving a final value for Ddn of 10). This produces model behaviour in the range evidenced in the Solar Analytics data, as outlined in Section 7.

2.3.7 Volt-var representation

The DER_A model features a reactive power-voltage control loop, which could be applied to represent the volt-var response of inverters (defined in the AS/NZS4777.2 standards). However, for this release of the model the net reactive power-voltage control loop contribution to the dynamic behaviour of the model has been zeroed out, by setting the gains of the voltage control loop (Kqv1, Kqv2) to zero.

[36] AEMO (May 2021) Behaviour of distributed resources during power system disturbances, at https://aemo.com.au/-/media/files/initiatives/der/2021/capstone-report.pdf?la=en&hash=BF184AC51804652E268B3117EC12327A.

[37] AEMO. Final Report – Queensland and South Australia system separation on 25 August 2018, January 2019, at https://aemo.com.au/-/media/files/electricity/nem/market_notices_and_events/power_system_incident_reports/2018/qld---sa-separation-25-august-2018-incident-report.pdf.

[38] AEMO. Final Report – South Australia and Victoria Separation Event on 16 November 2019, November 2020, at https://aemo.com.au/-/media/files/electricity/nem/market_notices_and_events/power_system_incident_reports/2019/final-report-sa-and-victoria-separation-event-16-november-2019.pdf.

[39] AEMO. Final Report – Victoria and South Australia Separation Event on 31 January 2020, November 2020, at https://aemo.com.au/-/media/files/electricity/nem/market_notices_and_events/power_system_incident_reports/2020/final-report-vic-sa-separation-31-jan--2020.pdf.

This has been done for several reasons:

1. Inverter bench testing has shown that the volt-var response of inverters, once activated, takes a minimum of several seconds to respond. There is little evidence to indicate inverters will provide voltage support during a fault (which may have a duration of only ~100ms). The reactive power-voltage control loop in the DER_A model does not include a time constant that would allow this observed slower speed of response to be represented accurately. This means the present form of the model would likely over-state the voltage support provided by installed DPV during a typical fault.
2. Distributed PV inverters are connected at the street level. There is typically a large amount of impedance between the street-level connected inverter, and the transmission network. As a result, aggregate reactive power injection at the street level is likely to have a limited effect at the transmission network level (where severe faults occur). Since the DER_A model is connected at the transmission bus, the model would likely overstate the contribution of DPV to supporting voltages at the transmission level.
3. Field measurements indicate very low compliance in delivery of volt-var behaviour (70-80% of inverters appear to not deliver this response as specified)[40].

In future revisions of the model, volt-var response could be reinstated in some capacity. What may be important to represent is how reactive power priority injection can trade off against active power injection when inverters hit their maximum current injection limit during a fault. The aggregate reduction in active power during fault conditions may be visible at the transmission level and may need to be represented in future model revisions.

2.3.8 Frequency trip parameters

Inverters installed under the 2005 standard

Survey of frequency trip settings for inverters

In 2016, AEMO surveyed DPV manufacturers about their default frequency trip settings for inverters installed under the 2005 standard[41]. This survey accounts for 45% of the DPV capacity installed in the NEM under the 2005 standard.

These frequency trip settings were used to set 12 (of 13) under-frequency trip stages (fl2 to fl13, frac_fl2 to frac_fl13, tfl2 to tfl13), and 11 (of 13) over-frequency trip stages (fh3 to fh13, frac_fh3 to frac_fh13, tfh3 to tfh13) for inverters under the 2005 standard.

Additional trip bands based on field observations

Figure 18 shows field measurements of DPV inverters during power system disturbances, based on datasets provided by Solar Analytics. This data suggests that some frequency tripping occurs between 49 Hz ≥ f ≤ 51Hz[42]. This could reflect inverters that were not included in those surveyed or inverters that have tripped due to installation errors or maloperation of other inverter protection controls.

[40] CitiPower/Powercor (7 October 2021) Re. Governance of distributed energy resources technical standards - ERC0319, https://www.aemc.gov.au/sites/default/files/documents/211007_submission_by_citipower_powercor_and_united_energy.pdf.

[41] AEMO (April 2016) Response of existing PV inverters to frequency disturbances, https://aemo.com.au/-/media/files/electricity/nem/security_and_reliability/reports/response-of-existing-pv-inverters-to-frequency-disturbances-v20.pdf.

[42] AEMO (May 2021) Behaviour of distributed resources during power system disturbances, https://aemo.com.au/-/media/files/initiatives/der/2021/capstone-report.pdf.

Several additional frequency trip bands were included in the model, to replicate these findings. The additional frequency trip bands, which include one under-frequency trip stage (fl1, tfl1, frac_fl1) and two over-frequency trip stages (fh1 to fh2, tfl1 to tfl2, frac_fh1 to frac_fh2), are shown in **Table 14** (and overlayed on the frequency tripping field measurements in Figure 18).

- The parameter frac_fl1 represents the proportion of DPV that disconnects on under-frequency below 49.6 Hz. This was set to 2% for inverters under the 2005 standard and 1% for inverters installed under the 2015 standard, based on field measurements shown in Figure 18.
- For over-frequency, frac_fh1 and frac_fh2 represent the proportion of DPV that disconnects for over-frequency above 50.5 Hz and 50.8 Hz respectively. These were set to the values shown in Table 14 and largely represent the orange and purple trendline for 2005 and 2015 inverters in Figure 18, respectively.

During the validation process, it was found that the DPV model was underestimating the percentage of inverters tripping on under-frequency (49.3 Hz) and over-frequency (51.5 Hz and 51.8 Hz); these additional trip parameters allowed for more accurate representation of frequency-based trip behaviour.

Figure 18 The proportion of disconnections depending on the minimum or maximum frequency reached during frequency excursion

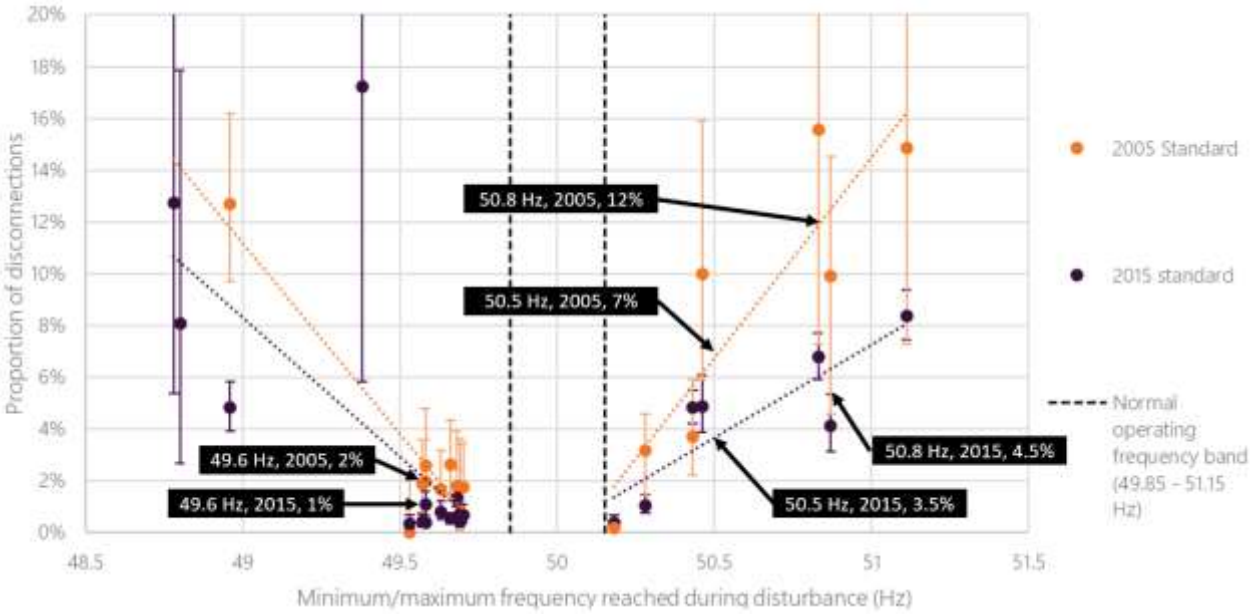

Table 14 Additional DPV frequency disconnection assumptions applied in DERAEMO1

		Parameter	Parameters applied (2005 standard)	Parameters applied (2015 standard)
Under-frequency Trip 1	Trip frequency	fl1	49.6 Hz	49.6 Hz
	Trip timer	tfl1	1.9 s	1.9 s
	Fraction of DPV that trips	frac_fl1	2%	1%
Over-frequency Trip 1	Trip frequency	fh1	50.5 Hz	50.5 Hz
	Trip timer	tfh1	1.9 s	1.9 s
	Fraction of DPV that trips	frac_fh1	7%	3.5%
Over-frequency Trip 2	Trip frequency	fh2	50.8 Hz	50.8 Hz
	Trip timer	tfh2	1.9 s	1.9 s
	Fraction of DPV that trips	frac_fh2	5% (12% cumulative)	1% (4.5% cumulative)

Inverters installed under the 2015 standard

AS/NZS4777.2:2015 requires that inverters remain connected for frequency disturbances within 47-52Hz. However, field measurements (shown in Figure 18) suggest that some inverters installed under the 2015 standard do disconnect in frequency disturbances. As shown in Figure 18, the average disconnection rate in frequency disturbances appears to be approximately half that of inverters installed under the 2005 standard.

The CER has been investigating the installation compliance level of DPV inverters since 2011 and has observed a low compliance level in installations from 2011 to 2018[43]. More recent investigations have focused on the compliance levels for inverter protection settings, including the selection of the correct standard with respect to

[43] Australian National Audit Office (ANAO). 2018. Administration of the Renewable Energy Target (see Figure 4.1), at https://www.anao.gov.au/work/performance-audit/administration-renewable-energy-target.

the installation date. The most recent inspection update[44] shows an average regional non-compliance level of ~18% of the more than 26,000 DPV installed fleet audited in the NEM. The audited inverters account for an estimated 130 MW[45] of installed capacity in the NEM.

To represent these findings, the frequency trip proportions were halved and applied to inverters installed under the 2015 standard (for all frequency trip stages except those shown in Table 14. This is discussed in more detail in AEMO's report on DER behaviour in disturbances[42].

[44] CER. 2020. Small-scale Renewable Energy Scheme inspections – Inspection Update No 19, at http://www.cleanenergyregulator.gov.au/DocumentAssets/Pages/Inspections-Update-No-19.aspx.

[45] 26,000 inverters in the NEM * 5kW average capacity = 130 MW.

3 CMLD model development process

3.1 Developing a Composite Load Model

AEMO, NSPs and other stakeholders in the NEM conducting power system studies have used a traditional polynomial static load (ZIP) model to represent the majority of NEM load for over 20 years. Load composition has changed considerably over this time, and more sophisticated load models are now available.

A review of international literature identified that much of the recent leading work on composite load models had been conducted by the North American Electric Reliability Corporation (NERC) and the Electric Power Research Institute (EPRI). They recommended the Composite Load (CMLD) model developed by the Western Electricity Coordinating Council's (WECC) Modelling and Validation Working Group[46]. Adoption of the CMLD model is generally considered industry best practice[47,48].

The model structure is shown in **Figure 19**[49]. It consists of six load components at the end of a feeder equivalent circuit, which is represented by a series impedance and shunt compensation. It is intended to emulate various load components' aggregate behaviour. It includes three three-phase (3P) induction motor models (Motor A, B and C), a single-phase (1P) capacitor-start motor performance model (Motor D), static load components (constant current and constant impedance), and a power electronic load model (constant active and reactive power).

Figure 19 The CMLD model structure

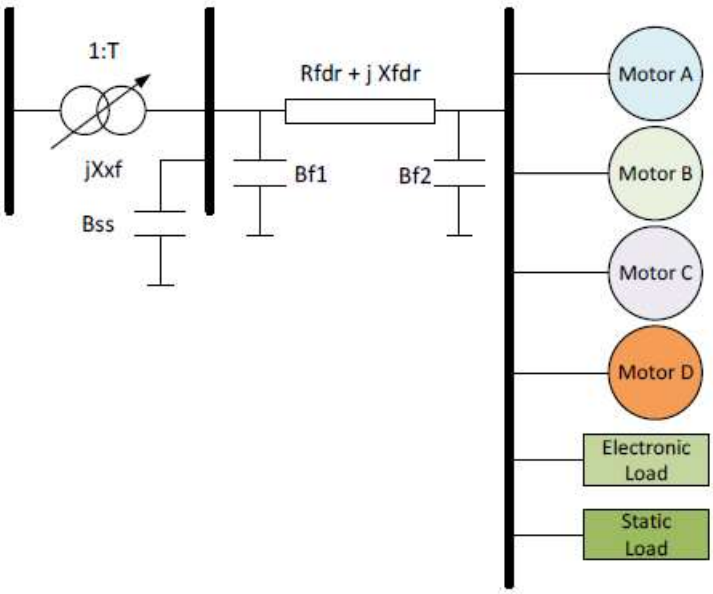

[46] WECC. Dynamic Composite Load Model Specifications, January 2015, at http://home.engineering.iastate.edu/~jdm/ee554/WECC%20Composite%20Load%20Model%20Specifications%2001-27-2015.pdf.

[47] NERC Reliability Guideline – Developing Load Model Composition Data, March 2017, at https://www.nerc.com/comm/PC_Reliability_Guidelines_DL/Reliability_Guideline_-_Load_Model_Composition_-_2017-02-28.pdf.

[48] NERC Technical Reference Document – Dynamic Load Modelling, December 2016, at https://www.nerc.com/comm/PC/LoadModelingTaskForceDL/Dynamic%20Load%20Modeling%20Tech%20Ref%202016-11-14%20-%20FINAL.PDF.

[49] Power and Energy, Analysis, Consulting and Education (PEACE®). Developing Dynamic Load Models for the Australian Eastern Interconnected System, June 2019, at https://aemo.com.au/-/media/files/initiatives/der/2020/aemo-load-modeling-062819-final.pdf?la=en.

The details of each component are summarised in **Table 15**[50].

Table 15 Components of the CMLD Model

Motor A	Motor A represents 3P induction motors with high locked-rotor torque, low inertia (H = 0.1 s) and driving constant torque loads. This motor type is common in commercial/industrial air conditioning compressors and refrigeration systems. The typical rating for small motors is between 4 to 11 kW and 150 to 370 kW for large motors.
Motor B	Motor B represents 3P induction motors with high inertia (H = 0.25 to 1.0 s) driving loads whose torque is proportional to speed squared. This motor type is common in commercial ventilation fans and air-handling systems. The typical rating is 4 to 19 kW.
Motor C	Motor C represents 3P induction motors with low inertia (H = 0.1 to 0.2 s) driving loads whose torque is proportional to speed squared. This motor type is common in commercial water circulation pumps in central cooling systems. The typical rating is 4 to 19 kW.
Motor D	Motor D is a specially developed performance model intended to represent single-phase (1P) compressors of residential air-conditioning loads in the United States of America, based on laboratory tests of such devices. A constant torque load characteristic and minimal inertia make these motors prone to stall. This motor type is common in 1P residential and light commercial refrigerator compressor motors in Australia. The typical rating is between 2 to 4 kW.
Power Electronic Load	Power electronic load represents consumer electronics (computers, televisions), appliances (dishwasher), office equipment, and variable frequency drives (VFDs)[51] used in commercial and industrial settings.
Static Load	Static load represents the remainder of the unclassified aggregate loads, including constant impedance loads such as incandescent lighting.
Distribution transformer	A representation of the distribution transformer (jXxf) and an on-load tap-changer (OLTC) if an OLTC is present.
Substation shunt capacitors	A representation of any explicit substation shunt capacitors (Bss) if they are present.
Equivalent distribution feeder	A single equivalent representation of distribution feeders of the actual end-use loads (Rfdr + jXfdr). The feeder compensation (Bf1 and Bf2) are not user inputs but are instead calculated internally by the model to balance out the reactive losses on the feeder to ensure that the net load MW/MVar at the transmission bus matches that in the power flow case.

3.2 Approach overview

A "bottom-up" methodology was applied to the development of the load model parameters, separately estimating two types of parameters in the CMLD model:

- **Load composition parameters** give the percentage of load in each category (Motor A, B, C, D, power electronics and static load) in each region in a particular snapshot of the power system. This was estimated using various data sources on load composition to estimate the breakdown of total customer load in a region in a specific time interval (depending on the time of day and season).
- **Load behaviour parameters** define the behaviour of each of the load categories during power system disturbances (for example, these parameters determine tripping and stalling behaviours for the CMLD motors). These parameters were applied identically for all NEM regions in all time periods.

[50] The NERC 'Dynamic Load Modelling Technical Reference Document' outlines the components of the CMLD model. AEMO have converted the typical motor ratings in Table 15 to SI units. NERC Technical Reference Document – Dynamic Load Modelling, December 2016, at https://www.nerc.com/comm/PC/LoadModelingTaskForceDL/Dynamic%20Load%20Modeling%20Tech%20Ref%202016-11-14%20-%20FINAL.PDF.

[51] The NERC load modelling task force (LMTF) has indicated it plans to separate VFDs into their own load category in the future. These updates will be incorporated by AEMO when available. Please refer to the following reference for details: https://www.wecc.org/Administrative/Kosterev - LMTF Update_August 2020.pdf.

Further elaboration on the determination of each parameter set is outlined in the following sections.

3.3 Load composition parameters

A bottom-up estimate of load composition in each region was developed by first estimating the breakdown of load into residential, commercial, and industrial loads, then further breaking down each category into various sectors and load types, then estimating the proportion of Motor A, B, C, D, power electronics and static loads within each load sector and type using "Rules of Association" (RoA).

The RoA provides a proportional breakdown of load into the categories in Table 15 by sector class (such as “retail shopping centres”) and end-use category (such as “exhaust fans”). Some RoA assigns 100% of the end-use load for the sector class or end-use load type to a single component (e.g. residential microwaves are assigned to the power electronics component) while others decompose the end-use load to multiple components (e.g. retail cooling towers are assigned 60% to Motor B and 40% to the power electronics component).

This bottom-up decomposition process was done individually for each NEM region, incorporating variation by time of day and season. An illustration for a particular time interval in South Australia is illustrated in **Figure 20**[52].

[52] ‘Other’ category for Residential End-Use Loads is comprised of loads less than or equal to 1% of total end-use, such as Dishwashers and Freezers. ‘Other’ category for Commercial End-Use Loads is comprised of loads less than or equal to 2% of total end-use, such as Onsite Transportation and Refrigeration and Process Cooling.

Figure 20 Illustration of bottom-up development of CMLD model composition (example for South Australia for Sunday 24 January 2021, 4:30-5:00 pm)

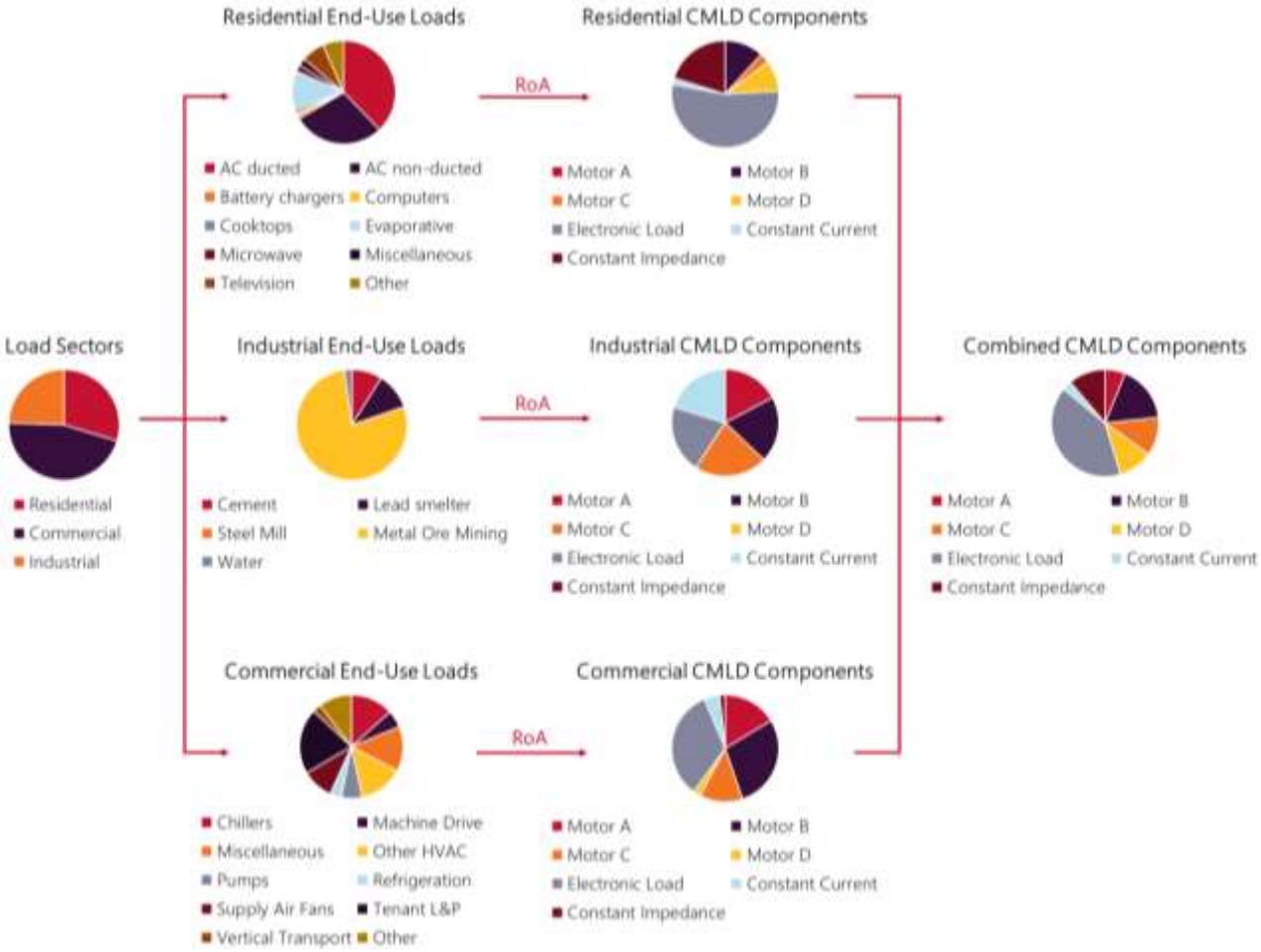

An overview of the data sources used for this process is summarised in **Table 16**.

Table 16 Data sources used to inform load composition parameters in the CMLD model

Data	Source
Residential, commercial and industrial load for each region	The 2020 AEMO Electricity Statement of Opportunities (ESOO)[53] provides an estimated breakdown into these three load sectors for the reference year 2020, for each NEM region. Due to the varying level of data available to AEMO, ESOO load estimates were then broken down to seasonal and hourly estimates for the commercial sector, seasonal estimates for the residential sector, and kept at an annual basis for the industrial sector.
Residential load breakdown	The Residential Baseline study[54], prepared by the Department of the Industry and Science, released in 2015, provides detailed appliance specific energy consumption in typical Australian homes. Estimates are provided for each NEM region, for summer and winter. Some adjustments were made to account for likely changes in residential load composition since 2015, detailed in the Rules of Association description below. An updated Residential Baseline study is expected to be released in 2023 and may be used to inform future updates to the residential RoA.

[53] At https://aemo.com.au/-/media/files/electricity/nem/planning_and_forecasting/nem_esoo/2020/2020-electricity-statement-of-opportunities.pdf?la=en.

[54] Energy Consult. Report: Residential Baseline Study for Australia 2000-2030, October 2015, at https://www.energyrating.gov.au/document/report-residential-baseline-study-australia-2000-2030.

Data	Source
Commercial load breakdown	Delta Q was engaged by AEMO to develop an estimate of commercial load composition. Delta Q's report is available on AEMO's website[55]. They used data from Australian energy statics and energy audits, applying a combination of firm data, soft data, extrapolation and estimation. Commercial load was defined as any load that is not residential and is not one of the largest ~200 industrial loads in Australia. This includes small manufacturing, office buildings, shopping centres, warehouses, hospitals, schools, universities, hotels, etc. Commercial loads were broken down into various load types (e.g. HVAC, fans, pumps, office equipment, heating, CFL lighting, incandescent lighting, refrigeration, tenant plug loads, etc). Delta Q used ESOO commercial demand data to break down load by region, then sector, and then season and day type (weekday or weekend). They created average daily load profiles (24 hours) and assigned load categories (compressors, fans, pumps, lighting) before converting them to load components. The result is a seasonal, daily breakdown of commercial CMLD components for each region.
Industrial load breakdown	AEMO used annual industrial demand data to breakdown industrial load individually for 140 Large Industrial Loads (LILs) into sectors (e.g. coal mining, LNG production, paper milling, etc). To manage model complexity, a single set of RoA was applied to each industrial sector in each region, irrespective of season, assuming relatively constant load composition for these customers. Of these 140 LILs, it was possible to assign explicit load models with their own CMLD parameters to 72 LILs, based on the LIL type. The load data and associated PSS®E bus of these 72 LILs were easily identifiable from the resolution of data available to AEMO and therefore modelled explicitly. For the remaining 68 LILs, industrial loads are connected to the same bus as residential or commercial load and cannot be isolated. A generalised model based on the general CMLD model for the region was employed for these 68 LILs (combining the estimated load composition of these LILs with the residential and commercial loads). This approach was used for loads such as rail (transport support services). Bell Bay, Alcoa Portland (APD), Tomago and Boyne Island smelters were all modelled independently using a static IEEE load model, each with established parameters agreed with the relevant TNSP.
Rules of Association (RoA) - break down of end-use loads to equivalent CMLD model components	The Lawrence Berkeley National Laboratory (LBNL) New England study[56] was identified as the most comprehensive reference available, providing estimates of RoA for a wide range of sectors and end-use loads. Some adjustments were made in consultation with NSPs to account for Australian specific factors, including: • Increasing adoption of power electronic products across many categories in the industrial sector. For example, industrial direct-on-line motors (DOL) are commonly replaced with VFDs at the end of their life or if there is a financial incentive for the plant operator to do so. • Commercial end-use categories are increasingly powered electronic driven, as VFD devices increase penetration in markets such as space cooling. Furthermore, water heating is transitioning from constant impedance to inverter, power electronic based technology as device cost and efficiency approach parity. • Retail sales and power factors trending to 1 indicate that newer end-use loads are increasingly inverter-driven, especially white goods such as refrigerators and washings machines. Additionally, constant impedance components are considered negligible in modern-day electronics.
Motor D load composition	AEMO commissioned energy Efficient Strategies (EES) to estimate the proportion of NEM load in the Motor D category. The EES report is available on AEMO's website[57]. NERC and PEACE documentation and AEMO's sensitivity analysis indicated that the Motor D category is particularly influential in the CMLD model behaviour, with even small changes in Motor D composition leading to differing model outcomes. Furthermore, international analysis to date on Motor D has focused on the behaviour of air conditioners in the United States of America (USA) which are predominantly 1P motor compressors. In contrast, the Australian residential air conditioner market is predominantly inverter interfaced motors. For these reasons, a specific study to refine estimates of the proportion of Motor D in Australian NEM regions was commissioned. EES used sales data to estimate the proportion of Motor D in the NEM, accounting for increasing adoption of inverter-based resources (in refrigerators, washing machines, etc).

[55] Delta Q (22 April 2020) AEMO Commercial Load Model, at https://aemo.com.au/-/media/files/initiatives/der/2020/2020-06-26-deltaq-final-report-aemo-commercial-load-model-user-guide-revb.pdf?la=en.

[56] W. Gifford, J. Lopes, C. Driscoll, N. Ghosh, A. Kanungo, J. Metoyer and T. Ledyard. End-Use Data Development for Power System Load Model in New England - Methodology and Results, April 2014, at https://certs.lbl.gov/sites/all/files/data-development-for-ne-end-use-load-modeling.pdf.

[57] Energy Efficient Strategies. Air Conditioning and Refrigerator Load Composition (report), August 2020, at https://aemo.com.au/-/media/files/initiatives/der/2020/2020-08-05-ees-ac-load-composition.pdf?la=en.

LNG industrial loads

AEMO collaborated with Powerlink and Energy Queensland to update the RoA for LNG loads in the Surat Basin, a heavily concentrated LNG region dominated by VFD type loads. This was necessary to improve the load loss estimates for faults occurring in the region, as some historic disturbances showed an underestimation of load disconnection in PSS®E. To address this issue and improve load disconnection estimates, the following has been implemented:

- Reduced the fraction of motor A, B, and C for the LNG loads RoA (from the original LNBL estimate).
- Increased the fraction of power electronic load for the LNG RoA to align with the fraction of Direct-On-Line (DOL) and VFD motors found in the Surat region, as estimated by Powerlink.
- Reduced the proportion of power electronic loads that reconnect following a fault (frcel) to align load disconnection with observations.

To validate the new parameters for LNG loads, AEMO performed validation studies for three QLD events (refer to Queensland events in Sections 5 to 7), with a particular focus on the 9 October 2018 as in this case the fault occurs on the transmission line from Braemar to Bulli Creek, which is geographically close to the Surat Basin. AEMO verified the accuracy of the CMLD model (load loss estimates) using internal SCADA data for the Surat region and cross-checking this data with distribution level data from Powerlink.

3.4 Load behaviour parameters

The parameters that define the behaviour of the model components (Motor A, B, C, D, power electronics and static loads) were adopted from international literature[58]. Default parameter values were taken from the NERC Technical Reference Document for Dynamic Load Modelling[59].

Some adjustments were applied to account for Australian conditions, based on engineering judgement, validation studies, discussions with NSPs and advice from PEACE consulting[60]. The motor standards applied in Australia were compared with relevant international standards, and motor torque-speed curves were checked to confirm they were appropriate, and to confirm the validity of the parameters selected. This is outlined further in Section 3.4.1 and Section 3.4.2.

Initialisation (D-STATE) errors for Motor A occurred in PSS®E simulations when using the default stator resistance (Rs) from the NERC Technical Reference Document for Dynamic Load Modelling. In line with the EPRI Technical Guide on Composite Load Modelling[61], a value of 0.02 p.u. for the stator resistance was adopted and found to correct the initialisation errors.

[58] NERC Reliability Guideline – Developing Load Model Composition Data, March 2017, at https://www.nerc.com/comm/PC_Reliability_Guidelines_DL/Reliability_Guideline_-_Load_Model_Composition_-_2017-02-28.pdf.

[59] Technical Reference Document – Dynamic Load Modelling, December 2016. See Appendix A – Composite Load Model Data of NERC, at https://www.nerc.com/comm/PC/LoadModelingTaskForceDL/Dynamic%20Load%20Modeling%20Tech%20Ref%202016-11-14%20-%20FINAL.PDF.

[60] PEACE (28 June 2019) Developing Dynamic Load Models for the Australian Eastern Interconnected System, at https://aemo.com.au/-/media/files/initiatives/der/2020/aemo-load-modeling-062819-final.pdf?la=en.

[61] EPRI Technical Guide on Composite Load Modelling (Draft), August 2020. See Table 3-2 Motor A parameters for commercial constant torque loads, at https://www.wecc.org/Administrative/Mitra%20-%20Technical%20Guide%20on%20Composite%20Load%20Modeling.pdf.

Given the known influence of the Motor D component to model performance, and the known issues with motor D type loads, in terms of delayed voltage recovery, AEMO commissioned EES[62] to perform bench tests on 1P residential (and light commercial) refrigeration units to inform select Motor D parameters. They conducted tests on 14 household refrigerators and freezers, and 28 commercial refrigerators and freezers. This is outlined further in Section 3.4.4.

For a detailed list of the parameters and notes on changes from international literature, refer to Appendix A2.

3.4.1 Comparison of international motor standards

Two industry bodies develop standards for electric motors globally – the National Electrical Manufacturers Association (NEMA) and the International Electrotechnical Commission (IEC). NEMA published the MG 1-2016 standard, which defines the manufacturing requirements for alternating-current (AC) and direct-current (DC) motors in North America. The IEC publishes IEC 60034-12:2016[63], which is the standard outside of North America. For Australia, the IEC standard was revised and redesignated as AS60034: 2009[64].

To provide confidence that the 3P motor parameters adopted from international literature are appropriate, North American motor standards (NEMA) were compared with the International (IEC) standards on which the Australian standard (AS) is based.

NEMA and IEC motors are similar in size, efficiency, and output power. Both also have standards in place to specify frame size dimensions, minimum efficiency levels and testing methods. The norm for general purpose applications is NEMA Design B or IEC Design N from a performance standpoint.

To determine the adequacy of the CMLD (3P) motor parameters, AEMO considered the following:

- Torque characteristics to assess whether the default NERC torque exponent parameter (etrq) could be applied to Australian motors (see **Figure 21**[65] for an illustration of the definitions of various motor torque characteristics).
- Default motor size for a given class of motor, because transient and sub-transient reactance (X' and X") vary with motor size. Reactance's also vary with the number of poles of a motor, so it is important to consider matching the number of poles when comparing motor data across the standards.

[62] Energy Efficient Strategies. Stall Measurements for Refrigerators (bench test report), August 2020, at https://aemo.com.au/-/media/files/initiatives/der/2020/2020-08-05-ees-results-of-stall-measurements-on-motor-d-and-inverter-systems.pdf?la=en.

[63] IEC. Rotating electrical machines - Part 12: Starting performance of single-speed three-phase cage induction motors, at https://webstore.iec.ch/publication/31304.

[64] Standards Australia. AS 60034.12-2009 Rotating Electrical Machines – Part 12: Starting Performance of single-speed three-phase cage induction motors, at https://www.standards.org.au/standards-catalogue/sa-snz/electrotechnology/el-009/as--60034-dot-12-2009.

[65] Engineering ToolBox, (2004). Electrical Induction Motors - Torque vs. Speed [online] at https://www.engineeringtoolbox.com/electrical-motors-torques-d_651.html [accessed 10 December 2021].

Figure 21 Torque characteristics in electrical induction motors

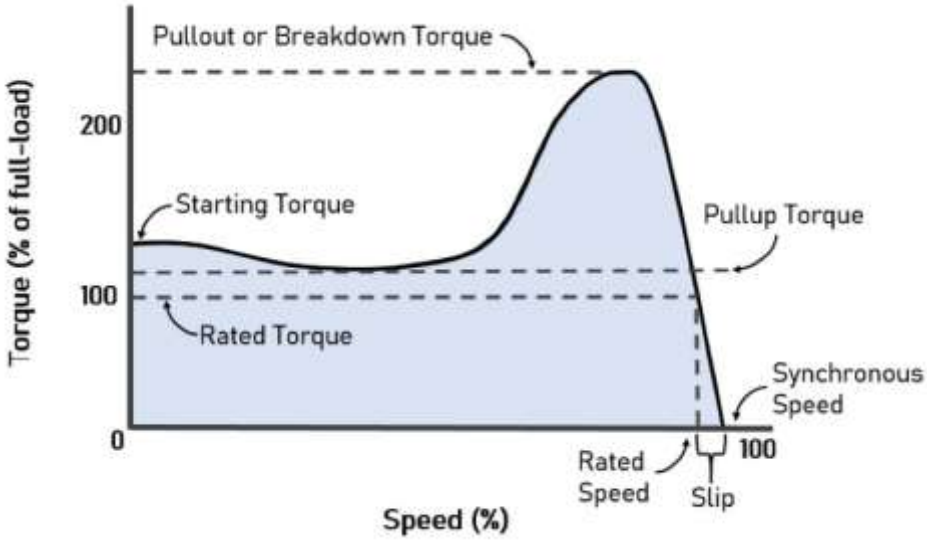

Source: Thomasnet. What is a Squirrel Cage Motor and How Does it Work? See Figure 1, at https://www.thomasnet.com/articles/machinery-tools-supplies/what-is-a-squirrel-cage-motor-and-how-does-it-work/.

Torque and power input data for each torque characteristic was collected from documentation for 1500 revolution per minute (rpm), 4-pole NEMA[66] Motor A/B and IEC[67] Motor N. The response of each torque characteristic as input power varies for NEMA and IEC motors is shown in **Figure 22** to **Figure 24**. NEMA motor data was recorded in horsepower, and then converted to SI units for comparison with IEC motor data. From the figures, for the motor sizes applicable to Motors A, B and C (shown in green) the torque characteristics are comparable.

Figure 22 Minimum breakdown torque

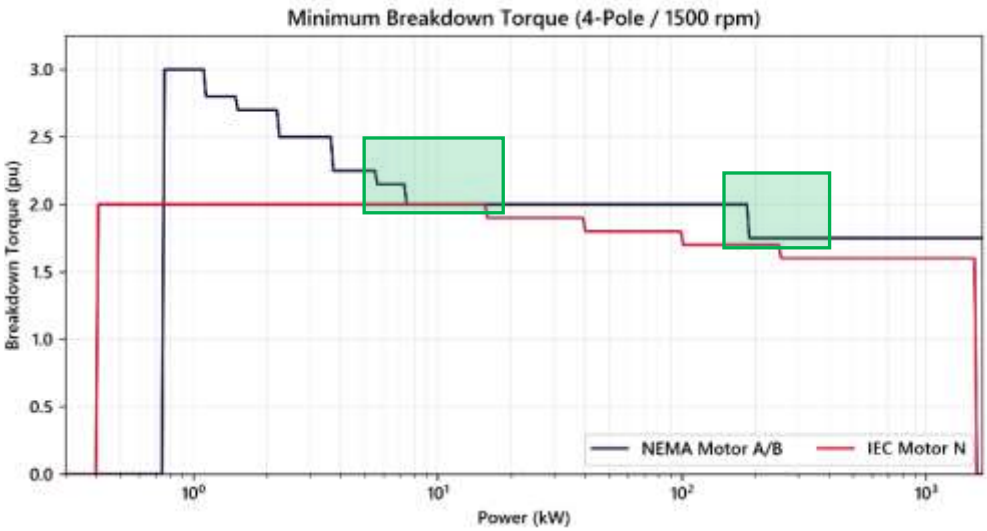

[66] ANSI, NEMA MG. (2016). MG 1-2016-Motors and Generators. National Electrical Manufacturers Association. See Table 12-2, Part 12-Page 10, at https://www.nema.org/standards/view/motors-and-generators.

[67] IEC. Rotating electrical machines - Part 12: Starting performance of single-speed three-phase cage induction motors. See Table 1, page 5, at https://webstore.iec.ch/publication/31304.

Figure 23 Minimum locked rotor torque

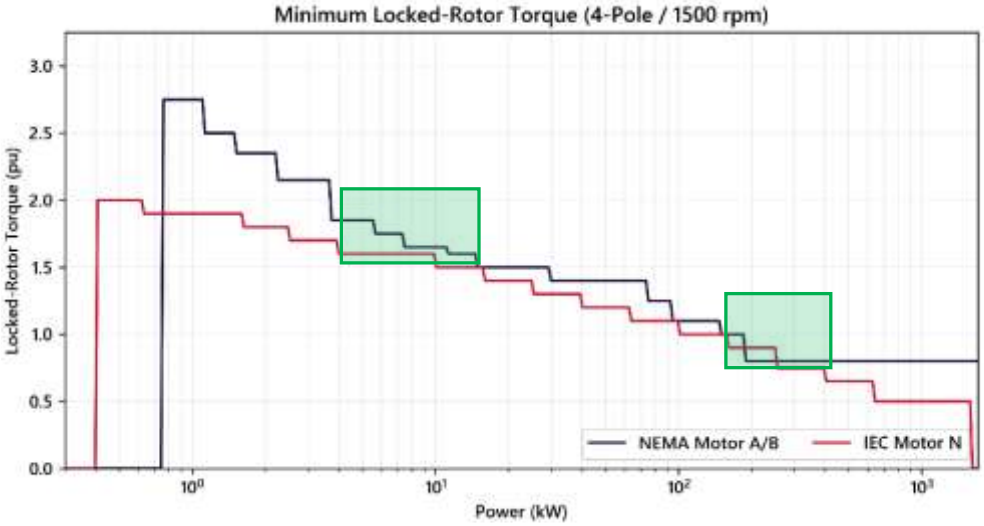

Figure 24 Minimum pull up torque

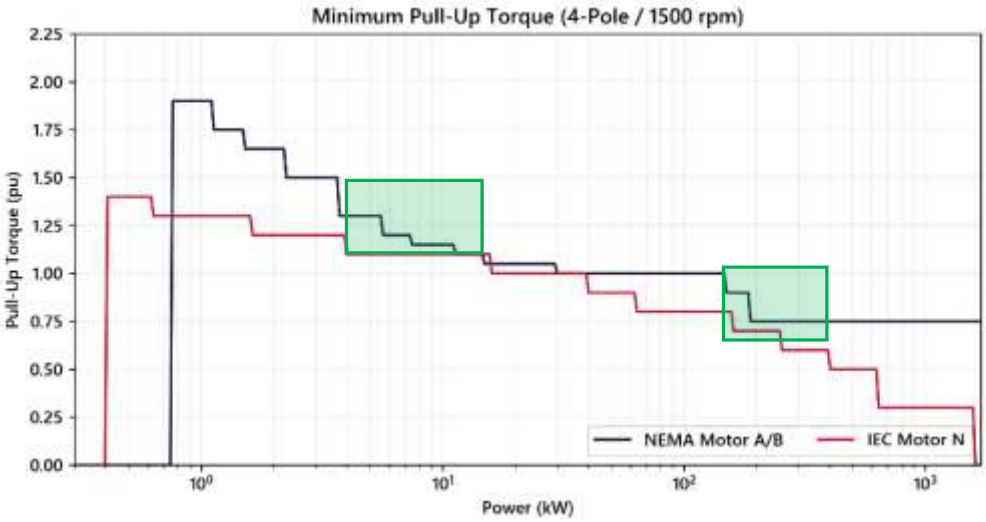

Table 17 compares the minimum breakdown, locked rotor, and pull-up torque characteristics for 4 pole NEMA and IEC motors of a given size. Given the torque characteristics are similar between standards, for the size of motor represented in the CMLD models, the etrq parameter is considered to be suitable for Australian applications. Figure 22 to Figure 24 reaffirm that for a specific motor size, the NEMA and IEC characteristics are comparable. Given the similarities between the torque characteristics vs the size of the motors, the reactance parameters were also considered to be suitable.

On this basis, the default etrq, X' and X" parameters from the NERC documentation were applied to the 3P motors in the CMLD model.

Table 17 CMLD motor type classification and general specifications

	Motor A		Motor B	Motor C
Size (kW)	4-11	150-370	4 – 19	4 – 19
NEMA Class	A		B	B
IEC Class	N		N	N
Breakdown Torque[68] NEMA/IEC (pu)	2-2.3 / 2	1.7-2 / 1.6-1.7	2-2.2 / 2	
Locked Rotor Torque[69] NEMA/IEC (pu)	1.6-1.8 / 1.5-1.7	0.8-1 / 0.8-1	1.5-1.8/ 1.4-1.6	
Pull-up Torque[70] NEMA/IEC (pu)	1.1-1.3 / 1.1	0.8-0.9 / 0.6-0.8	1.1-1.3 / 1-1.1	
Is NEMA and IEC comparable?	Yes	Yes	Yes	

3.4.2 Motor torque-speed curves

To provide further confidence that the 3P motor parameters adopted are appropriate, motor torque-speed curves were calculated for Motors A, B and C to confirm these are within a physically appropriate range.

The parameters applied to the CMLD model for Motors A, B and C are summarised in **Table 18**. These were converted to equivalent two-cage squirrel induction motor (CIM6BL)[71] model parameters, then the PSS®E motor tool was used to calculate torque speed curves.

Table 18 CMLD motor parameters adopted

Parameter	Description	Motor A	Motor B	Motor C
LF	Real power to power base ratio	0.75	0.75	0.75
Ra (pu on motor base)	Stator resistance	0.02	0.03	0.03
X (pu)	Synchronous reactance	1.8	1.8	1.8
X' (pu)	Transient reactance	0.12	0.19	0.19
X" (pu)	Sub-transient reactance	0.104	0.14	0.14
T_o' (s)	Transient open-circuit time constant	0.095	0.2	0.2
T_o" (s)	Sub-transient open-circuit time constant	0.0021	0.0026	0.0026
H (s)	Inertia constant	0.1	0.5	0.1
e_{trq}	Exponent for variation of torque with speed	0	2	2

Figure 25 shows the resulting torque speed curves for Motor A, and **Figure 26** shows the torque speed curves for Motor B and Motor C. The black curve shows the torque (y-axis) relative to the speed (x-axis), the red curve shows the current (y-axis) relative to the speed, and the green curve shows the power factor (y-axis) relative to the speed.

[68] Breakdown torque is the maximum torque a motor develops with rated voltage applied at rated frequency, without an abrupt drop in speed.

[69] Locked rotor torque is the torque a motor develops at a standstill.

[70] Pull-up torque is the minimum torque a motor develops when it runs from zero to full-load speed (before reaching the breakdown torque point).

[71] Siemens. 2019. Model Library: PSS®E 34.7.0. Page 446.

Motor A is intended to represent constant torque loads such as commercial air conditioner compressors and therefore has a flatter curve between the locked rotor torque and breakdown torque (compared to a quadratic curve). The curves illustrated in Figure 25 provide a realistic representation of motors of this type.

Figure 25 Motor A torque speed curve

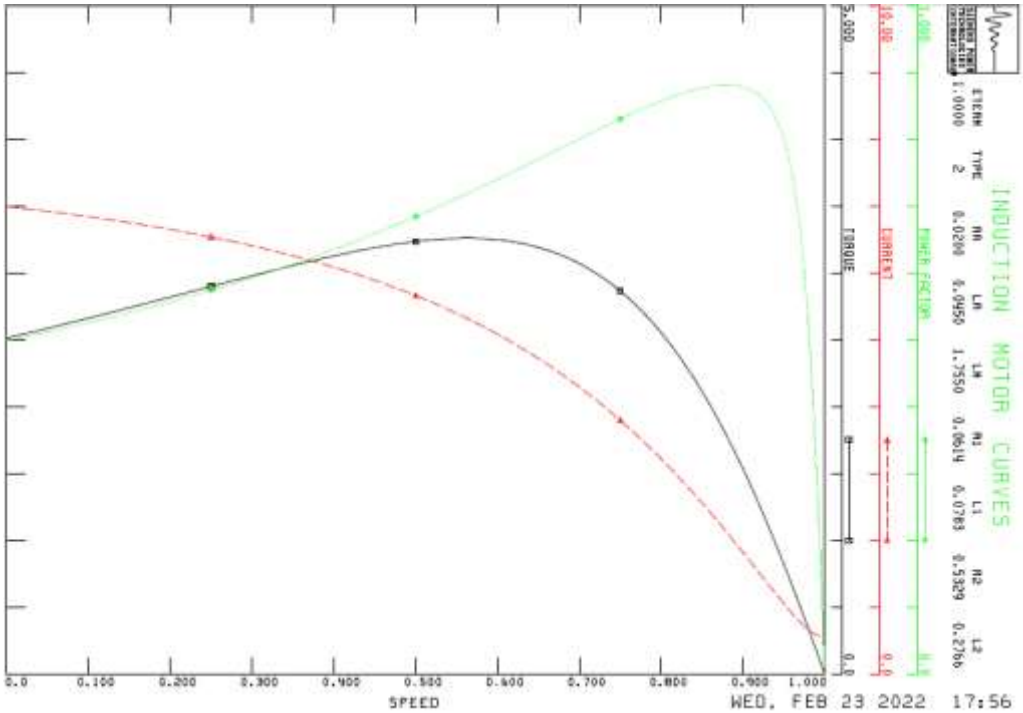

Motor B and C are intended to represent loads such as centrifugal pumps and fans, and therefore have a quadratic curve which indicates that torque is proportional to speed squared. The curves represented in **Figure 26** provide a realistic representation of motors of this type.

Figure 26 Motor B & C torque speed curve

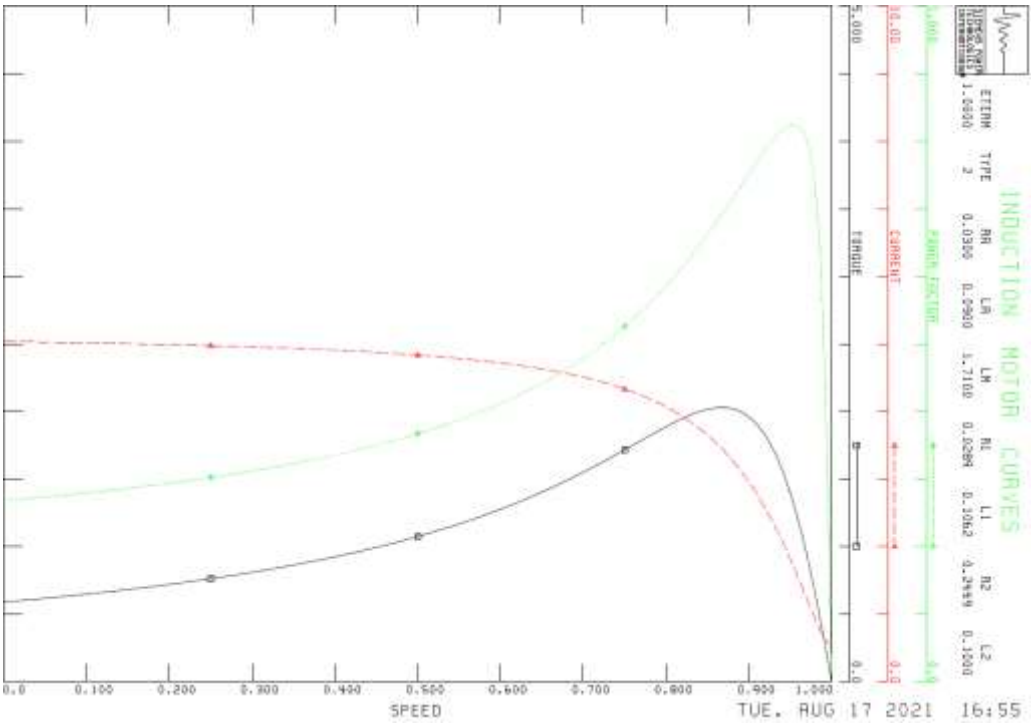

Based on these results, the motor parameters appear to be physically realistic, and suitably demonstrate the behaviours of the motor types they are intended to represent.

Motor D is a 1P performance model, derived from lab testing of the behaviour of these loads, and the parameters are not intended to translate to a torque speed curve. The development of Motor D parameters is outlined in the following section.

3.4.3 Frequency response of CMLD load components

The six load types in the CMLD model react differently to frequency disturbances. To demonstrate, a frequency ramp to 48 Hz then back to 50 Hz was performed for each of the load components. The results in **Figure 27** represent an under-frequency ramp but have been mirrored for over-frequency as well to check for consistency.

The Motor B and Motor C loads behave similarly and have a greater response to frequency disturbances than the other CMLD load types. This is because the torque of these motors is proportional to speed squared (etrq = 2), whereby the load torque decreases as frequency drops. This relationship simulates load relief. Motor B has a more aggressive response than Motor C as it has a higher inertia constant.

As Motor A represents constant torque (etrq = 0) loads, there is no variation in torque with a change in frequency. Hence, the load only exhibits a slight change during the transient periods of the frequency ramp but settles at the pre-disturbance level when the ramp flattens.

Motor D represent single-phase compressor motors, and the load response is proportional to the frequency response, as the load torque varies linearly with speed. For example, a 4% frequency reduction (50 Hz to 48 Hz) will result in a 4% power reduction (100 MW to 96 MW).

Both the power electronic load and static load components exhibit no frequency dependency in the CMLD model and are only voltage dependent.

Figure 27 Load model response to an under-frequency ramp (50 Hz to 48Hz and back)

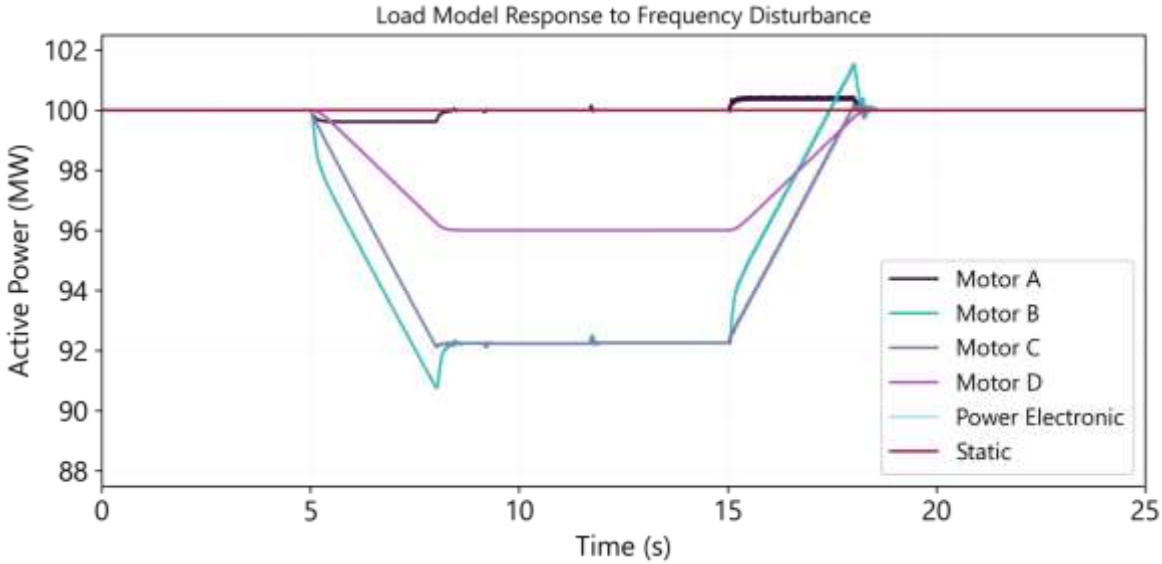

3.4.4 Motor D behaviour parameters

Two Motor D trip-related parameters were adjusted from the default values in international literature based on the findings from EES[72], from the testing of more than 40 1P refrigerators. A summary of the trip results is shown in **Table 19**. These parameters inform the fraction of motors that can restart after a stall (Frst) and the fraction of motors that disconnect on undervoltage (and do not stall) and do not reconnect (Fuvr). The other values do not apply to any parameters and are only included to illustrate the completeness of the Motor D testing undertaken and provide support for the parameters that were used in the Motor D model (as the sum of all trips shown in the table add to 100%)

Table 19 Summary of findings from Motor D testing

Finding	Units demonstrating the relevant behaviour	Relevant CMLD Parameter	Parameter value
10% of the motors can restart after a stall	22, 23, 28, 36	Frst – Motor D fraction capable of restart after stall	0.1
32.5% of the motors disconnect on under-voltage (do not stall) due to a digital thermostat and do not reconnect	6, 9, 11, 13, 15, 17, 18, 20, 24, 26, 29, 31, 33	Fuvr – Motor D fraction with under-voltage relays	0.325

[72] EES Results of low voltage stall measurements on single phase induction motors and inverter systems, June, 2020, at https://aemo.com.au/-/media/files/initiatives/der/2020/2020-08-05-ees-results-of-stall-measurements-on-motor-d-and-inverter-systems.pdf?la=en.

Motor D temperature parameters

The Motor D temperature parameters (Th1t, Th2t) are also updated based on the EES findings. While the motor temperature was not measured in the tests, the temperature may be derived. To derive motor temperature, the motor is modelled as a first order system (low pass filter), whereby:

- Tth is the Motor D heating time constant (s) which is the time constant associated with the thermal overload protection of the motors that physically disconnects the motor. This is assumed to be 15 s according to NERC documentation and is based on thermal relay characteristic testing[73].
- Pstall is the stall power of the motor. This is assumed to be 7 pu based on the motor testing data.
- Ttrip is the assumed tripping temperature, measured as a percentage from nominal, whereby Th1t is the starting temperature and Th2t is the final temperature with all motors tripped. For example, if Th1t is 1.98, then the temperature at which motors start to trip is 198% of nominal temperature.

Modelling Motor D as a first order system (low pass filter), these values are related as follows[74]:

$$Tth * \frac{dTtrip}{dt} + Ttrip = Pstall$$

Performing a Laplace transform of the differential equation, if the stall power is a unit step, then the solution to the differential equation is:

$$Ttrip = Pstall . \left(1 - e^{\frac{-t}{Tth}}\right)$$

Table 20 Motor trip temperature calculation

Motor #	1	2	3	4	5	7	10	12	14	16	19	22	25	34	35	36	38
Trip time (s)	16	39	21	30	35	5	12	54	17	7	10	7	11	26	14	8	26
Ttrip (%)	4.59	6.48	5.27	6.05	6.32	1.98	3.85	6.81	4.75	2.61	3.41	2.61	3.64	5.76	4.25	2.89	5.76

Table 20 shows the measured trip times, and calculated Ttrip values (based on Tth = 15 and Pstall = 7). In the CMLD model, Th1t (starting temperature) was set to the lowest trip temperature (1.98). Th2t (final temperature with all motors tripped) was set to the median of the trip temperatures (4.59). The median temperature was considered more appropriate for Th2t as HSM data suggests significantly more stall behaviour than modelled during significant historic undervoltage events. This implies that more 1P motor stalling is required for a given undervoltage disturbance. The Th2t parameter will be reviewed again in future as further data becomes available. This is best assessed by reviewing HSM data for several night-time disturbances on radial distribution feeders with a high concentration of residential load. If the active power spikes significantly in the first minute following an event (thermal overload) followed by a drop below pre-fault values of active power (disconnection on thermal overload) then the Th2t value can be matched appropriately.

[73] NERC. Technical Reference Document – Dynamic Load Modelling, December 2016. See Figure 42, page 42, at https://www.nerc.com/comm/PC/LoadModelingTaskForceDL/Dynamic%20Load%20Modeling%20Tech%20Ref%202016-11-14%20-%20FINAL.PDF.

[74] NERC. Technical Reference Document – Dynamic Load Modelling, December 2016. See Figure 39, page 41, at https://www.nerc.com/comm/PC/LoadModelingTaskForceDL/Dynamic%20Load%20Modeling%20Tech%20Ref%202016-11-14%20-%20FINAL.PDF.

4 Consolidated model development process

4.1 The CMLD and DPV model

The PSS®E CMLD and DER model implementation is shown in **Figure 28**. The DER model is integrated at the transmission network level. This is different to the approach proposed in NERC documentation[75,76]. At the time of model development, suitable models were not yet available in PSS®E to enable the integration of the DER_A model with the CMLD model at the low voltage bus.

This approach is considered likely to provide a reasonable representation:

- One international study[77] has indicated that the distribution DER_A model is minimally sensitive to feeder impedance assumptions. This study tested moving ZIP transmission loads at the transmission voltage level (100 kV) to the distribution network (12.47 kV), adding distribution transformers and feeders, and connecting DPV.
- In discussions, EPRI indicated that the behaviour of the DER_A model (the original DPV model developed by WECC) is not expected to vary significantly with feeder voltage.

This suggests that the DPV model is minimally affected by voltage level or feeder impedance. In future model updates, integration of the DPV and CMLD models at the low voltage bus may be explored.

Figure 28 The combined CMLD and DPV model structure

a) NERC proposed implementation of DER_A model (original design)

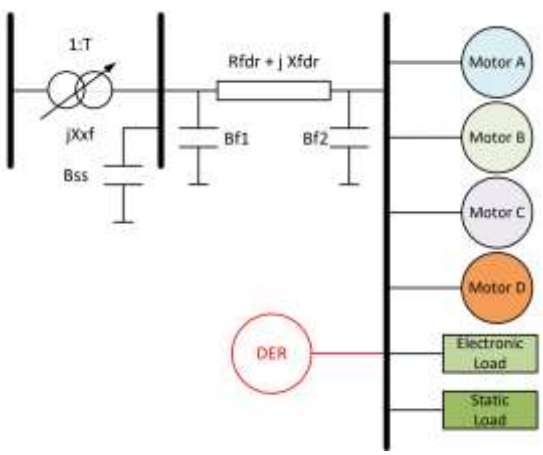

b) DERAEMO1 as implemented by AEMO

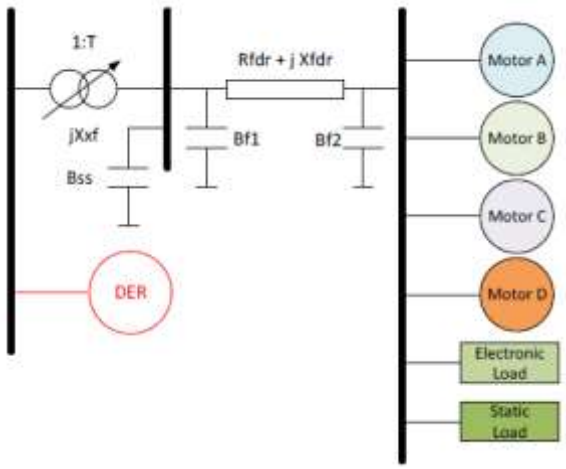

[75] NERC. Reliability Guideline – Parameterization of the DER_A Model, September 2019, at https://www.nerc.com/comm/PC_Reliability_Guidelines_DL/Reliability_Guideline_DER_A_Parameterization.pdf.

[76] NERC. Reliability Guideline - Model Verification of Aggregate DER Models used in Planning Studies, at https://www.nerc.com/comm/RSTC_Reliability_Guidelines/Reliability_Guideline%20_DER_Model_Verification_of_Aggregate_DER_Models_used_in_Planning_Studies.pdf.

[77] PJM. DER Trip Impact Study: Methods, Results, and Conclusions. Page 11 and 27, at https://www.pjm.com/-/media/committees-groups/task-forces/derrttf/20190614/20190614-item-01-der-trip-impact-study-results.ashx.

4.2 The CMLD and DPV model in a power system network

Figure 29[78] shows how the models fit into a broader perspective of the power system network.

Figure 29 NEM network topology

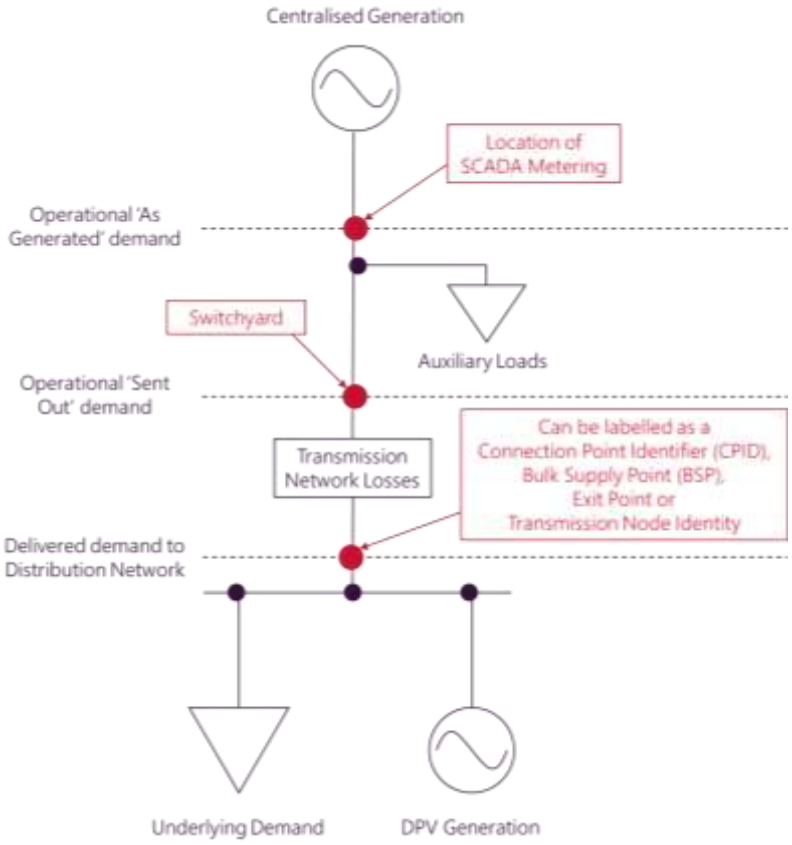

The diagram above can be used to define a relationship between operational demand, underlying demand and DPV generation:

$$OD = UD - DPV + NL + AL$$

where:

- Operational demand in a region is demand that is met by local scheduled generation, semi-scheduled generation, and non-scheduled wind/solar generation of aggregate capacity ≥ 30 MW, and by generation imports to the region, excluding the demand of local scheduled loads, and including Wholesale Demand Response. Operational demand does not include demand met by DPV generation. This type of demand can typically be measured in real-time (through SCADA readings).

[78] Centralised generation is defined as generation supplied by scheduled, semi-scheduled and significant non-scheduled generating units. Refer to the following document for a more detailed diagram: https://www.aemo.com.au/-/media/Files/Electricity/NEM/Planning_and_Forecasting/Demand-Forecasts/Operational-Consumption-definition.pdf.

- Underlying demand (UD) is electricity used at a particular time by residential, commercial and large industrial consumers, as supplied by scheduled, semi-scheduled and significant non-scheduled generating units as well as DPV generation. This type of demand is not easily measured in real-time.
- DPV is solar power generated behind the meter (typically residential homes and light commercial properties).
- Network losses (NL) result from the transport of electricity across the transmission and distribution networks.
- Auxiliary loads (AL) refer to electricity used by auxiliary equipment required to generate electricity at power generation facilities.

To be able to compare the results of PSSE simulations with real world data, the definition of underlying demand has been broadened in this document to include auxiliary loads. This means the above equation can be simplified as follows.

$$OD = UD - DPV + NL$$

where

$$UD = EUL + AL,$$

and EUL refers to End Use Loads (industrial, commercial or residential).

All model comparisons to real world data were made based on changes in the discussed quantities. This means the pre fault value was compared with the post fault value, to give an idea of the "delta" (Δ) or change in the relevant number. This can be expressed as follows.

$$\Delta OD = \Delta UD - \Delta DPV + \Delta NL$$

It was assumed that the network was large enough that any change in network configuration due to a power system disturbance would not significantly change aggregate network losses. For this reason, this term in the above equation could be considered negligible. This leads to the following simplified equation.

$$\Delta OD = \Delta UD - \Delta DPV$$

Figure 30 below provides a visual representation of this simplified formula, for considering the response of the models to a power system fault.

Figure 30 A simplified NEM network topology (valid when analysing the effect of a change in the network)

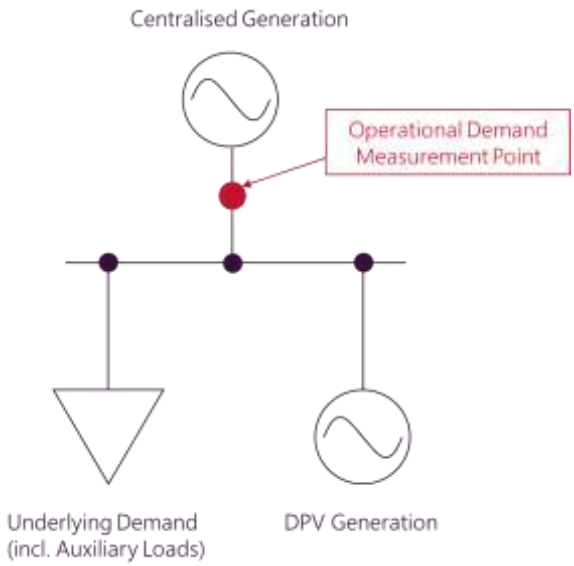

4.2.1 Calculating changes in the observed quantities

Observed operational demand is recorded at the SCADA metering location seen in Figure 30 and is considered operational 'as generated' demand. For this reason, change in observed operational demand has been calculated simply as the change in SCADA readings pre and post fault.

Change in observed DPV generation has been estimated using datasets from Solar Analytics, which provide statistical representation based on the behaviour of a sample of DPV installed across the network[79].

Change in observed underlying demand was estimated by rearranging the equation discussed on the previous page, to make underlying demand the subject.

$$\Delta UD_{observed} = \Delta OD_{observed} + \Delta DPV_{observed}$$

Note that SCADA readings are inclusive of auxiliary loads, so calculating underlying demand in this way is inclusive of changes in auxiliary load. SCADA readings also include changes in network losses, but it is assumed this change is small enough to be disregarded.

4.2.2 Calculating changes in the modelled quantities

Change in operational demand estimated from the simulations was calculated by summing the change in underlying demand, predicted by the CMLD model, and then subtracting the change in DPV generation, predicted by the DPV model.

$$\Delta OD_{modelled} = \Delta UD_{modelled} - \Delta DPV_{modelled}$$

[79] AEMO. Behaviour of distributed resources during power system disturbances. Refer to Appendix A1 for estimated pre and post fault DPV generation levels for each disturbance discussed in this report: https://aemo.com.au/-/media/files/initiatives/der/2021/capstone-report.pdf?la=en&hash=BF184AC51804652E268B3117EC12327A.

As discussed previously, modelled underlying demand is inclusive of both end-use and auxiliary loads[80]. Again, changes in network losses were considered to be negligible and were not accounted for in the analysis of simulation results.

4.2.3 Analysing the impact on operational demand of changes in underlying load and DPV generation

Figure 31 shows illustrative examples of how changes in load or DPV generation after a fault impact operational demand:

- Scenario 1 shows a scenario where 10 MW of underlying load disconnects, at the same time as 10 MW of DPV is lost. The net contingency size is 0 MW.
- In scenario 2, a 10 MW load increase is offset by a 10 MW increase in DPV. The net contingency size is 0 MW.
- Scenarios 3 and 4 demonstrate what can occur if alternating responses are explored. If 10 MW of load is gained, at the same time as 10 MW of DPV is lost, the net contingency size is +20 MW. Likewise, if 10 MW of load is lost, at the same time as 10 MW of DPV is gained, the net contingency size is -20 MW.

Where the models underestimate a change in DPV, and overestimate a change in load, the error in the operational demand estimate will compound[81].

However, where the models both underestimate a change in DPV, and underestimate a change in load, there will be a cancellation effect which reduces the error in the operational demand estimate[82].

[80] Meaning the CMLD model was applied to auxiliary loads, as well as end use loads.

[81] A similar issue will occur if the models overestimate a change in DPV, and underestimate a change in load.

[82] A similar phenomenon is applicable to an overestimation of the change in DPV, and an overestimation of the change in load.

Figure 31 Diagram showing how to analyse a change in the various quantities

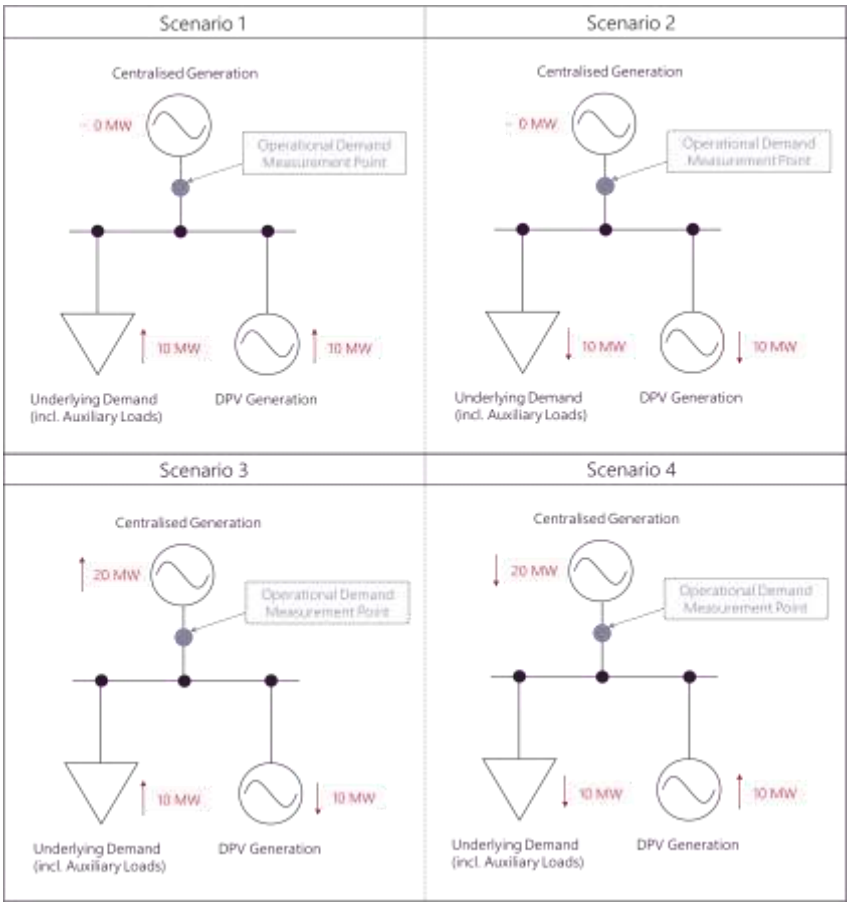

4.3 Selection of events for model validation

AEMO identified a selection of historic disturbances to assess and validate the CMLD and DPV model performance. Significant disturbances experienced in the NEM over the past several years were selected, aiming to capture:

- Disturbances across as many NEM regions as possible[83].
- Events with no DPV generating (to allow testing of the CMLD model in isolation) as well as events with significant levels of DPV generating (to facilitate testing of the DPV model with the CMLD model).
- A range of voltage disturbances (covering a variety of faulted regions, depth of voltage depressions, fault times, and fault locations on the transmission network) to allow tuning of voltage trip parameters.
- Several frequency disturbances including a mix of under-frequency, over-frequency, separation events, and load shedding.
- Events where significant changes in net load were observed, to test the model's ability to represent this behaviour accurately. A selection of events where significant changes in net load were not observed were also included, to ensure the model replicated this accurately.

[83] Given low levels of DPV installation, no events occurring in Tasmania were selected to assess the CMLD and DPV models.

- A range of dates (2017 to 2020) to capture the changing proportion of DPV inverters installed under older standards (ASNZS4777.3:2005) versus newer standards (ASNZS4777.2:2015).

Table 21 lists the voltage events used for validation studies, while **Table 22** lists the frequency events used. Incident reports are available for most of these events on AEMO's website[84], with hyperlinks provided by clicking on the dates in the first column.

Table 21 Voltage events used for validation studies

Date	Region	Event type	DPV generating	Used for CMLD	Used for DPV
03-03-2017	SA	Under-voltage	✓	✓	✓
18-01-2018	VIC	Under-voltage	✓	✓	✓
08-03-2018	VIC	Under-voltage	✗	✓	✗
11-04-2018	SA	Under-voltage	✗[85]	✓	✗
09-10-2018	QLD	Under-voltage	✓	✓	✓
18-02-2019	VIC	Under-voltage	✗	✓	✗
03-03-2019	VIC	Under-voltage	✓	✓	✓
17-04-2019	SA	Under-voltage	✗	✓	✗
26-11-2019	QLD	Under-voltage	✓	✓	✓
24-01-2021	SA	Under-voltage	✓	✓	✓
22-02-2021	QLD	Under-voltage	✓	✓	✓
12-03-2021	SA	Under-voltage	✓	✓	✓

Table 22 Frequency events used for validation studies

Date	Region	Event type	DPV generating	Used for CMLD	Used for DPV
25-08-2018	QLD	Over-frequency	✓	✓	✓
	SA	Over-frequency	✓	✓	✓
	NSW	Under-frequency	✓	✓	✓
	VIC	Under-frequency	✓	✓	✓
16-11-2019	SA	Over-frequency	✓	✓	✓
31-01-2020	SA	Over-frequency	✓	✓	✓
	VIC	Under-frequency	✓	✓	✓

The CMLD + DPV model was tuned against the validation studies in the following order to isolate and determine model parameters:

1. Night-time undervoltage events – CMLD model only.
2. Day-time undervoltage events – CMLD + DPV model.
3. Day-time frequency events – CMLD + DPV model.

[84] AEMO, Power system operating incident reports, at https://aemo.com.au/en/energy-systems/electricity/national-electricity-market-nem/nem-events-and-reports/power-system-operating-incident-reports.

[85] This event occurred at 4.47 pm with approximately 190 MW of DPV online. There was relatively little DPV generation online at the time of the fault (compared to the other events considered), so this event was not used for DPV model validation.

Suitable validation events are relatively rare, which is one of the main limitations in confirming model validity. AEMO will continue to add more events to this calibration set as further disturbances occur.

4.4 Data collection

The following data was collected for each event to inform the validation studies:

- **High Speed Monitoring (HSM) data** (20 ms sampling period) to compare the dynamic profiles (voltage, active power, reactive power, frequency) of buses in PSS®E and determine if they match HSM data. Voltage depressions at the nearest HSM device were used to assess the severity of the fault. Voltage depressions were measured using the positive sequence voltage depression.
- **SCADA regional demand data** (4 s sample period) to estimate net load change.
  - Regional demand SCADA channels are calculated by summing the active power of the locally scheduled and semi-scheduled generators in the region, non-scheduled wind generators in the region, and interconnector flows between regions. These measurements may not always be fully time synchronised (with errors sometimes occurring over a significant duration of time) and may not always accurately represent total demand in the region. These measurements therefore represent an approximate estimate of total demand in the region.
  - The net change in load was estimated by using a trendline to determine the net pre-fault and post-fault load change over a number of intervals, accounting for variability between four second intervals.
  - In some disturbances, the settling point of minimum load change was unclear – load may appear to reach a stable point in the several minutes following the disturbance, but then decline further in the subsequent minutes. It is unclear whether this represents real behaviour of load, or errors in the measurement. In these cases, the minimum load reached over the 0-3 minutes following the disturbance was used as the target value for load loss, but ranges are noted to account for the considerable uncertainty in these estimates. The values used as targets in each case are shown as green dashed lines in figures in the subsequent sections of this report.
  - Limitations in the accuracy of these regional load measurements represents one of the most significant limitations in the tuning and validation of these models.
- **DPV disconnection and curtailment data from Solar Analytics**, who measure the response of thousands of individual DPV systems across the NEM with a mix of 5s/30s/60s sample periods. The behaviour of this sample set of individual DPV systems was analysed to estimate the behaviour of the DPV fleet in the region, Including identifying the proportion that disconnected, and the curtailment behaviour observed. A detailed outline of the way these datasets were analysed is outlined elsewhere[86].

[86] AEMO (May 2021) Behaviour of distributed resources during power system disturbances, https://aemo.com.au/-/media/files/initiatives/der/2021/capstone-report.pdf.

- **DPV capacity factor data** from AEMO's DPV forecasting system, ASEFS2[87], to determine the amount of DPV generation in the region at the time of the event. This was interpolated between half-hourly forecast intervals to estimate DPV generation at the exact time of the disturbance.

The data sets available did not provide complete and thorough coverage of the network in many cases. The best datasets available were used for this analysis, and AEMO is working to improve them for future model validation. For example, improved tools for estimating DPV behaviour will be developed through initiatives such as Project MATCH[88], and AEMO is working with NSPs to improve the availability of HSM datasets, particularly at radial network locations with load and DPV. As improved datasets become available for future disturbances, this will improve the potential for calibrating these models.

4.5 Assessing model performance

The following approach was applied to assess, validate, and fine tune the response of the CMLD and DPV models. These steps were undertaken for each of the disturbances outlined above, with parameters tuned as a single set to provide the best possible match against all disturbances simultaneously.

- **Step 1: Validate against high speed measurements (HSM)**:
  - Identify the transmission buses where HSM data is available and plot the waveforms (V, P, Q for voltage disturbances and V, P, Q, f for frequency disturbances). Compare the waveforms of the HSM data and the PSS®E output results.
  - Tune a select set of CMLD parameters to improve the match of PSS®E results with HSM measurements. Only a select set of parameters were tuned, where there was minimal information available to inform bottom-up determination.
  - The following parameters were tuned to improve the match with HSM:
    - Vtr1/ Vtr2 – motor undervoltage trip voltages
    - Ttr1/Ttr2 – motor undervoltage trip delay
    - Ftr1/Ftr2 – motor undervoltage trip fraction
    - Trc1/Trc2 – motor undervoltage reclose delay
  - Sensitivity studies were also conducted adjusting the following parameters, but they were found to not significantly improve the match against HSM, and so were not adjusted from default values in the final parameter set:
    - R - Motor stator resistance.
    - X - Motor synchronous reactance.
    - X' - Motor transient reactance.
    - X" - Motor sub transient reactance.

[87] AEMO, Australian Solar Energy Forecasting System, https://aemo.com.au/en/energy-systems/electricity/national-electricity-market-nem/nem-forecasting-and-planning/operational-forecasting/solar-and-wind-energy-forecasting/australian-solar-energy-forecasting-system.

[88] Australian Government, Australian Renewable Energy Agency (ARENA), Project MATCH, https://arena.gov.au/projects/project-match/.

  - To' - Motor transient open circuit time constant.
  - To" - Motor sub transient open circuit time constant.
  - H - Motor inertia constant.
- Baseline simulations were also conducted for comparison with the existing ZIP load model. This helps identify the degree to which the dynamic response at that location is due to the CMLD or DPV model parameters, or whether mismatches may be due to other issues, such as representation of the network configuration in the model snapshot. Corrections to the snapshot were made where possible (for example, confirming whether network components such as capacitor banks should be in/out of service). Two baseline comparisons were used:
  - **ZIP model alone** – this simulation applies the ZIP model to represent the net demand at each bus (underlying demand minus DPV generation, exactly as measured and shown in the OPDMS snapshot). This allows direct comparison of the CMLD+DPV models with the present load and DPV modelling approach, where DPV is represented only as negative load.
  - **ZIP + DPV** – this simulation applies the ZIP model to represent the total underlying demand at each bus, and the DPV model to represent the total DPV generation at each bus. This allows direct comparison of the performance of the CMLD and ZIP load models, representing total underlying load, while the DPV model is applied in the same way.

- **Step 2: Validate against net load change (SCADA measurements)**:
  - The net load change in the CMLD+DPV models in the region in PSS®E was compared with the SCADA measurements for the total load in the region of interest.
  - The estimate of net load change varies depending on when it is measured:
    - For the PSS®E estimate: For disturbances with deep voltage depressions (deeper than 0.5 pu), the PSS®E load loss needs to be measured at greater than ~50 s post fault. This accounts for the delayed stall and subsequent trip response of Motor D. For shallower disturbances less than 0.5pu, the load loss can be measured earlier, though this is not necessary. A 60 s simulation time was considered adequate for PSS®E simulations for all historical disturbances.
    - For the SCADA measurement: Net load loss was measured from the average measurement trendline immediately pre-event, against an average measurement trendline 60 s to 100 s post event (once the data has settled), accounting for scatter and variability inherent with SCADA data. The estimation of net load loss using SCADA is a rough approximation, but no other data sources were available to estimate net change in regional load. This is one of the most significant limitations in this model development process.
  - The following parameters were tuned to improve the match of the CMLD model against the net load change estimate:
    - frcel - fraction of electronic load that can reconnect.
    - Vd1 - voltage electronic loads start to drop.
    - Vd2 - Voltage all electronic load has dropped.

  - UVtr1 - Motor D 1st undervoltage pick-up.
  - Ftr1/Ftr2 – motor undervoltage trip fraction.

- **Step 3: Validate against estimates of DPV response (Solar Analytics measurements)**:
  - The change in total DPV generation in the region from the DPV model was compared with the estimates from Solar Analytics datasets.
  - For over-frequency disturbances involving controlled curtailment responses from inverters installed under the AS/NZS4777.2:2015 standard, the DPV model response was split into disconnection responses and over-frequency curtailment responses and calibrated against each element from the Solar Analytics datasets separately.
  - The following parameters were tuned to improve the match:
    - vl0 - first breakpoint for low voltage cut-out.
    - Ddn - reciprocal of droop for over-frequency conditions.
    - fl1, fl2, fl3 - low frequency trip limits 1, 2 and 3 respectively.
    - fh1, fh2, fh3 - high frequency trip limits 1, 2 and 3 respectively.
    - frac_fl1 - fraction for low frequency trip 1.
    - frac_fh1 – fraction for high frequency trip limit 1.
    - frac_fh2 – fraction for high frequency trip limit 1.

CMLD model parameters were tuned first since these can be calibrated in isolation for events without significant DPV generation. The DPV model parameters were then calibrated against events with meaningful levels of DPV generating.

The above approach was conducted for voltage disturbances first, and then for frequency disturbances in a second stage. DPV disconnection in response to voltage disturbances is known to be significant, and there are a wide selection of events in the sample set where a significant voltage disturbance occurred but the frequency disturbance was minimal, and the response of DPV inverters to frequency in that range is known to be minimal. This allows the voltage disturbance response of the DPV model to be calibrated in isolation. The calibration of the frequency response parameters against events with more significant frequency deviation was then calibrated in the final stage.

All dynamic simulations were performed using PSS®E 34.7.0.

4.5.1 Weighted model evaluation function for disconnection estimates

To evaluate the relative success of a parameter change to the overall model performance in representing load and DPV disconnection across a set of events, a weighting function was developed to give a performance "score" of the model's predictions. The performance "score" is calculated using model load loss or DPV disconnection as a percentage of the observed load loss or DPV disconnection respectively. For cases with minimal load or DPV loss, the score was set to 100% accuracy as long as the model accurately represented minimal load or DPV loss.

The weighting function was derived with the aim to optimise both the accuracy and precision of the models estimates of load and DPV disconnection. It provided a standardised way to ensure model tuning was improving accuracy and precision of DPV and load disconnection estimates across the whole set of disturbances.

The weighting function is defined as:

$$S = |\bar{x} - 1| + \sigma$$

where:

	Explanation	Purpose
$\boldsymbol{S}$	Performance score for the CMLD or DPV model for a particular set of parameters across a set of events.	Overall performance score
$\bar{\boldsymbol{x}}$	Average percentage of actual load or DPV disconnection captured by the model across a set of events. For example, if the CMLD model estimates load loss that was 78% of the actual observed load loss estimate from SCADA in one event, and 112% of actual load loss in another event, for a sample size of 2, $\bar{x}$=(0.78+1.12)/2=0.95 or 95%. This was calculated across the full set of 15 events.	If $\bar{x} = 1$ then across the set of events, on average, the model accurately predicts load loss. If $\bar{x} < 1$ this means the model consistently underestimates load loss for the set of events. If $\bar{x} > 1$ this means the model consistently overestimates load loss for the set of events.
$\boldsymbol{\lvert\bar{x} - 1\rvert}$	The magnitude of the average error for estimates of load or DPV disconnection across a set of events. $\bar{x} - 1$ recentres $\bar{x}$ about 0 so any number other than zero indicates some level of inaccuracy. By taking an absolute value of $\bar{x} - 1$ such that we have $\lvert\bar{x} - 1\rvert$ we ensure any amount of inaccuracy is strictly positive.	Indicates the model's level of **accuracy** estimating load or DPV disconnection.
$\boldsymbol{\sigma}$	The standardised sample standard deviation of load or DPV disconnection across a set of events.	Indicates the model's level of **precision** (spread or range) in estimating load or DPV disconnection.

The objective is to minimise both $|\bar{x} - 1|$ and σ, giving the lowest overall score for both models. There was some interaction between the scores for the CMLD and DPV models observed during tuning since changes in either model will affect the behaviour of the power system and therefore affect the outcomes for the other model. This was managed with successive iterations.

4.5.2 Validation studies

The validation studies for each event are outlined in detail in Section 5 (voltage events with no DPV generating), Section 6 (voltage events with DPV generating), and Section 7 (frequency events). For each event analysed, the following is provided:

- A short summary of the key elements of the disturbance event.
- An indication of how the event was replicated in PSS®E.
- A discussion of the model performance at key transmission buses, compared with HSM and SCADA from the actual disturbance, and compared with the existing (ZIP) load model as well as a combined ZIP + DPV model.

A performance summary is provided for each disturbance summarising model performance across all the SCADA and HSM channels available to AEMO for each event. Only a subset of the HSM and SCADA measurements examined are included directly in this report, with general commentary provided on the observations related to others.

Model performance is categorised as a "Good match" where it represents the event reasonably accurately, "Fair match" where it is acceptable, and "Poor match" where the event is not represented accurately. Shaded colours in

the tables ("Good match" – green, "Fair match" – yellow, and "Poor match" – red) are used to emphasise these assessment categories visually.

A column in the tables also indicate for each event the performance of the CMLD load model compared with the existing ZIP model. A cross indicates where the ZIP model performs better than CMLD, a tick shows where the CMLD model performs at least as well as the ZIP model, and a double tick indicates where the CMLD model performs significantly better than the ZIP model.

5 Validation: voltage disturbances without DPV

This section presents the validation studies conducted for the Composite Load Model (CMLD) responding to voltage disturbances in periods with minimal or no DPV generating.

5.1 8 March 2018 – Victoria

5.1.1 Event overview

Table 23 Event summary – 8 March 2018

Date and time	8 March 2018, 04:37
Region	Victoria
Description of the event	Multiple contingency events. Loy Yang Power Station B1 (LYPS B1) generator trip due to explosion/fire at the generator transformer. Subsequent trip of Loy Yang A2 (LYPS A2) generator due to boiler protection (04:39 ~2 min after the first event).
Minimum voltage recorded	**0.56** pu positive sequence recorded at Loy Yang Power Station (from HSM data)
Operational demand prior to the event	**4,420** MW (from SCADA data)
Estimated change in operational demand	**243** MW decrease (from SCADA data)

Figure 32 Map – 8 March 2018

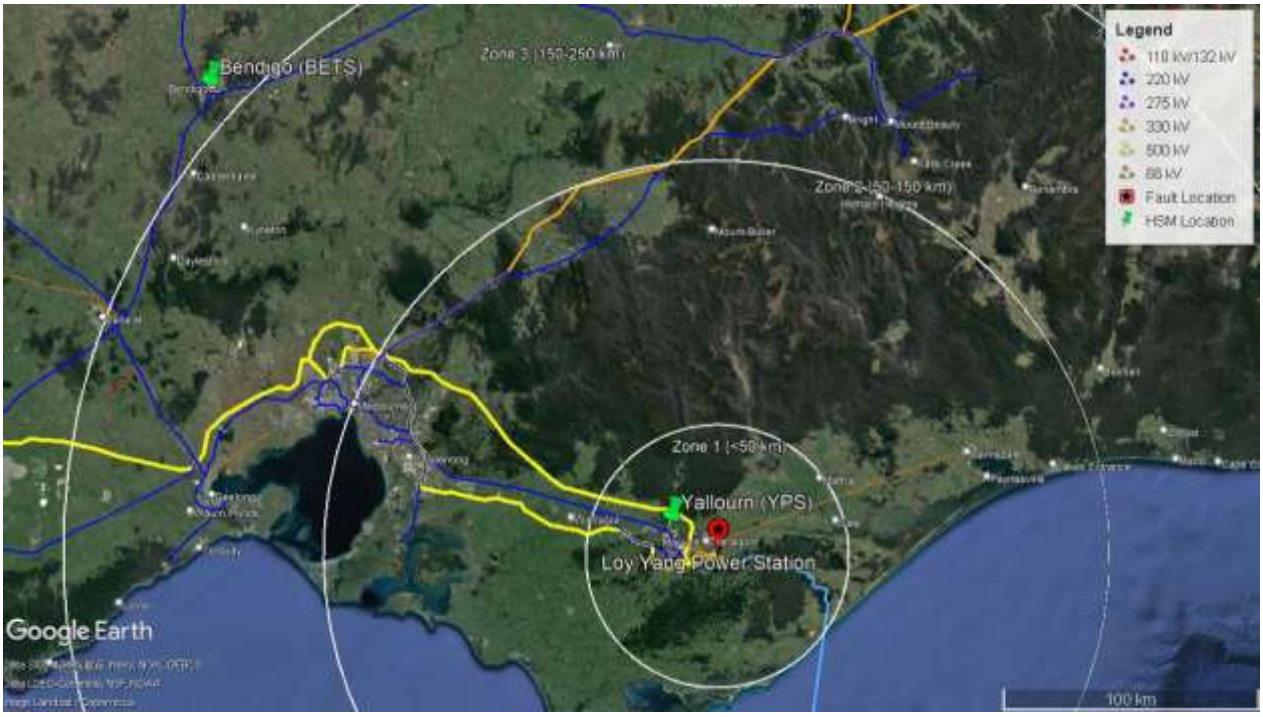

5.1.2 Replication in PSS®E

The following element changes were made in PSS®E to replicate this case:

Table 24 Simulation event summary – 8 March 2018

Time (s)	Events/comments
0.0	Start simulation
1.0	Apply branch fault at Loy Yang Power Station B1 (LYPS B1) generator transformer (PSS®E bus 35446 to PSS®E bus 30445)
1.06	Clear branch fault at Loy Yang Power Station B1 (LYPS B1) generator transformer (PSS®E bus 35446 to PSS®E bus 30445) Trip 500/20 kV LYPS B1 transformer feeder (PSS®E bus 35446 to PSS®E bus 30445)
60	End simulation

5.1.3 High speed measurements

Figure 33 and **Figure 34** show the voltages at LYPS (close to the fault) and Bendigo Terminal Station (BETS), which is further away but also affected.

Observations at LYPS (Figure 33) illustrate the voltage response at most locations in the network[89]. In this disturbance, and at most locations, the CMLD model shows a slower voltage recovery profile than observed in HSM, although voltages still recover within 0.25 s, which is not unreasonable[90]. Voltage overshoot is minimal and in line with observations. The steady-state voltage after the disturbance is also comparable with observations.

The BETS HSM, shown in Figure 34, monitors the distribution level (22 kV). At this more remote and lower voltage location, the PSS®E model shows a deeper voltage depression during the fault than observed in the HSM. This occurs for both the ZIP and CMLD load models, suggesting this mismatch is unrelated to the load models. Given that the fault impedance applied at LYPS matches well with the HSM closest to the fault (Figure 33). this suggests misrepresentation of distribution network components (and perhaps the component impedance data) in the PSS®E model.

[89] HSM data was available for the following locations: Yallourn Power Station G4, Loy Yang Power Station A1, A2, and A3 transformers, and Bendigo Terminal Station.

[90] The fault clearance times set out in Table S5.1a.2 of the National Electricity Rules (NER) state that primary and backup protection should operate within 0.25 s for faults occurring on 275 kV network. In this disturbance, with the CMLD representation voltage recovers to >90% of nominal voltage in less than 0.25 s. It is therefore assumed that there are no adverse impacts in the delayed voltage recovery which may cause spurious tripping of surrounding protection elements.

Figure 33 Voltage – 8 March 2018 – 500 kV Loy Yang Power Station (LYPS)

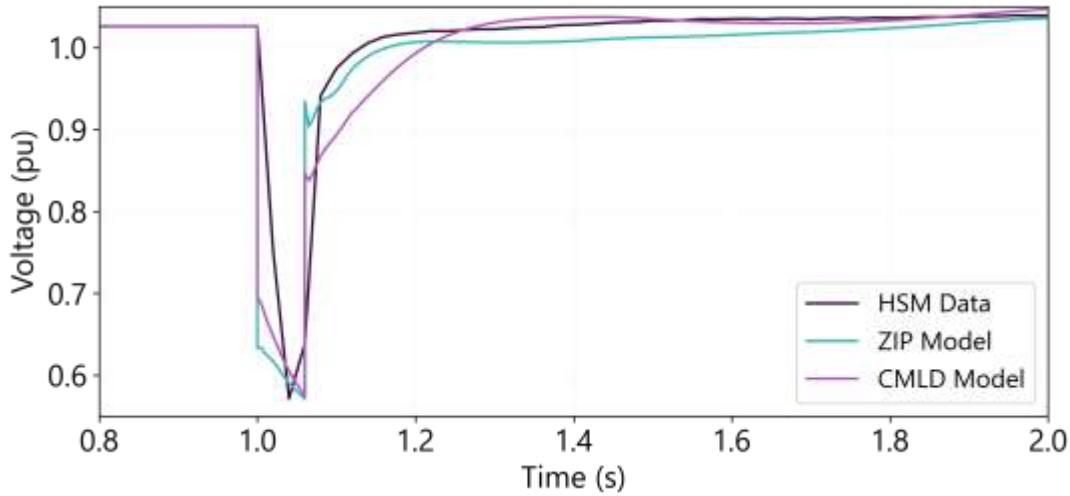

Figure 34 Voltage – 8 March 2018 – 22 kV Bendigo Terminal Station (BETS)

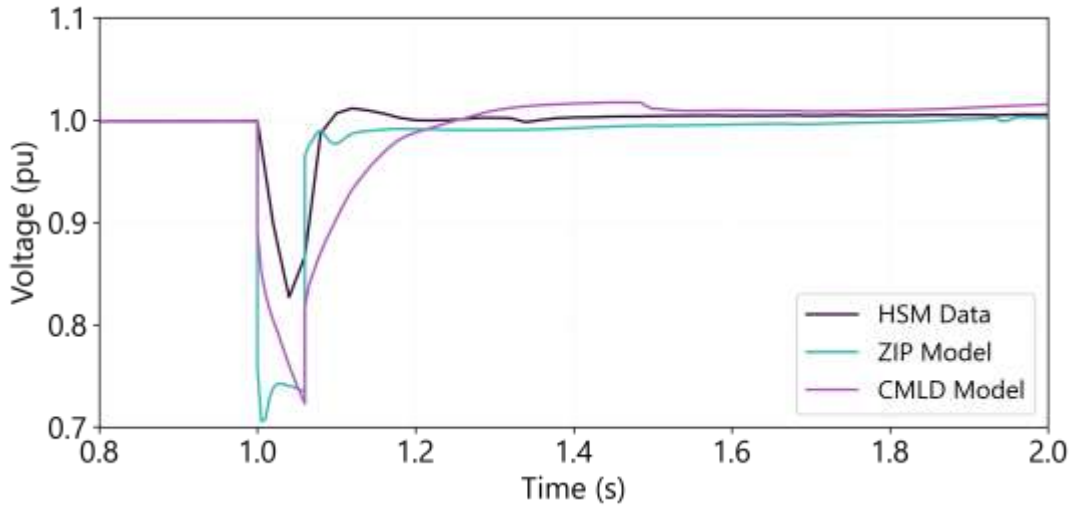

Figure 35 shows the active and reactive power measurements at the same locations. Observations at LYPS are illustrative of typical measurements at most other locations in the network where monitoring was available. Active power is represented well during the transient and steady-state periods. For reactive power, both the CMLD and ZIP models somewhat overestimate peak reactive power flows during the fault, and the CMLD model shows slightly longer recovery times, likely related to the voltage discrepancies. This overestimation of peak reactive flows is a known limitation in PSS®E and, in some cases, PSCAD. It may be partially attributed to the lack of transformer saturation data in PSS®E and the lack of under-excitation and over-excitation limiter modelled for the generator Automatic Voltage Regulators (AVRs) in the region, which would effectively damp and limit peak reactive power flows. It may also be attributed to the shortcomings of existing HSM data[91] which cannot accurately

[91] The HSMs that AEMO has access to at the transmission level are Phasor Measurement Units (PMUs) with low (20 ms) sampling rates. PMUs perform extensive waveform filtering and data processing to create synchrophasors. This distorts the resulting data relative to the source waveform.

capture transient or fault events because in such cases the waveform is not sinusoidal and changes amplitude, phase angle and frequency over a very short interval. This is discussed in more detail in Section 9.7.

The HSM data indicates a small decrease in steady state reactive power post disturbance (when measured at 60 s post disturbance, not shown in the figures below). This is reasonably well replicated by both the CMLD and ZIP models.

Figure 35 Active/reactive power – 8 March 2018

500/21 kV Loy Yang Power Station (LYPS) Transformer A1 Feeder

Active power

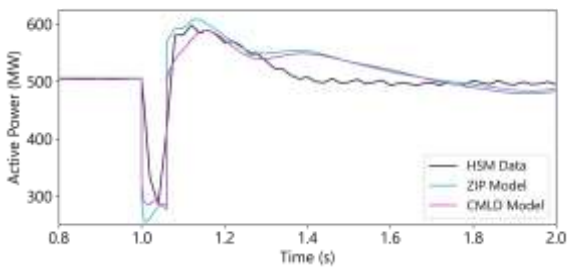

Reactive power

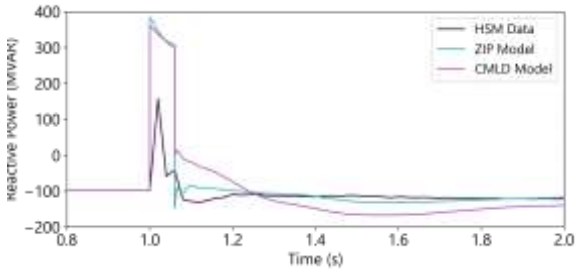

22 kV Bendigo Terminal Station (BETS) Transformer 2 Feeder

Active power

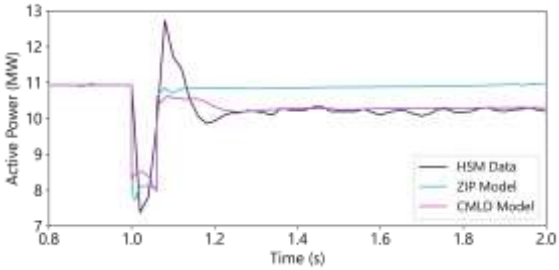

Reactive power

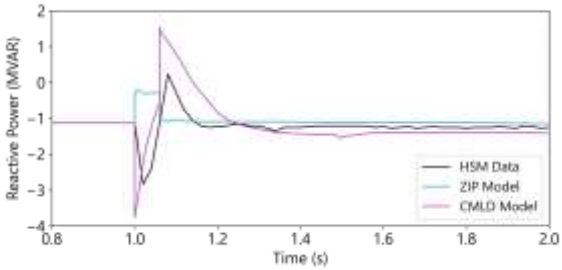

At BETS, also shown in Figure 35, neither the CMLD nor ZIP model accurately captures the spike in active power immediately post fault. However, the CMLD model matches steady-state recovery well, providing a significant improvement over the ZIP model. Reactive power measurements at BETS are also better matched by the CMLD model than the ZIP model. The minimum and maximum peaks are somewhat overestimated, and recovery is somewhat slower than HSM observations. This may be attributed to the limited sampling rate of HSM (50 Hz), whereby sub-transient phenomena during a fault may peak and decay in less than three cycles, and may not be captured with 50 Hz sampling rates (discussed further in Section 9.7). Steady-state reactive power shows a good match.

Where mismatches with observations are apparent for both the CMLD and ZIP models, it appears unrelated to the load model. This is likely due to network misrepresentation in PSS®E and limitations of the state estimator to determine an accurate network state. It could also be attributed to incorrect positive sequence transmission line

data. AEMO has opted to leave the network state as represented in OPDMS and tune the models as close to the OPDMS representation as possible[92].

5.1.4 SCADA measurements

Figure 36 shows the total measured load (from SCADA) in Victoria, compared with the performance of the CMLD model and the existing ZIP model. The CMLD model was tuned to match the load change measured at 60s post disturbance (represented by the green dashed line in Figure 36). The green "target range" indicates the margin of uncertainty. For this event, the target load change is 243 MW, and the load disconnection is estimated to be in the range of 155 MW to 300 MW.

The CMLD model predicts the target estimated load disconnection to within the uncertainty margin (slightly over-predicting the central target range). The ZIP model cannot represent any load disconnection.

Figure 36 Operational demand measurements (SCADA) – Victoria Total – 8 March 2018

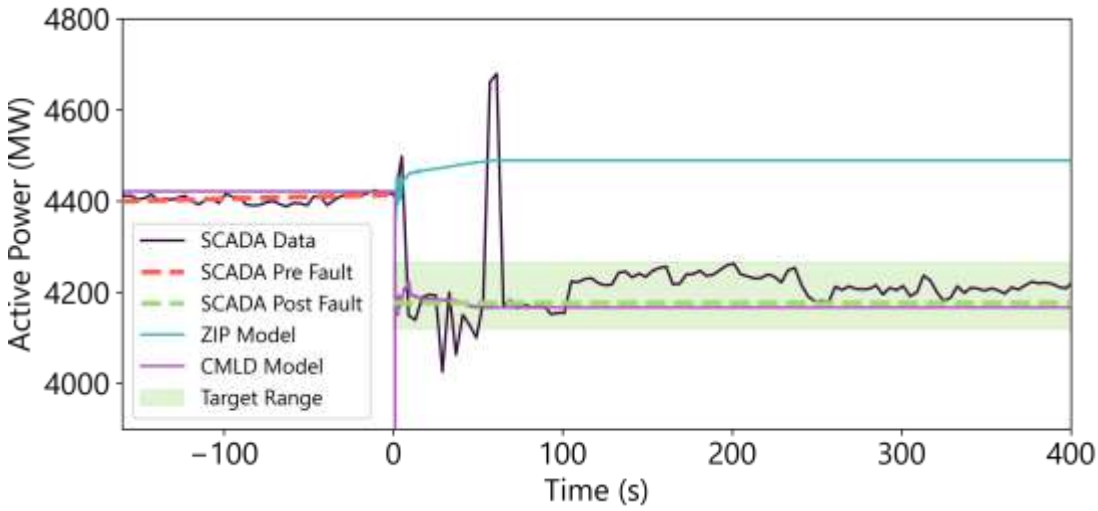

Load change in the Melbourne metropolitan area was also measured and found to be comparable between the SCADA and CMLD model representation.

5.1.5 Assessment of model performance

Table 25[93] summarises the performance of the CMLD model for this disturbance. Green indicates the CMLD model provides a good match to HSM, orange indicates the CMLD model provides a fair match to HSM, red indicates the CMLD model provides a poor match to HSM. A cross indicates where the ZIP model performs better than CMLD, a tick shows where the CMLD model performs at least as well as the ZIP model, and a double tick indicates where the CMLD model performs significantly better than the ZIP model.

[92] Some preliminary tuning of bus voltages and generator reactive power limits is required prior to dynamic simulation in PSS®E.

[93] See Section 4.5.2 for further explanation on this table.

Table 25 Assessment of model performance – 8 March 2018

Quantity	Characteristic	CMLD estimate	CMLD model equal (✓) or better (✓✓) than ZIP?	Commentary
Voltages	Voltage overshoot	Good match	✓	CMLD accurately estimates peak voltage overshoot magnitude and stays within normal voltages as defined in the NER (0.9 to 1.1 pu).
	Voltage recovery rate	Fair match	✗	CMLD voltage recovery speed is slower than HSM data but still recovers to the normal voltage in < 0.25s.
	Steady-state post disturbance	Good match	✓	CMLD voltages are accurate (settle to within 5% of the HSM data for all voltage channels).
Active power	During dynamic state	Fair match	✓	CMLD aligned with HSM for most assessed channels. Peak magnitudes are sometimes overestimated.
	Steady-state post disturbance	Good match	✓✓	CMLD aligned with HSM
Reactive power	During dynamic state	Fair match	✓✓	CMLD trajectory aligned with HSM data for all channels. Peak flows are somewhat overestimated, and CMLD shows slightly longer recovery times.
	Steady-state post disturbance	Good match	✓	CMLD aligned with HSM
Load	Load change	Good match	✓✓	SCADA: 243 MW decrease (60 s post disturbance) CMLD: 254 MW decrease CMLD overestimates load disconnection by ~5%% but is within the target range.

5.2 11 April 2018 – South Australia

5.2.1 Event overview

Table 26 Event summary – 11 April 2018

Date and time	11 April 2018, 16:47 Although this event occurred during the daytime, minimal DPV was generating, so it was modelled in PSS®E with no DPV generation operating.
Region	South Australia
Description of the event	Unplanned transmission system outage in South Australia. The Cherry Gardens – Torrens Island B (TIPS B) line tripped.
Minimum voltage recorded	0.69 pu positive sequence at Torrens Island A Power Station (TIPS A) (from HSM Data)
Operational demand prior to the event	2,270 MW (from SCADA data)
Estimated change in operational demand	144 MW decrease (from SCADA data)

Figure 37 Map – 11 April 2018

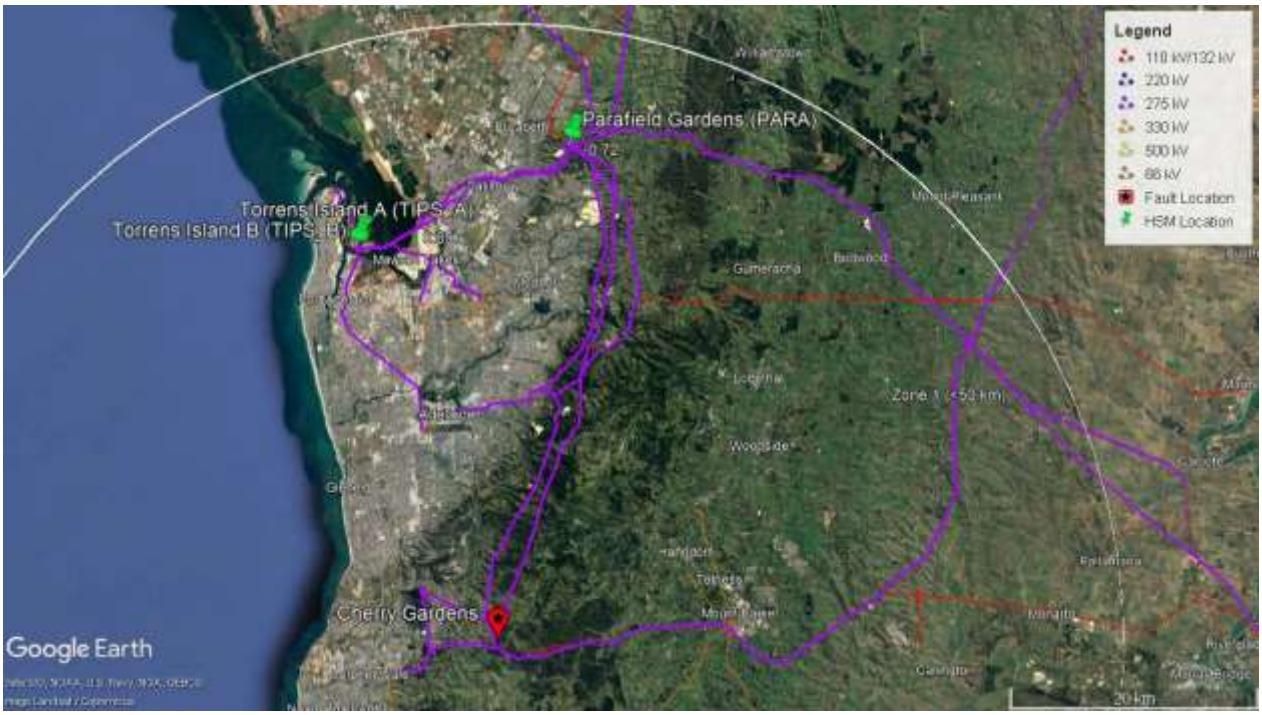

5.2.2 Replication in PSS®E

The following element changes were made in PSS®E to replicate this case:

Table 27 Simulation event summary – 11 April 2018

Time (s)	Events/comments
0.0	Start simulation
1.0	Apply branch fault on the 275 kV Torrens Island B generator 2 (TIPS B G2) (PSS®E bus 53385) to Cherry Gardens (PSS®E bus 53770) line
1.07	Clear branch fault on the 275 kV Torrens Island B generator 2 (TIPS B G2) (PSS®E bus 53385) to Cherry Gardens (PSS®E bus 53770) line Trip 275 kV TIPS B bus (PSS®E bus 53385) to Cherry Gardens (PSS®E bus 53770) line
60	End simulation

5.2.3 High speed measurements

Figure 38 shows the voltages at the 275 kV Para bus close to the fault. Observations at Para West illustrate the voltage response at all locations with HSM data available[94], with the voltage depressions (from the applied fault impedance) closely matching the 275 kV measurements. In this disturbance, the CMLD model shows a similar voltage recovery profile to the HSM and demonstrates an improvement compared with the ZIP model, which shows a voltage recovery rate that is too rapid. Voltage overshoot is slightly higher than observed in HSM but

[94] HSM data was available at the following locations: 275 kV Davenport, 275 kV Para West, 275 kV South East, 275 kV TIPS B, and 275 kV TIPS A.

remains well less than 1.1 pu and relatively consistent with observations. The overshoot may be attributed to the lack of transformer saturation characteristics in PSS®E, as mentioned in Section 5.1.3.

The steady-state voltage after the disturbance is comparable with observations for all models.

Figure 38 Voltage – 11 April 2018 – Para West Bus 275 kV

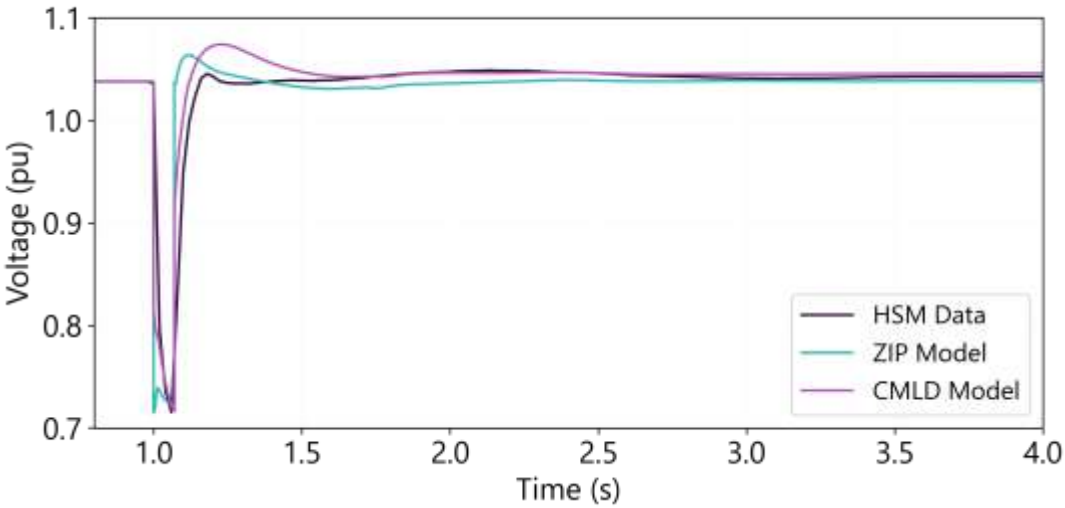

Figure 39 shows the active and reactive power measurements at the 275 kV Torrens Island A (TIPS A) to Northfield line and 275 kV TIPS B G1 feeder, both in the vicinity of the disturbance. Observations on the TIPS A to Northfield line are illustrative of typical measurements recorded in this event. The spike in active power flows immediately following the fault is underestimated by both CMLD and ZIP. Steady-state active and reactive power (measured at 60 s post disturbance, not shown in the figures below) is reasonably well represented by CMLD and somewhat overestimated by ZIP. The trajectory of the reactive power is accurately represented by CMLD, although the minimum and maximum peak reactive flows are overestimated during the transient period (for possible reasons as discussed in Section 9.7). This presents an improvement over the ZIP model, which does not accurately depict the dynamic reactive power response trajectory in some observations (including the TIPS A to Northfield line HSM).

The TIPS B G1 feeder is shown for comparison since peak reactive power flows are misrepresented at this location. Figure 39 shows that the active power trajectory and peak flows during the fault and post-fault steady-state response are reasonably well represented. The reactive power trajectory during the transient period and steady-state post fault aligns with observations. However, the peak reactive power flows during the transient period significantly exceed the observations (for both the CMLD and ZIP models). Because this mismatch is observed for both the CMLD and ZIP models, this suggests misrepresentation of the network components in the PSS®E model at this location, so mismatches are likely unrelated to the load model.

Figure 39 Active/reactive power – 11 April 2018

275 kV TIPS A to Northfield Feeder

Active power

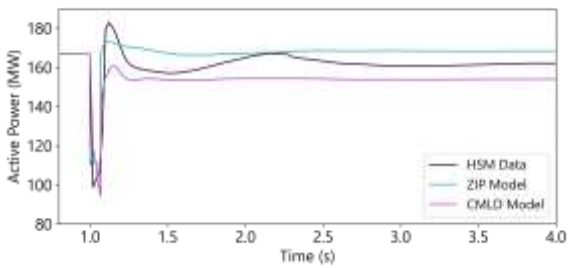

Reactive power

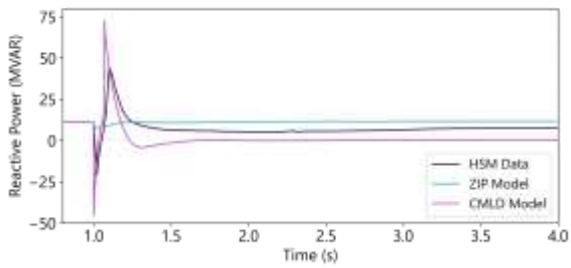

275 kV TIPS B G1 Feeder

Active power

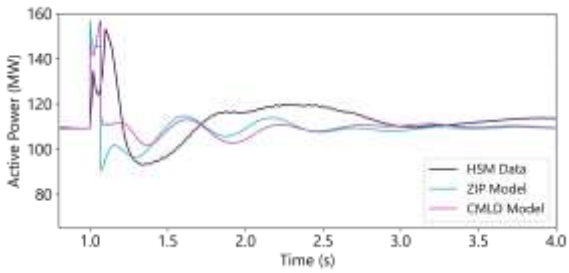

Reactive power

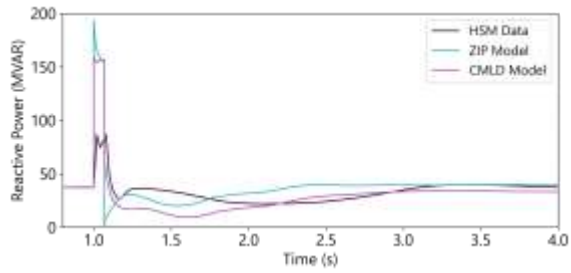

5.2.4 SCADA measurements

Figure 40 shows the total measured load (from SCADA) in South Australia, compared with the performance of the CMLD model and the existing ZIP model. For this case, approximately 144 MW of load disconnection in South Australia was estimated, but due to uncertainty in the measured SCADA data, this has a relatively wide uncertainty range (represented by the green range band in Figure 40).

Figure 40 Operational demand measurements (SCADA) – South Australia total – 11 April 2018

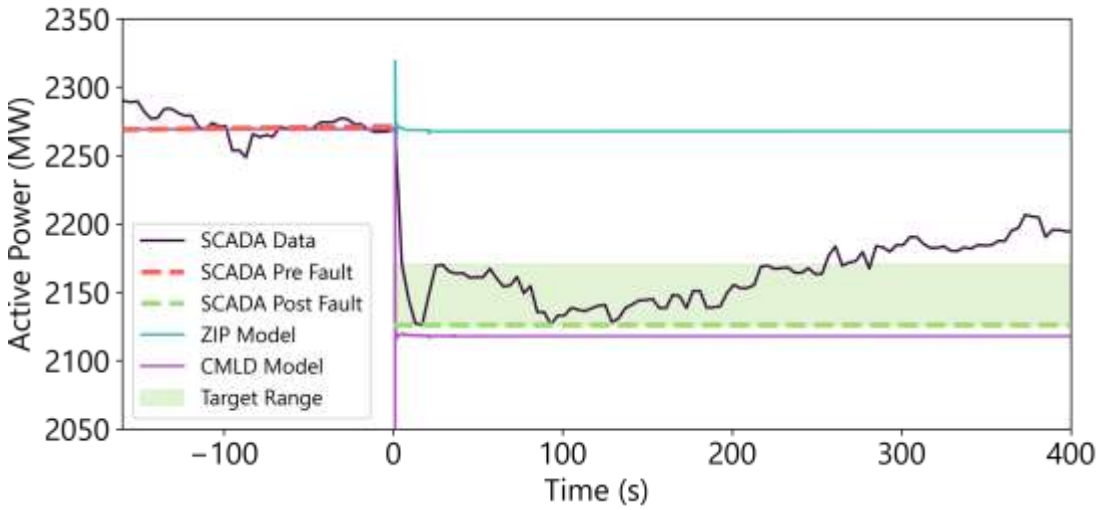

The CMLD model achieves a satisfactory estimate of load disconnection, overpredicting only slightly by ~5% (measured at 92 s post disturbance). In contrast, the ZIP model cannot represent any load disconnection.

Load change in the Adelaide metropolitan area was also measured and found to be comparable between the SCADA and CMLD model representation.

5.2.5 Assessment of model performance

Table 28[95] summarises the performance of the CMLD model for this disturbance. Green indicates the CMLD model provides a good match to HSM, orange indicates the CMLD model provides a fair match to HSM, red indicates the CMLD model provides a poor match to HSM. A cross indicates where the ZIP model performs better than CMLD, a tick shows where the CMLD model performs at least as well as the ZIP model, and a double tick indicates where the CMLD model performs significantly better than the ZIP model.

Table 28 Assessment of model performance – 11 April 2018

Quantity	Characteristic	CMLD estimate	CMLD model equal (✓) or better (✓✓) than ZIP?	Commentary
Voltages	Voltage overshoot	Fair match	✗	CMLD marginally overestimates peak voltage overshoot magnitude, although it stays within the normal voltage as defined in the NER (0.9 to 1.1 pu).
	Voltage recovery rate	Good match	✓✓	CMLD aligned with HSM
	Steady-state post disturbance	Good match	✓	CMLD accurate (settles to within 5% of the HSM data for all voltage channels).
Active power	During dynamic state	Fair match	✓	Peak magnitudes are underestimated.
	Steady-state post disturbance	Good match	✓✓	CMLD aligned with HSM
Reactive power	During dynamic state	Fair match	✓✓	The trajectory of the CMLD reflects the HSM data for most channels. Peak min/max flows are slightly overestimated.
	Steady-state post disturbance	Good match	✓	CMLD aligned with HSM
Load	Load change	Good match	✓✓	SCADA: 144 MW decrease (92 s post disturbance) CMLD: 151 MW decrease CMLD slightly underestimates load disconnection by 5% and is within range (when measured at 92 s post disturbance).

[95] See Section 4.5.2 for further explanation on this table.

5.3 18 February 2019 – Victoria

5.3.1 Event overview

Table 29 Event summary – 18 February 2019

Date and time	18 February 2019, 19:56[96]
Region	Victoria
Description of the event	Trip of the 500 kV Sydenham to Moorabool No 2 (SYTS-MLTS 2) line and the 500 kV Sydenham to Keilor (SYTS-KTS) line. The trip of the SYTS-MLTS 2 line was due to a high voltage (HV) fault on the line, and all protection equipment operated as designed and as expected to clear the fault. The cause of the fault has not been conclusively determined. The trip of the SYTS-KTS line was due to the operation of a redundant element of the protection system that should not have been in service. There was no HV fault on the SYTS-KTS line.
Minimum voltage recorded	0.78 pu positive sequence recorded at Tarrone Terminal Station (TRTS) (from HSM data)
Operational demand prior to the event	5,313 MW (from SCADA data)
Estimated change in operational demand	100 MW decrease (from SCADA data)

Figure 41 Map – 18 February 2019

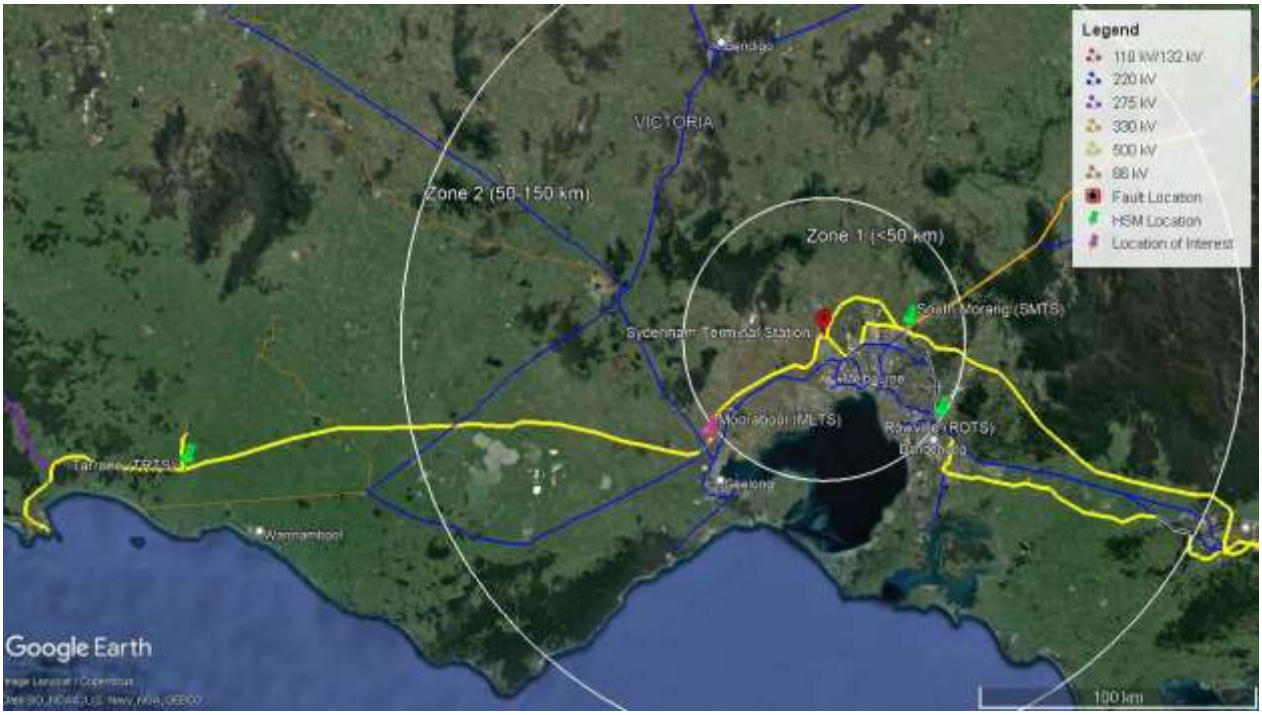

5.3.2 Replication in PSS®E

The following element changes were made in PSS®E to replicate this case:

[96] AEMO. Trip of the Sydenham – Moorabool No. 2,500 kV line and the Sydenham – Keilor 500 kV line on 18 February 2019, October 2019, at https://aemo.com.au/-/media/files/electricity/nem/market_notices_and_events/power_system_incident_reports/2019/mlts-syts-syts-kts-lines-18-feb.pdf?la=en&hash=D6F8378372E53C31F3A42F91B780F358.

Table 30 Simulation event summary – 18 February 2019

Time (s)	Events/comments
0.0	Start simulation
1.0	Apply branch fault on the 275 kV Sydenham (PSS®E bus 35760) to Moorabool (PSS®E bus 35480) line 2 (SYTS-MLTS 2)
1.07	Clear branch fault on the 275 kV Sydenham (PSS®E bus 35760) to Moorabool (PSS®E bus 35480) line 2 (SYTS-MLTS 2) Trip 275 kV SYTS (PSS®E bus 35760) to MLTS (PSS®E bus 35480) line 2
60	End simulation

5.3.3 High speed measurements

Figure 42 and **Figure 43** show the voltages close to the fault at 132 kV Tarrone Terminal Station (TRTS) and 330 kV South Morang Terminal Station (SMTS), respectively. Observations at these locations illustrate the voltage response observed at most locations in the network. The fault impedance applied to the 275 kV SYTS-MLTS line was correctly matched at all 132 kV, 220 kV and 330 kV HSM locations where HSM data was available[97].

The CMLD model shows a similar voltage recovery profile to the HSM (as well as can be determined from the resolution of the HSM). The CMLD model recovers slightly more slowly than HSM when voltage exceeds 0.9 pu, while the ZIP model recovers slightly more rapidly, especially at SMTS. Voltage overshoot is slightly underestimated but largely in line with observations. The steady-state voltage (measured at ~8 s after the disturbance, not shown) is also comparable with observations.

Figure 42 Voltage – 18 February 2019 – Tarrone Terminal Station (TRTS) 132 kV

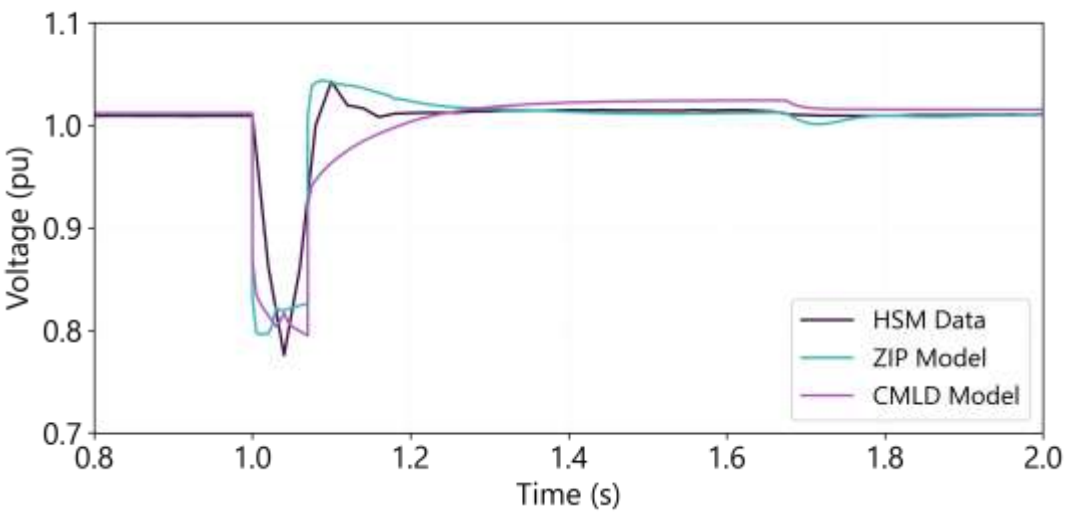

[97] HSM data was available at the following locations: 220/66 kV Red Cliffs, 132 kV Tarrone Terminal Station, 500/330 kV South Morang Terminal Station, 220 kV East Rowville Terminal Station.

Figure 43 Voltage – 18 February 2019 – South Morang Terminal Station (SMTS) 330 kV

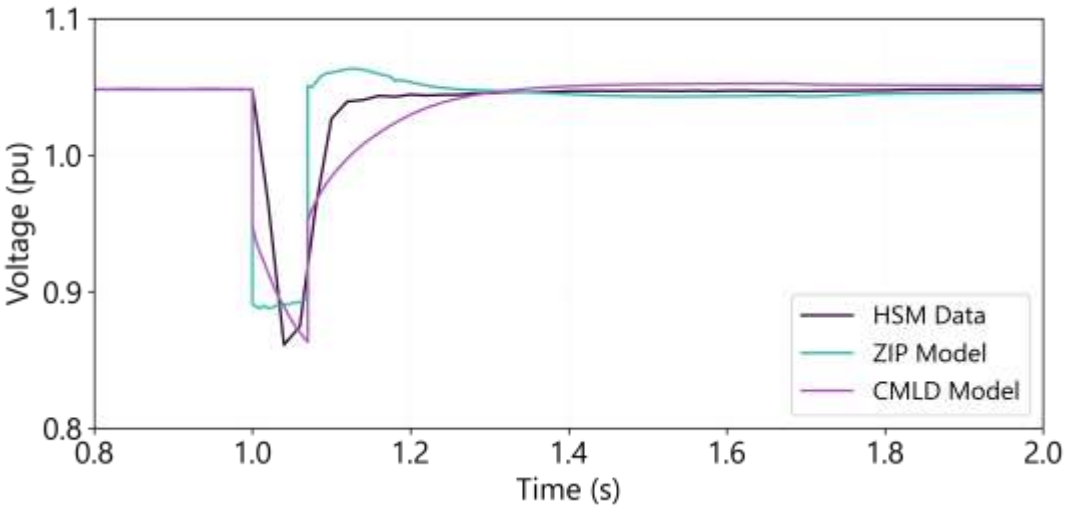

Figure 44 shows the active and reactive power measurements as seen from the 330 kV SMTS H1 transformer feeder (in the vicinity of the disturbance). Observations at this location are illustrative of typical measurements at most locations observed.

Figure 44 Active/reactive power – 18 February 2019

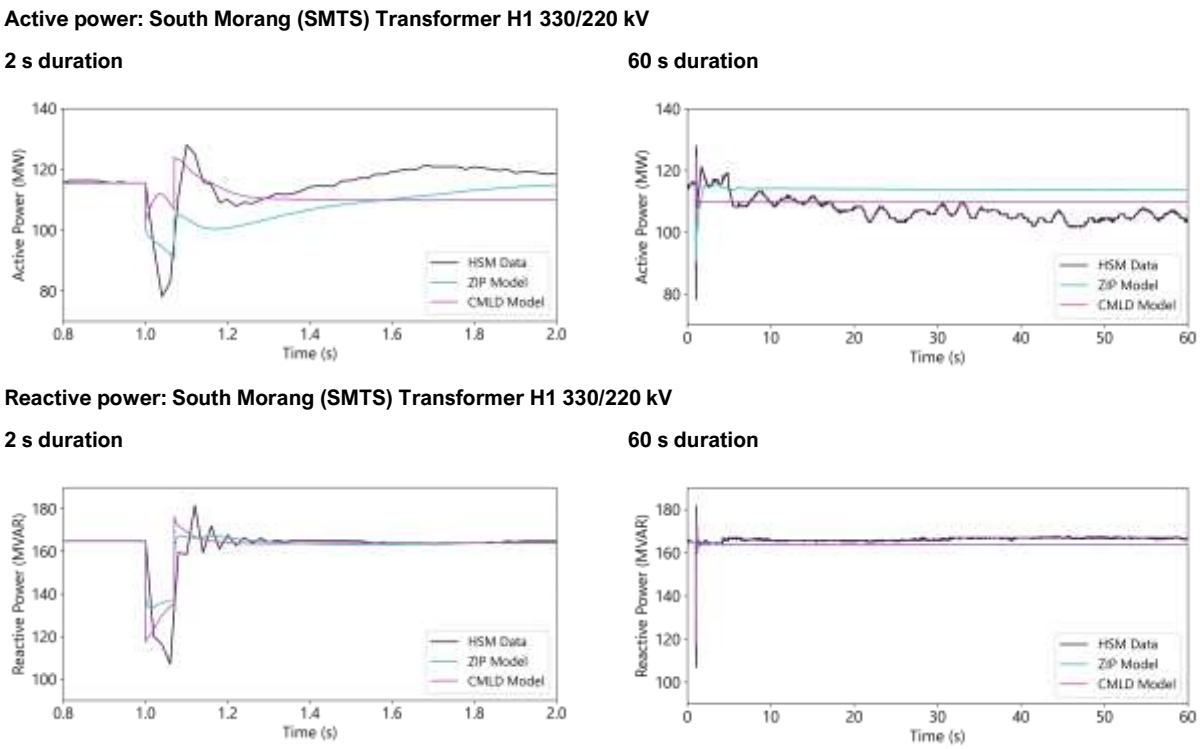

At SMTS, the CMLD approximately captures the trajectory of the active power flow on the line but underestimates the maximum and minimum flow during the transient period. Possible explanations for this mismatch include a misrepresentation of the transformer (and on-load tap-changer) in the PSS®E snapshot, or inability of the power

electronic logic block in the CMLD model to capture variable frequency drive (VFD) response during voltage disturbances accurately (see Section 9.7 for more details). The CMLD predicts an immediate decrease in active power at this location, while the HSM shows an initial return to pre-fault values, followed by a gradual decrease in the period 5-20 s to a level similar to that predicted by the CMLD. The CMLD model is unable to represent this gradual reduction in power flows. The ZIP model is unable to represent the observed reduction in the steady-state active power, over any timeframe.

The reactive power during the dynamic state, immediately post fault, and in the steady-state is well matched by CMLD for most cases but peak flows are sometimes overestimated (for example, at East Rowville, not shown).

5.3.4 SCADA measurements

Figure 45 shows the total measured load (from SCADA) in Victoria, compared with the performance of the CMLD model and the existing ZIP model. In this case, the target estimated load disconnection is 100 MW (with a range of uncertainty between 72 MW and 111 MW).

The CMLD model very accurately predicts this target load loss. The ZIP model cannot represent any load disconnection.

Figure 45 Operational demand measurements (SCADA) – Victoria total – 18 February 2019

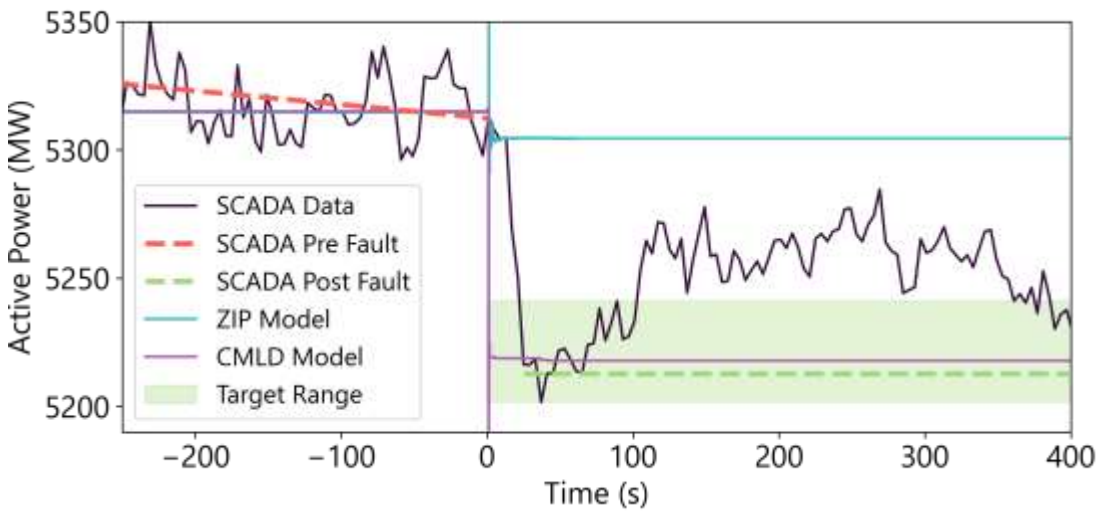

5.3.5 Assessment of model performance

Table 31 summarises the performance of the CMLD model for this disturbance. Green indicates the CMLD model provides a good match to HSM, orange indicates the CMLD model provides a fair match to HSM, red indicates the CMLD model provides a poor match to HSM. A cross indicates where the ZIP model performs better than CMLD, a tick shows where the CMLD model performs at least as well as the ZIP model, and a double tick indicates where the CMLD model performs significantly better than the ZIP model.

Table 31 Assessment of model performance – 18 February 2019

Quantity	Characteristic	CMLD estimate	CMLD model equal (✓) or better (✓✓) than ZIP?	Commentary
Voltages	Voltage overshoot	Good match	✓	The CMLD accurately estimates peak voltage overshoot magnitude and stays within the normal voltage as defined in the NER (0.9 to 1.1 pu).
	Voltage recovery rate	Good match	✓	CMLD is comparable to HSM.
	Steady-state post disturbance	Good match	✓	CMLD voltages are accurate (settles to within 5% of the HSM data for all voltage channels).
Active power	During dynamic state	Fair match	✓	CMLD has a reasonably similar trajectory to the HSM, although it underestimates peak power flows.
	Steady-state post disturbance	Good match	✓	CMLD is aligned with HSM at 40-60s post disturbance but underestimates active power immediately post disturbance.
Reactive power	During dynamic state	Fair match	✓	The trajectory of the CMLD reflects the HSM data for all channels. Peak flows are sometimes overestimated
	Steady-state post disturbance	Good match	✓	Comparable steady-state reactive power outcomes post disturbance, aligned with HSM.
Load	Load change	Good match	✓✓	SCADA: 100 MW decrease (40 s post disturbance) CMLD: 98 MW decrease CMLD very accurately predicts load loss (within the estimated target range).

5.4 17 April 2019 – South Australia

5.4.1 Event overview

Table 32 Event summary – 17 April 2019

Date and time	17 April 2019, 06:13
Region	South Australia
Description of the event	Torrens Island – Magill 275 kV line trip due to bushfire.
Minimum voltage recorded	0.62 pu positive sequence at Torrens Island B Power Station (TIPS B) (from HSM Data)
Operational demand prior to the event	1,389 MW (from SCADA data)
Estimated change in operational demand	127 MW decrease (from SCADA data)

Figure 46 Map – 17 April 2019

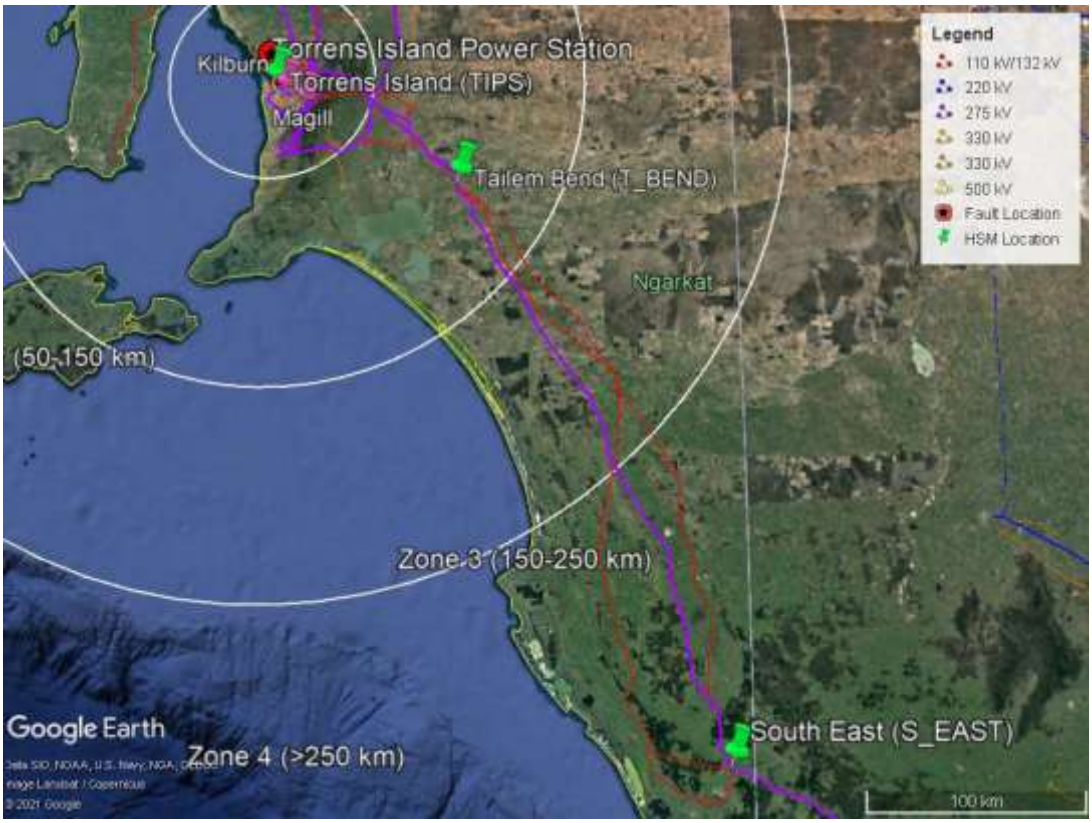

5.4.2 Replication in PSS®E

The following element changes were made in PSS®E to replicate this case:

Table 33 Simulation event summary – 17 April 2019

Time (s)	Events/comments
0.0	Start simulation
1.0	Apply branch fault on the 275 kV Torrens A Power Station (TIPS A) (PSS®E bus 53080) to Magill (PSS®E bus 53550) line
1.1	Clear branch fault on the 275 kV Torrens A Power Station (TIPS A) (PSS®E bus 53080) to Magill (PSS®E bus 53550) line Trip 275 kV TIPS A (PSS®E bus 53080) to Magill (PSS®E bus 53550) line
60	End simulation

5.4.3 High speed measurements

Figure 47 and **Figure 48** show the voltages at TIPS A (close to the fault), and a more remote South East bus location that experienced overvoltage's. Observations at TIPS A illustrate the voltage response at most measured locations in the network[98]. At the South East bus (close to the Victoria border), voltages are accurately represented during and post fault, implying that the line data is well represented in PSS®E in this snapshot.

[98] HSM data was available at the following locations: 275 kV South East to Heywood Feeder, 275 kV Tailem Bend to Cherry Gardens Feeders, 275 kV Tailem Bend to South East Feeder, 275 kV Torrens Island A to Northfield Feeder, 275 kV Torrens Island A (Kilburn), and 275 kV Torrens Island to Cherry Gardens Feeder.

In this disturbance, the CMLD model shows a very accurate voltage recovery profile compared to the HSM, demonstrating a good improvement from the ZIP model (which recovers too quickly). The voltage overshoot estimated by the CMLD model is in line with observations.

At the South East bus, the CMLD model shows a significant improvement over the ZIP model since the ZIP model overestimates the voltage overshoot.

The steady-state voltage after the disturbance is comparable with observations for both models.

Figure 47 Voltage – 17 April 2019 – 275 kV Torrens Island Power Station A (TIPS A)

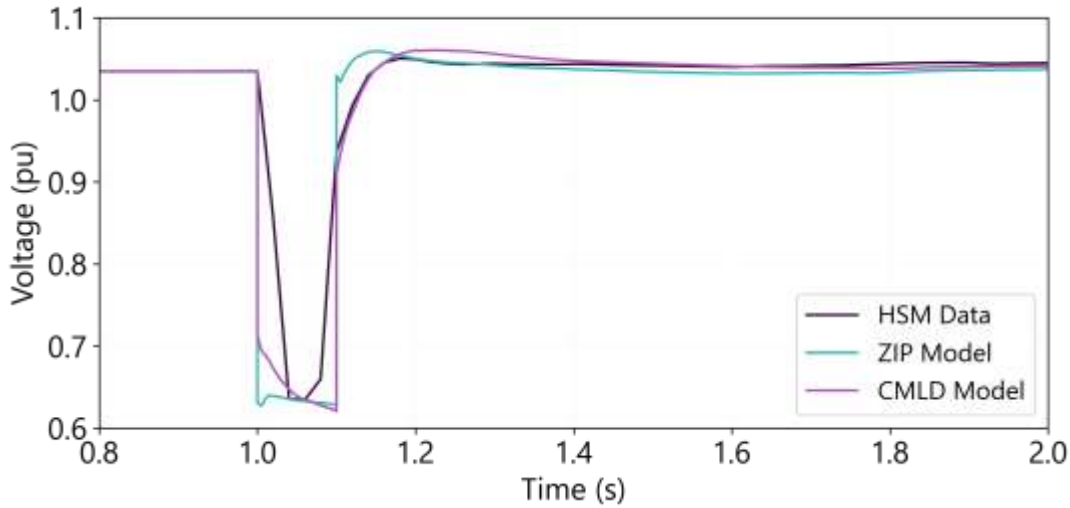

Figure 48 Voltage – 17 April 2019 – 275 kV South East Bus

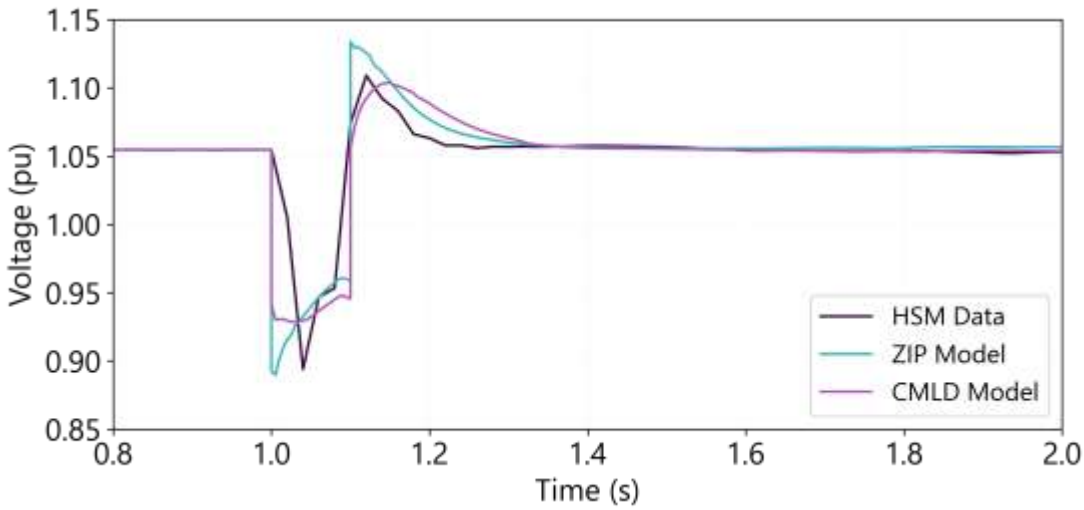

Figure 49 shows the active power measurements for TIPS A to Kilburn. This illustrates typical measurements at most locations in the network. The CMLD reasonably accurately predicts the trajectory of the transient active power measurements at this location, but the peak magnitude immediately after the fault is somewhat

underestimated. This may be due to the inability of the power electronic logic block in the CMLD model to capture the VFD response during voltage disturbances (see Section 9.7).

The CMLD model accurately predicts steady state active power following the fault, while the ZIP model is unable to replicate the observed reduction in steady-state active power following the fault (shown in the 15 s duration figure on the right).

Figure 49 Active power – 17 April 2019 – Torrens Island Power Station A (TIPS A) to Kilburn

2 s duration **15 s duration**

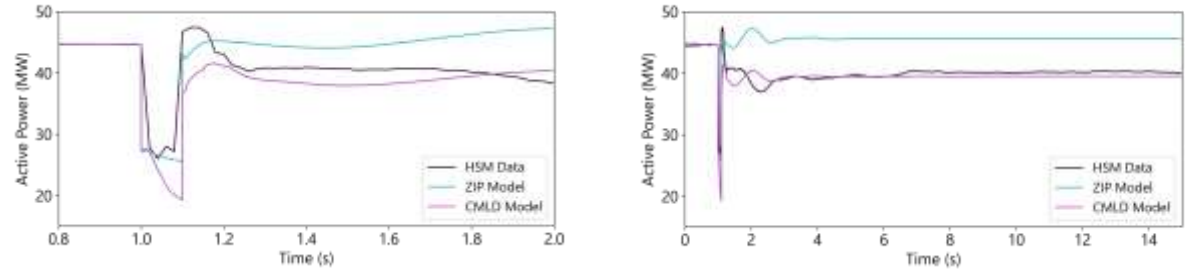

For contrast, **Figure 50** shows observations at South East, at the same voltage level as the faulted line, but over 400 km away. The ZIP and CMLD models show some inaccuracy during and immediately following the fault, but the CMLD model matches steady-state recovery levels reasonably well, providing a significant improvement over the ZIP model.

Figure 50 Active power – 17 April 2019 – 275 kV South East to Heywood Feeder (HYTS) 2

2 s duration **15 s duration**

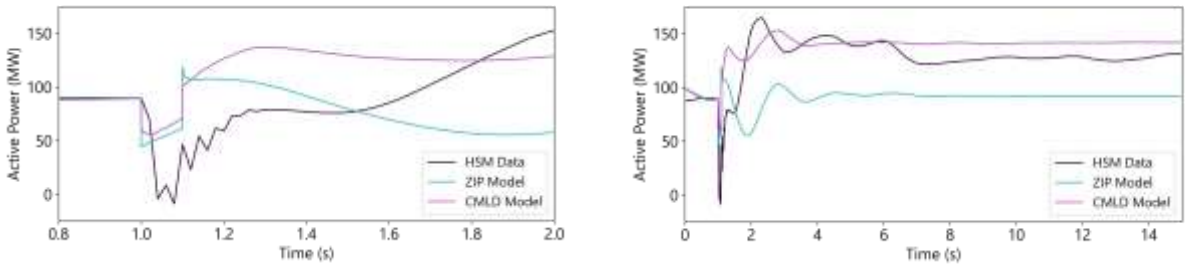

Figure 51 shows reactive power measurements at the same locations. The CMLD accurately captures the general trajectory and post fault steady-state values for reactive power measurements but somewhat overestimates the magnitude of reactive power changes during the transient period (possible reasons for this are discussed in Section 9.7).

Where mismatches are apparent for both the CMLD and ZIP models, these are likely related to the misrepresentation of network components in PSS®E, which is particularly influential in this disturbance due to the close proximity of the selected HSM's to generator transformers, large synchronous generators and associated auxiliary loads.

Figure 51 Active/reactive power – 17 April 2019

Torrens Island Power Station (TIPS) A to Kilburn

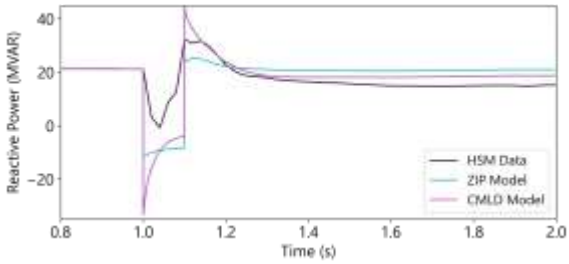

South-East to Heywood Branch (HYTS) 2

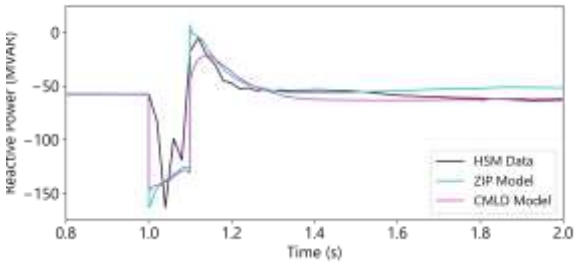

5.4.4 SCADA measurements

Figure 52 shows the total measured load (from SCADA) in South Australia, compared with the performance of the CMLD model and the existing ZIP model. The CMLD relatively somewhat underpredicts the 127 MW of load loss estimated from SCADA measurements (measured at 60 s post disturbance) for the South Australia region for this case. The ZIP model cannot represent any load disconnection.

Figure 52 Operational demand measurements (SCADA) – South Australia total – 17 April 2019

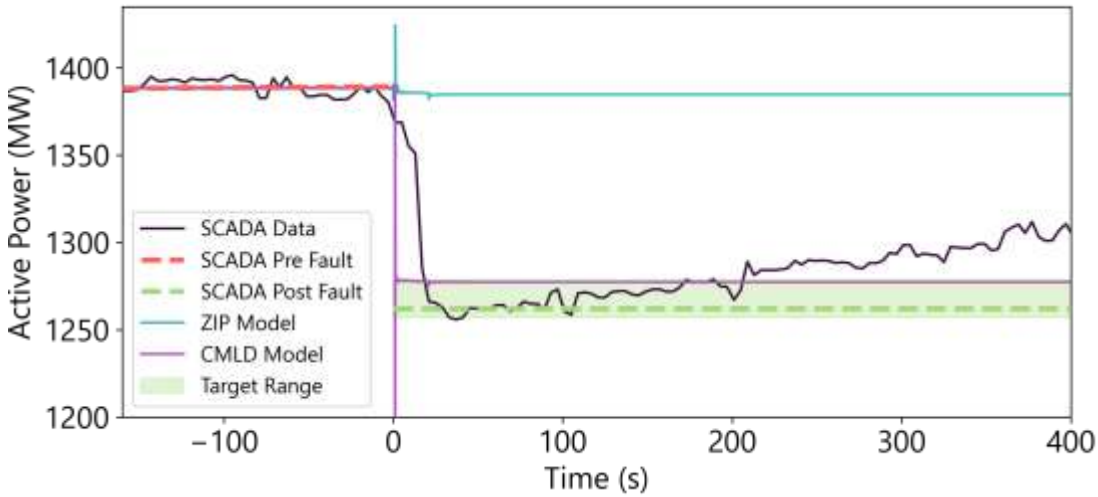

Load change in the Adelaide metropolitan area was also measured and found to be comparable between the SCADA and CMLD model representation.

5.4.5 Assessment of model performance

Table 34[99] summarises the performance of the CMLD model for this disturbance. Green indicates the CMLD model provides a good match to HSM, orange indicates the CMLD model provides a fair match to HSM, red indicates the CMLD model provides a poor match to HSM. A cross indicates where the ZIP model performs better

[99] See Section 4.5.2 for further explanation on this table.

than CMLD, a tick shows where the CMLD model performs at least as well as the ZIP model, and a double tick indicates where the CMLD model performs significantly better than the ZIP model.

Table 34 Assessment of model performance – 17 April 2019

Quantity	Characteristic	CMLD estimate	CMLD model equal (✓) or better (✓✓) than ZIP?	Commentary
Voltages	Voltage overshoot	Good match	✓✓	CMLD accurately estimates peak voltage overshoot magnitude even when bus voltages during the fault exceed the normal voltage as defined in the NER (0.9 to 1.1 pu).
	Voltage recovery rate	Good match	✓✓	CMLD aligned with HSM
	Steady-state post disturbance	Good match	✓	CMLD voltages are accurate (settles to within 5% of the HSM data for all voltage channels).
Active power	During dynamic state	Fair match	✓	CMLD matches the general trajectory of the power waveform, but the peak power flows are not well represented.
	Steady-state post disturbance	Good match	✓✓	CMLD steady-state power is representative of the HSM data.
Reactive power	During dynamic state	Fair match	✓	The trajectory of the CMLD reflects the HSM data for all channels. Peak flows are overestimated.
	Steady-state post disturbance	Good match	✓	Comparable steady-state reactive power outcomes post disturbance, aligned with HSM.
Load	Load change	Good match	✓✓	SCADA: 127 MW decrease (60 s post disturbance) CMLD: 111 MW decrease CMLD underestimates load disconnection by 12% but is within range (when measured at 60 s post disturbance)

5.5 22 February 2021 - Queensland

5.5.1 Event overview

Table 35 Event summary – 22 February 2021

Date and time	22 February 2021, 21:20[100]
Region	Queensland
Description of the event	2PG fault (direct lightning strike) on the Mt England to Wivenhoe (Feeder 824) line. South Pine SVC tripped due to AC changeover failure. All equipment returned to service by 2214 hrs.
Minimum voltage recorded	0.15 pu positive sequence recorded at Swanbank E Substation (from HSM data)
Operational demand prior to the event	7,977 MW (from SCADA data)
Estimated change in operational demand	533 MW decrease (from SCADA data)

[100] AEMO. Trip of Mount England to Wivenhoe Power Station 275 kV Line and South Pine Static Var Compensator on 22 February 2021, July 2021, at https://aemo.com.au/-/media/files/electricity/nem/market_notices_and_events/power_system_incident_reports/2021/trip-of-mount-england-to-wivenhoe-power-station-275-kv-line-and-south-pine-static-var-compensator.pdf?la=en.

Figure 53 Map – 22 February 2021

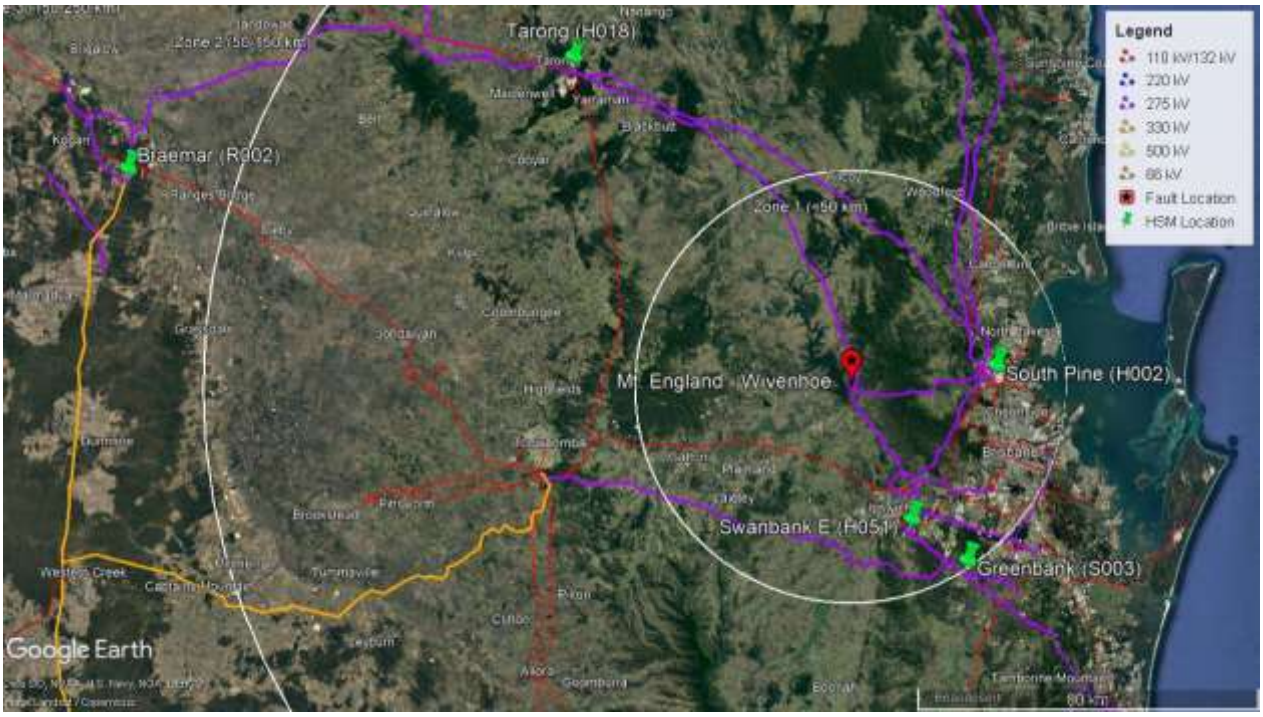

5.5.2 Replication in PSS®E

The following element changes were made in PSS®E to replicate this case:

Table 36 Simulation event summary – 22 February 2021

Time (s)	Events/comments
0.0	Start simulation
1.0	Apply 2PG fault on the 275 kV Mt England bus (PSS®E bus 441280)
1.07	Clear 2PG fault on the 275 kV Mt England bus (PSS®E bus 441280) Trip 275 kV Mt England (PSS®E bus 441280) to Wivenhoe (PSS®E bus 442880) line (branch 2)
3.07	Trip South Pine SVC (PSS®E bus 440282)
60	End simulation

5.5.3 High speed measurements

Figure 54 and **Figure 55** show the voltages at South Pine and Swanbank (both close to the fault). Observations at South Pine are illustrative of the voltage response observed at most locations in the transmission network[101], while the observations at Swanbank are somewhat different, and similar to observations at Greenbank[102].

The HSM data indicates a deep voltage measurement (0.2 pu) at Swanbank and a moderate depth at South Pine (0.5 pu). When the fault is calibrated in the PSS®E model to produce the observed voltage depth at South Pine,

[101] HSM data was available for the following locations: 275 kV Mt England, 275 kV Rocklea, 275 kV Belmont, 275 kV Braemar and 275 kV Tarong buses.

[102] HSM data in this vicinity included: 275 kV Greenbank to Molendinar Feeder, 275 kV Greenbank to Mudgeeraba Feeders, and 275 kV Swanbank bus.

the voltage depth at Swanbank is underestimated by both the CMLD and ZIP models. Similar observations are made at Greenbank. Powerlink has noted discrepancies between the Queensland positive sequence impedance line data (in OPDMS) and its network model data, which manifests as a mismatch in voltage when a fault is applied during dynamic simulations, as observed in this case. The mismatch seems to be a misrepresentation of the network components in PSS®E. Following discussions with Powerlink, AEMO opted to leave the network state as represented in OPDMS.

In this disturbance, the CMLD model shows a similar voltage recovery profile to the HSM, significantly improving on the ZIP model (which consistently recovers too quickly). The ZIP model also shows a significant voltage overshoot at all locations, which is not observed in HSM, while the CMLD model matches voltage overshoot observations well.

Figure 54 Voltage – 22 February 2021 – 275 kV South Pine H002 bus

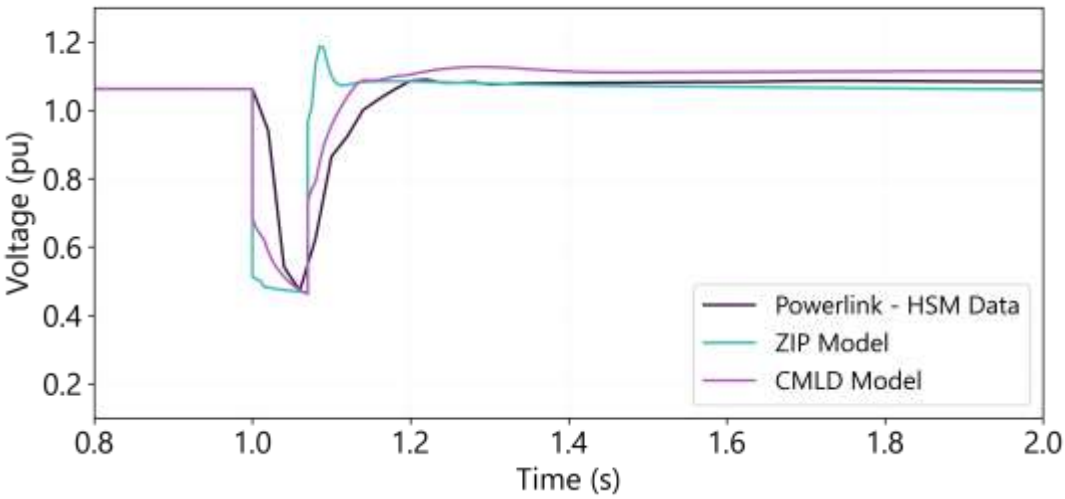

Figure 55 Voltage – 22 February 2021 – 275 kV Swanbank E H051 bus

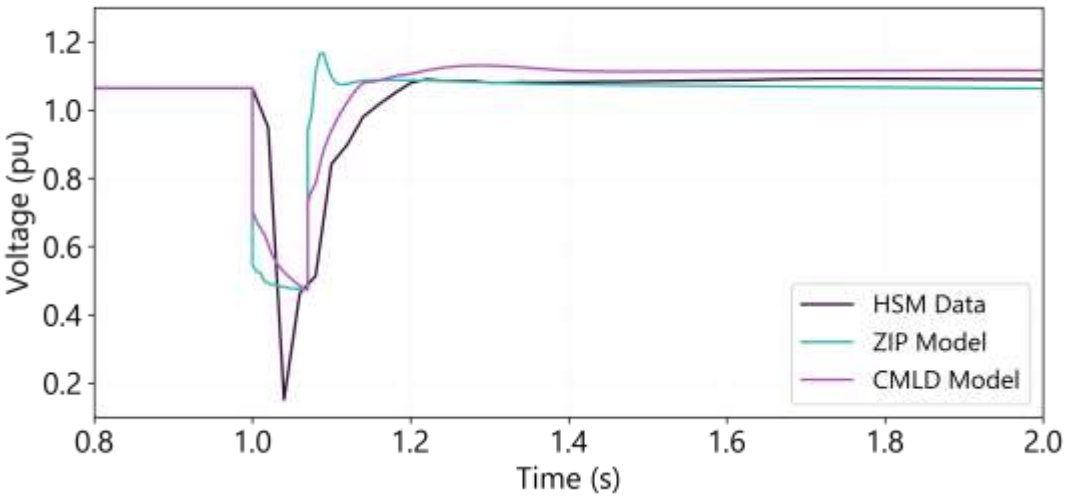

Figure 56 shows the active/reactive power measurements at South Pine, which illustrates typical measurements at most locations in the network. At South Pine, the CMLD model reasonably represents the active power during the transient and steady-state (measured at 60 s post fault) but slightly underestimates maximum flows immediately following the fault. This may be due to the inability of the power electronic logic block to capture the VFD response during voltage disturbances or the shortcomings of existing HSM data, as discussed in Section 9.7.

The ZIP model overestimates steady-state active power.

For reactive power, the CMLD trajectory is similar to observations, but the minimum and maximum flows are overestimated during the transient period. The steady-state reactive power outcomes post disturbance aligns well with the HSM. In contrast, the ZIP model does not reflect the observed trajectory and cannot represent the maximum and minimum and steady-state reactive power flows.

Figure 56 Active/reactive power – 22 February 2021 – South Pine 275 kV bus feeder to 275/110 kV H2 Transformer

Active power **Reactive power**

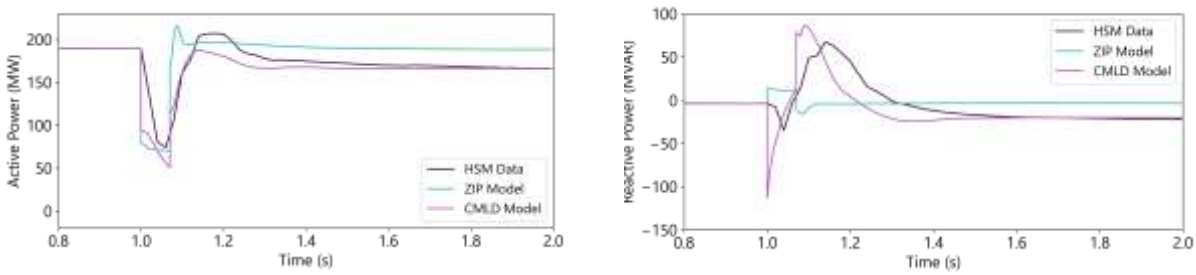

Figure 57 shows the active and reactive power measurements at the Swanbank to Greenbank line (unique to this location). At this location, the active and reactive power response of the CMLD model is comparable to the South Pine results. However, the lowest peak reactive power flows are four times that observed. Given the misrepresentation of the voltage levels at Swanbank, this is likely related to the network's misrepresentation in PSS®E, and the CMLD (or any other load model) is not expected to behave accurately.

Figure 57 Active/reactive power – 22 February 2021 – 275 kV Swanbank (SBK2) to Greenbank H051 Feeder 805

Active power **Reactive power**

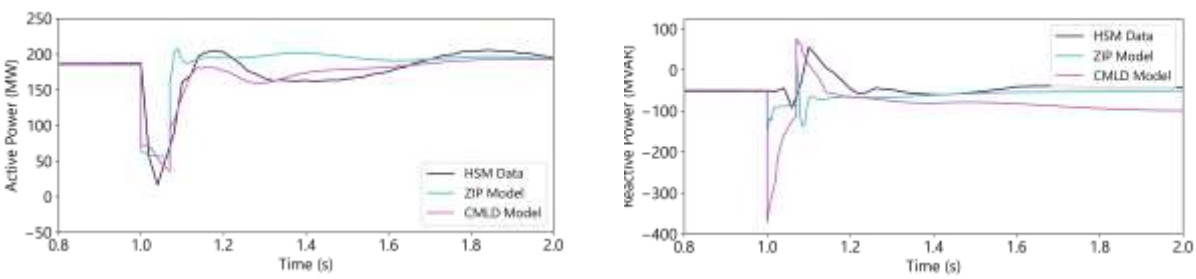

5.5.4 SCADA measurements

Figure 58 shows the total measured load (from SCADA) in Queensland, compared with the performance of the CMLD model and the existing ZIP model. The CMLD accurately predicts the 533 MW of load loss estimated from SCADA measurements for the Queensland region for this case when measured at 60 s post disturbance, to within the uncertainty range.

The ZIP model cannot represent any load disconnection.

Figure 58 Operational demand measurements (SCADA) – Queensland total – 22 February 2021

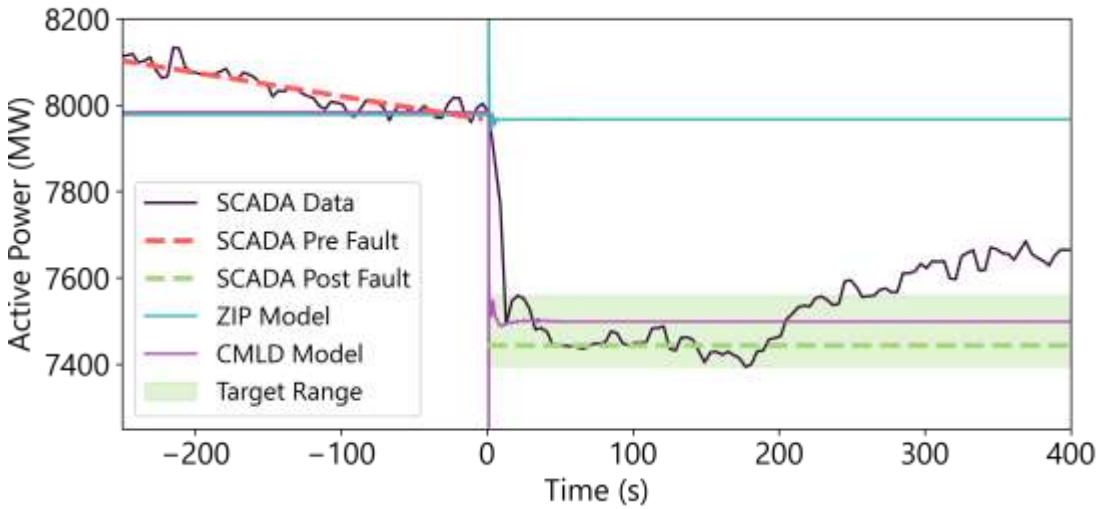

Load change in the Brisbane metropolitan area was also measured and found to be comparable between the SCADA and CMLD model representation.

5.5.5 Assessment of model performance

Table 37[103] summarises the performance of the CMLD model for this disturbance. Green indicates the CMLD model provides a good match to HSM, orange indicates the CMLD model provides a fair match to HSM, red indicates the CMLD model provides a poor match to HSM. A cross indicates where the ZIP model performs better than CMLD, a tick shows where the CMLD model performs at least as well as the ZIP model, and a double tick indicates where the CMLD model performs significantly better than the ZIP model.

Table 37 Assessment of model performance – 22 February 2021

Quantity	Characteristic	CMLD estimate	CMLD model equal (✓) or better (✓✓) than ZIP?	Commentary
Voltages	Voltage overshoot	Good match	✓✓	CMLD accurately estimates peak voltage overshoot magnitude and stays within the normal voltage as defined in the NER (0.9 to 1.1 pu).
	Voltage recovery rate	Good match	✓✓	CMLD aligned with HSM

[103] See Section 4.5.2 for further explanation on this table.

Quantity	Characteristic	CMLD estimate	CMLD model equal (✓) or better (✓✓) than ZIP?	Commentary
	Steady-state post disturbance	Good match	✓	CMLD voltages are accurate (settles to within 5% of the HSM data for all voltage channels).
Active power	During dynamic state	Good match	✓✓	CMLD has a similar trajectory to the HSM data. Max peak flows are somewhat underestimated.
	Steady-state post disturbance	Good match	✓✓	CMLD aligned with HSM
Reactive power	During dynamic state	Fair match	✓✓	The trajectory of the CMLD reflects the HSM data for all channels. Min/max power flows are overestimated.
	Steady-state post disturbance	Good match	✓✓	CMLD aligned with HSM
Load	Load change	Good match	✓✓	SCADA: 533 MW decrease (60 s post disturbance) CMLD: 485 MW decrease CMLD accurately predicts load disconnection (underestimates load disconnection by 9% at 60 s post disturbance.

6 Validation: voltage disturbances with DPV

This section presents the validation studies conducted for the CMLD and DPV models during voltage disturbances in periods with significant levels of DPV generating.

6.1 3 March 2017 – South Australia

6.1.1 Event overview

Table 38 Event summary – 3 March 2017

Date and time		3 March 2017, 15:03[104]
Region		South Australia
Description of the event		A series of three faults occurred at the Torrens Island switchyard. These faults resulted in the loss of five generating units in South Australia. The event is summarised as: **Fault 1 (15:03:46):** Capacitor Voltage Transformer (CVT) at Torrens Island Switchyard • Trip of TIPS B unit 4 from 134 MW • Trip of PPCCGT from 218 MW (steam turbine trip at 1505 hrs) **Fault 2 (15:03:46):** Torrens Island Switchyard trip due to debris/smoke from the explosion of the CVT. • Trip of TIPS B 275 kV West Bus **Fault 3 (15:03:47):** TIPS B3 trip due to debris/smoke from the explosion of the CVT causing a flashover of TIPS B3 bus support insulators. • Trip of TIPS B unit 3 from 134 MW • TIPS B unit 2 starts to run back from 132 MW due to the boiler air pre-heater drive loss
Minimum voltage recorded		0.48 pu positive sequence recorded at TIPS B (from HSM data)
Installed capacity of DPV		Total installed capacity in South Australia: 739 MW (from APVI) • 95% installed under AS4777.3:2005 (from CER) • 5% installed under AS/NZS4777.2:2015 (from CER)
Prior to the event	**DPV**	440 MW, 60% capacity factor (from ASEFS2, interpolated)
	Operational demand	1,987 MW (from SCADA data)
	Underlying demand	2,427 MW (estimate from SCADA + ASEFS2)
Estimated change (post disturbance vs pre disturbance)	**DPV**	133 MW (range of 44-260 MW) decrease (from Solar Analytics data)
	Operational demand	280 MW (range of 269-428 MW) decrease (from SCADA data)
	Underlying demand	413 MW (range of 313-687 MW) decrease (from SCADA & Solar Analytics data)

[104] AEMO. Fault at Torrens Island Switchyard and Loss of Multiple Generating Units on 3 March 2017, March 2017, at https://www.aemo.com.au/-/media/Files/Electricity/NEM/Market_Notices_and_Events/Power_System_Incident_Reports/2017/Report-SA-on-3-March-2017.pdf.

Figure 59 Map – 3 March 2017

6.1.2 Replication in PSS®E

The following element changes were made in PSS®E to replicate this case:

Table 39 Simulation event summary – 3 March 2017[105]

Time (s)	Events/comments
0.0	Start simulation
1.28	Apply 1PG fault on the 275 kV Torrens Island B Power Station bus (PSS®E bus 53385)[106]
1.38	Clear 1PG fault on the 275 kV Torrens Island B Power Station bus (PSS®E bus 53385) Trip TIPS B G4 generator (PSS®E bus 50388) Trip TIPS G4 275/16 kV transformer (PSS®E bus 50388 to 53385) Trip Pelican Point GT11 generator (PSS®E bus 50371) Trip Pelican Point GT11 275/16 kV transformer (PSS®E bus 50371 to 53378)
1.88	Apply 2PG fault on the 275 kV Torrens Island B Power Station bus (PSS®E bus 53385)[106]
1.98	Clear 2PG fault on the 275 kV Torrens Island B Power Station bus (PSS®E bus 53385)
2..78	Apply 1PG fault on the 275 kV Torrens Island B Power Station bus (PSS®E bus 53385)[106]
2.88	Clear 1PG fault on the 275 kV Torrens Island B Power Station bus (PSS®E bus 53385) Trip TIPSB G3 generator (PSS®E bus 50387) Trip TIPS G3 275/16 kV transformer (PSS®E bus 50387 to 53385)
60	End simulation

[105] This snapshot is unstable during ZIP and ZIP+DPV simulations. For ZIP+DPV, by increasing generation in South Australia by 170 MW, and subsequently reducing imports over Heywood by ~100 MW, this case is made stable and load loss is estimated. Similarly, for ZIP, by increasing generation by 100 MW, and subsequently reducing imports over Heywood by ~60 MW, this case is made stable. This is a testament to the improved accuracy of the CMLD over the ZIP model for reproducing historical disturbances.

[106] CMLD+DPV. ZIP+DPV, and ZIP models' fault impedance were individually tuned to better match with HSM data.

6.1.3 High speed measurements

Voltages

Figure 60 shows the voltages at the faulted 275 kV Torrens Island Power Station B bus. The only other bus with HSM data available for this event was the relatively close 275 kV Lefevre bus, which demonstrated a similar response.

In this disturbance, the CMLD+DPV model replicates the HSM voltage recovery profile reasonably closely. Voltage over-shoot is marginally overestimated following the first and (to a lesser degree) third fault but remains within the normal voltage range of 0.9 pu to 1.1 pu. The CMLD+DPV steady-state voltage after the disturbance is also comparable with observations. In contrast, simulations with the ZIP or the ZIP+DPV models recover too quickly immediately after the first and third fault with the ZIP+DPV showing signs of a delayed volage recovery following the second fault. The voltage in the ZIP+DPV case sags slightly more than the CMLD+DPV after the third fault for multiple seconds before recovering to steady state. This is primarily due to the inability of the ZIP model to represent the load disconnection that occurred. When the ZIP model is coupled with the DPV model, which accurately replicates the DPV disconnection that occurred, this leads to underestimation of the decrease in operational demand that occurred, and the ZIP+DPV model therefore indicates a voltage sag for several seconds that was not observed in the HSM. This illustrates why it is not appropriate to use the DPV model without the ZIP model in cases where DPV disconnection occurs, since load disconnection will also typically occur in these cases, and the net change in operational demand is not accurately represented by the ZIP+DPV model representation.

Both the cases with the ZIP model also underestimate the steady-state voltage, while the CMLD+DPV model represents steady state voltage reasonably accurately (at 60 s, not shown).

Figure 60 Voltage – 3 March 2017 – 275 kV Torrens Island Power Station (TIPS) B bus

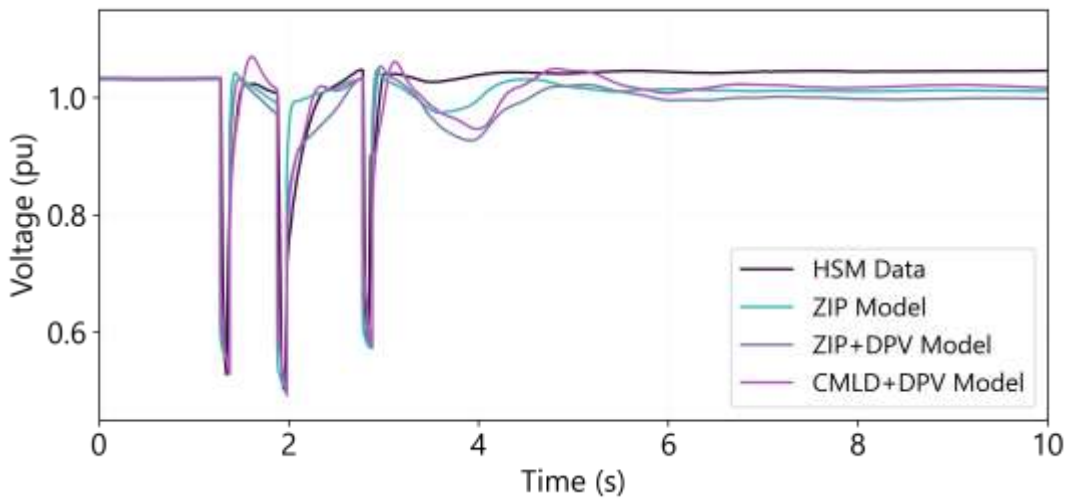

Active power flows

Figure 61 shows the active power observations at the TIPS B generator 1 feeder. All models overestimate the minimum active power flows during the fault, but maximum power flows and the general trajectory of the active

power response align with observations and have similar recovery times. The post fault steady-state active power for all models matches observations relatively well.

Figure 61 Active power – 3 March 2017 – 275 kV Torrens Island Power Station (TIPS) B Generator 1 Feeder

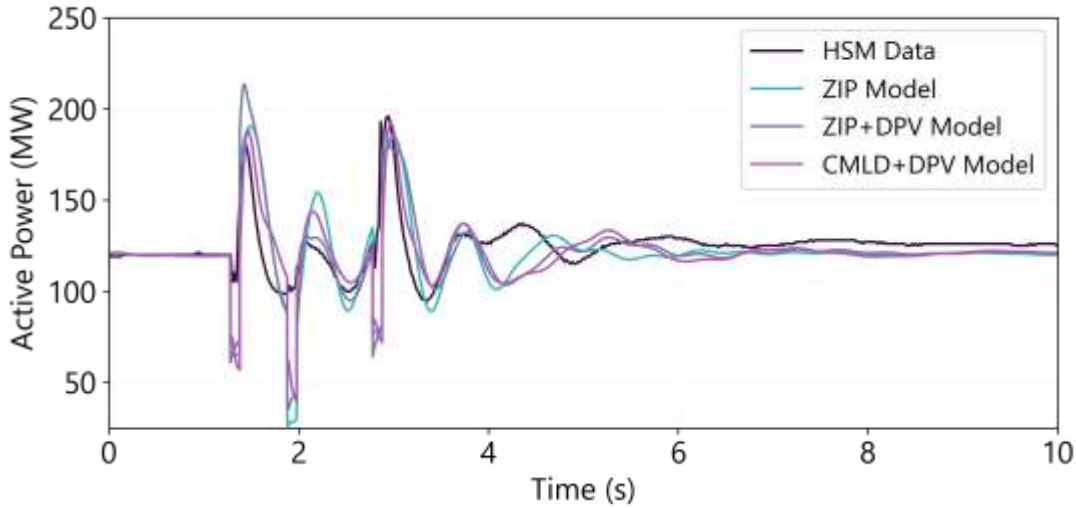

6.1.4 DPV measurements

Figure 62 shows the total measured DPV generation in South Australia (initial value estimated from ASEFS2, and the change post disturbance estimated from Solar Analytics datasets) compared with the performance of the CMLD+DPV model and the ZIP+DPV model. In both simulations, the DPV model reasonably accurately predicts the 133 MW DPV disconnection estimated for this event. The uncertainty range for this estimate is wide due to the relatively small sample of DPV inverters in the Solar Analytics sample for this older event occurring in early 2017.

Figure 62 DPV measurements – South Australia total – 3 March 2017

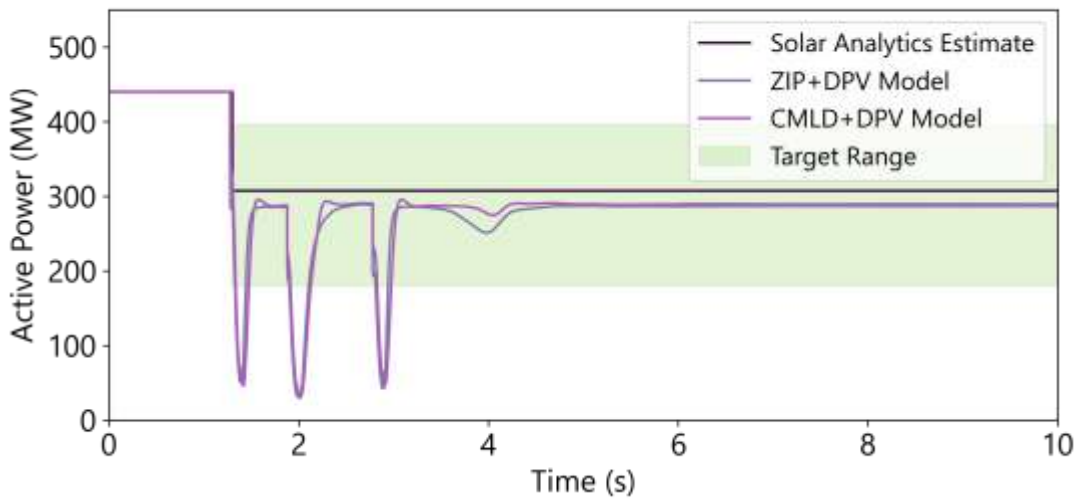

6.1.5 SCADA measurements

Figure 63 shows the total measured operational demand in South Australia (from SCADA), compared with the performance of the various models.

As shown in Figure 63, in this event, the post disturbance operational demand declined gradually, reaching a minimum at approximately two minutes after the disturbance. It is unclear whether this gradual decline is representative of real load behaviour or if this may represent inaccuracies in the SCADA measurement (for example, due to misalignment of time measurements when summing SCADA). If this is representative of real load behaviour, this gradual decline cannot be represented by any of the load models (CMLD or ZIP). The CMLD+DPV model was therefore tuned to match the load change measured at 60 s post disturbance (represented by the green dashed line in Figure 63), but it is acknowledged that there are significant inaccuracies in the SCADA measurement for this event. The green "target range" band in Figure 63 indicates the margin of uncertainty.

Figure 63 Operational demand measurements (SCADA) – 3 March 2017

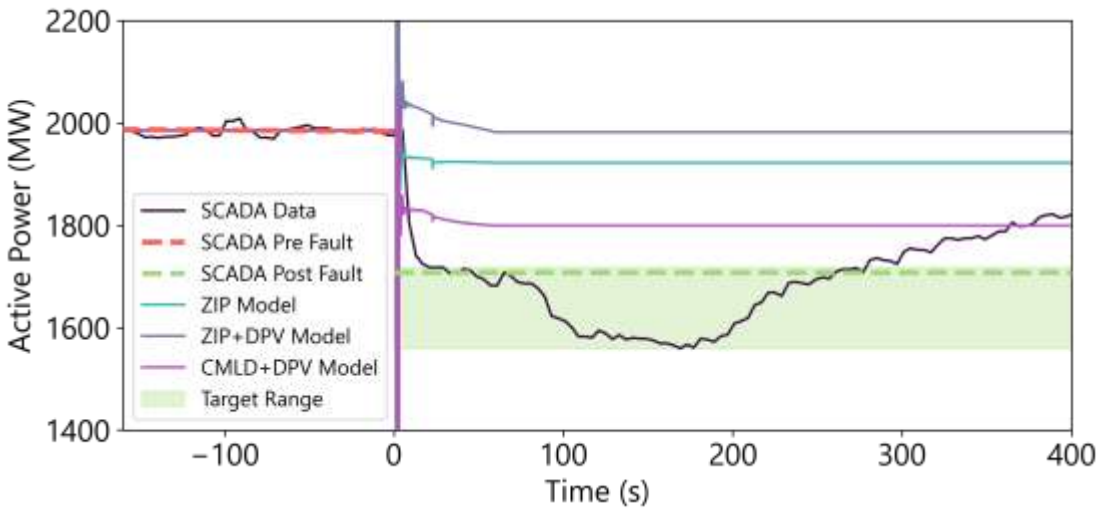

As shown in Figure 63, the CMLD+DPV model somewhat underpredicts the estimated net 280 MW decrease in operational demand. The CMLD model predicts 336 MW of total underlying load loss, offset by 151 MW of DPV disconnection predicted by the DPV model, leading to a total net decrease in operational demand of 185 MW. The comparison with estimated actuals is shown in **Table 40**. In this case, an underestimation of load disconnection compounds with a small overestimation of DPV disconnection, leading to a larger proportional overall error in the net change in operational demand.

Table 40 Summary of change in demand and distributed PV – 3 March 2017

	Actuals (estimated)	CMLD+DPV prediction
Change in distributed PV generation (estimated from Solar Analytics sample)	133 MW (44 – 260 MW) decrease	151 MW decrease (overestimates by 14%, but within range)
Change in underlying demand (estimated from SCADA & Solar Analytics)	412 MW (313 – 687 MW) decrease	336 MW decrease (underestimates by 18%, but within range)
Change in operational demand (estimated from SCADA, 60s post disturbance)	280 MW (269 – 428 MW) decrease	185 MW decrease (underestimates by 34%, outside of range)

The ZIP model cannot represent any load disconnection but does show a moderate reduction in total regional load following the disturbance. This is partially due to the disconnection of auxiliary loads at the generating units that tripped during the disturbance[107] and partially due to the voltage dependant characteristics of the (constant current) ZIP model (as shown in Figure 60, the simulations with the ZIP and ZIP+DPV models show somewhat depressed steady-state voltages post fault). For the ZIP+DPV case, this mild reduction in ZIP load is offset by DPV disconnection, so the combined ZIP+DER model indicates minimal change in operational demand following the disturbance, which is clearly misaligned with the SCADA observations. The CMLD+DPV model therefore provides a clear improvement over the existing ZIP model.

Load change in the Adelaide metropolitan area was also measured and found to be comparable between the SCADA and CMLD+DPV model representation.

6.1.6 Assessment of model performance

Table 41[108] provides a summary of the model performance for this event. Green indicates the CMLD model provides a good match to HSM, orange indicates the CMLD model provides a fair match to HSM, red indicates the CMLD model provides a poor match to HSM. A cross indicates where the ZIP model performs better than CMLD, a tick shows where the CMLD model performs at least as well as the ZIP model, and a double tick indicates where the CMLD model performs significantly better than the ZIP model.

Table 41 Assessment of model performance – 3 March 2017

Quantity	Characteristic	CMLD+DPV estimates	CMLD+DPV model equal (✓) or better (✓✓) than ZIP?	Commentary
Voltages	Voltage overshoot	Fair match	✗	The CMLD+DPV marginally overestimates peak voltage overshoot magnitude, but it stays within the normal voltage range of 0.9 to 1.1 pu
	Voltage recovery rate	Good match	✓✓	CMLD+DPV aligned with HSM
	Steady-state post disturbance	Good match	✓	CMLD+DPV voltages are accurate (settles to within 5% of the HSM data for all voltage channels).
Active power	During dynamic state	Fair match	✓	CMLD has a similar trajectory to the HSM, although it overestimates peak minimum flows during the fault.
	Steady-state post disturbance	Good match	✓	CMLD+DPV aligned with HSM
Reactive power	During dynamic state	-	-	Reactive power data is not available.
	Steady-state post disturbance	-	-	Reactive power data is not available.
DPV	DPV change	Good match	✓✓	Estimated actuals: 133 MW decrease DPV: 151 MW decrease The DPV model overestimates DPV disconnection by 13%, but within range.
CMLD	Underlying load change	Good match	✓✓	Estimated actuals: 412 MW decrease (60 s post disturbance) CMLD: 336 MW decrease

[107] Auxiliary loads tripped: TIPS B G4 7 MW, PEL G11 5 MW, TIPS B G3 7 MW.

[108] See Section 4.5.2 for further explanation on this table.

Quantity	Characteristic	CMLD+DPV estimates	CMLD+DPV model equal (✓) or better (✓✓) than ZIP?	Commentary
				The CMLD underestimates load disconnection by 19% when measured at 60 s post disturbance, but within range.
Operational Demand	Net load change	Poor match	✓✓	Estimated actuals: 280 MW decrease (60 s post disturbance) CMLD+DPV: 185 MW decrease The CMLD+DPV model underestimates net load change by 34% and is outside the range.

6.2 18 January 2018 – Victoria

6.2.1 Event overview

Table 42 Event summary – 18 January 2018

Date and time		18 January 2018, 15:19[109]
Region		Victoria
Description of the event		A 1PG fault occurred at the Rowville terminal station due to a 500 kV CT failure associated with the A2 busbar. The event is summarised as: • Fault at Rowville (ROTS) No 2 500 kV Busbar • Trip of ROTS No 2 500/220 kV Transformer • Rowville - South Morang No 3 500 kV line (ROTS–SMTS line) opened at South Morang The load loss occurred in the distribution networks, and no bulk transmission network supply points were disconnected.
Minimum voltage recorded		0.64 pu positive sequence recorded at Cranbourne Terminal Station (from HSM data)
Installed capacity of DPV		Total installed capacity: 1,237 MW (from APVI) • 80% installed under AS4777.3:2005 (from CER) • 20% installed under AS/NZS4777.2:2015 (from CER)
Prior to the event	**DPV**	680 MW, 55% capacity factor (from ASEFS2, interpolated)
	Operational demand	8,736 MW (from SCADA data)
	Underlying demand	9,416 (estimate from SCADA + ASEFS2)
Estimated change (post disturbance vs pre disturbance)	**DPV**	123 MW (range of 57-218 MW) decrease (from Solar Analytics data)
	Operational demand	506 MW (range of 450-598 MW) decrease (from SCADA data)
	Underlying demand	629 MW (range of 507-815 MW) decrease (estimate from SCADA + Solar Analytics data)

[109] AEMO, Trip of the Rowville No. 2 500 kV Busbar and A2 500/220 kV Transformer on 18 January 2018, March 2019, at https://www.aemo.com.au/-/media/files/electricity/nem/market_notices_and_events/power_system_incident_reports/2018/trip-of-rots-bus-on-18-jan-2018---published.pdf.

Figure 64 Map – 18 January 2018

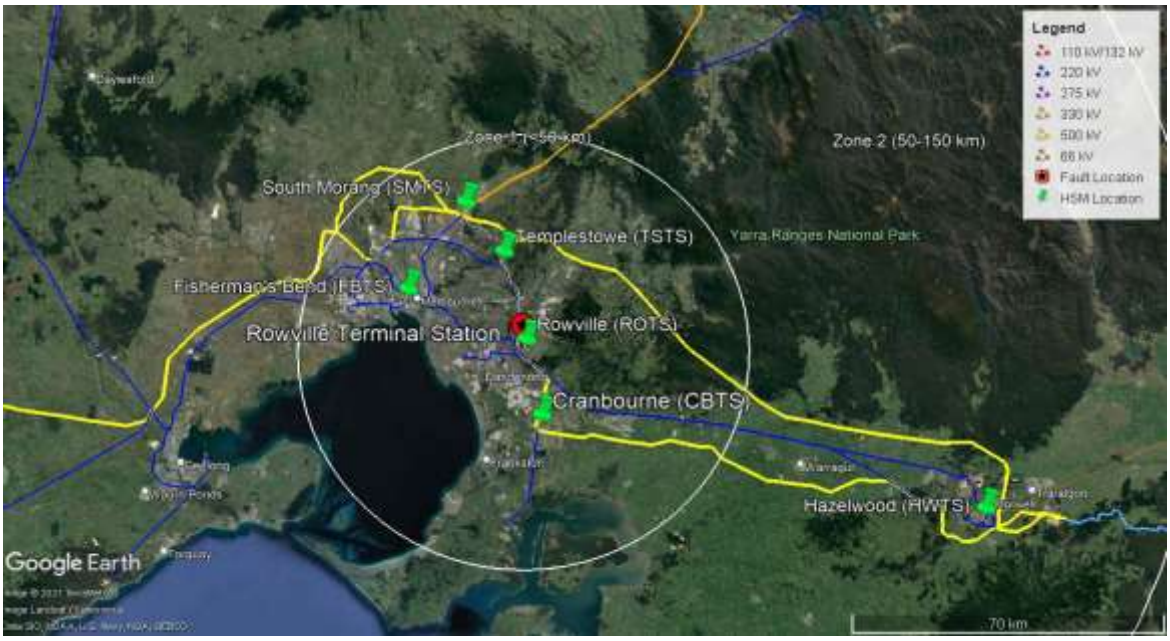

6.2.2 Replication in PSS®E

The following element changes were made in PSS®E to replicate this case:

Table 43 Simulation event summary – 18 January 2018

Time (s)	Events/comments
0.0	Start simulation
1.0	Apply 1PG fault at Rowville No.2 500 kV bus (PSS®E bus 35641)[110]
1.08	Trip Rowville No2 500/220 kV transformer (PSS®E bus 32649 to 35641)
1.16	Clear 1PG fault at Rowville No.2 500 kV bus (PSS®E bus 35641) Trip 500 kV Rowville (PSS®E bus 35641) to South Morang (PSS®E bus 35720) line
60	End simulation

6.2.3 High speed measurements

Voltages

Figure 65 and **Figure 66** show the voltages observed at the 220 kV Rowville and 66 kV Cranbourne Terminal Stations, close to the fault. Observations at Rowville were found to be illustrative of the voltage response at all locations with HSM data available[111]. Observations at Cranbourne were included to show that voltage sags are also well represented at lower voltage levels, suggesting an accurate PSS®E network representation in this case.

[110] CMLD+DPV. ZIP+DPV, and ZIP models' fault impedance were individually tuned to better match with HSM data.

[111] HSM data was available at the following locations: 220 kV Rowville, 220 kV Altona, 220 kV Bendigo, 66 kV Brooklyn, 66 kV Cranbourne, 66 kV Fishermans Bend, 22 kV Red Cliffs, and 66 kV Templestowe buses.

In both figures, the CMLD+DPV model replicates the HSM voltage recovery profile closely. Voltage over-shoot is overestimated and exceeds the normal voltage operating range of 0.9 pu to 1.1 pu. This may be due to an overestimation of motor load disconnection or misrepresentation of the types of loads in this area. In future CMLD revisions, it may be possible to obtain specific information about the types of loads in this part of the network to improve this match. The CMLD+DPV model's steady-state voltage (after ~8s) is comparable with observations.

In contrast, the ZIP and ZIP+DPV models recover too quickly immediately after the fault and underestimate the steady-state voltage. However, the voltage overshoot estimated by the ZIP and ZIP+DPV models is a better match to the observed data (compared with the CMLD equivalent).

Figure 65 Voltage – 18 January 2018 – 220 kV Rowville Terminal Station (ROTS)

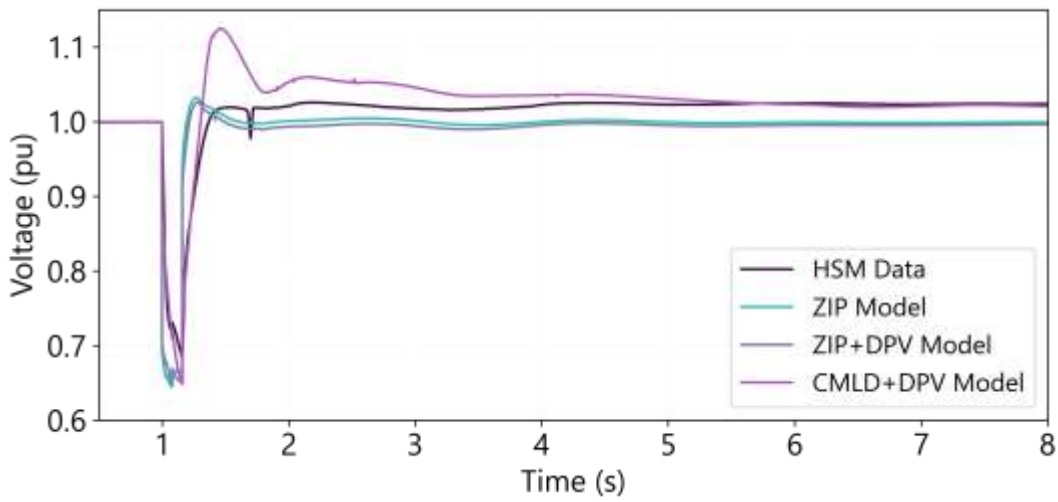

Figure 66 Voltage – 18 January 2018 – 66 kV Cranbourne Terminal Station

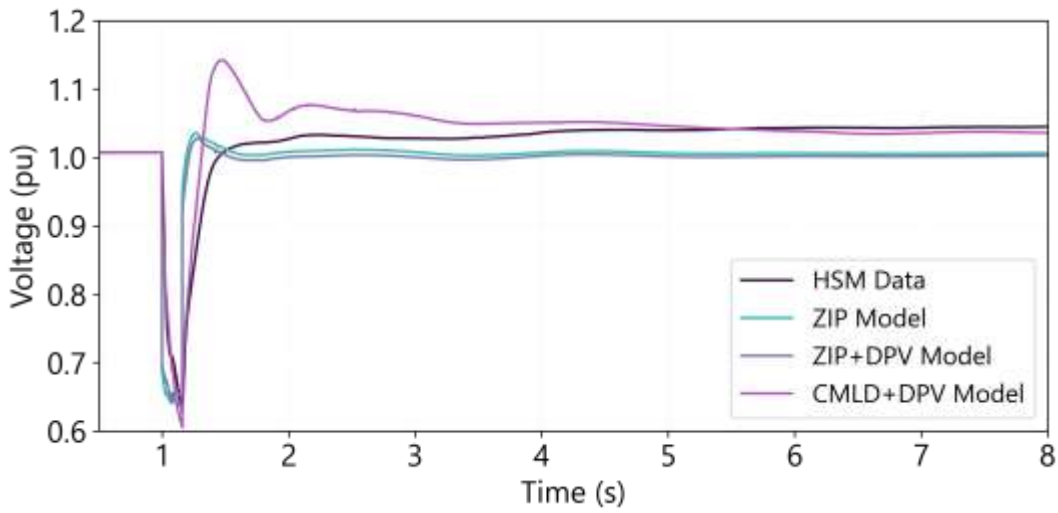

Active and reactive power flows

Figure 67 shows the active and reactive power measurements at the same locations. Observations at the 220 kV Rowville location are illustrative of typical measurements at most locations in the network. For the CMLD+DPV model, peak minimum active power is slightly overestimated during the fault but well represented in the steady-state. Reactive power peak flows and steady-state power are comparable to the observations. In contrast, the ZIP/ZIP+DPV models significantly overestimate steady-state active power flows, and completely misrepresent the trajectory of reactive power flows. The misrepresentation of reactive power at the 220 kV level was observed across several available HSM locations (not shown).

Observations at Cranbourne (66 kV) show similar characteristics to those at the 220 kV Rowville HSM. The underestimation of active and reactive power immediately following the fault may be due to the inability of the power electronic logic block to capture the VFD response during voltage disturbances (see Section 9.7).

Figure 67 Active/reactive power – 18 January 2018

220 kV Rowville Terminal Station (ROTS) to Springvale Terminal Station Feeder

Active power

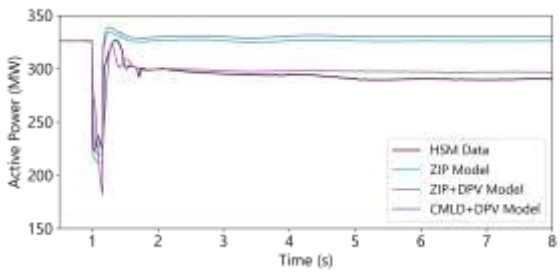

Reactive power

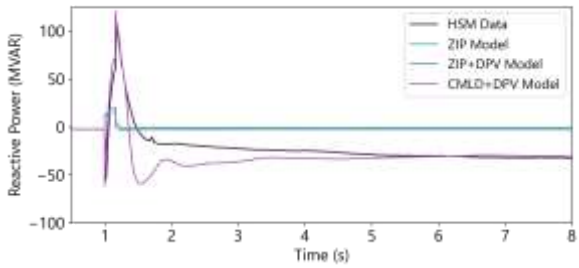

66 kV Cranbourne Terminal Station (CBTS) Transformer B1 Feeder

Active power

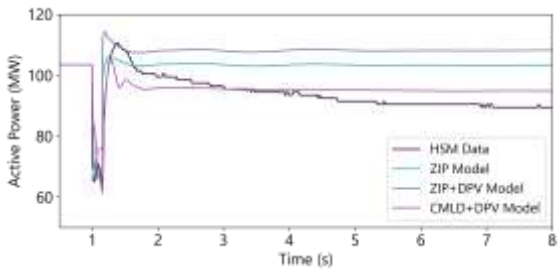

Reactive power

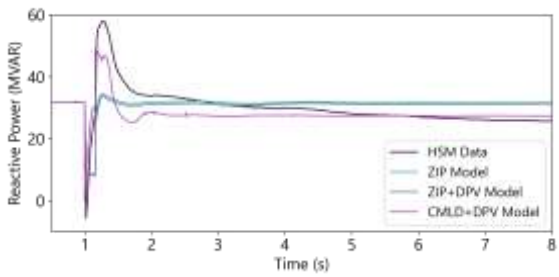

6.2.4 DPV measurements

Figure 68 shows the total measured DPV generation in Victoria (initial value estimated from ASEFS2 and the change post disturbance estimated from Solar Analytics datasets) compared with the performance of the CMLD+DPV model and the ZIP+DPV model. In both cases, the DPV model predicts DPV disconnection within the target range (underestimating by 25%, when applied with the CMLD model).

Figure 68 DPV measurements – Victoria total – 18 January 2018

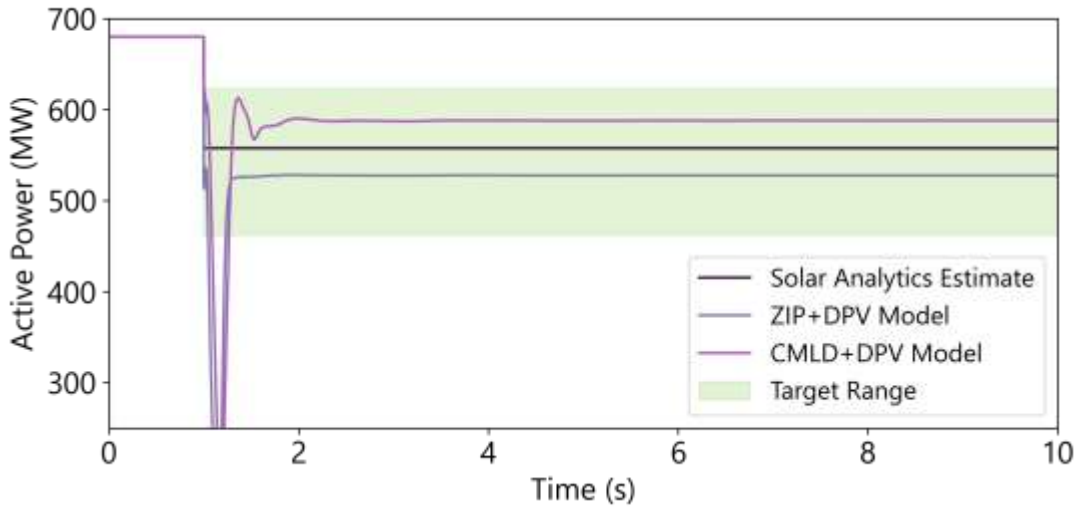

6.2.5 SCADA measurements

Figure 69 shows the total measured operational demand in Victoria (from SCADA), compared with the performance of the various models. The CMLD+DPV model was tuned to match the load change measured at 92 s post disturbance (represented by the green dashed line in Figure 69), selected as a reasonably central estimate of the SCADA observations post disturbance, but it is acknowledged that there are significant inaccuracies in the SCADA measurement (represented by the green shaded "target range").

Figure 69 Operational demand measurements (SCADA) – Victoria total – 18 January 2018

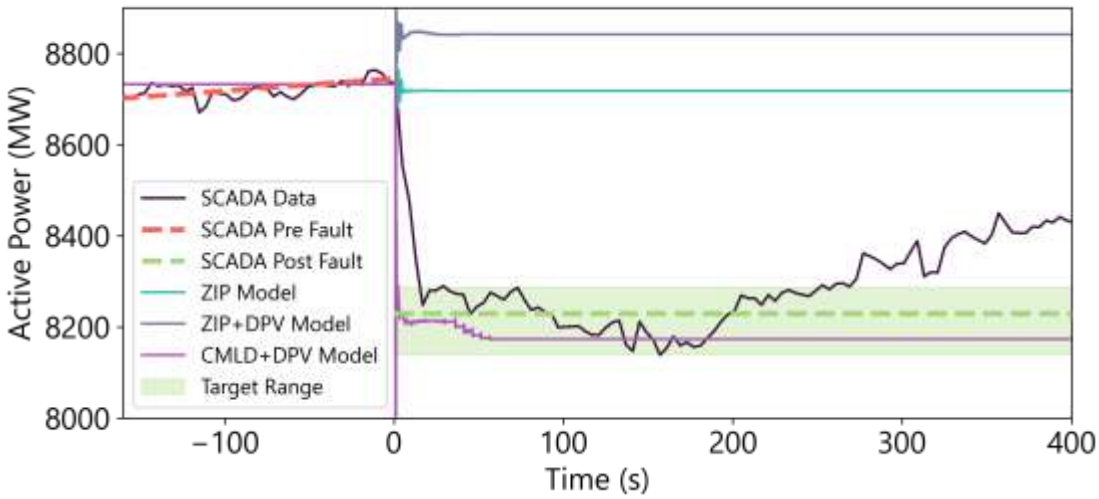

As shown in Figure 69, the CMLD+DPV model slightly overpredicts the estimated net 506 MW decrease in operational demand. The CMLD model slightly overestimates underlying load loss, while the DPV model slightly underestimates DPV loss, leading to a larger overall uncertainty in the estimate of net change in operational demand. The comparison with estimated actuals is shown in **Table 44**.

Table 44 Summary of change in demand and distributed PV – 18 January 2018

	Actuals (estimated)	CMLD+DPV prediction
Change in DPV generation (estimated from Solar Analytics sample)	122 MW (57 – 218 MW) decrease	92 MW decrease (underestimates by 25% but within range)
Change in underlying demand (estimated from SCADA & Solar Analytics)	629 MW (507 – 815 MW) decrease	652 MW decrease (overestimates by 4% but within range)
Change in operational demand (estimated from SCADA, 92s post disturbance)	506 MW (450 – 598 MW) decrease	560 MW decrease (overestimates by 11% but within range)

In contrast, the ZIP model cannot represent any load disconnection. For the ZIP+DPV case, the DPV disconnection results in an apparent increase in operational demand. Both cases are clearly misaligned with the SCADA observations.

Load change in the Melbourne metropolitan area was also measured and found to be comparable between the SCADA and CMLD+DPV model representation.

6.2.6 Assessment of model performance

Table 45 provides a summary of model performance for this event. Green indicates the CMLD model provides a good match to HSM, orange indicates the CMLD model provides a fair match to HSM, red indicates the CMLD model provides a poor match to HSM. A cross indicates where the ZIP model performs better than CMLD, a tick shows where the CMLD model performs at least as well as the ZIP model, and a double tick indicates where the CMLD model performs significantly better than the ZIP model.

Table 45 Assessment of model performance – 18 January 2018

Quantity	Characteristic	CMLD+DPV estimates	CMLD+DPV model equal (✓) or better (✓✓) than ZIP?	Commentary
Voltages	Voltage overshoot	Poor match	✗	The CMLD+DPV model overestimates peak voltage overshoot magnitude and exceeds the normal operating range (0.9 to 1.1 pu) for 120ms.
	Voltage recovery rate	Good match	✓✓	CMLD+DPV comparable to HSM.
	Steady-state post disturbance	Good match	✓✓	CMLD+DPV voltages are accurate (settles to within 5% of the HSM data for all voltage channels).
Active power	During dynamic state	Good match	✓✓	CMLD+DPV aligned with HSM for most assessed channels. Peak min/max magnitudes are sometimes over/underestimated respectively.
	Steady-state post disturbance	Good match	✓✓	CMLD+DPV aligned with HSM.
Reactive power	During dynamic state	Fair match	✓✓	CMLD+DPV trajectory aligned with HSM data for all channels. Peak min/max flows are sometimes under/overestimated.
	Steady-state post disturbance	Good match	✓✓	CMLD+DPV aligned with HSM.
DPV	DPV change	Fair match	✓✓	Estimated actuals: 122 MW decrease DPV: 92 MW decrease

Quantity	Characteristic	CMLD+DPV estimates	CMLD+DPV model equal (✓) or better (✓✓) than ZIP?	Commentary
				The DPV model underestimates DPV disconnection by 25%.
CMLD	Underlying load change	Good match	✓✓	Estimated actuals: 629 MW decrease (92 s post disturbance) CMLD: 652 MW decrease The CMLD slightly overestimates load disconnection by 4% when measured at 92 s post disturbance.
Operational Demand	Net load change	Fair match	✓✓	Estimated actuals: 506 MW decrease (92 s post disturbance) CMLD+DPV: 560 MW decrease The CMLD+DPV model overestimates the change in operational demand by 11%.

6.3 9 October 2018 – Queensland

6.3.1 Event overview

Table 46 Event summary – 9 October 2018

Date and time		9 October 2018, 15:35
Region		Queensland
Description of the event		Lightning in the vicinity of the Braemar to Bulli Creek 330 kV line (bus no. 9902) caused the line to trip, and auto reclose. A significant amount of load disconnected at the Surat Basin, which is largely LNG industrial loads.
Minimum voltage recorded		0.75 pu positive sequence recorded at Braemar Power Station (from HSM data)
Installed capacity of DPV		Total installed capacity: 2,295 MW (from APVI) • 71% installed under AS4777.3:2005 (from CER) • 29% installed under AS/NZS4777.2:2015 (from CER)
Prior to the event	**DPV**	460 MW, 20% capacity factor (from ASEFS2, interpolated)
	Operational demand	6,684 MW (from SCADA data)
	Underlying demand	7,144 MW (estimate from SCADA + ASEFS2)
Estimated change (post disturbance vs pre disturbance)	**DPV**	2 MW (range of 1-3 MW) decrease (from Solar Analytics data)
	Operational demand	190 MW (range of 173-238 MW) decrease (from SCADA data)
	Underlying demand	192 MW (range of 173-241 MW) decrease (estimate from SCADA + Solar Analytics data)

Figure 70 Map – 9 October 2018

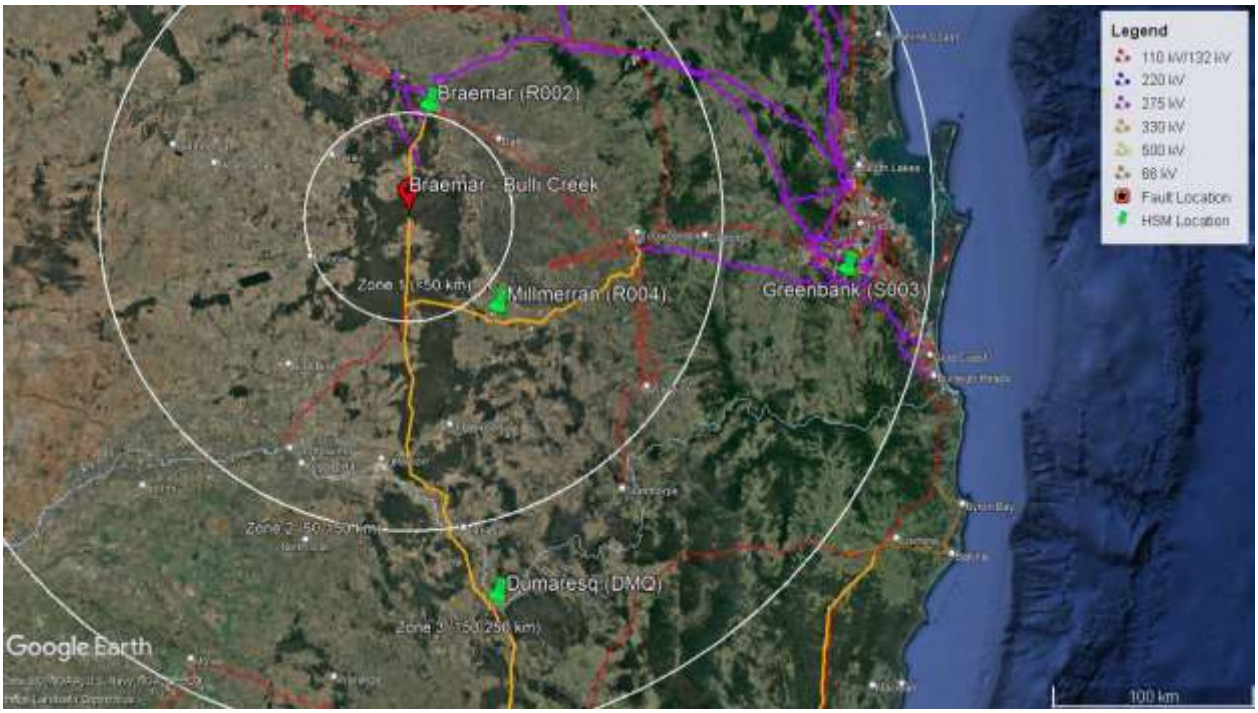

6.3.2 Replication in PSS®E

The following element changes were made in PSS®E to replicate this case:

Table 47 Simulation event summary – 9 October 2018

Time (s)	Events/comments
0.0	Start simulation
1.0	Apply 1PG fault on the 330 kV Braemar bus (PSS®E bus 49020)
1.08	Clear 1PG fault on the 330 kV Braemar bus (PSS®E bus 49020) Trip 330 kV Braemar (PSS®E bus 49020) to Bulli Creek (PSS®E bus 49031) line (branch 2)
60	End simulation

6.3.3 High speed measurements

Voltages

Figure 71 shows the voltages at the 275 kV Braemar bus, which is close to the fault. Braemar observations were illustrative of the voltage response at all locations with HSM data available[112], with the voltage depressions (from the applied fault impedance) closely matching the 275 kV and 330 kV measurements.

[112] HSM data was available at the following locations: 275 kV Braemar Power Station, 275 kV Greenbank, 330 kV Millmerran, and 330 kV Dumaresq to Bulli Creek Feeder.

In this disturbance, the CMLD+DPV model shows a somewhat slower voltage recovery profile compared with the HSM, although voltages still recover in less than 0.1 s, which is not unreasonable[113]. Voltage overshoot and steady-state levels are comparable with observations. The ZIP/ZIP+DPV models overestimate voltage overshoot.

Figure 71 Voltage – 9 October 2018 – 275 kV Braemar bus

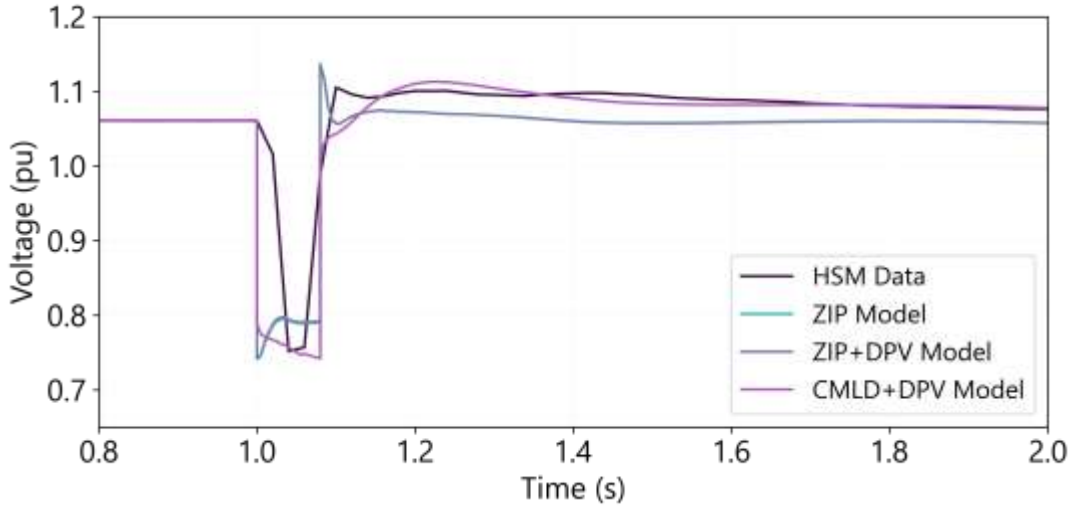

Active and reactive power flows

Figure 72 shows the active and reactive power measurements at two 330 kV feeders at the same voltage level as the faulted line: Millmerran to Millchester feeder and Dumaresq to Bulli Creek feeder. Observations at Millmerran are illustrative of typical measurements at most locations in the network. All models represent active power well during the transient and steady-state period with only minor mismatches of the peak transient flows. The CMLD model more accurately represents the observed post fault dip in active power. All models somewhat overestimate reactive power peak flows during the fault, although the CMLD model provides a better match, especially for the minimum peak flows at 1.2 s immediately post fault. All models represent the steady-state reactive power well, settling to close to the observed value at 60 s (not shown).

The only location to show contrasting results was the Dumaresq to Bulli Creek feeder, shown in Figure 72. At this location, all models represent the dynamic, active power trajectory and peak flow well up to ~1.2 s, but all models then diverge for the subsequent 60 s. The CMLD model underestimates observed active power flows over this period but is closer to HSM than the ZIP model. From 60 s (not shown), and once the active power on the line has reached steady state, the CMLD+DPV model matches HSM well. All models overestimate the peak reactive power flows during the fault, but the general dynamic trajectory and steady-state flows (after 60 s, not shown) are well represented. The mismatches shown by all models for this location are thought to be due to mismatches in the pre-fault flows on interconnectors in the vicinity of the Dumaresq to Bulli Creek feeder, drawn from the system snapshot, which has led to mismatches in the post-fault interconnector flows.

[113] The fault clearance times set out in Table S5.1a.2 of the National Electricity Rules (NER) state that primary and backup protection should operate within 0.25 s for faults occurring on 275 kV network. In this disturbance, with the CMLD representation voltage recovers to >90% of nominal voltage in less than 0.25 s.

Figure 72 Active/reactive power plots – 9 October 2018

330 kV Millmerran to Millchester R004 9905 Feeder

Active power

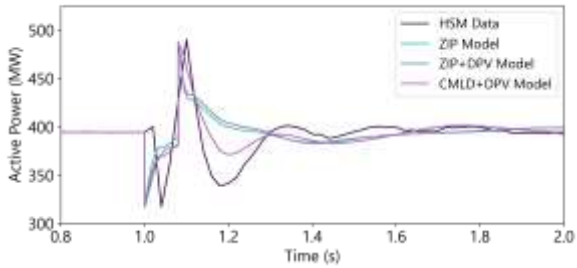

Reactive power

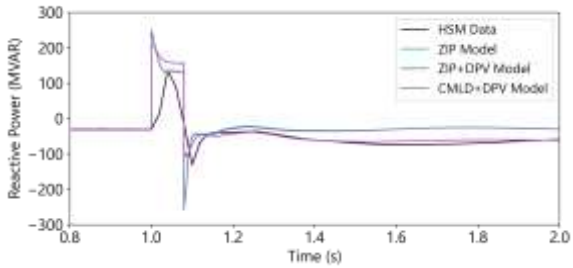

330 kV Dumaresq to Bulli Creek 8L Feeder

Active power

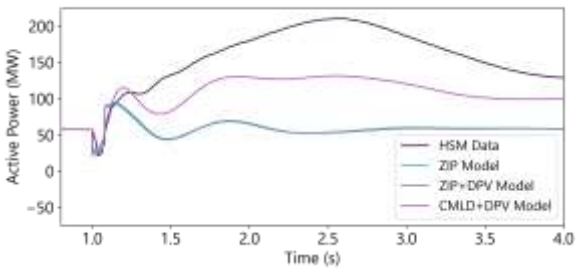

Reactive power

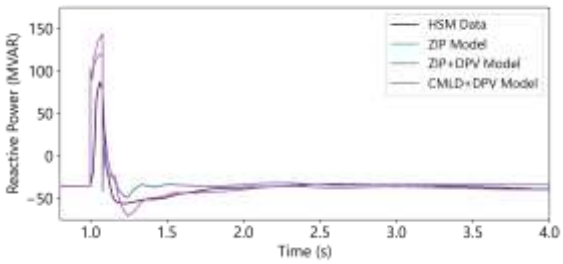

6.3.4 DPV measurements

Figure 73 shows the total measured DPV generation in Queensland (initial value estimated from ASEFS2 and the change post disturbance estimated from Solar Analytics datasets) compared with the performance of the CMLD+DPV model and the ZIP+DPV model. In both simulations, the DPV model accurately predicts the minimal amount of DPV disconnection estimated for this event.

Figure 73 DPV measurements (Solar Analytics) – Queensland total – 9 October 2018

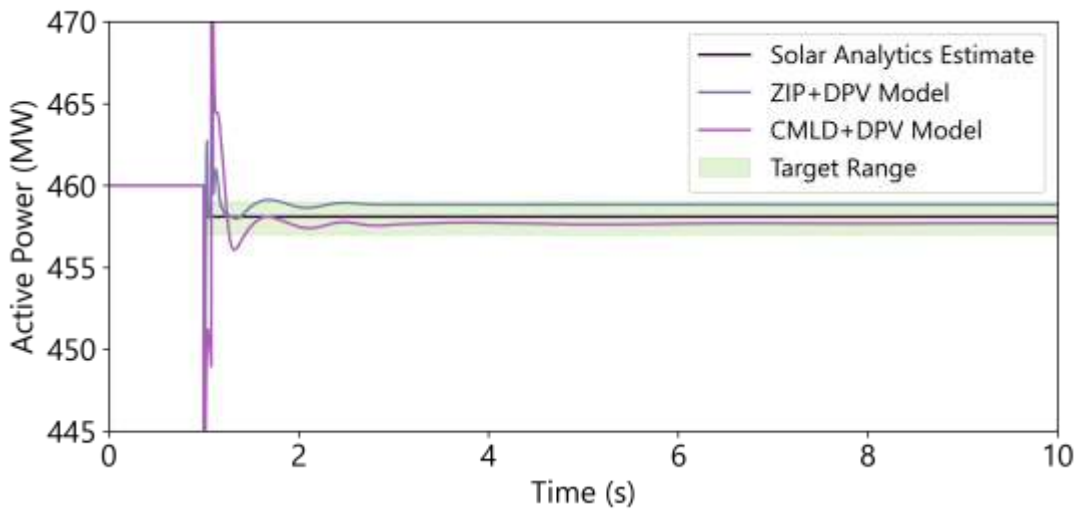

6.3.5 SCADA measurements

Figure 74 shows the total operational demand in Queensland (from SCADA), compared with the performance of the various models. The CMLD+DPV model was tuned to match the net load change measured at 60 s post disturbance (represented by the green dashed line in Figure 74).

Figure 74 Operational demand measurements (SCADA) – 9 October 2018

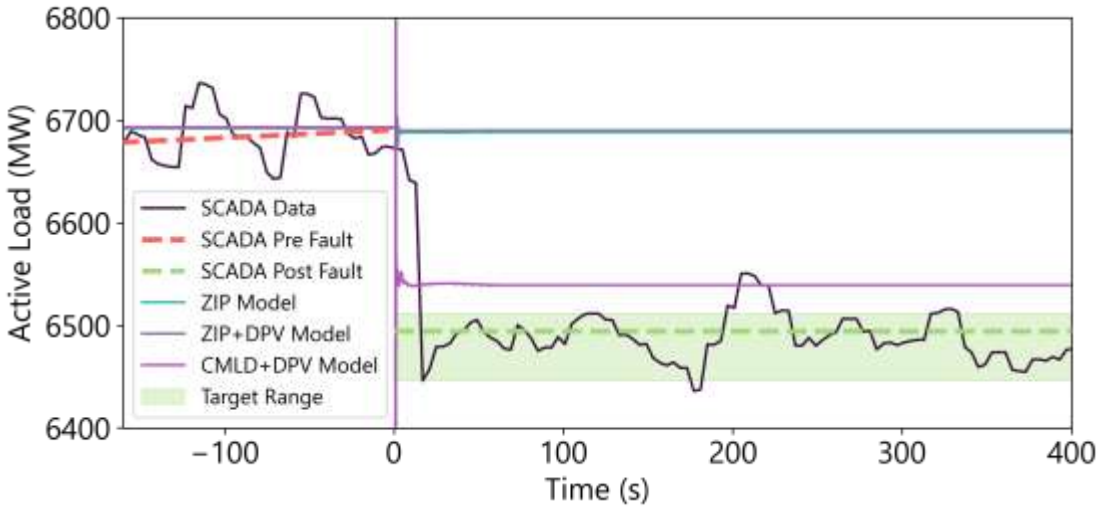

As shown in Figure 74, the CMLD+DPV model somewhat underpredicts the estimated net 190 MW decrease in operational demand. The comparison with estimated actuals is shown in **Table 48**. Given the minimal DPV disconnection for this case, the underestimation of load disconnection is the primary reason for underestimating the net change in operational demand.

Table 48 Summary of change in demand and distributed PV – 9 October 2018

	Actuals (estimated)	CMLD+DPV prediction
Change in DPV generation (estimated from Solar Analytics sample)	2 MW (1 – 3 MW) decrease	2 MW decrease (accurately predicts minimal DPV disconnection)
Change in underlying demand (estimated from SCADA & Solar Analytics)	192 MW (173 – 241 MW) decrease	156 MW decrease (underestimates by 18% and outside of target range)
Change in operational demand (estimated from SCADA, 60s post disturbance)	190 MW (173 – 238 MW) decrease	154 MW decrease (underestimates by 19% and outside of target range)

The ZIP model cannot represent any load disconnection, and therefore the ZIP and ZIP+DPV models are misaligned with observations.

Load change in the Brisbane metropolitan area was also measured and found to be comparable between the SCADA and CMLD+DPV model representation.

6.3.6 Assessment of model performance

Table 49 provides a summary of the performance of the CMLD+DPV model for this disturbance. Green indicates the CMLD model provides a good match to HSM, orange indicates the CMLD model provides a fair match to HSM, red indicates the CMLD model provides a poor match to HSM. A cross indicates where the ZIP model performs better than CMLD, a tick shows where the CMLD model performs at least as well as the ZIP model, and a double tick indicates where the CMLD model performs significantly better than the ZIP model.

Table 49 Assessment of model performance – 9 October 2018

Quantity	Characteristic	CMLD+DPV estimates	CMLD+DPV model equal (✓) or better (✓✓) than ZIP?	Commentary
Voltages	Voltage overshoot	Good match	✓✓	CMLD+DPV accurately estimates peak voltage overshoot magnitude and stays within the normal voltage range as defined in the NER (0.9 to 1.1 pu).
	Voltage recovery rate	Fair match	✓	The CMLD voltage recovery speed is slower than the HSM data but still recovers to the nominal voltage in < 0.1s.
	Steady-state post disturbance	Good match	✓	CMLD+DPV voltages are accurate and settle to within 5% of the HSM data for all voltage channels.
Active power	During dynamic state	Good match	✓✓	CMLD+DPV aligned with HSM for most assessed channels. Peak magnitudes are sometimes overestimated.
	Steady-state post disturbance	Good match	✓	CMLD+DPV aligned with HSM for most assessed channels. Peak flows during the transition from dynamic to steady-state are underestimated at one HSM location.
Reactive power	During dynamic state	Fair match	✓✓	The trajectory of the CMLD+DPV reflects the HSM data for all channels. Peak max flows are overestimated.
	Steady-state post disturbance	Good match	✓	CMLD+DPV aligned with HSM.
DPV	DPV change	Good match	✓	Estimated actuals: 2 MW decrease DPV: 2 MW decrease The DPV model accurately predicts minimal DPV disconnection.
CMLD	Underlying load change	Fair match	✓✓	Estimated actuals: 192 MW decrease (60 s post disturbance) CMLD: 156 MW decrease The CMLD slightly underestimates load disconnection by 18% when measured at 60 s post disturbance.
Operational demand	Net load change	Fair match	✓✓	Estimated actuals: 190 MW decrease CMLD+DPV: 154 MW decrease The CMLD+DPV model slightly underestimates operational demand change by 19%.

6.4 3 March 2019 – Victoria

6.4.1 Event overview

Table 50 Event summary – 3 March 2019

Date and time		3 March 2019, 15:13
Region		Victoria
Description of the event		Due to bushfires in the area, at 15:13, the HWTS – SMTS #2 500 kV line opened automatically following a 1PG fault on the line and reclosed ~12 s later.
Minimum voltage recorded		0.89 pu positive sequence recorded at Hazelwood Terminal Station (from HSM data)
Installed capacity of DPV		Total installed capacity: 1,681 MW (from APVI) • 59% installed under AS4777.3:2005 (from CER) • 41% installed under AS/NZS4777.2:2015 (from CER)
Prior to the event	**DPV**	325 MW, 19% capacity factor (from ASEFS2, interpolated)
	Operational demand	7,818 MW (from SCADA data)
	Underlying demand	8,143 MW (estimate from SCADA + ASEFS2)
Estimated change (post disturbance vs pre disturbance)	**DPV**	6 MW (range of 3-19 MW) decrease (from Solar Analytics data)
	Operational demand	11 MW increase (range of 8 MW decrease to 23 MW increase) (from SCADA data)
	Underlying demand	5 MW increase (range of 27 MW decrease to 20 MW increase) (estimate from SCADA + Solar Analytics data)

Figure 75 Map – 3 March 2019

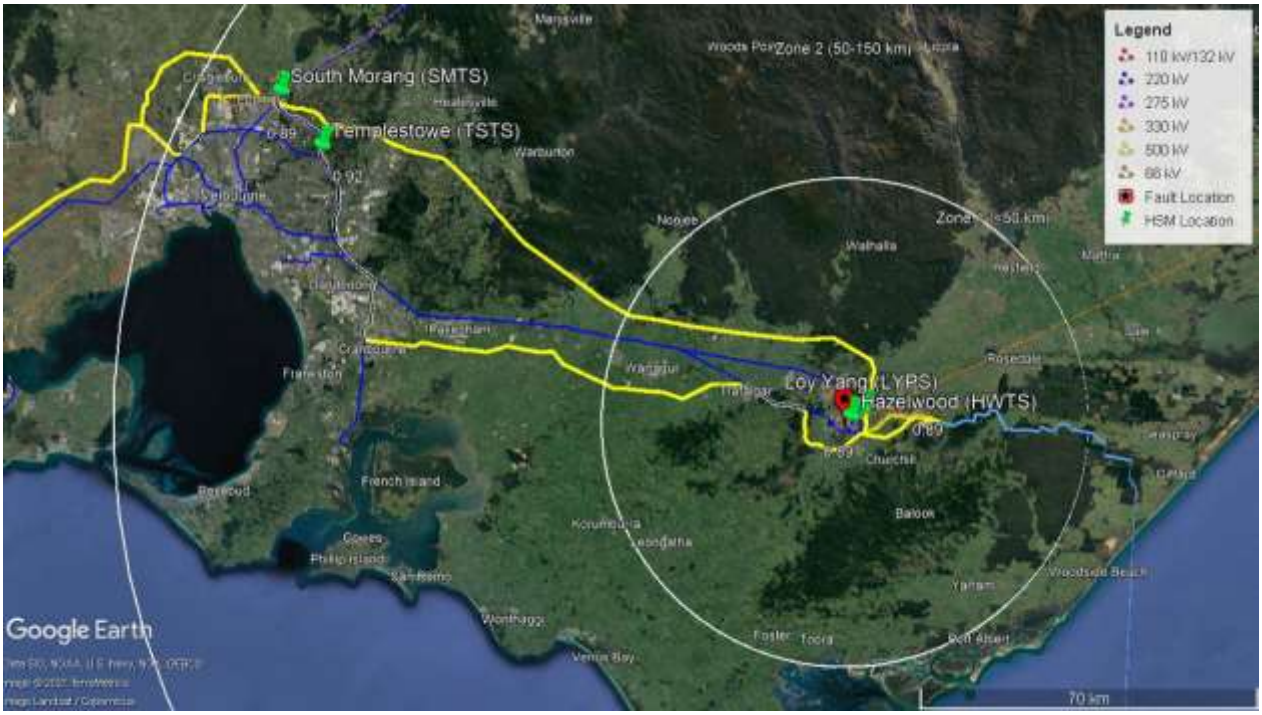

6.4.2 Replication in PSS®E

The following element changes were made in PSS®E to replicate this case:

Table 51 Simulation event summary – 3 March 2019

Time (s)	Events/comments
0.0	Start simulation
1.0	Apply 1PG fault on the 500 kV Hazelwood bus (PSS®E bus 35310) Trip 500 kV Hazelwood (PSS®E bus 35310) to South Morang (PSS®E bus 35720) line (branch 2)
1.08	Clear 1PG fault on the 500 kV Hazelwood bus (PSS®E bus 35310)
12.21	Close 500 kV Hazelwood (PSS®E bus 35310) to South Morang (PSS®E bus 35720) line (branch 2)
60	End simulation

6.4.3 High speed measurements

Voltages

Figure 76 shows the voltages at the faulted 500 kV Hazelwood Terminal Station bus. Observations at this location are illustrative of the observed voltage response at most locations in the network[114].

In this disturbance, the CMLD+DPV model voltage recovery profile is slower than observed but recovers to normal voltage level within 0.1s, which is considered adequate. In contrast, the ZIP/ZIP+DPV model recovers too quickly after each fault.

Voltage over-shoot is marginally overestimated by all models following the fault (and line opening) and after line closing at 13 s (shown in **Figure 77**) but stays within the normal voltage range of 0.9 pu to 1.1 pu. This may be due to the misrepresentation of active power flows on the second (parallel) line (see **Figure 78**) after the first line opens.

All models show steady-state voltages (after 60 s, not shown) after the disturbance comparable with observations.

[114] HSM data was available at the following locations: 500 kV Hazelwood Terminal Station, 500 kV South Morang Terminal Station, 500 kV Loy Yang Power Station, 500 kV Templestowe Terminal Station.

Figure 76 Voltage – 3 March 2019 – 500 kV Hazelwood Terminal Station (HWTS) bus

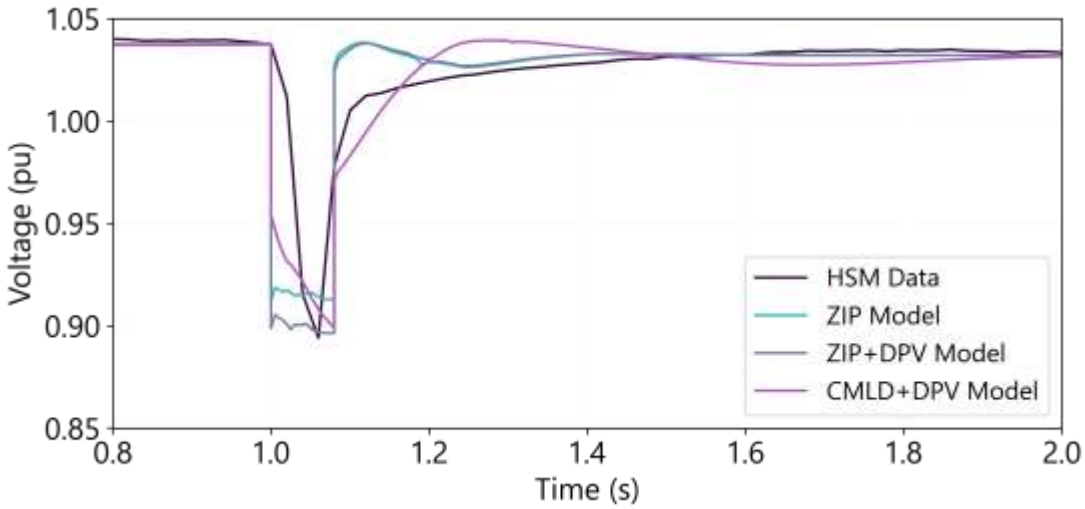

Figure 77 Voltage – 3 March 2019 – 500 kV Hazelwood Terminal Station (HWTS) bus (15 s duration)

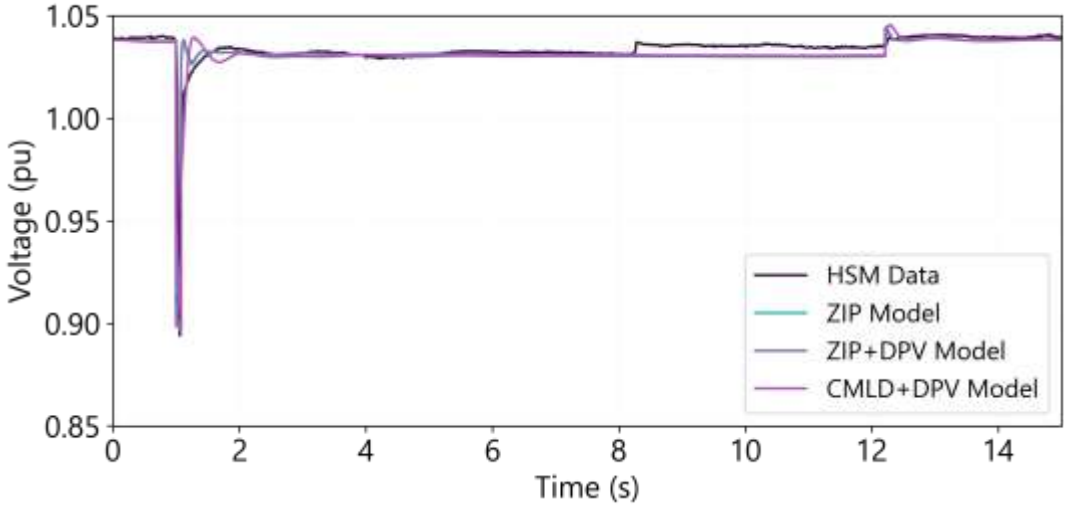

Active and reactive power flows

Figure 78 shows the active and reactive power measurements at the same location. Active and reactive power observations at this location are illustrative of typical measurements at some locations, such as Loy Yang. At these locations, all models overestimate active power flows by ~100 MW as the recloser opens following the fault; at this 500 kV location, active power flows are often in the GW range, so this does not represent a significant error on a percentage basis. For all models, active and reactive power returns to pre-fault flows after the line recloses, as observed in HSM.

At some other locations (such as Templestowe and South Morang), all models show an underestimation of steady-state active power flows in the network after line opening.

Following recloser operation, all models represent steady-state reactive power flows well. During the fault, all models overestimate peak levels. At the HWTS-SMTS feeder (shown in Figure 78), the trajectory of the models is not representative of observations immediately following the fault (at 1 s), although this was only evident at this feeder for this event.

Since these mismatches are observed identically for all models, they are unlikely to be related to the load and DPV models.

Figure 78 Active/reactive power – 3 March 2019 – 500 kV Hazelwood to 500kV South Morang Feeder 1 (HWTS_SMTS1)

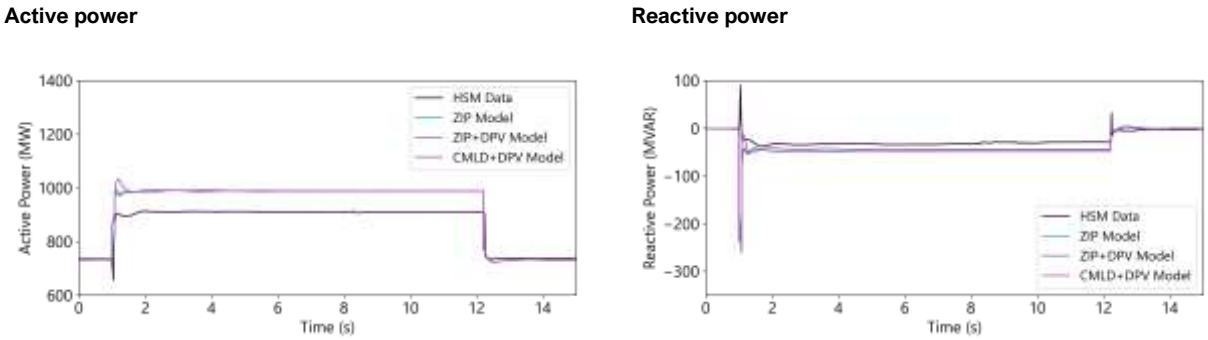

6.4.4 DPV measurements

Figure 79 shows the total measured DPV generation in Victoria (initial value estimated from ASEFS2 and the change post disturbance estimated from Solar Analytics datasets) compared with the performance of the CMLD+DPV model and the ZIP+DPV model. In both simulations, the DPV model accurately predicts minimal DPV disconnection for this event.

Figure 79 DPV measurements (Solar Analytics) – Victoria total – 3 March 2019

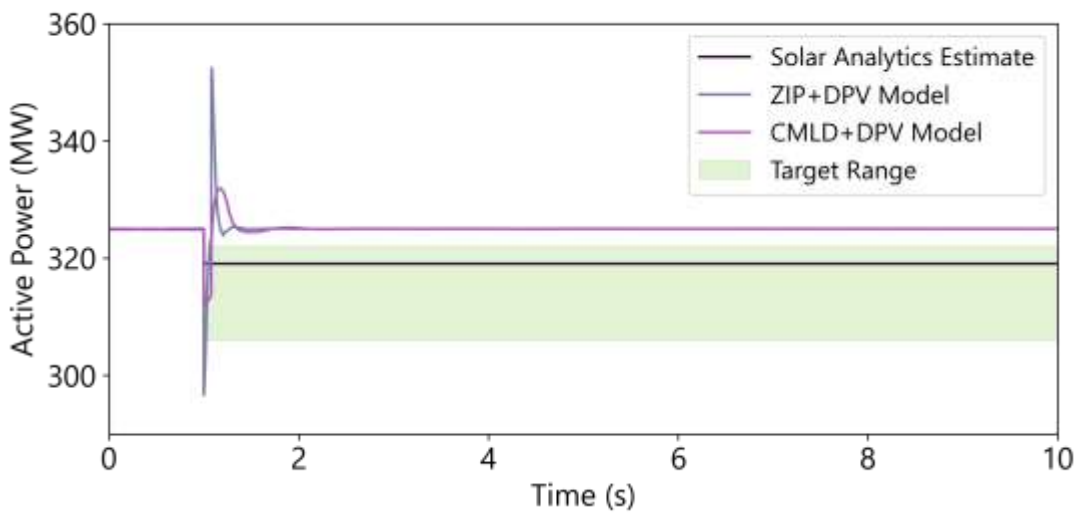

6.4.5 SCADA measurements

Figure 80 shows the total operational demand in Victoria (from SCADA), compared with the performance of the various models. Operational demand was relatively unchanged during this event. The CMLD+DPV model was tuned to match the load change represented by the green dashed line in Figure 80, with the uncertainty margin represented by the shaded green target range.

Figure 80 Operational demand measurements (SCADA) – 3 March 2019

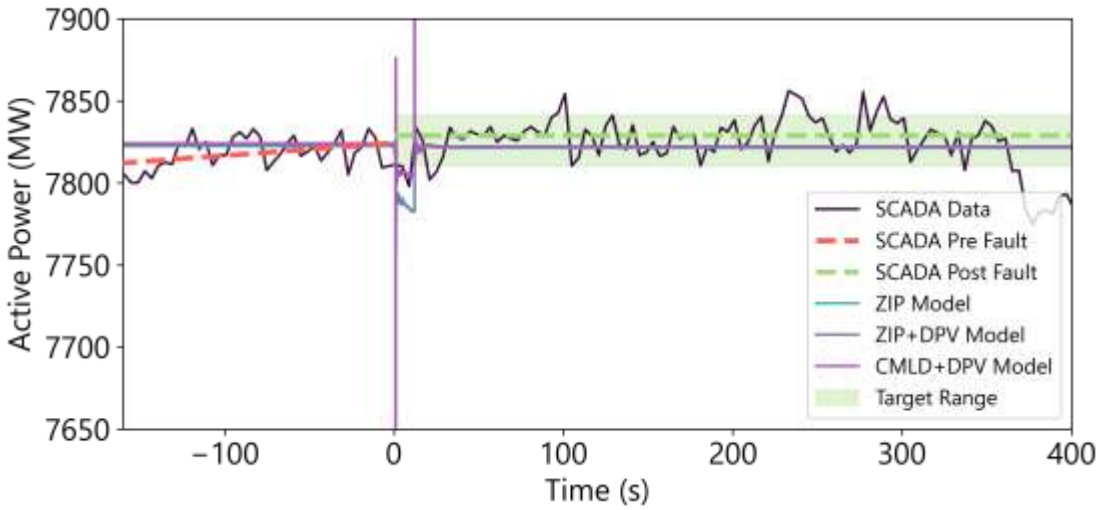

As shown in Figure 80, and summarised in **Table 52**, all models accurately represent the minimal change in operational demand observed in this event.

Table 52 Summary of change in demand and distributed PV – 3 March 2019

	Actuals (estimated)	CMLD+DPV prediction
Change in DPV generation (estimated from Solar Analytics sample)	6 MW (3 – 19 MW) decrease	No change, 0 MW decrease (accurately predicts minimal change)
Change in underlying demand (estimated from SCADA & Solar Analytics)	5 MW increase (27 decrease to 20 MW increase)	Minimal change, 1 MW increase (accurately predicts minimal change, and within range)
Change in operational demand (estimated from SCADA, 112s post disturbance)	11 MW increase (8 MW decrease to 23 MW increase)	Minimal change, 1 MW increase (accurately predicts minimal change, and within range)

This validation case demonstrates that the CMLD+DPV model is not significantly overestimating DPV and load disconnection in events where none occurred. For this event, because minimal disconnection occurred, the ZIP model provides comparable outcomes.

6.4.6 Assessment of model performance

Table 53 provides a summary of the CMLD+DPV model performance in this case. Green indicates the CMLD model provides a good match to HSM, orange indicates the CMLD model provides a fair match to HSM, red indicates the CMLD model provides a poor match to HSM. A cross indicates where the ZIP model performs better

than CMLD, a tick shows where the CMLD model performs at least as well as the ZIP model, and a double tick indicates where the CMLD model performs significantly better than the ZIP model.

Table 53 Assessment of model performance – 3 March 2019

Quantity	Characteristic	CMLD+DPV estimates	CMLD+DPV model equal (✓) or better (✓✓) than ZIP?	Commentary
Voltages	Voltage overshoot	Fair match	✓	The CMLD+DPV marginally overestimates peak voltage overshoot magnitude, although it stays within the normal voltage as defined in the NER (0.9 to 1.1 pu).
	Voltage recovery rate	Fair match	✓	The CMLD+DPV voltage recovery speed is slightly slower following the fault but is within the normal range within 0.2s.
	Steady-state post disturbance	Good match	✓	CMLD+DPV voltages are accurate (settles to within 5% of the HSM data for all voltage channels).
Active power	During dynamic state	Fair match	✓	CMLD+DPV is reasonably aligned with HSM. Peak magnitudes are overestimated.
	Steady-state post disturbance	Good match	✓	CMLD+DPV returns to pre-fault conditions after the line recloses.
Reactive power	During dynamic state	Fair match	✓	CMLD+DPV is reasonably aligned with HSM. Peak magnitudes somewhat under/overestimated.
	Steady-state post disturbance	Good match	✓	CMLD+DPV returns to pre-fault conditions after the line recloses.
DPV	DPV change	Good match	✓	Estimated actuals: 6 MW decrease DPV: No change (0 MW decrease) The DPV model accurately predicts minimal DPV disconnection.
CMLD	Underlying load change	Good match	✓	Estimated actuals: 5 MW increase (112s post disturbance) CMLD: Minimal change (1 MW increase) The CMLD model accurately predicts minimal load disconnection.
Operational demand	Net load change	Good match	✓	Estimated actuals: 11 MW increase CMLD+DPV: Minimal change (1 MW increase) The CMLD+DPV model accurately predicts minimal change in operational demand.

6.5 26 November 2019 – Queensland

6.5.1 Event overview

Table 54 Event summary – 26 November 2019

Date and time	26 November 2019, 12:14[115]
Region	Queensland

[115] AEMO. Trip of South Pine 275 kV No. 1 Busbar and 275/110 kV No. 5 Transformer on 26 November 2019, July 2020, at https://aemo.com.au/-/media/files/electricity/nem/market_notices_and_events/power_system_incident_reports/2019/incident-report-south-pine-incident-on-26-nov-19.pdf.

Date and time		26 November 2019, 12:14[115]
Description of the event		At 12:14 hours, a fault occurred internal to a 275 kV CT associated with CB 5452 at South Pine Substation. Concurrent with this incident, there was an unexpected protection trip of the 110 kV 1 Capacitor Banks at West Darra Substation due to the operation of the capacitor balance protection. The following network components were tripped following the incident: • H002 South Pine 275 kV No. 1 Busbar (No. 1 Busbar). • H002 South Pine 275/110 kV No. 5 Transformer (No. 5 Transformer). • T155 West Darra 110 kV No. 1 Capacitor Bank (No. 1 Capacitor).
Minimum voltage recorded		0.68 pu positive sequence recorded at Mudgeeraba (from HSM data)
Installed capacity of distributed PV		Total installed capacity: 2,833 MW (from APVI) • 57% installed under AS4777.3:2005 (from CER) • 43% installed under AS/NZS4777.2:2015 (from CER)
Prior to the event	Distributed PV	1,820 MW, 64% capacity factor (from ASEFS2, interpolated)
	Operational demand	6,323 MW (from SCADA data)
	Underlying demand	8,143 MW (estimate from SCADA + ASEFS2)
Estimated change (post disturbance vs pre disturbance)	Distributed PV	299 MW (range of 218-419 MW) decrease (from Solar Analytics data)
	Operational demand	330 MW (range of 213-330 MW) decrease (from SCADA data)
	Underlying demand	629 MW (range of 431-749 MW) decrease (estimate from SCADA + Solar Analytics data)

Figure 81 Map – 26 November 2019

6.5.2 Replication in PSS®E

The following element changes were made in PSS®E to replicate this case:

Table 55 Simulation event summary – 26 November 2019

Time (s)	Events/comments
0.0	Start simulation
1.0	Apply 1PG fault on the 275 kV South Pine bus (PSS®E bus 46020)
1.2	Clear 1PG fault on the 275 kV South Pine bus (PSS®E bus 46020) Trip South Pine 2 275/110 kV transformer (PSS®E bus 46020 to 45023)
60	End simulation

6.5.3 High speed measurements

Voltages

Figure 82 shows the voltages at the 275 kV Greenbank bus (close to the fault). Observations at this location were found to be illustrative of the voltage response at all locations with HSM data available[116].

In this disturbance, the CMLD+DPV model shows a similar voltage recovery profile to the HSM and demonstrates a significant improvement compared with the excessively rapid voltage recovery of the ZIP/ZIP+DPV models.

The ZIP models show a significant voltage over-shoot that is higher than observed and outside of the normal range (>1.1 pu) for 100 ms. The voltage overshoot is reduced but still present for the CMLD+DPV model. Greenbank was the only location with voltage overshoot exceeding 1.1 pu. This is not desirable, but the short duration should not cause unintended operation of transmission protection devices modelled in PSS®E.

The steady-state voltage after the disturbance (measured at 60s, not shown) is comparable with observations for all models.

Figure 82 Voltage – 26 November 2019 – 275 kV Greenbank Bus

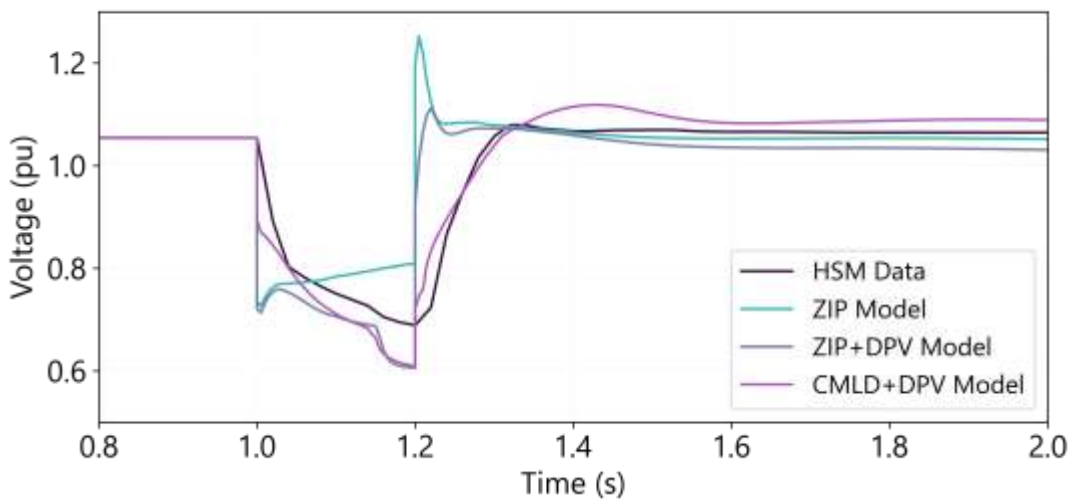

[116] HSM data was available for the following locations: 275 kV Greenbank bus, 275/110 kV South Pine Transformers (P, Q only), 275 kV Braemar, 275 kV Gladstone Power Station, 275 kV Tarong Power Station, 275 kV Millmerran bus, 275 kV Calvale bus, and 110 kV Mudgeeraba bus (V only).

Active and reactive power flows

Figure 83 shows the active and reactive power measurements at the 275 kV Greenbank (HSM location) to Mudgeeraba line 1, which is in the vicinity of the disturbance. Observations at this location are illustrative of typical measurements recorded in this event. At Greenbank and most locations, active power is reasonably well represented during the transient period, although peak flows immediately post fault are somewhat underestimated. This may be attributable to the inability of the power electronics load component in CMLD to model the dynamic response of VFD loads in the area, as discussed further in Section 9.7. Steady-state active power post disturbance (measured at 60s, not shown) is predicted reasonably well by all models.

The trajectory of the reactive power measured at Greenbank is accurately represented by CMLD, although the minimum peak reactive flows are slightly over-estimated during the fault. This may be attributed to the shortcomings of existing HSM data[117] which cannot accurately capture transient or fault events because in such cases the waveform is not sinusoidal and changes amplitude, phase angle and frequency over a very short interval, as discussed further in Section 9.7.

In this case, the CMLD+DPV model provides a considerable improvement over the ZIP/ZIP+DPV models, which do not depict the general dynamic reactive power response trajectory at all in some observations, as shown in the figure below. This could be due to AEMO's implementation of the ZIP model which represents all loads as constant current load. The diverse load types in the NEM are better captured by the CMLD model.

Figure 83 Active/reactive power – 26 November 2019 – 275 kV Greenbank (GBK) to Mudgeeraba Line 1

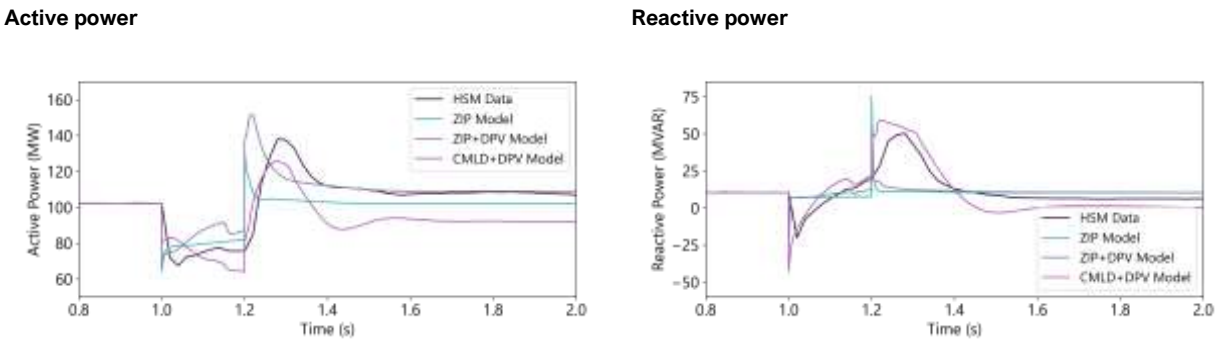

For comparison, **Figure 84** shows the active and reactive power measurements at South Pine[118]. There is 266 MW of DPV (~15% of all DPV generating in Queensland during this period) connected to the South Pine bus in PSS®E during this event.

At this location, active power measurements are reasonably well represented by all models during the dynamic and steady-state periods. The small difference between the ZIP model and ZIP+DPV model responses suggests that even large amounts of connected DPV at the South Pine bus is not significantly influencing the active power

[117] The HSM's that AEMO has access to at the transmission level are Phasor Measurement Units (PMU's) with low (20ms) sampling rates. PMU's perform extensive waveform filtering and data processing to create synchrophasors. This distorts the resulting data relative to the source waveform.

[118] Note that the static var compensator and switched shunts at South Pine were off at the time of the event and do not play a role in the dynamic response.

response in this disturbance. The response is much more strongly affected by the load model, and the CMLD model demonstrates a closer match to observations compared with the ZIP model.

The reactive power measurements at this location are poorly represented by all models. This suggests misrepresentation of the surrounding network components in the PSS®E model such as the South Pine transformer. Measurements at the nearby South Pine to Rocklea feeder are less influenced by the South Pine transformer and it is evident that at this more distant location all models better represent the trajectory observed.

Figure 84 Active/reactive power – 26 November 2019

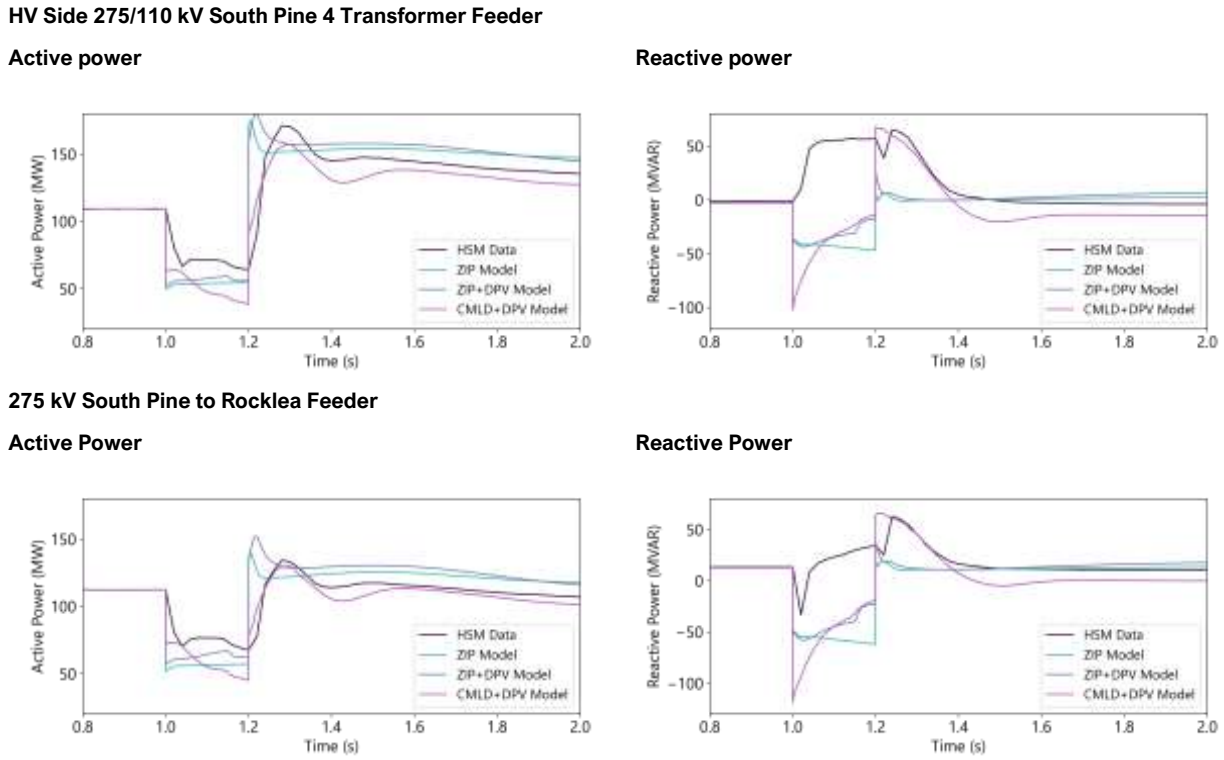

6.5.4 DPV measurements

Figure 85 shows the total measured DPV generation in Queensland (initial value estimated from ASEFS2 and the change post disturbance estimated from Solar Analytics datasets) compared with the performance of the CMLD+DPV model and the ZIP/ZIP+DPV model. The CMLD+DPV model underestimates the estimated 299 MW DPV disconnection for this event by 21%.

Figure 85 DPV measurements (Solar Analytics) – Queensland total – 26 November 2019

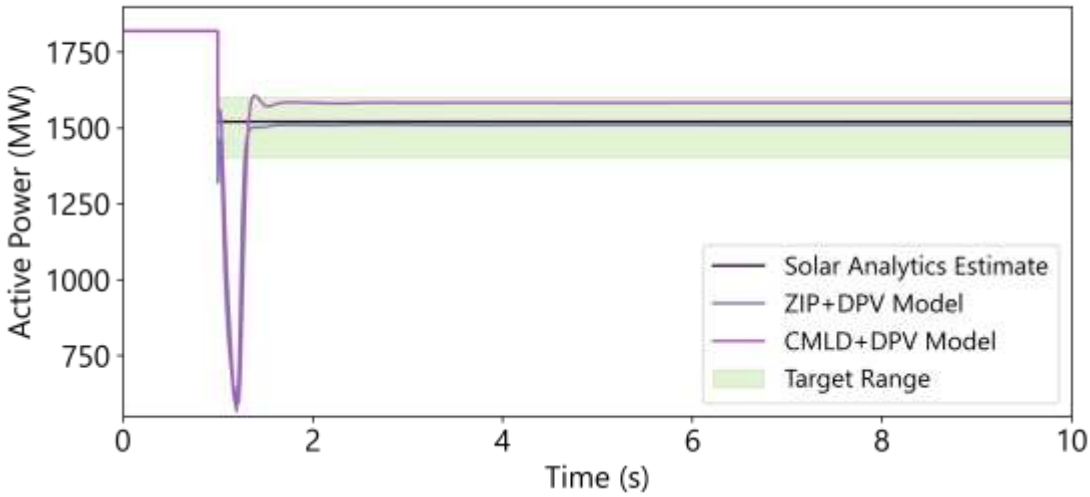

6.5.5 SCADA measurements

Figure 86 shows the total measured load in Queensland (from SCADA), compared with the performance of the various models.

As shown in Figure 86, in this event, the post disturbance operational demand declined gradually, reaching a minimum approximately 2-3 minutes after the disturbance. It is unclear whether this gradual decline is representative of real load behaviour, or if this may represent inaccuracies in the SCADA measurement. Similarly, and due to the severity of the fault, the Motor D component of the CMLD stalls (for the first ~11 s), followed by a gradual reduction in active power (over the next 60 s).

The CMLD+DPV model was tuned to match the load change measured at 168 s post disturbance (represented by the green dashed line in Figure 86), but it is acknowledged that there are significant inaccuracies in the SCADA measurement for this event.

Figure 86 Operational demand measurements (SCADA) – 26 November 2019

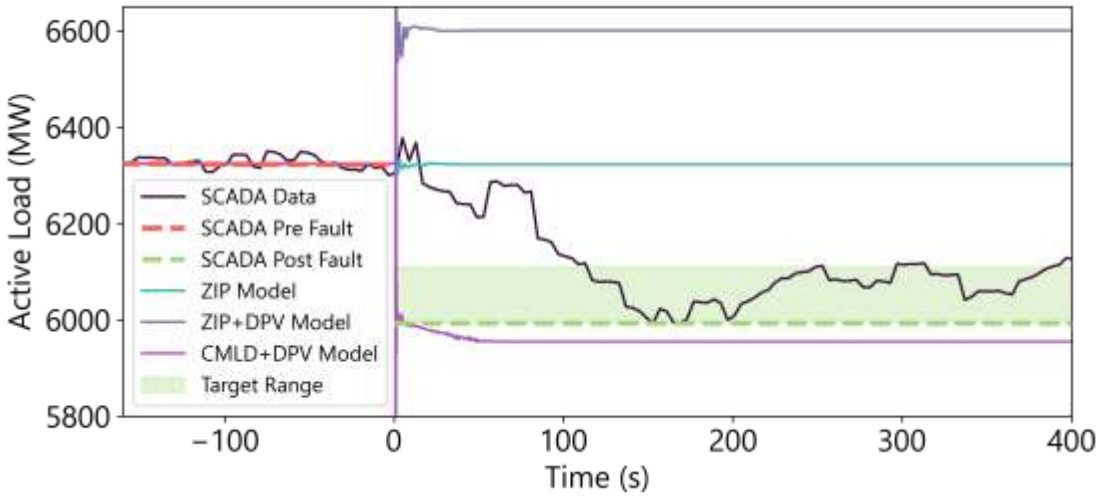

As shown in Figure 86, the CMLD+DPV model somewhat overestimates the net 330 MW decrease in operational demand. The CMLD model predicts 607 MW of total underlying load loss, offset by 237 MW of DPV disconnection predicted by the DPV model, leading to a total net decrease in operational demand of 369 MW. The comparison with estimated actuals is shown in **Table 56**. In this case, the CMLD model slightly underestimates load disconnection and the DPV model underestimates DPV disconnection, with errors offsetting each other and leading to a reasonably accurate estimate of operational demand.

Table 56 Summary of change in demand and distributed PV – 26 November 2019

	Actuals (estimated)	CMLD+DPV prediction
Change in DPV generation (estimated from Solar Analytics sample)	299 MW (218 – 419 MW) decrease	237 MW decrease (underestimates by 21% but within the target range)
Change in underlying demand (estimated from SCADA & Solar Analytics)	629 MW (431 – 749 MW) decrease	607 MW decrease (underestimates by 4%, but within range)
Change in operational demand (estimated from SCADA, 280s post disturbance)	330 MW (213 – 330 MW) decrease	369 MW decrease (overestimates by 12%, and marginally outside target range)

The ZIP model cannot represent any load disconnection, but the ZIP+DPV model does show an increase in operational demand following the disturbance (as shown in Figure 86). For this case, the accurate estimate of DPV disconnection from the DPV model is not offset by corresponding load disconnection (since this cannot be replicated by the ZIP model), resulting in a net load gain which is clearly misaligned with the SCADA observations. This highlights the importance of applying the CMLD model whenever using the DPV model in events where DPV disconnection is occurring.

Load change in the Brisbane metropolitan area was also measured and found to be comparable between the SCADA and CMLD+DPV model representation (although also underestimated by a similar proportion).

6.5.6 Assessment of model performance

Table 57 provides a summary of the CMLD+DPV model performance for this event. Green indicates the CMLD model provides a good match to HSM, orange indicates the CMLD model provides a fair match to HSM, red indicates the CMLD model provides a poor match to HSM. A cross indicates where the ZIP model performs better than CMLD, a tick shows where the CMLD model performs at least as well as the ZIP model, and a double tick indicates where the CMLD model performs significantly better than the ZIP model.

Table 57 Assessment of model performance – 26 November 2019

Quantity	Characteristic	CMLD+DPV estimates	CMLD+DPV model equal (✓) or better (✓✓) than ZIP?	Commentary
Voltages	Voltage overshoot	Poor match	✓✓	CMLD+DPV overestimates peak voltage overshoot magnitude and exceeds normal voltages (for ~100ms) as defined in the NER (0.9 to 1.1 pu).
	Voltage recovery rate	Good match	✓✓	CMLD+DPV aligned with HSM
	Steady-state post disturbance	Good match	✓	CMLD+DPV voltages are accurate (settles to within 5% of the HSM data for all voltage channels).
Active power	During dynamic state	Fair match	✓	CMLD+DPV has a similar trajectory to the HSM, although it over/underestimates peak max flows during the dynamic state.
	Steady-state post disturbance	Good match	✓	CMLD+DPV aligned with HSM
Reactive power	During dynamic state	Fair match	✓✓	CMLD+DPV trajectory aligned with HSM data for most channels (excluding South Pine transformer feeder). Peak flows during and after the fault are sometimes over/underestimated, respectively.
	Steady-state post disturbance	Good match	✓	CMLD+DPV aligned with HSM.
DPV	DPV change	Fair match	✓✓	Estimated actuals: 299 MW decrease DPV: 237 MW decrease The DPV model underestimates DPV disconnection by 21%, within target range.
CMLD	Underlying load change	Good match	✓✓	Estimated actuals: 629 MW decrease (168 s post disturbance) CMLD: 607 MW decrease The CMLD model slightly underestimates load disconnection by 4%, but within range.
Operational demand	Net load change	Fair match	✓✓	Estimated actuals: 330 MW decrease CMLD+DPV: 369 MW decrease The CMLD+DPV model slightly overestimates the change in operational demand by 12%, marginally outside of range.

6.6 24 January 2021 – South Australia

6.6.1 Event overview

Table 58 Event summary – 24 January 2021

Date and time		24 January 2021, 16:43[119]
Region		South Australia
Description of the event		There were six faults in the area, which resulted in the following three transmission lines being tripped: • Cherry Gardens – Mount Barker 132 kV (fault 1, 2, and 6, not modelled, as described below) • Cherry Gardens – Mount Barker South 275 kV (fault 3, modelled) • Cherry Gardens – Tailem Bend 275 kV (fault 4 and 5, modelled) At 15:17 the NEM SCADA system experienced intermittent failures, and at 15:46 all SCADA failed[120]. The SCADA failure did not contribute to or exacerbate this incident.
Minimum voltage recorded		0.70 pu positive sequence recorded at Para (from HSM data)
Installed capacity of DPV		Total installed capacity: 1,558 MW • 45% installed under AS4777.3:2005 (from CER) • 55% installed under AS/NZS4777.2:2015 (from CER)
Prior to the event	**DPV**	576 MW, 37% capacity factor (from ASEFS2, interpolated)
	Operational demand	2,601 MW before the first fault (not modelled) 2,483 MW before the third fault (modelled) (from SCADA data)
	Underlying demand	3,059 MW (estimate from SCADA + ASEFS2)
Estimated change (post disturbance vs pre disturbance)	**DPV**	115 MW (range of 69-138 MW) decrease (from Solar Analytics data)
	Operational demand	225 MW (range of 211-280 MW) decrease (from SCADA data) Total operational demand change measured for this event was 306 MW, but only the more severe faults three to five (which caused a 225 MW decrease in operational demand) has been explicitly modelled in these validation studies.
	Underlying demand	340 MW (range of 281-419 MW) decrease (estimate from SCADA + Solar Analytics data)

[119] AEMO. Trip of Multiple Cherry Gardens Lines on 24 January 2021, June 2021, at https://aemo.com.au/-/media/files/electricity/nem/market_notices_and_events/power_system_incident_reports/2021/trip-of-multiple-cherry-gardens.pdf.

[120] AEMO. Total Loss of AEMO SCADA Systems on 24 January 2021, September 2021, at https://aemo.com.au/-/media/files/electricity/nem/market_notices_and_events/power_system_incident_reports/2021/final-report-total-loss-of-nem-scada-data.pdf.

Figure 87 Map – 24 January 2021

6.6.2 Replication in PSS®E

Due to dynamic simulation time constraints, AEMO only modelled the most severe load disconnection associated with the third, fourth and fifth faults (trip of the 275 kV Cherry Gardens – Mt Barker and 275 kV Tailem Bend – Cherry Gardens lines) and did not model the Cherry Gardens – Mount Barker 132 kV line faults. This line was set to out of service for the PSS®E simulation.

The following element changes were made in PSS®E to replicate this case:

Table 59 Simulation event summary – 24 January 2021

Time (s)	Events/comments
0.0	Start simulation
1.0	Apply 2PG fault on the 275 kV Cherry Gardens bus (PSS®E bus 511580)
1.085	Clear 2PG fault on the 275 kV Cherry Gardens bus (PSS®E bus 511580) Trip 275 kV Cherry Gardens (PSS®E bus 511580) to Mt Barker South (PSS®E bus 553580) line
37.76	Apply 1PG fault on the 275 kV Tailem Bend bus (PSS®E bus 586580)
37.846	Clear 1PG fault on the 275 kV Tailem Bend bus (PSS®E bus 586580) Trip 275 kV Tailem Bend (PSS®E bus 586580) to Cherry Gardens (PSS®E bus 511580) line
60	End simulation

6.6.3 High speed measurements

Voltages

Figure 88 shows the voltages at the 275 kV Para bus, one of the closer HSM buses to the faulted location. Observations at Para are illustrative of the voltage response at all 275 kV HSM locations assessed[121].

In this disturbance, the CMLD+DER model closely replicates the HSM voltage recovery profile, especially once the voltage recovers to the normal range of 0.9 pu to 1.1 pu. In contrast, the ZIP/ZIP+DPV models recover too quickly immediately following the fault.

All models overestimate voltage over-shoot but stay within the normal range. The post fault steady-state voltage predicted by all models is also comparable with observations.

Figure 88 Voltage – 24 January 2021 – 275 kV Para bus (Third fault – Cherry Gardens – Mount Barker South trip)

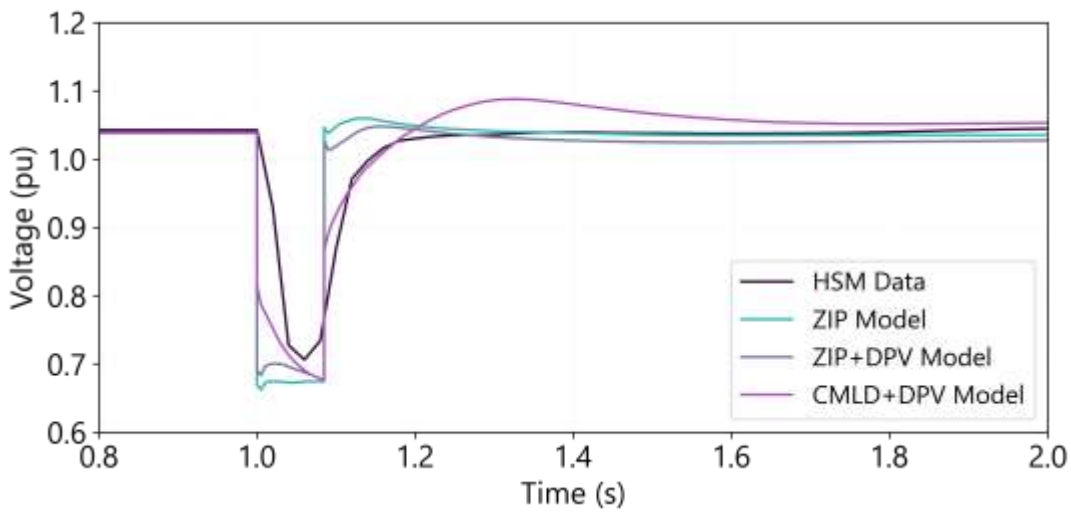

Active and reactive power flows

Figure 89 shows observations at the TIPS B to City West feeder, which is in the vicinity of the fault, and shows results that are typical of most observed locations. The CMLD+DPV model approximately captures the general trajectory of the active power measurements at this location but misrepresents the peak (minimum and maximum) power flow during the transient period. This may be due to factors discussed further in Section 9.7.

Immediately following the initial fault, active power falls gradually over the subsequent ~5 s. The CMLD+DPV model captures this more accurately than the ZIP models (which show an increase in active power that is clearly misaligned with observations). However, the CMLD+DPV model does not show the full extent of active power reduction and is unable to capture the slow rate of decline.

[121] HSM data was available at the following locations: 275 kV Para, 275 kV Pelican Point, 275 kV Tailem Bend, 275 kV TIPS B, 275 kV Robertstown to Mokota and Tungkillo Feeders (P, Q only).

Figure 89 Active power – 275 kV TIPS B to City West Feeder – 24 January 2021

Third fault – Cherry Gardens – Mount Barker South trip

2 s duration **45 s duration**

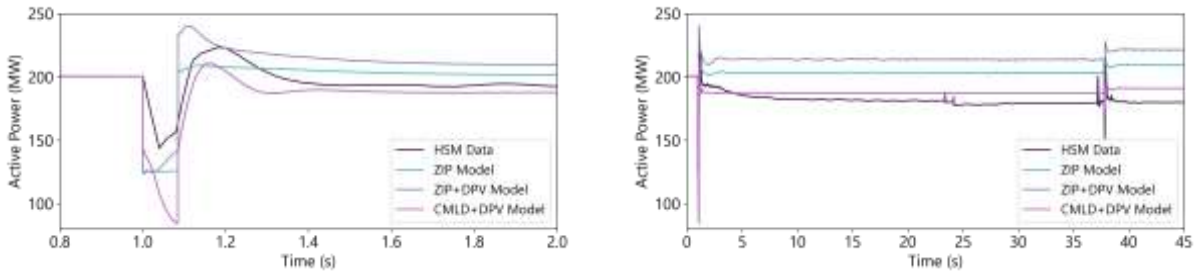

The reactive power result at this location is shown in **Figure 90**. The dynamic trajectory is in line with observations, but the peak flows during the fault are slightly overestimated for the CMLD+DPV model. Both City West reactors were in service and represented in PSS®E for this disturbance.

Steady state flows are shown in Figure 90 on the right, illustrating the longer-term dynamics measured at this location. Following the initial fault, the CMLD+DPV model accurately captures the steady state reactive power levels, although the slow decline over the first ~5 s is not well captured. The ZIP models do not capture the reduction in steady state reactive power at all. The causes for the observed reduction in reactive power at 23 s is unknown, and therefore not represented in the simulation.

Figure 90 Reactive power – 275 kV TIPS B to City West Feeder – 24 January 2021

Third fault – Cherry Gardens – Mount Barker South trip

2 s duration **45 s duration**

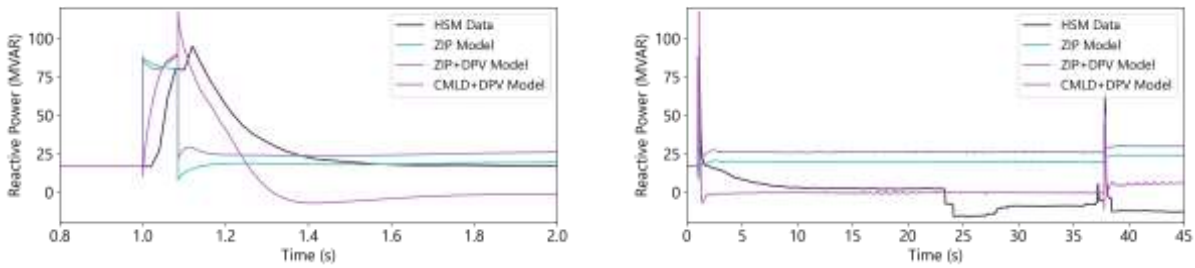

Observations on the Robertstown feeder are also included below to show the dynamic and steady-state response further away from the fault. Active power measurements are shown in **Figure 91**. At this location, the general trajectory of the CMLD+DPV model active power are well represented, but peak flows are underestimated during and immediately following the fault.

In steady-state following each disturbance, the CMLD+DPV model over-predicts active power, while the ZIP models underestimate active power.

Figure 91 Active power – 275 kV Robertstown to Tungkillo Feeder 1 – 24 January 2021

Third fault – Cherry Gardens – Mount Barker South trip

2 s duration

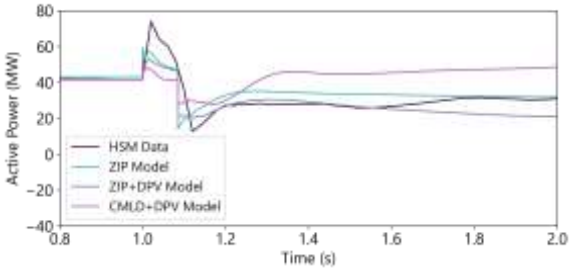

Fourth and fifth fault – Cherry Gardens – Tailem Bend trip

2 s duration

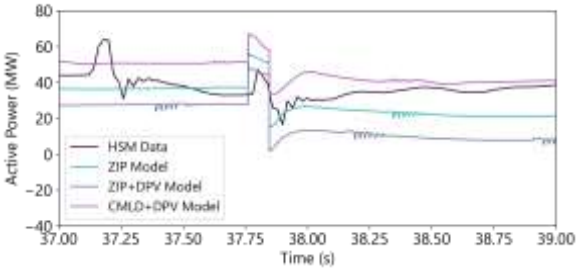

Whole duration (45 s)

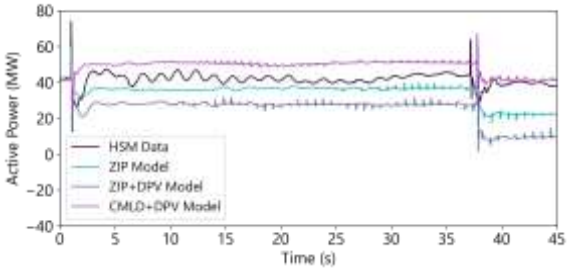

Reactive power observations at this feeder are shown in **Figure 92**. The dynamic trajectory is accurate, but the peak reactive power during the fault is slightly underestimated for all models.

The CMLD+DPV model overestimates the steady-state reduction in reactive power flows, while the ZIP models underestimate the steady-state reduction in reactive power flows.

Figure 92 Reactive power – 275 kV Robertstown to Tungkillo Feeder 1 – 24 January 2021

Third fault – Cherry Gardens – Mount Barker South trip

2 s duration

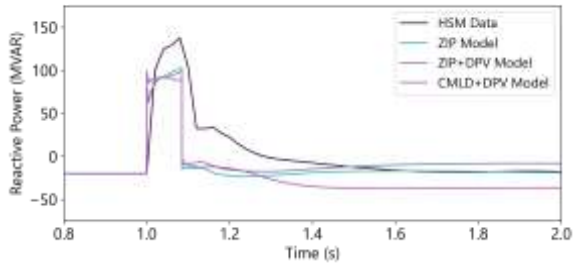

Fourth and fifth fault – Cherry Gardens – Tailem Bend trip

2 s duration

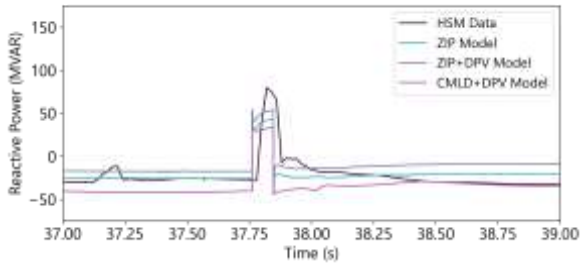

Whole duration (45 s)

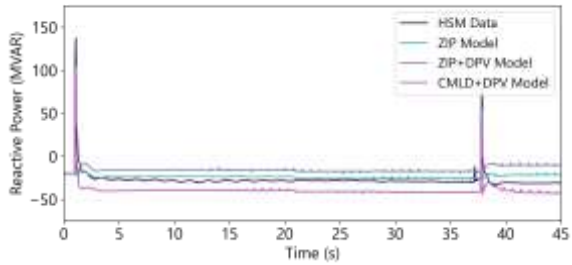

6.6.4 DPV measurements

Figure 93 shows the total measured DPV generation in South Australia (initial value estimated from ASEFS2 and the change post disturbance estimated from Solar Analytics datasets) compared with the performance of the various models. In both simulations, the DPV model accurately predicts the 104 MW DPV disconnection estimated for this event.

Figure 93 DPV measurements (Solar Analytics) – South Australia total – 24 January 2021

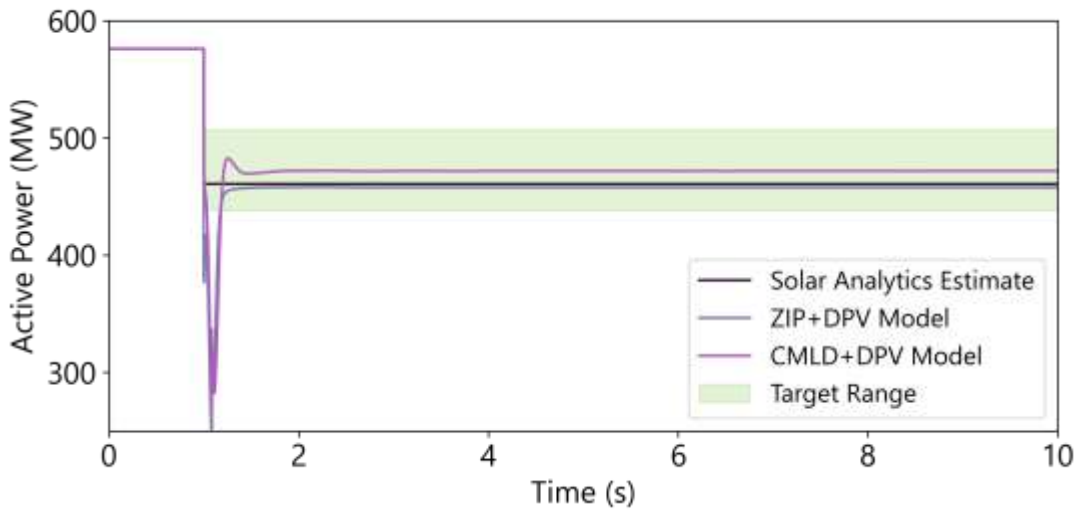

6.6.5 SCADA measurements

Figure 94 shows the total measured load in South Australia (from SCADA), compared with the performance of the various models. The CMLD+DPV model was tuned to match the load change measured at 60 s post disturbance (represented by the green dashed line in **Figure 94**), but it is acknowledged that there are inaccuracies in the SCADA measurement.

Figure 94 Operational demand measurements (SCADA) – 24 January 2021

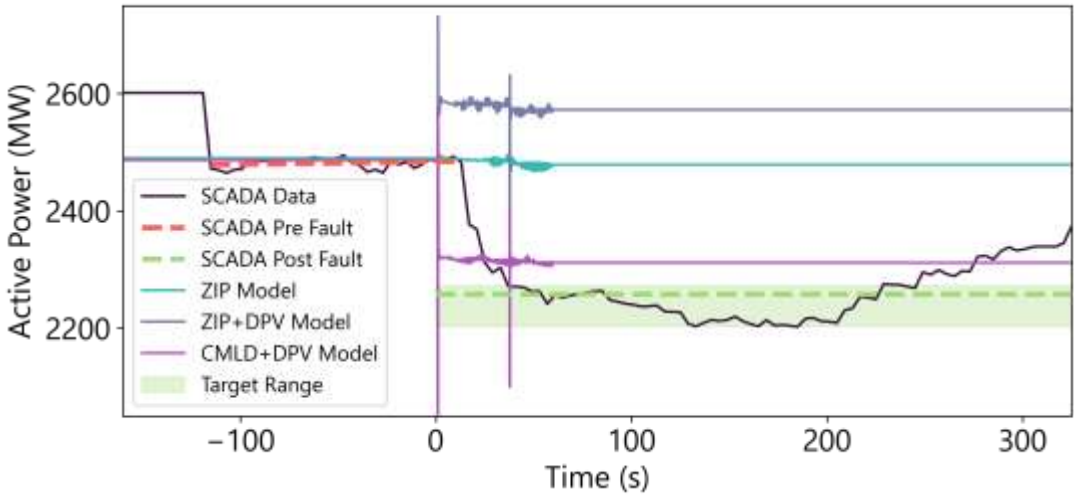

The CMLD+DPV model somewhat underpredicts the estimated net 225 MW decrease in operational demand. The comparison with estimated actuals is shown in **Table 60**. In this case, underestimation of load disconnection is the primary reason for the overall error in the net change in operational demand.

Table 60 Summary of change in demand and distributed PV – 24 January 2021

	Actuals (estimated)	CMLD+DPV prediction
Change in DPV generation (estimated from Solar Analytics sample)	115 MW (69 – 138 MW)	104 MW decrease (underestimates by 10%, but within range)
Change in underlying demand (estimated from SCADA & Solar Analytics)	340 MW (281 – 419 MW) decrease	279 MW decrease (underestimates by 18%, and marginally outside of range)
Change in operational demand (estimated from SCADA, 60s post disturbance)	225 MW (211 – 280 MW) decrease	175 MW decrease (underestimates by 22%, and outside of range)

The ZIP model cannot represent any load disconnection. For the ZIP+DPV case, the lack of load disconnection is compounded with DPV disconnection, resulting in a net load gain which is clearly misaligned with the SCADA observations. This highlights the importance of applying the CMLD model when using the DPV model to analyse severe voltage disturbances.

Load change in the Adelaide metropolitan area was also measured and found to be comparable between the SCADA and CMLD+DPV model representation (although also underestimated by a similar proportion).

6.6.6 Assessment of model performance

Table 61 provides a summary of the CMLD+DPV model performance for this event. Green indicates the CMLD model provides a good match to HSM, orange indicates the CMLD model provides a fair match to HSM, red indicates the CMLD model provides a poor match to HSM. A cross indicates where the ZIP model performs better than CMLD, a tick shows where the CMLD model performs at least as well as the ZIP model, and a double tick indicates where the CMLD model performs significantly better than the ZIP model.

Table 61 Assessment of model performance – 24 January 2021

Quantity	Characteristic	CMLD+DPV estimates	CMLD+DPV model equal (✓) or better (✓✓) than ZIP?	Commentary
Voltages	Voltage overshoot	Fair match	✓	The CMLD+DPV marginally overestimates peak voltage overshoot magnitude, but it stays within the normal range (0.9 to 1.1 pu).
	Voltage recovery rate	Good match	✓✓	CMLD+DPV comparable to HSM after voltages return to normal range.
	Steady-state post disturbance	Good match	✓	CMLD+DPV voltages are accurate (settles to within 5% of the HSM data for all voltage channels).
Active power	During dynamic state	Fair match	✓	CMLD+DPV has a similar trajectory to the HSM, although it slightly underestimates peak flows during the fault.
	Steady-state post disturbance	Good match	✓✓	CMLD+DPV aligned with HSM for first disturbance in all cases and aligned with HSM for second disturbance in most cases.
Reactive power	During dynamic state	Fair match	✓	CMLD+DPV has a similar trajectory to the HSM, although it slightly underestimates peak flows during the fault.
	Steady-state post disturbance	Good match	✓✓	CMLD+DPV aligned with HSM and significantly better than ZIP+DPV for 50% of HSM channels.
DPV	DPV change	Good Match	✓	Estimated actuals: 115 MW decrease DPV: 104 MW decrease The DPV model underestimates DPV disconnection by 10%, within uncertainty range.
CMLD	Underlying load change	Good match	✓✓	Estimated actuals: 340 MW decrease CMLD: 279 MW decrease The CMLD underestimates load disconnection by ~18% when measured at 60 s post disturbance.
Operational demand	Net load change	Fair match	✓✓	Estimated actuals: 225 MW decrease (60 s post disturbance) CMLD+DPV: 175 MW decrease. The CMLD+DPV underestimates the change in operational demand by 22%, and this is attributed mainly to the CMLD underestimating underlying load disconnection.

6.7 12 March 2021 – South Australia

6.7.1 Event overview

Table 62 Event summary – 12 March 2021

Date and time		12 March 2021, 17:08[122]
Region		South Australia (SA)
Description of the event		Torrens Island A and B West 275 kV Busbars tripped due to a current transformer failure associated with the Torrens Island substation West bus section circuit breaker. This disconnected Barkers Inlet power station from 111 MW and the Torrens West 275/66 kV West transformer. All equipment was returned to service at 0922 hrs on 14 March.
Minimum voltage recorded		0.54 pu positive sequence at Torrens Island Power Station A (from HSM Data)
Installed capacity of DPV		Total installed capacity: 1,637 MW • 43% installed under AS4777.3:2005 (from CER) • 57% installed under AS/NZS4777.2:2015 (from CER)
Prior to the event	**DPV**	460 MW, 28% capacity factor (from ASEFS2, interpolated)
	Operational demand	1,516 MW (from SCADA data)
	Underlying demand	1,976 MW (estimate from SCADA + ASEFS2)
Estimated change (post disturbance vs pre disturbance)	**DPV**	74 MW (range of 51-106 MW) decrease (from Solar Analytics data)
	Operational demand	96 MW (range of 42-96 MW) decrease (from SCADA data)
	Underlying demand	170 MW (range of 92-202 MW) decrease (estimate from SCADA + Solar Analytics data)

[122] AEMO. Final Report – Trip of Torrens Island A and B West 275 kV busbars on 12 March 2021, November 2021, at https://aemo.com.au/-/media/files/electricity/nem/market_notices_and_events/power_system_incident_reports/2021/final-report-torrens-island-275-kv-west-busbar-trip.pdf?la=en.

Figure 95 Map – 12 March 2021

6.7.2 Replication in PSS®E

The following element changes were made in PSS®E to replicate this case:

Table 63 Simulation event summary – 12 March 2021

Time (s)	Events/comments
0.0	Start simulation
1.0	Apply 1PG fault on the 275 kV TIPS A bus (PSS®E bus 590580)
1.08	Clear 1PG fault on the 275 kV TIPS A bus (PSS®E bus 590580) Trip 275 kV TIPS A (PSS®E bus 590580) to TIPS B (PSS®E bus 591080) line (branch 2) Trip 275 kV Barker Inlet Power Station (BIPS) bus (PSS®E bus 505680) Trip 275 kV BIPS (PSS®E bus 505680) to TIPS B (PSS®E bus 591080) line Trip BIPS GN1 275/15 kV transformer (PSS®E bus 505611 to 505680) Trip 15 kV BIPS GN1 (PSS®E bus 505611) to 5DMY02421 (PSS®E bus 52421) line Trip BIPS GN1 generator (PSS®E bus 52421) operating at 111 MW[123] Trip TIPS A 275/66 kV transformer (PSS®E bus 590580 to 590530)
60	End simulation

[123] Barker Inlet Power Station is modelled as a negative load as AEMO does not have a dynamic PSS®E models for this generator.

6.7.3 High speed measurements

Voltages

Figure 96 shows the voltages at the faulted 275 kV TIPS A bus. Observations at this location are illustrative of the voltage response at all 275 kV HSM locations assessed[124].

In this disturbance, the CMLD+DPV model replicates the HSM voltage recovery profile closely. Voltage over-shoot is marginally overestimated following the fault but stays within the normal voltage range of 0.9 pu to 1.1 pu. The CMLD+DPV steady-state voltage is also comparable with observations. The ZIP/ZIP+DPV models recover too quickly following the fault but otherwise have a similar response to the CMLD+DPV model.

Figure 96 Voltage – 12 March 2021 – Torrens Island A bus

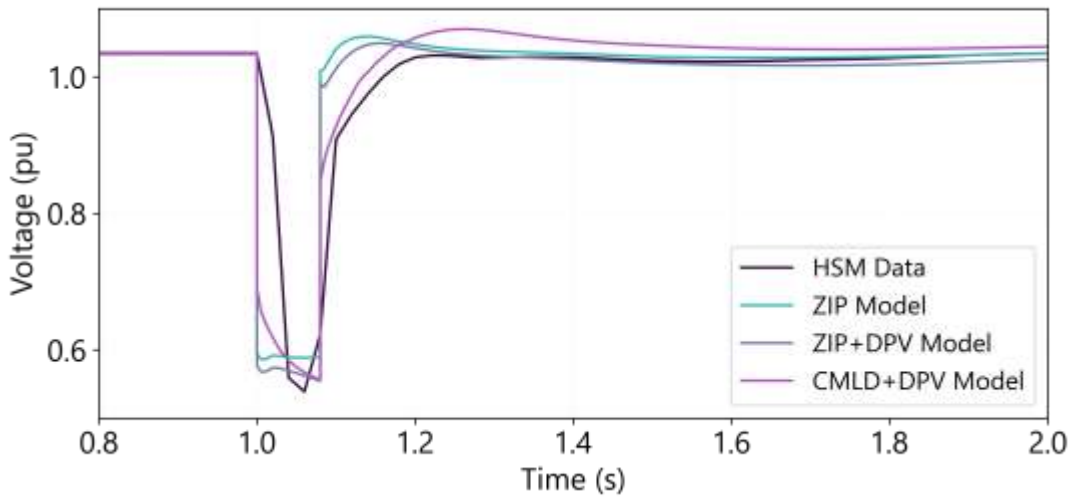

Active and reactive power flows

Figure 97 shows the active and reactive power measurements at the 275 kV TIPS A to Kilburn feeder, close to the disturbance. Observations on this line are illustrative of typical measurements recorded in this event.

Active power is well represented during the fault and in the steady-state. Minimum peak power flows during the fault are sometimes over-estimated by the CMLD+DPV model, while maximum peak power flows immediately after the fault are sometimes under-estimated. This mismatch may be due to the power electronics component of the load model being unable to represent the dynamic response of VSDs following a voltage disturbance, as discussed further in Section 9.7.

For reactive power, the approximate trajectory is accurately represented by the CMLD+DPV model, although the min/max reactive power flows are slightly over-estimated. The model presents an improvement over both ZIP models, which do not replicate the dynamic reactive power response trajectory in some observations.

[124] HSM data was available at the following locations: 275 kV TIPS A and TIPS B, 275 kV TIPS B to Lefevre and TIPS B to City West (P,Q only), and 275 kV Tailem Bend to South East feeder (V only).

The CMLD+DPV model accurately estimates steady state active power flows following the fault (measured at ~15s post fault, not shown in figures below), providing a significant improvement over the ZIP models which do not replicate this behaviour. All models replicate steady-state reactive power flows reasonably well.

Figure 97 Active/reactive power plots – 12 March 2021 – Torrens Island Power Station (TIPS) A to Kilburn Line 1 275 kV

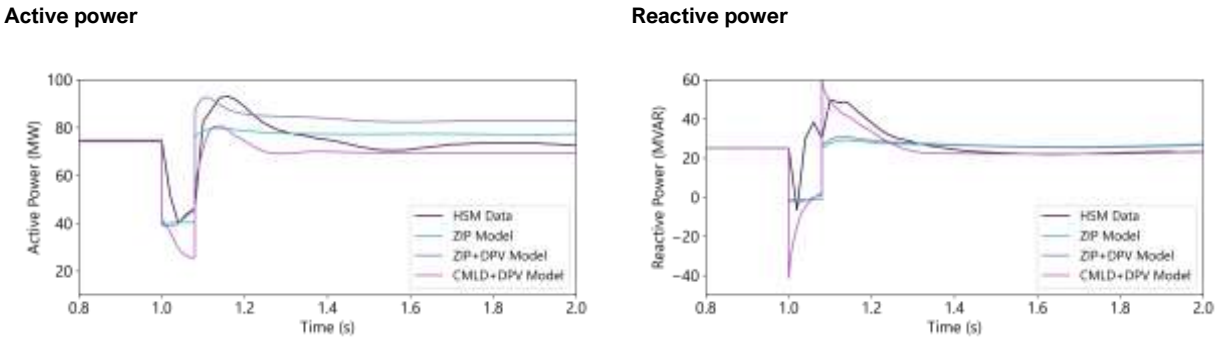

6.7.4 DPV measurements

Figure 98 shows the total measured DPV generation in South Australia (initial value estimated from ASEFS2 and the change post disturbance estimated from Solar Analytics datasets) compared with the performance of the various models. The CMLD+DPV slightly overestimates the 74 MW DPV disconnection estimated for this event but is within the uncertainty range.

Figure 98 DPV measurements (Solar Analytics) – South Australia Total – 12 March 2021

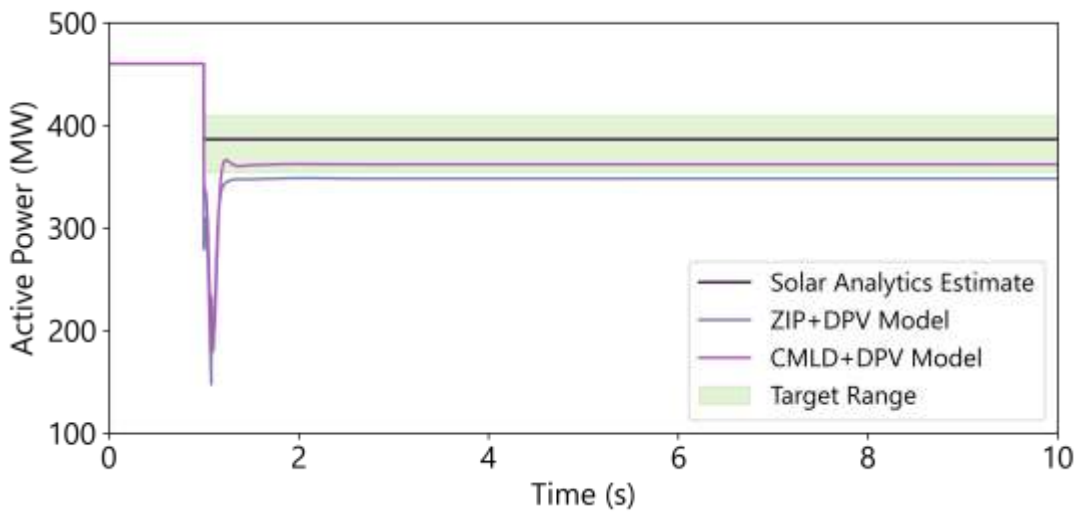

6.7.5 SCADA measurements

Figure 99 shows the total measured load in South Australia (from SCADA), compared with the performance of the various models. The CMLD+DPV model was tuned to match the load change measured at 212 s post disturbance (represented by the green dashed line in Figure 99) as an approximate measure of average post disturbance operational demand, but it is acknowledged that there are inaccuracies in the SCADA measurement.

Figure 99 Operational demand measurements (SCADA) – South Australia total – 12 March 2021

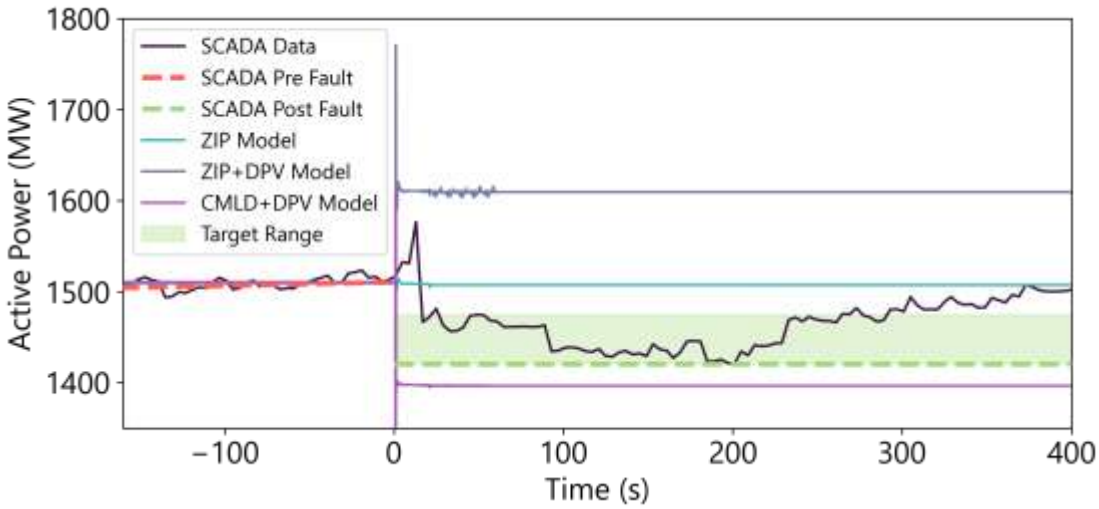

In this event, the CMLD+DPV model somewhat overpredicts the estimated net 96 MW decrease in operational demand. The CMLD model predicts 213 MW of total underlying load loss, offset by 98 MW of DPV disconnection predicted by the DPV model, leading to a total net decrease in operational demand of 115 MW. The comparison with estimated actuals is shown in **Table 64**.

Table 64 Summary of change in demand and distributed PV – 12 March 2021

	Actuals (estimated)	CMLD+DPV prediction
Change in DPV generation (estimated from Solar Analytics sample)	74 MW (51 –106 MW) decrease	98 MW decrease (overestimates by 33%, but within range)
Change in underlying demand (estimated from SCADA & Solar Analytics)	170 MW (92 –202 MW) decrease	213 MW decrease (overestimates by 25%, not within range)
Change in operational demand (estimated from SCADA, 76s post disturbance)	96 MW (42 –96 MW) decrease	115 MW decrease (overestimates by 20%, not within range).

Load change in the Adelaide metropolitan area was also measured and found to be comparable to SCADA (in underestimating net load change).

6.7.6 Assessment of model performance

Table 65 provides a summary of the performance of the CMLD+DPV model for this event. Green indicates the CMLD model provides a good match to HSM, orange indicates the CMLD model provides a fair match to HSM, red indicates the CMLD model provides a poor match to HSM. A cross indicates where the ZIP model performs better than CMLD, a tick shows where the CMLD model performs at least as well as the ZIP model, and a double tick indicates where the CMLD model performs significantly better than the ZIP model.

Table 65 Assessment of model performance – 12 March 2021

Quantity	Characteristic	CMLD+DPV estimates	CMLD+DPV model equal (✓) or better (✓✓) than ZIP?	Commentary
Voltages	Voltage overshoot	Fair match	✓	CMLD+DPV marginally overestimates peak voltage overshoot magnitude, although it stays within the 0.9 to 1.1 pu range.
	Voltage recovery rate	Good match	✓✓	CMLD+DPV comparable to HSM.
	Steady-state post disturbance	Good match	✓	CMLD+DPV voltages are accurate (settles to within 5% of the HSM data for all voltage channels).
Active power	During dynamic state	Fair match	✓	CMLD+DPV has a similar trajectory to the HSM, although it slightly over/underestimates peak flows during and immediately following the fault, respectively.
	Steady-state post disturbance	Good match	✓✓	CMLD+DPV aligned with HSM.
Reactive power	During dynamic state	Fair match	✓	CMLD+DPV has a similar trajectory to the HSM, although it slightly overestimates peak flows during and immediately following the fault.
	Steady-state post disturbance	Good match	✓	CMLD+DPV aligned with HSM.
DPV	DPV change	Fair match	✓✓	Estimated actuals: 74 MW decrease DPV: 98 MW decrease The DPV model overestimates PV disconnection by 33%.
CMLD	Underlying load change	Fair match	✓✓	Estimated actuals: 170 MW decrease CMLD: 213 MW decrease The CMLD overestimates load disconnection by 25% when measured at 212 s post disturbance.
Operational demand	Net demand change	Fair match	✓✓	Estimated actuals: 96 MW decrease CMLD+DPV: 115 MW decrease. The CMLD+DPV model overestimates the change in operational demand by 20%.

7 Validation: frequency disturbances

This section presents the validation studies conducted for the CMLD and DPV models during frequency disturbances in periods with significant levels of DPV generating.

7.1 25 August 2018 – South Australia

This section describes observations in South Australia during this event. Refer to sections 7.2 to 7.4 for the analysis relevant to Queensland, Victoria, and New South Wales.

7.1.1 Event overview

Table 66 Event summary – 25 August 2018 – South Australia

Date and time		25 August 2018, 13:11[125]
Region		South Australia
Description of the event		Both Queensland – New South Wales Interconnector (QNI) lines tripped, resulting in separation of the Queensland region from the rest of the NEM. This was followed by the separation of South Australia from the rest of the NEM, and under-frequency load shedding (UFLS) in New South Wales, Victoria, and Tasmania.
Minimum voltage recorded		1.00 pu positive sequence at TIPS B (from HSM Data)
Maximum voltage recorded		1.17 pu positive sequence at South East (from HSM Data)
Frequency nadir or zenith		Nadir: 49.13 Hz Zenith: 50.46 Hz
Installed capacity of DPV		Total installed capacity in South Australia: 938 MW (from APVI) • 75% installed under AS4777.3:2005 (from CER) • 25% installed under AS/NZS4777.2:2015 (from CER)
Prior to the event	**DPV**	590 MW, 63% capacity factor (from ASEFS2, interpolated)
	Operational demand	779 MW (from SCADA data)
	Underlying demand	1,369 MW (estimate from SCADA + ASEFS2)
Estimated change (post disturbance vs pre disturbance)	**DPV**	71 MW (38 – 122 MW) decrease (from Solar Analytics data)
	Operational demand	74 MW (8 – 135 MW) increase (from SCADA data)
	Underlying demand	2 MW increase (113 MW decrease – 97 MW increase) (from SCADA & Solar Analytics data)

[125] AEMO. Final Report – Queensland and South Australia system separation on 25 August 2018, January 2019. At https://aemo.com.au/-/media/files/electricity/nem/market_notices_and_events/power_system_incident_reports/2018/qld---sa-separation-25-august-2018-incident-report.pdf.

7.1.2 Replication in PSS®E

Table 67 Simulation event summary – 25 August 2018

Time (s)	Region	Events simulated	Comments
0.0		Start simulation	
1.0	QLD	Apply 1PG fault on the 330 kV Bulli Creek bus (PSS®E bus 49032)	
1.1	QLD	Clear 1PG fault on the 330 kV Bulli Creek bus (PSS®E bus 49032)	
3.0	QLD/NSW	Trip 330 kV Bulli Creek (PSS®E bus 49032) to Dumaresq (PSS®E bus 21256) line Trip 330 kV Armidale (PSS®E bus 21078) to Tamworth (PSS®E bus 21770) line (branch 2)	
3.2	QLD	Trip 11 kV Condamine Generator 2 bus (PSS®E bus 41007) Trip 11 kV Condamine Generator 3 bus (PSS®E bus 41005)	
5.0	NSW	Trip 106 MW 330 kV Tomago potline (PSS®E bus 21790)	Automatic UFLS scheme tripped 622 MW of two potlines after SA separation from VIC. Adjustments were made to better represent frequency responses in SA and VIC and so potlines were tripped at two time intervals (5 s and 10.1 s).
8.0	SA	Trip 700V Hallett Hill Wind Farm Generator bus (PSS®E bus 50960) Trip 700V Hallett Wind Farm Generator bus (PSS®E bus 50330) Trip 700V The Bluff Wind Farm Generator bus (PSS®E bus 50335) Trip 700V North Brown Hill Wind Farm Generator 1B bus (PSS®E bus 50092) Trip 700V North Brown Hill Wind Farm Generator 2A bus (PSS®E bus 50093)	Four wind farms reduced output to zero due to an incorrect protection setting after SA separation. Adjustments were made to better represent frequency responses in SA and VIC.
8.72	VIC	Trip 275 kV South East (PSS®E bus 34341) to Heywood Terminal Station (PSS®E bus 53900) line (branch 1) Trip 275 kV South East (PSS®E bus 34341) to Heywood Terminal Station (PSS®E bus 53900) line (branch 2)	
10.0	VIC	Trip 300 MW 33 kV Alcoa Portland (APD) potline (PSS®E bus 38588)	Tripped PSS®E bus does not fully represent the actual event. The incident report shows a staged trip of 282 MW of APD load, while the PSS®E simulation consisted of a single 300 MW load trip. This was done to better match the frequency response in Victoria.
10.1	NSW	Trip 506 MW 330 kV Tomago potline (PSS®E bus 21790)	Tripped PSS®E bus does not fully represent the actual event. Automatic UFLS scheme tripped 622 MW of two potlines during the actual event, whereas a total of 612 MW of Tomago load is tripped in the simulation.
10.2	NSW	Trip 23.3 MW 11 kV Top Ryde load (PSS®E bus 29730) in Sydney Trip 23.0 MW 132 kV Clovelly load (PSS®E bus 23858) in Sydney Trip 22.8 MW 132 kV Port Hacking load (PSS®E bus 25550) in Sydney Trip 22.3 MW 132 kV Wanniassa load (PSS®E bus 25715) in Canberra	Automatic UFLS scheme trip load from the following distributors: AusGrid (52 MW) Endeavour Energy (12 MW) Evoenergy (6 MW) Essential Energy (7 MW) TransGrid (16.3 MW) Total: 93.3 MW

Time (s)	Region	Events simulated	Comments
			PSS®E buses were chosen based on the summation of load tripped in the DNSP's operating region (91.9 MW). Hence, tripped buses do not fully represent the actual event. Note, PSS®E buses were not tripped; loads were reduced to zero output. As a result, DPV at the PSS®E buses (6.6 MW) were not disconnected.
60		End simulation	

7.1.3 High speed measurements

Frequency

Figure 100 shows the grid frequency in South Australia. Prior to the disturbance, 870 MW of power was flowing from QLD to NSW on QNI. When QNI tripped, QLD experienced a supply surplus, resulting in a rise in frequency to 50.9 Hz (as discussed in Section 7.2 which presents model results for QLD). The remainder of the NEM (including South Australia, discussed in this section) experienced a supply deficit, with frequency reducing to ~49 Hz, as shown in **Figure 100**. At this point, South Australia then separated from the rest of the NEM, causing frequency to rise in South Australia, reaching a maximum of 50.46 Hz.

As shown in Figure 100, the frequency response of all models in the first ~8.7 s (prior to the SA-VIC separation) is comparable to observations. Following the islanding of South Australia (~9 s), all models show a somewhat higher frequency zenith than the observations. The overshoot is most severe for the ZIP model alone.

In this disturbance, the CMLD and ZIP models both provide a reasonably accurate representation of the limited load disconnection observed. When included in the simulation, the DPV model provides a similar DPV reduction estimate regardless of the load model (see **Figure 103**). In contrast, the ZIP model alone does not capture the anticipated reduction of DPV in response to over-frequency, which leads to the more severe frequency overshoot. The reduction in DPV generation represented by the DPV model has been calibrated to represent a combination of over-frequency curtailment specified in the AS/NZS4777.2:2015 standard and some over-frequency disconnection anticipated based on manufacturer surveys and field measurements[126] and is discussed further in Section 7.1.4.

The remaining frequency overshoot observed for all models is likely explained by known misrepresentation of generator governor controls in PSS®E (supported by the nature and timing of the observed mismatch, which only occurs in the later part of the simulation when governors start to respond).

All models provide a reasonably accurate representation of the steady-state frequency following the event (reached at ~60s).

[126] AEMO (May 2021) Behaviour of distributed resources during power system disturbances, https://aemo.com.au/-/media/files/initiatives/der/2021/capstone-report.pdf. See Section 3.

Figure 100 Frequency – 25 August 2018 – 275 kV Para bus (SA)

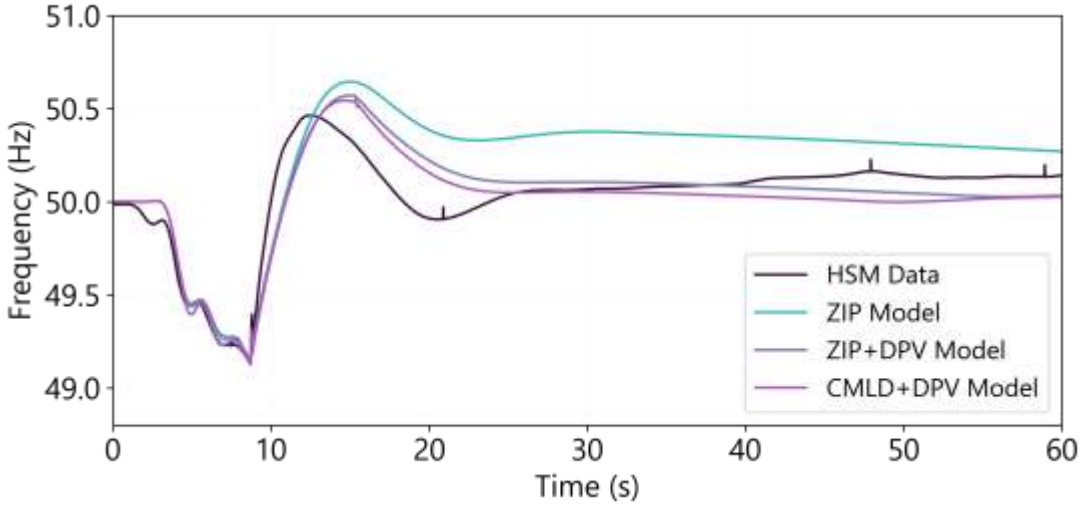

Voltages

Figure 101 shows the voltages at the 275 kV Para bus in the Adelaide metropolitan region. Observations at this location were illustrative of the voltage response at all locations with HSM data available[127].

All models show a similar voltage recovery profile to the HSM in this disturbance. For all models, the peak voltages align with observations and are within the normal range (0.9 to 1.1 pu), although the recovery to post fault levels is slightly depressed. The steady-state voltage after the disturbance is comparable with observations.

Figure 101 Voltage – 25 August 2018 – Para bus (SA)

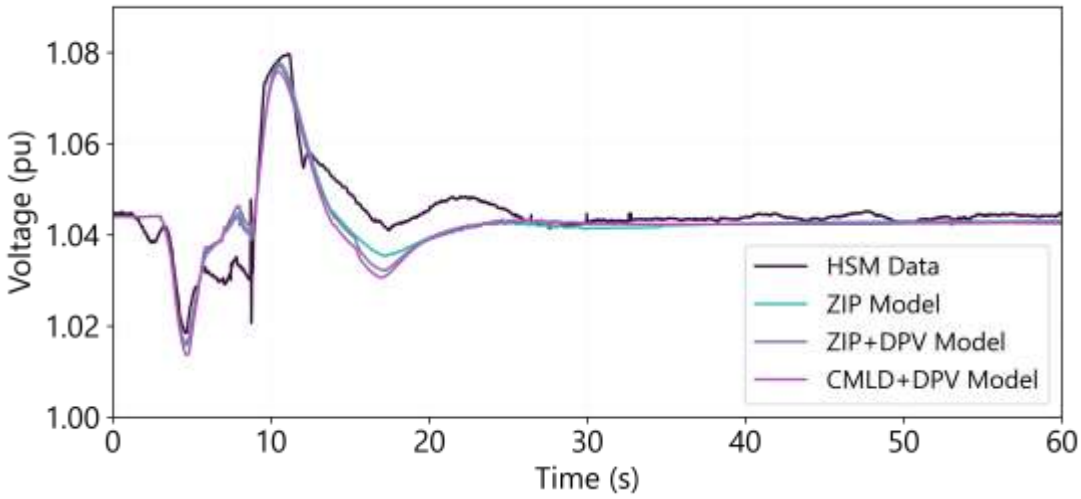

[127] HSM data was available for the following locations: 275 kV Davenport, 275 kV Para, 275 kV Pelican Point, 275 kV Robertstown (P & Q only), 275 kV South East, 275 kV Torrens Island.

Active and reactive power flows

Figure 102 shows the active and reactive power measurements at the 275 kV Para to TIPS A feeder (in the Adelaide metropolitan area). Observations at this location are illustrative of typical measurements recorded in this event. Active power is reasonably well represented during the initial under frequency period on this feeder and most locations. All models somewhat overestimate peak active power flows during the subsequent over frequency period (from ~9 s onwards). This overestimation is likely linked to the overestimate of the frequency zenith, related to inaccuracies in the PSS®E generator governors.

The trajectory of the reactive power measured on this feeder is accurately represented by all models, although the minimum peak reactive flows are slightly underestimated in the 5 s to 11 s simulation period. As seen in Figure 101, this may be partially attributed to the overestimate of voltage that occurs from 5 s to 9 s.

Steady-state active and reactive power is reasonably well represented by all models.

Figure 102 Active/reactive power – 25 August 2018 (SA) – 275 kV Para to TIPS A Feeder

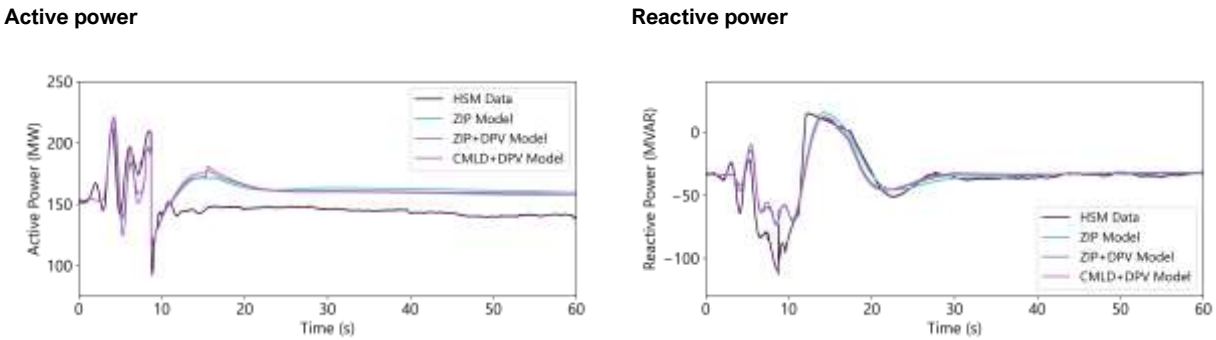

7.1.4 DPV measurements

Figure 103 shows the total measured DPV generation in South Australia (initial value estimated from ASEFS2, and the change post disturbance estimated from Solar Analytics datasets) compared with the performance of the CMLD+DPV model and the ZIP+DPV model.

Figure 103 DPV measurement (Solar Analytics) – 25 August 2018 – (SA)

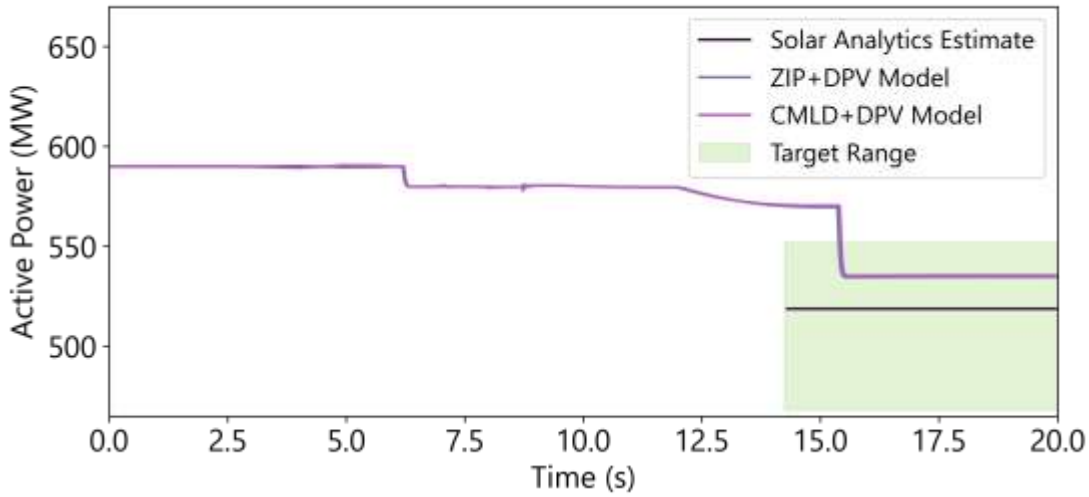

In the simulation of this event, the DPV response can be summarised as follows:

- A small amount of DPV disconnection occurs at ~6 s in response to the under-frequency. The DPV model includes a block of 1.75% of DPV that trips when frequency falls below 49.6 Hz for 1.9 s, for this event.
- DPV curtailment then occurs at 11 s to 14 s in response to the over-frequency (as required for the proportion of DPV installed under AS/NZS4777.2:2015).
- There is a small amount of further DPV disconnection at 15 s as frequency reaches the zenith.

These behaviours are consistent with the model's design, aiming to replicate the available evidence on DPV behaviour in frequency disturbances based on manufacturer surveys and field observations[126].

The Solar Analytics dataset is only available at a 60 s resolution, so it cannot be plotted to compare model performance at the timescales shown in Figure 103. However, **Table 68** summarises estimates from the Solar Analytics dataset of the proportion of inverters that demonstrated disconnection (suddenly dropping generation to close to zero and remaining close to zero for at least one minute) versus curtailment (reducing generation based on the over-frequency observed, consistent with the specified droop response in AS/NZS4777.2:2015). The DPV model represents these behaviours within the uncertainty margin, although it slightly under-estimates DPV disconnection in this case.

Table 68 Summary of distributed PV behaviour – 25 August 2018 (SA)

	Actuals (estimated)	CMLD+DPV prediction
DPV curtailment	8 MW (6 – 9 MW) decrease	9 MW decrease (accurately estimates minimal DPV curtailment)
DPV disconnection	64 MW (31 – 112 MW) decrease	46 MW decrease (underestimates by 28% but within range)
DPV total	71 MW (38 – 122 MW) decrease	55 MW decrease (underestimates by 23% but within range)

7.1.5 Load measurements

Figure 104 shows the active power responses of each of the load components in the CMLD model, in aggregate across the region. The following observations can be made:

- Motor A has a low inertia and assumed constant mechanical torque, to represent mechanical type loads. As such the etrq (torque speed exponent) parameter is set to zero to represent constant torque loads that are not dependent on speed (such as compressors). This means the output power will vary minimally with frequency, as observed.
- Motor B and Motor C are CIM6BL induction motor models with undervoltage motor protection settings. The active power output of these motors changes somewhat with a decrease/increase in frequency. In this event, the active power response of these motor loads moderately tracks the frequency response of the network.
- Motor D somewhat follows the trajectory of the power system frequency. The Motor D model is a performance model developed to simulate the response of single-phase capacitor start compressor motors to voltage disturbances. It does not include frequency trip parameters and is explicitly voltage dependent. The contribution of Motor D load at the time of this event is estimated to be small, so this has minimal impact on the overall load response.
- The power electronic load component includes voltage trip parameters, which are not reached in this event. It is insensitive to frequency. The power electronics load therefore does not change in this event.

The static load component has a significant voltage dependency and no frequency dependency. Pfrq (the fraction of load that is not voltage dependent) is set to zero. For this disturbance, static load response tracks the voltage response (shown in Figure 101).

Figure 104 Active power responses of the CMLD load components – 25 August 2018 (SA)

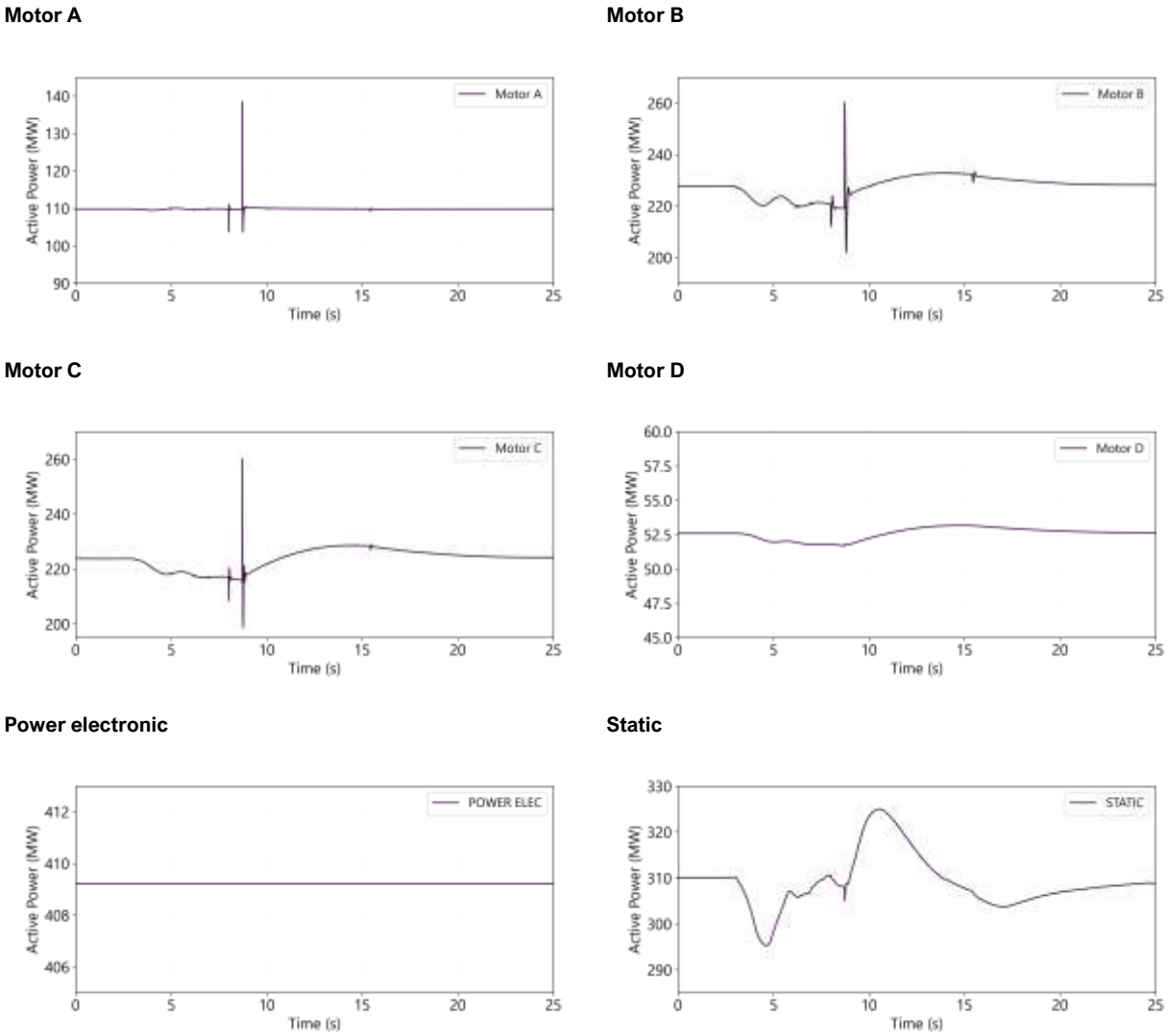

7.1.6 SCADA measurements

Figure 105 shows the total operational demand in South Australia (from SCADA) compared with the performance of the various models.

From Figure 105, the post-disturbance operational demand in this event suddenly increased by ~100 MW, then declined gradually over the subsequent minutes. Given known inaccuracies in the SCADA data (for example, the potential for misalignment of time measurements when summing SCADA from generator terminals), it is unclear what change in operational demand really occurred in the fast timescales represented by the PSS®E model. Furthermore, this gradual decline cannot be represented by any load models (CMLD or ZIP). The CMLD+DPV model was therefore tuned to match the load change measured at 120 s post disturbance (represented by the green dashed line in Figure 105), but it is acknowledged that there are significant inaccuracies in the SCADA measurement for this event.

Figure 105 Operational demand measurements (SCADA) – 25 August 2018 (SA)

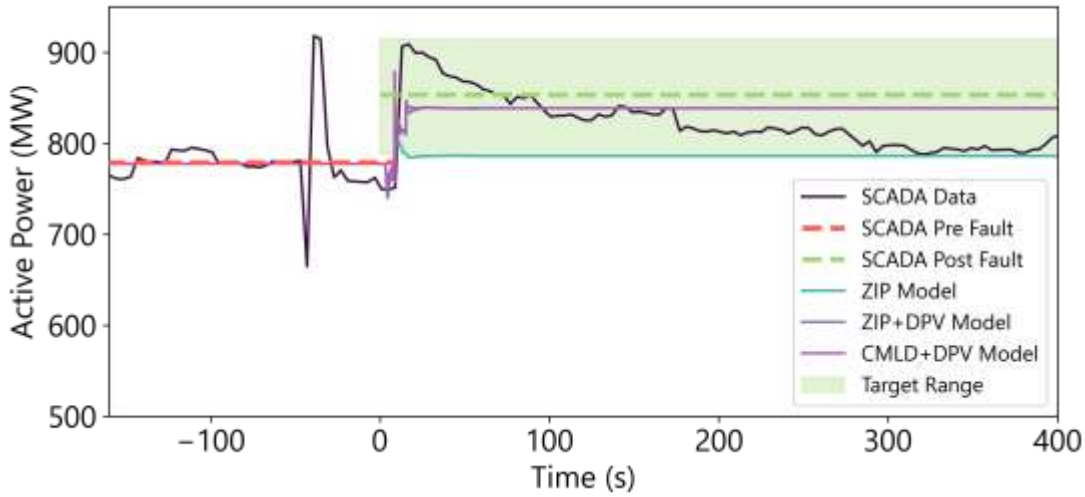

As shown in Figure 105, all models somewhat underpredict the increase in operational demand. The CMLD model predicts 7 MW of total underlying load increase, offset by 55 MW of DPV reduction predicted by the DPV model, leading to a total net increase in operational demand of 61 MW. The comparison with estimated actuals is shown in **Table 69**.

Table 69 Summary of change in demand and distributed PV – 25 August 2018 (SA)

	Actuals (estimated)	CMLD+DPV prediction
Change in DPV generation (estimated from Solar Analytics sample)	71 MW (38 – 122 MW) decrease	55 MW decrease (underestimates by 23% but within range)
Change in underlying demand (estimated from SCADA & Solar Analytics)	2 MW increase (113 MW decrease to 97 MW increase)	7 MW increase (accurately predicts minimal change)
Change in operational demand (estimated from SCADA, 120s post disturbance)	74 MW (8 MW – 135 MW) increase	61 MW increase (underestimates by 17% but within range)

In this disturbance, there was minimal voltage disturbance, so the ZIP model does not predict any significant change in load. When the ZIP model alone is applied, the estimated DPV decrease in this event is not captured, and the observed increase in operational demand is underestimated.

7.1.7 Assessment of model performance

Table 70 provides a summary of the performance of the CMLD+DPV models.

Table 70 Assessment of model performance – 25 August 2018 (SA)

Quantity	Characteristic	CMLD+DPV estimates	CMLD+DPV model equal (✓) or better (✓✓) than ZIP?	Commentary
Frequency	During dynamic state	Fair match	✓✓	All models aligned with HSM during initial under-frequency but overshoot during subsequent over-frequency, likely due to misrepresentation of generator governors.
	Steady-state post disturbance	Good match	✓	CMLD+DPV aligned with HSM
Voltage	During dynamic state	Good match	✓	CMLD+DPV aligned with HSM
	Steady-state post disturbance	Good match	✓	CMLD+DPV aligned with HSM
Active power	During dynamic state	Good match	✓	CMLD+DPV has a similar trajectory to the HSM, although it somewhat overestimates peak flows after separation of SA-VIC
	Steady-state post disturbance	Good match	✓	CMLD+DPV aligned with HSM
Reactive power	During dynamic state	Good match	✓	CMLD+DPV aligned with HSM
	Steady-state post disturbance	Good match	✓	CMLD+DPV aligned with HSM
DPV	DPV curtailment	Good match	✓✓	Estimated actuals: 8 MW decrease DPV: 9 MW decrease The DPV model accurately estimates DPV curtailment.
	DPV disconnection	Fair match	✓✓	Estimated actuals: 64 MW decrease DPV: 46 MW decrease The DPV model underestimates DPV disconnection by 28% but within uncertainty margin.
	DPV total	Good match	✓✓	Estimated actuals: 71 MW decrease DPV: 55 MW decrease The DPV model underestimates DPV reduction by 23% but within uncertainty margin.
Load	Underlying load change	Good match	✓✓	Estimated actuals: 2 MW increase (120 s post disturbance) CMLD: 7 MW increase CMLD accurately estimates minimal underlying load change.
Operational demand	Net load change	Good match	✓✓	SCADA: 74 MW increase (120 s post disturbance) CMLD+DPV: 61 MW increase The CMLD+DPV model underestimates net load change by 14% but is within the uncertainty range

7.2 25 August 2018 – Queensland

7.2.1 Event overview

Table 71 Event summary – 25 August 2018 (QLD)

Date and time		25 August 2018, 13:11[128]
Description of the event		Both Queensland - New South Wales Interconnector (QNI) lines tripped, resulting in the separation of the Queensland region from the rest of the NEM. This was followed by the separation of South Australia from the rest of the NEM, and under-frequency load shedding (UFLS) in New South Wales, Victoria, and Tasmania.
Region		Queensland (QLD)
Minimum voltage recorded		0.91 pu positive sequence at Millmerran (from HSM Data)
Maximum voltage recorded		1.13 pu positive sequence at Millmerran (from HSM Data)
Frequency nadir or zenith		Zenith: 50.88 Hz
Installed capacity of DPV		Total installed capacity in Queensland: 2,225 MW (from APVI) • 73% installed under AS4777.3:2005 (from CER) • 27% installed under AS/NZS4777.2:2015 (from CER)
Prior to the event	**DPV**	1,020 MW, 46% capacity factor (from ASEFS2, interpolated)
	Operational demand	5,286 MW (from SCADA data)
	Underlying demand	6,306 MW (estimate from SCADA + ASEFS2)
Estimated change (post disturbance vs pre disturbance)	**DPV**	143 MW (90 – 230 MW) decrease (from Solar Analytics data)
	Operational demand	196 MW (77 – 206 MW) increase (from SCADA data)
	Underlying demand	53 MW increase (152 MW decrease – 117 MW increase) (from SCADA & Solar Analytics data)

7.2.2 Replication in PSS®E

Full details provided in Section 7.1.2.

7.2.3 High speed measurements

Frequency

Figure 106 shows the power system frequency in Queensland. At the time of the disturbance, 870 MW of power was flowing from Queensland to New South Wales interconnector (QNI). QLD experienced an immediate supply surplus, resulting in a rise in frequency to 50.9 Hz, as shown in Figure 106.

In this disturbance, all models deliver comparable results. The frequency response of all models before the QNI interconnector trip (~3s) is comparable to observations. Following the QNI trip, the CMLD+DPV and ZIP only models show a frequency zenith comparable to observations, followed by a frequency recovery that is somewhat faster than observations. The faster recovery speed of the CMLD+DPV model may be attributed to the DPV

[128] AEMO. Final Report – Queensland and South Australia system separation on 25 August 2018, January 2019. At https://aemo.com.au/-/media/files/electricity/nem/market_notices_and_events/power_system_incident_reports/2018/qld---sa-separation-25-august-2018-incident-report.pdf.

disconnection at the 50.8 Hz band. It is unclear why the ZIP model also shows a relatively fast recovery (compared to the HSM). In contrast, the ZIP+DPV model underestimates the over-frequency[129] and has a similar recovery rate to observations. The difference between the CMLD+DPV and ZIP+DPV models recovery rate may be because the ZIP+DPV does not reach the 50.8Hz frequency trip band for the aggregate DPV model and therefore recovers more slowly.

The misalignment of all models following the QNI trip is likely attributed to the misrepresentation of the primary frequency response (~10 s to 30 s) of the Queensland generators in PSS®E.

Following the event, frequency matches the observations for all models reasonably well, up to a simulation time of 60 s. For this event, the frequency in Queensland did not return to within 49.8 – 50.2 Hz for ~70 minutes.

Figure 106 Frequency – 25 August 2018 (QLD)

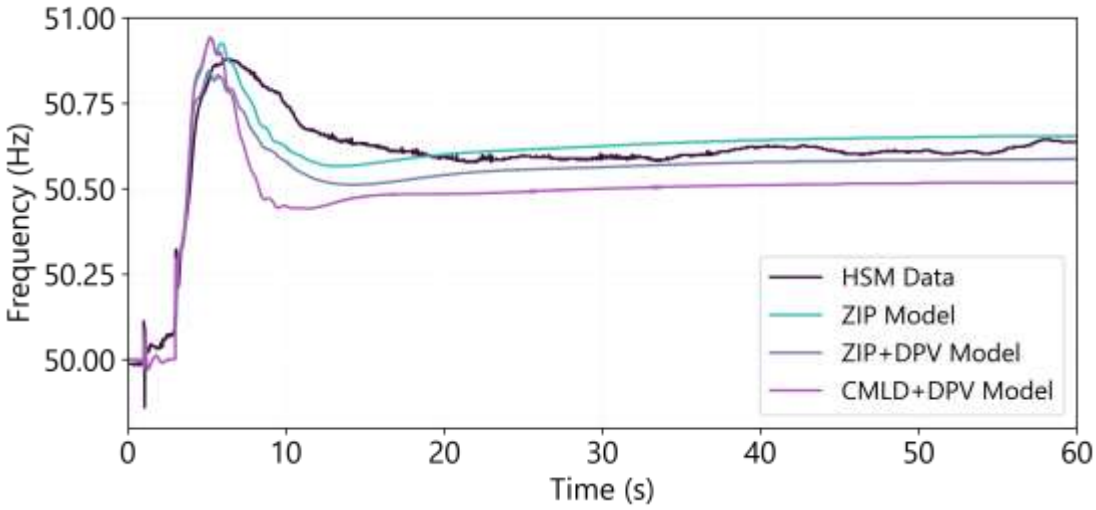

Voltages

Figure 107 shows the voltages at the 275 kV Braemar bus, on the QLD side of the 330 kV Braemar to Bulli Creek QNI. Observations at Braemar were found to be illustrative of the voltage response at most locations with HSM data available[130].

Following the trip of QNI (at 3 s), for all models, voltage over-shoot is marginally overestimated, voltage recovery is delayed compared with HSM, and the steady-stage voltage is over-estimated. Since these inaccuracies are observed for all models, they are likely due to misrepresentation of the network in the PSS®E snapshot or misrepresentation of the disturbance itself, rather than the load or DPV models.

[129] The snapshot with the ZIP model required an increase in generation in QLD and a subsequent reduction in other NEM regions to better match the frequency zenith of the HSM data.

[130] HSM data was available at the following locations: 275 kV South Pine, 275 kV Braemar, 110 kV Mudgeeraba, 275 kV Gladstone (PPS & F only), 275 kV Tarong (P & Q only), 275 kV Stanwell, 330 kV Millmerran, 275 kV Greenbank, 275 kV Lake Ross.

Figure 107 Voltage – 25 August 2018 (QLD) – 275 kV Braemar bus

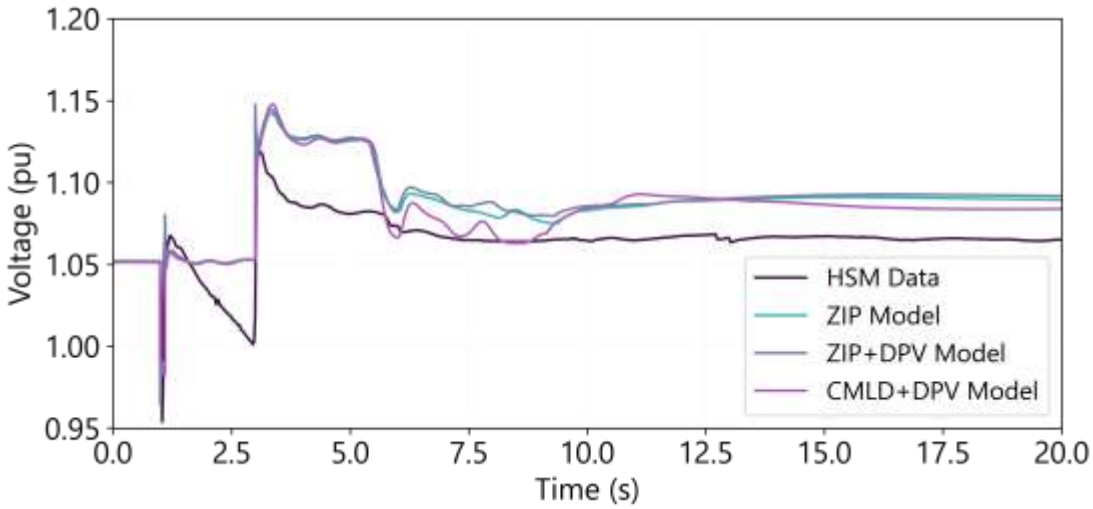

Active and reactive power flows

Figure 108 shows the active and reactive power measurements on the Greenbank to Molendinar feeder. Observations on this feeder are illustrative of typical measurements at most locations in the network. All models represent active power well during the initial period with only minor mismatches of the peak transient flows. Steady-state active power is somewhat underestimated by all models, with the best results seen by the CMLD model.

All models overestimate the peak min/max reactive power measurement peak flows immediately following the separation event that islanded QLD. All models represent the steady-state reactive power well, settling to the observed value at 60 s (not shown).

Figure 108 Active/reactive power – 25 August 2018 (QLD) – 275 kV Greenbank to Molendinar 8824 Feeder

Active power **Reactive power**

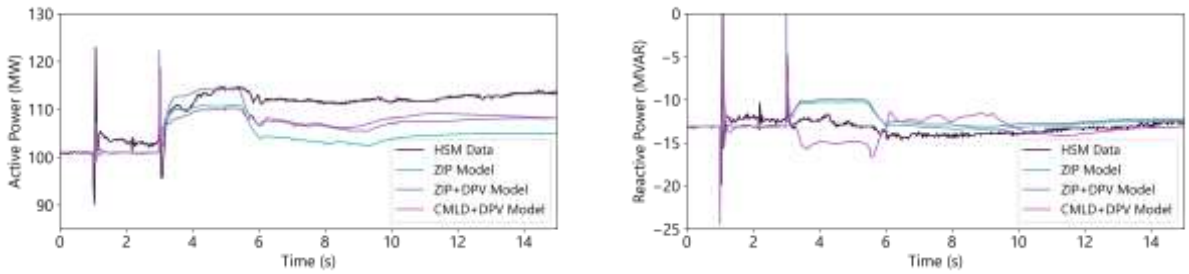

7.2.4 DPV measurements

Figure 109 shows the total measured DPV generation in Queensland (initial value estimated from ASEFS2, and the change post disturbance estimated from Solar Analytics datasets) compared with the performance of the CMLD+DPV model and the ZIP+DPV model. Both models accurately estimate the observed reduction in DPV in

this event. The CMLD+DPV model slightly underestimates DPV curtailment but accurately estimates disconnection on over frequency.

Figure 109 DPV measurement (Solar Analytics) – 25 August 2018 (QLD)

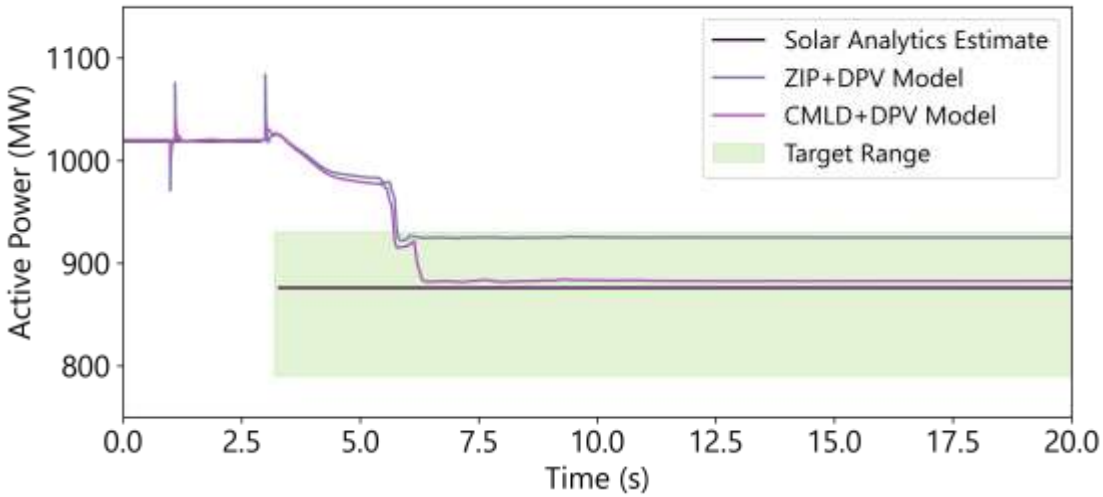

In the simulation of this event, the DPV response can be summarised as follows:

- DPV disconnection occurs at ~3 s in response to the over-frequency. In the ZIP+DPV model the first over-frequency DPV trip block is reached (at 50.5Hz), and in the CMLD+DPV model the frequency also reaches the second trip block (at 50.8Hz).
- DPV curtailment occurs at ~3-5 s in response to the over-frequency (as required under AS/NZS4777.2:2015).

These behaviours are consistent with the model's design, aiming to replicate the available evidence on DPV behaviour in frequency disturbances based on manufacturer surveys and field observations[126].

Table 72 summarises estimates from the Solar Analytics dataset of the proportion of inverters that demonstrated disconnection (suddenly dropping generation to close to zero and remaining close to zero for at least one minute) versus curtailment (reducing generation based on the over-frequency observed, consistent with the specified droop response in AS/NZS4777.2:2015)

The DPV model represents these behaviours within the uncertainty margin for DPV disconnection, although it slightly underestimates DPV curtailment in this case.

Table 72 Summary of distributed PV behaviour – 25 August 2018 (QLD)

	Actuals (estimated)	CMLD+DPV prediction
DPV curtailment	54 MW (47 – 60 MW) decrease	38 MW decrease (underestimates by 28% and outside of target range)
DPV disconnection	90 MW (43 – 169 MW) decrease	99 MW decrease (overestimates by 10%, but within range)
DPV total	143 MW (90 – 230 MW) decrease	137 MW decrease (underestimates by 4%, but within range)

7.2.5 Load measurements

Figure 110 shows the active power responses of each of the load components in the CMLD model, in aggregate across the region. The following observations can be made:

- Motor A represents constant torque loads that are not dependent on speed such as compressors, and is minimally affected by the frequency disturbance.
- Motor B and motor C are induction motor models. In this disturbance, the response of these motors primarily reflects the over-frequency excursion.
- Motor D reflects the frequency response. Motor D model is a performance model developed to simulate the response of single-phase capacitor start motors to voltage disturbances.
- Power electronic load shows no response in this event, given that the voltage trip settings for this model were not reached.
- The static load reflects the voltage disturbance (shown in Figure 107). The static load reflects the voltage excursion to ~1.15 pu and back to pre-fault levels.

Load disconnection is minimal in this event because voltages at most buses do not reach any of the model voltage trip setpoints.

Figure 110 Active power responses of the CMLD load components – 25 August 2018 (QLD)

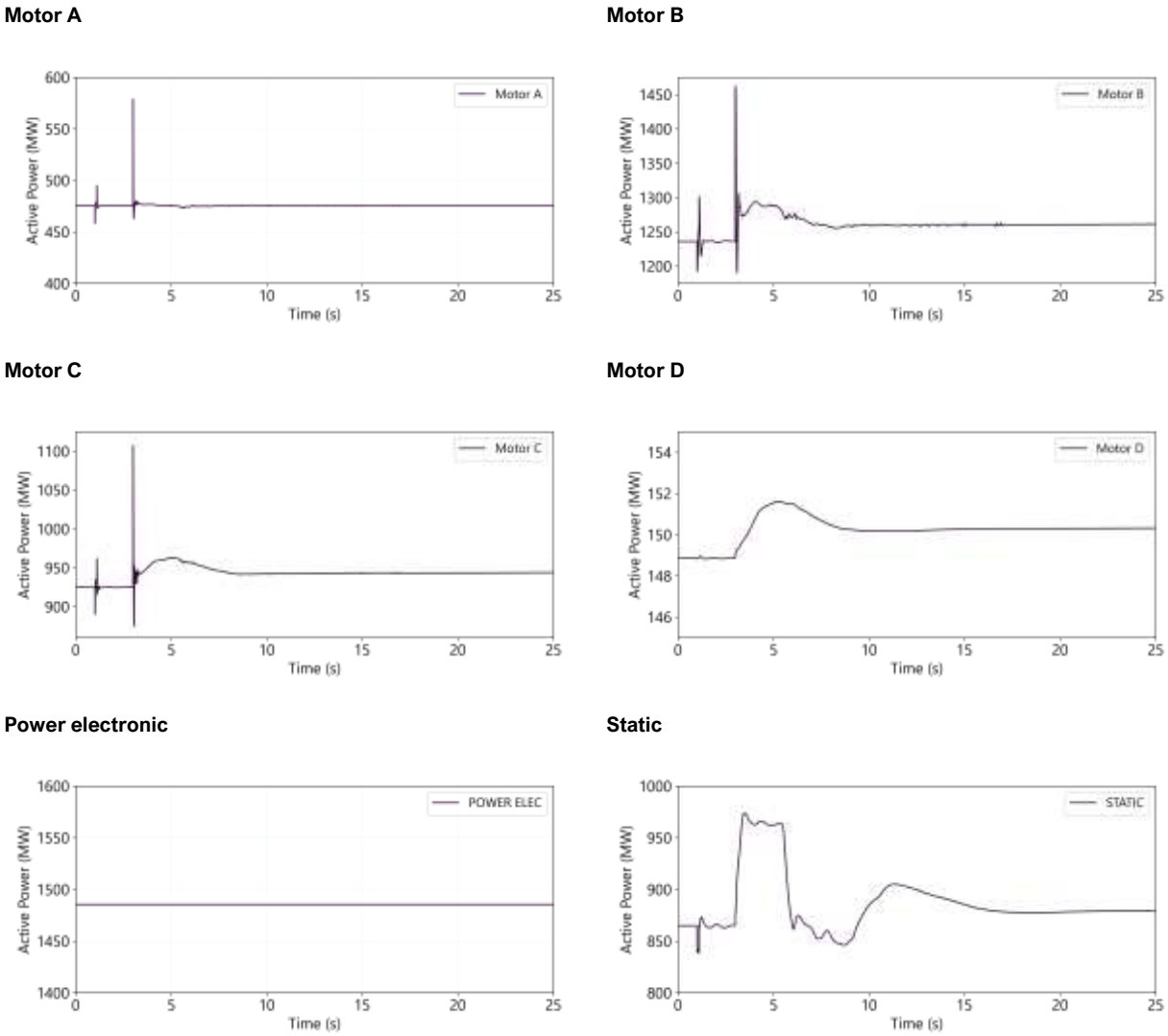

7.2.6 SCADA measurements

Figure 111 shows the total operational demand in Queensland (from SCADA), compared with the performance of the various models. The CMLD+DPV model was tuned to match the load change measured at 72 s post disturbance (represented by the green dashed line in Figure 111), but it is acknowledged that there are significant inaccuracies in the SCADA measurement.

Figure 111 Operational demand measurements (SCADA) – 25 August 2018 (QLD)

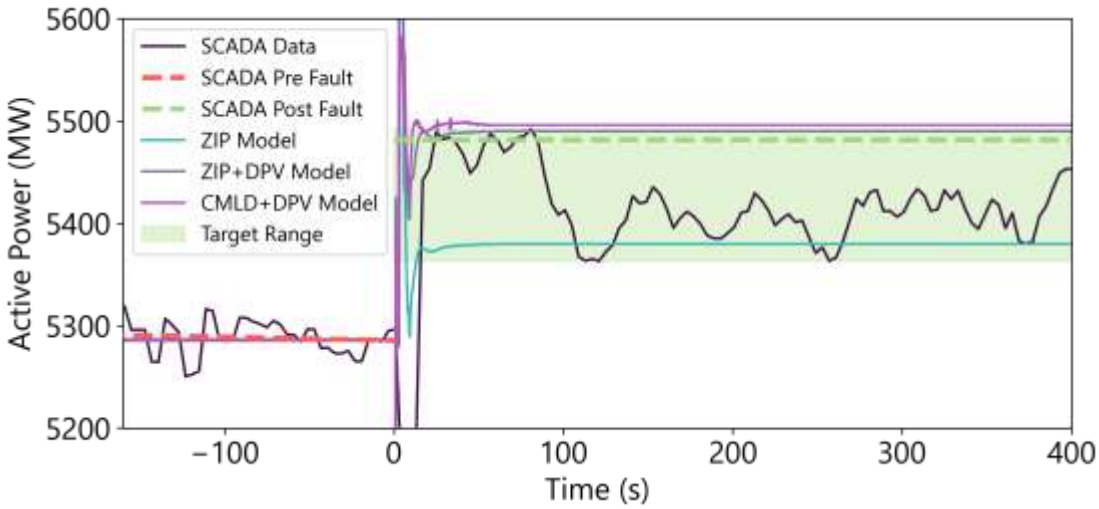

As shown in Figure 111, the CMLD+DPV model marginally overestimates the estimated net 196 MW increase in operational demand. The CMLD model predicts 73 MW of total underlying load increase, compounded by 137 MW of DPV loss predicted by the DPV model, leading to a total net increase in operational demand of 211 MW. The comparison with estimated actuals is shown in **Table 73**.

Table 73 Summary of change in demand and distributed PV – 25 August 2018 (QLD)

	Actuals (estimated)	CMLD+DPV prediction
Change in distributed PV generation (estimated from Solar Analytics sample)	143 MW (90 – 230 MW) decrease	137 MW decrease (underestimates by 4%, but within range)
Change in underlying demand (estimated from SCADA & Solar Analytics)	53 MW increase (152 MW decrease – 117 MW increase)	73 MW increase (overestimates by 38%, but within range)
Change in operational demand (estimated from SCADA, 72s post disturbance)	196 MW (77 – 206 MW) increase	211 MW increase (overestimates by 7% and marginally outside of range)

The ZIP model predicts a small increase in load, associated with post fault voltages being higher than pre-fault voltages, as shown in Figure 103.

7.2.7 Assessment of model performance

Table 74 provides a summary of the performance of the CMLD+DPV model for this event.

Table 74 Assessment of model performance – 25 August 2018 (QLD)

Quantity	Characteristic	CMLD+DPV estimates	CMLD+DPV model equal (✓) or better (✓✓) than ZIP?	Commentary
Frequency	During dynamic state	Fair match	✓	CMLD+DPV trajectory aligned with HSM and represents frequency zenith well, but the recovery rate is faster than observed.

Quantity	Characteristic	CMLD+DPV estimates	CMLD+DPV model equal (✓) or better (✓✓) than ZIP?	Commentary
	Steady-state post disturbance	Good match	✗	CMLD+DPV aligned with HSM
Voltage	During dynamic state	Fair match	✓	CMLD+DPV trajectory aligned with HSM, with slightly slower recovery.
	Steady-state post disturbance	Fair match	✓	CMLD+DPV voltages are reasonably accurate (settles to within 5% of the HSM data for all voltage channels)
Active power	During dynamic state	Good match	✓	CMLD+DPV aligned with HSM
	Steady-state post disturbance	Good match	✓✓	CMLD+DPV aligned with HSM, although flows are marginally underestimated.
Reactive power	During dynamic state	Good match	✓	CMLD+DPV aligned with HSM
	Steady-state post disturbance	Good match	✓	CMLD+DPV aligned with HSM
DPV	DPV curtailment	Fair match	✓✓	Estimated actuals: 54 MW decrease DPV: 38 MW decrease The DPV model underestimates DPV curtailment by 30%.
	DPV disconnection	Good match	✓✓	Estimated actuals: 90 MW decrease DPV: 99 MW decrease The DPV model overestimates DPV disconnection by 10%, but within range.
	DPV total	Good match	✓✓	Estimated actuals: 143 MW decrease DPV: 137 MW decrease The DPV model underestimates DPV reduction by 4%, but within range.
Load	Underlying load change	Fair match	✓✓	Estimated actuals: 53 MW increase (72 s post disturbance) CMLD: 73 MW increase The CMLD overestimates underlying load change by 38%, but within range.
Operational demand	Net load change	Good match	✓✓	SCADA: 196 MW increase (72 s post disturbance) CMLD+DPV: 211 MW increase CMLD+DPV overestimates by 8% and is marginally outside of range.

7.3 25 August 2018 – Victoria

7.3.1 Event overview

Table 75 Event summary – 25 August 2018 – Victoria

Date and time		25 August 2018, 13:11[131]
Region		Victoria
Description of the event		Both QNI lines tripped, resulting in the separation of the Queensland region from the rest of the NEM. This was followed by the separation of South Australia from the rest of the NEM, and UFLS in New South Wales, Victoria, and Tasmania.
Minimum voltage recorded		0.96 pu positive sequence at Yallourn (from HSM Data)
Maximum voltage recorded		1.09 pu positive sequence at Bendigo (from HSM Data)
Frequency nadir or zenith		Nadir: 48.95 Hz
Installed capacity of DPV		Total installed capacity in Victoria: 1,402 MW (from APVI) • 70% installed under AS4777.3:2005 (from CER) • 30% installed under AS/NZS4777.2:2015 (from CER)
Prior to the event	**DPV**	850 MW, 61% capacity factor (from ASEFS2, interpolated)
	Operational demand	4,226 MW (from SCADA data)
	Underlying demand	5,076 MW (estimate from SCADA + ASEFS2)
Estimated change (post disturbance vs pre disturbance)	**DPV**	123 MW (48 – 238 MW) decrease (from Solar Analytics data)
	Operational demand	229 MW (143 – 289 MW) decrease (from SCADA data) mainly attributed to UFLS[132]
	Underlying demand	352 MW (191 – 527 MW) decrease (from SCADA & Solar Analytics data)

7.3.2 Replication in PSS®E

Full details are provided in Section 7.1.2.

As noted in the incident report, the automatic UFLS scheme tripped 282 MW of APD load. To replicate this in the PSS®E simulation, APD UFLS load was modelled as a ZIP load representing each potline, and the tripping of the load was simulated by changing the APD load power from 300 MW to 0MW at 10s.

There is no DPV associated with the load buses that were tripped by the action of UFLS in this event.

7.3.3 High speed measurements

Frequency

Figure 112 shows the power system frequency in Victoria. Prior to the disturbance, 170 MW of power was flowing from SA to VIC on the Heywood interconnector. When Heywood tripped, VIC experienced a supply deficit,

[131] AEMO. Final Report – Queensland and South Australia system separation on 25 August 2018, January 2019. At https://aemo.com.au/-/media/files/electricity/nem/market_notices_and_events/power_system_incident_reports/2018/qld---sa-separation-25-august-2018-incident-report.pdf.

[132] Minor discrepancies for estimated change in OD are due to the selected pre and post disturbance SCADA measurements.

resulting in a decrease in frequency to 48.96 Hz. VIC remained connected to NSW throughout the event and remained connected to TAS via the Basslink HVDC interconnector.

As shown in Figure 112, the frequency response of all models in the first ~8.7 s (prior to the SA-VIC separation) is comparable to observations. Following the islanding of South Australia (~9 s), after frequency declined below 49 Hz, UFLS was trigged in NSW and VIC. This load shedding was sufficient to restore frequency in VIC to around 49.9 Hz (settling at ~4 minutes after the initial event, not shown).

Figure 112 Frequency – 25 August 2018 (VIC)

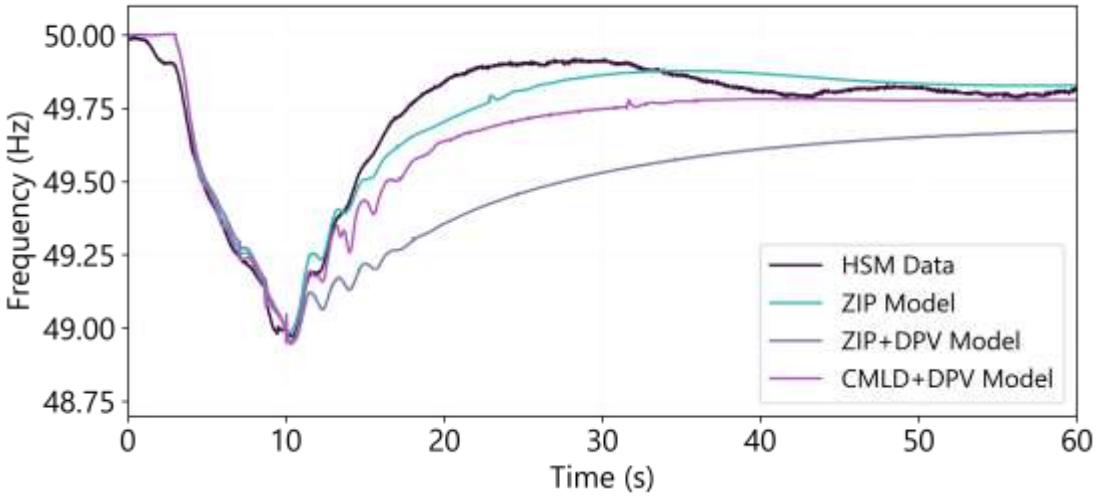

In this disturbance, all three cases include significant load disconnection due to the action of UFLS (modelled identically in all three cases). The CMLD model delivers an additional reduction in load due to the reduction in frequency (related to load relief in the motor models) and transient reduction in voltage during the 3-10s period. These load reductions are offset by the reduction in DPV due to under-frequency tripping. This case therefore shows a similar frequency recovery profile to the ZIP only model, which does not represent the frequency response of either the load or DPV. In contrast, the ZIP+DPV model shows a slower frequency recovery profile, since the DPV disconnection is represented, but the reduction in load in response to low frequency is not, so the overall profile recovers more slowly. This presents an example where it is important to use the CMLD model when applying the DPV model, to make sure all relevant factors are captured.

There is a known misrepresentation of generator governor controls in PSS®E, which is likely contributing to the delayed frequency recovery behaviour observed for all models (compared with HSM). This is supported by the nature and timing of the observed mismatch, which only occurs in the latter part of the simulation when governors start to respond.

All models provide a reasonably accurate representation of the steady-state frequency following the event (reached at ~4 minutes, not shown).

Voltage

Figure 113 shows the voltages at the 220 kV Rowville Terminal Station (ROTS) bus in the Melbourne metropolitan region. Observations at this location are illustrative of the voltage response at most locations in the network[133].

In this disturbance, all models overestimate min/max peak voltages compared with observations but remain within the normal range. All models show steady-state voltages (after 40 s) which are comparable with observations.

Figure 113 Voltage – 25 August 2018 – Rowville Terminal Station (ROTS) bus (VIC)

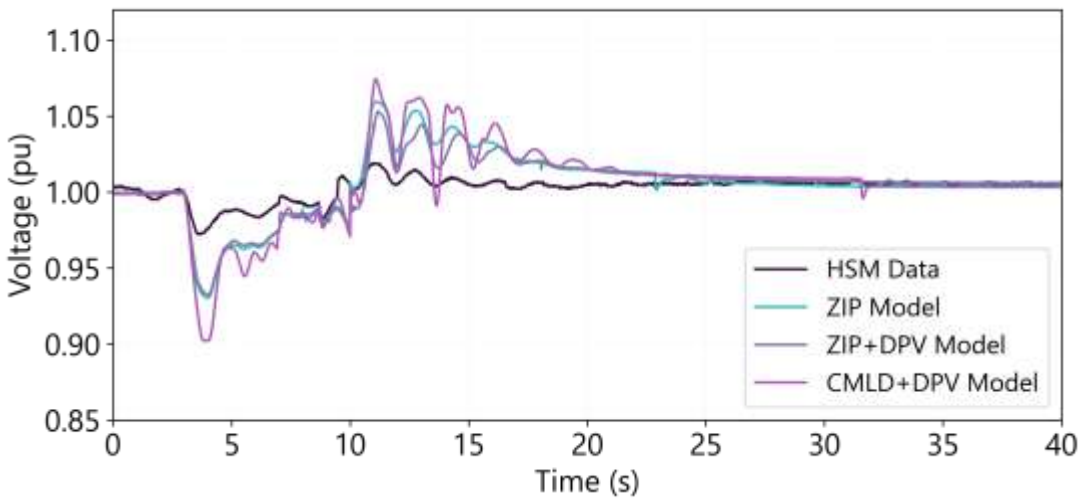

Active and reactive power flows

Figure 114 shows the active and reactive power measurements at the 500/220 kV ROTS feeder (in the vicinity of the Melbourne metropolitan area). Observations at this location are illustrative of typical measurements recorded in this event.

Active power is reasonably well represented during the initial period on this feeder and at most locations. All models somewhat overestimate peak active power flows following the subsequent trip of the Heywood interconnector (at ~9 s). This overestimation is likely linked to the delayed frequency recovery (related to inaccuracies in the PSS®E generator governors) and overestimation of min/max voltages.

The trajectory of the reactive power measured on this feeder is misrepresented by all models, including the minimum peak reactive flows in the 12 s to 17 s simulation period. This may be partially attributed to the overestimate of voltage that occurs in the same time range (see Figure 113), and partially attributed to the inability to represent transformer saturation accurately in PSS®E, which effectively damps temporary overvoltage's and peak reactive power flows.

All models represent steady-state active and reactive power reasonably well.

[133] HSM data was available at the following locations: 220 kV Altona, 220/66/22 kV Bendigo. 66/22 kV Brooklyn, 220 kV Cranbourne, 330 kV Dederang, 220/66/22 kV Fishermans Bends, 500/220 kV Hazelwood, 500 kV Loy Yang, 220 kV Mt Beauty, 330 kV Murray, 220/66/22 kV Red Cliffs, 220 kV Rowville, 500/330 kV South Morang, 132 kV Tarrone, 66 kV Templestowe, 220 kV Yallourn.

Figure 114 Active/reactive power – 25 August 2018 (VIC) – 500/220 kV Rowville (ROTS) Transformer A1 Feeder

Active power **Reactive power**

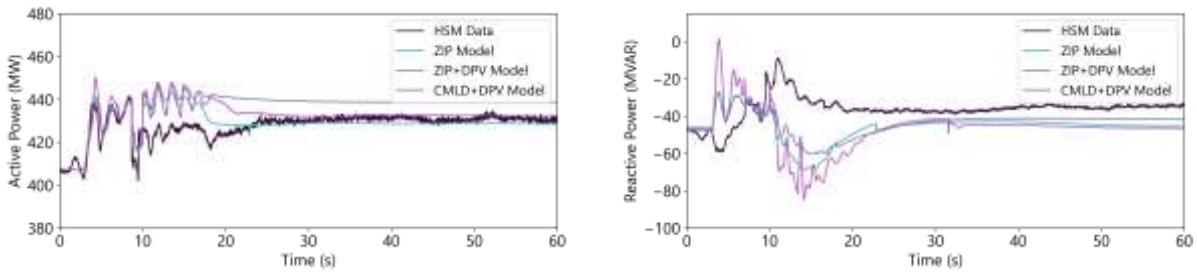

7.3.4 DPV measurements

Figure 115 shows the total measured DPV generation in Victoria (initial value estimated from ASEFS2, and the change post disturbance estimated from Solar Analytics datasets) compared with the performance of the CMLD+DPV model and the ZIP+DPV models.

Figure 115 DPV generation (estimated from Solar Analytics data) – 25 August 2018 (VIC)

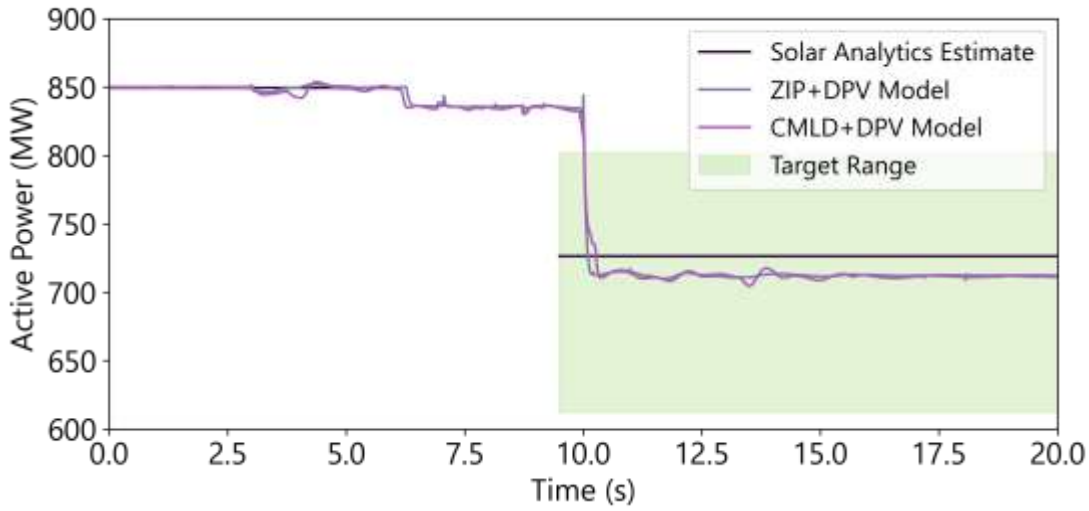

In the simulation of this event, the DPV response can be summarised as follows:

- A small amount of DPV disconnection occurs at ~6 s in response to the under-frequency reaching 49.6 Hz with a 1.9s delay.
- There is a large amount of further DPV disconnection at ~9 s as frequency reaches the nadir (below a larger DPV trip block at 49 Hz).

These behaviours are consistent with the model's design, aiming to replicate the available evidence on DPV behaviour in frequency disturbances based on manufacturer surveys and field observations[126].

Table 76 summarises estimates from the Solar Analytics dataset of the proportion of inverters that demonstrated disconnection versus curtailment. The DPV model represents these behaviours within the uncertainty margin.

Table 76 Summary of distributed PV behaviour – 25 August 2018 (VIC)

	Actuals (estimated)	CMLD+DPV prediction
DPV loss	123 MW (48 – 238 MW) decrease	139 MW decrease (overestimates by 13% but within range)

7.3.5 Load measurements

Figure 116 shows the active power responses of each of the load components in the CMLD model, in aggregate across the region. Motor B, C and D are observed to respond to the reduction in frequency (demonstrating load relief), while Motor A and the power electronics loads are relatively unaffected. The static load component demonstrates voltage dependency (comparing the trajectory with Figure 113) and is the most significant contributor to load change during this event due to the large proportion of load estimated to be static load in this snapshot period.

There was minimal load disconnection in this event since voltages at most buses did not reach any of the voltage trip setpoints.

Figure 116 Active power responses of the CMLD load components – 25 August 2018 (VIC)

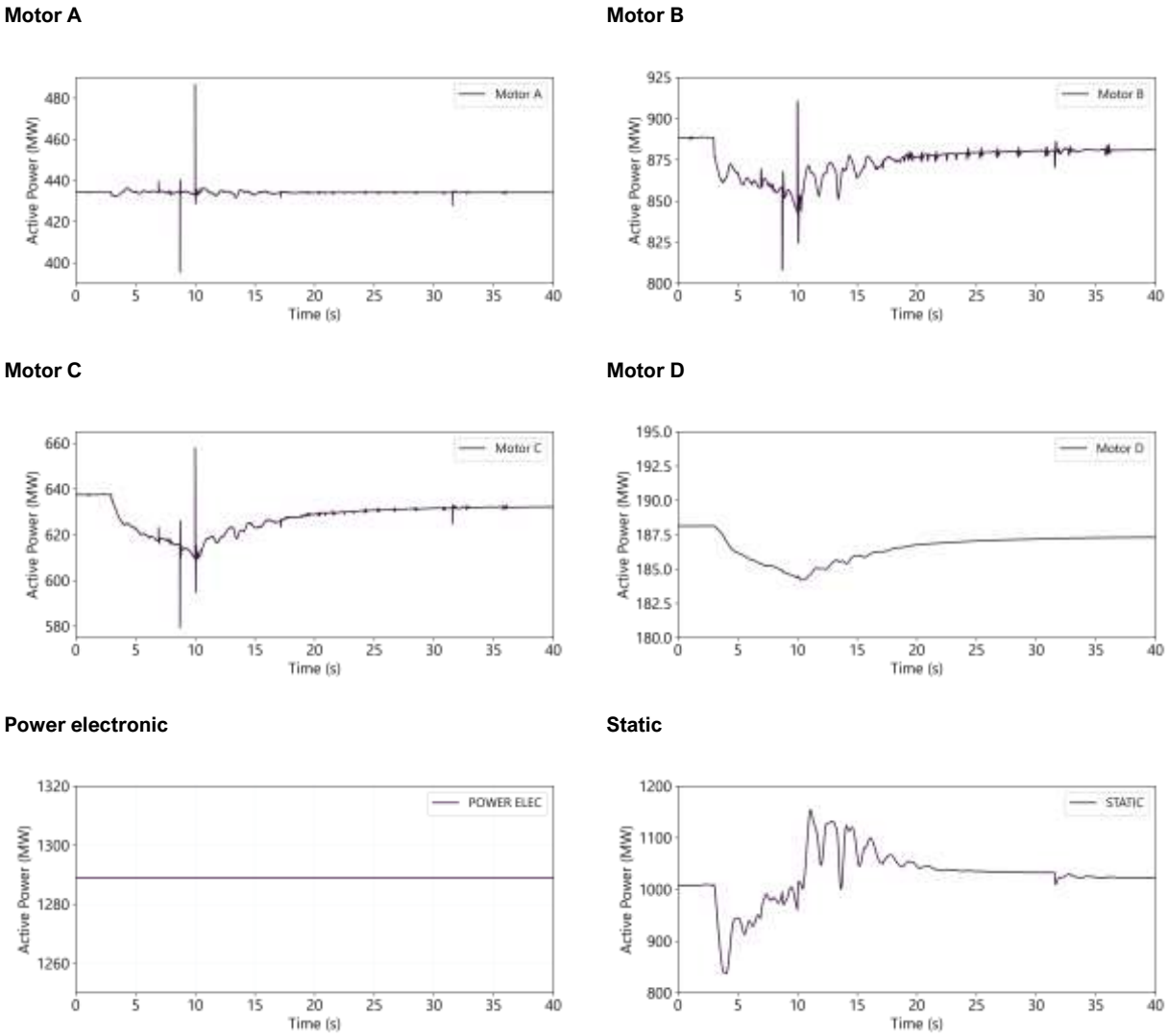

7.3.6 SCADA measurements

Figure 117 shows the total operational demand in Victoria (from SCADA) compared with the performance of the various models.

The CMLD+DPV model was tuned to match the load change measured at ~60 s post disturbance (represented by the green dashed line in Figure 117).

Figure 117 Operational demand measurements (SCADA) – 25 August 2018 (VIC)

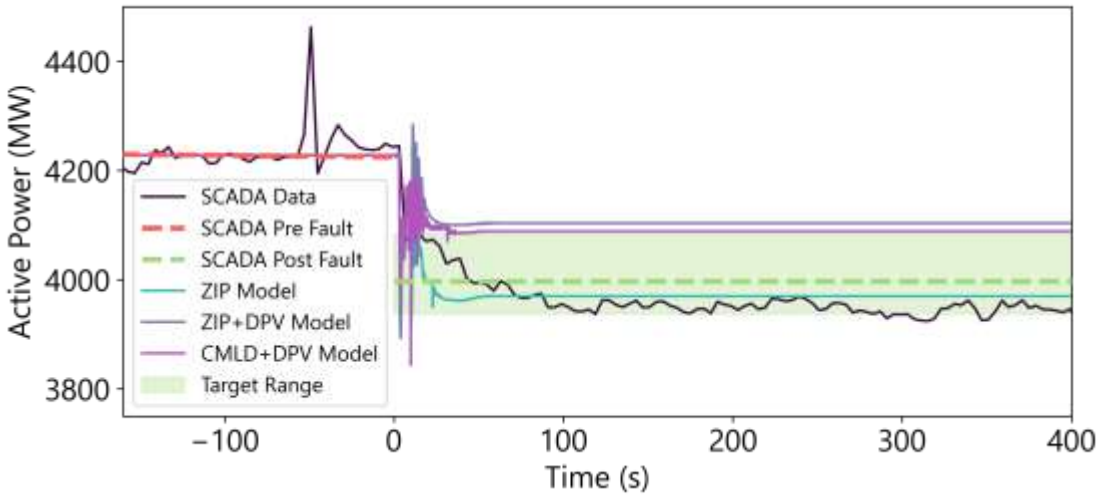

All the models shown in Figure 117 include a 300 MW change in underlying demand due to the UFLS trip. The SCADA data similarly includes the actual 282 MW of change in underlying demand due to the UFLS trip.

The comparison of the performance of the load models with estimated actuals is shown in **Table 77**. The columns on the right exclude the UFLS trip component, to allow direct comparison of the performance of the load models in reproducing the estimated net change in load that is not related to UFLS action. The CMLD+DPV models predict a 22 MW increase in underlying load, which is a better match to the estimated actuals than the predicted 39 MW increase in underlying load predicted by the ZIP+DPV models. However, the estimated actuals have wide uncertainty margins.

Note that the CMLD model predicts a small increase in underlying load for this under-frequency event. The reduction in load due to the load relief response of the motor models is offset by an increase in load related to the voltage dependency of the static load component. The ZIP+DPV model predicts a larger increase in underlying load, since the voltage dependency of the static load is not offset by the load relief components.

The constant current ZIP models used by AEMO are unable to represent load tripping or load change related to frequency. Instead, the constant current ZIP models increase/decrease output power based on voltage deviation. As the post-fault voltages in VIC are greater than the pre-fault voltages, the ZIP load represents an active power increase.

Table 77 Summary of change in demand and distributed PV – 25 August 2018 (VIC)

	Including UFLS trip		UFLS trip (MW)		Excluding UFLS trip		
	Actuals (estimated)	CMLD+DPV prediction	Actuals	CMLD+DPV	Actuals (estimated)	CMLD+DPV prediction	ZIP+DPV prediction
Change in distributed PV generation (estimated from Solar Analytics sample)	123 MW (48 – 238 MW) decrease	139 MW decrease (within range)	N/A	N/A	123 MW (48 – 238 MW) decrease	139 MW decrease (within range)	138 MW decrease

	Including UFLS trip		UFLS trip (MW)		Excluding UFLS trip		
Change in operational demand (estimated from SCADA, 60s post disturbance)	229 MW (143 – 289 MW) decrease	140 MW decrease (outside of range)	282	300	53 MW increase (7 MW decrease to 139 MW increase)	160 MW increase (marginally outside of range)	177 MW decrease
Change in underlying demand (estimated from SCADA & Solar Analytics)	352 MW (191 – 527 MW) decrease	278 MW decrease (within range)	282	300	70 MW decrease (245 MW decrease to 91 MW increase)	22 MW increase (within range)	39 MW increase[134]

7.3.7 Assessment of model performance

Table 78 provides a summary of the performance of the CMLD+DPV models.

Table 78 Assessment of model performance – 25 August 2018 (VIC)

Quantity	Characteristic	CMLD + DPV estimates	CMLD+DPV model equal (✓) or better (✓✓) than ZIP?	Commentary
Frequency	During dynamic state	Fair match	✓	CMLD+DPV trajectory aligned with HSM, replicates nadir well, but the recovery rate is slower than observed
	Steady-state post disturbance	Good match	✓	CMLD+DPV aligned with HSM
Voltages	During dynamic state	Fair match	✓	Overestimate's min/max peak voltages but remains within normal range.
	Steady-state post disturbance	Good match	✓	CMLD+DPV aligned with HSM
Active power	During dynamic state	Fair match	✓	CMLD+DPV has a similar trajectory to the HSM, although it somewhat overestimates peak maximum flows after separation of SA-VIC
	Steady-state post disturbance	Good match	✓	CMLD+DPV aligned with HSM
Reactive power	During dynamic state	Poor match	✓	CMLD+DPV does not have a comparable trajectory to the HSM, and peak flows are overestimated after the separation of SA-NEM
	Steady-state post disturbance	Good match	✓	CMLD+DPV aligned with HSM
DPV	DPV total	Good match	✓✓	Estimated actuals: 123 MW decrease DPV: 139 MW decrease The DPV model overestimates DPV reduction by 13%, but within target range.
Load	Underlying load change	Good match	✓✓	Estimated actuals (ex. UFLS): 70 MW decrease (104 s post disturbance) CMLD: 22 MW increase The CMLD is within target range.
Operational demand	Net load change	Fair match	✗	SCADA (ex. UFLS): 53 MW increase (104 s post disturbance)

[134] Attributed to large parts of the network having post-fault voltage greater than pre fault voltage causing an increase in overall (constant current) ZIP load. Figure 116 shows an example (for the CMLD model in this case) of static loads increasing in response to an increase in voltage.

Quantity	Characteristic	CMLD + DPV estimates	CMLD+DPV model equal (✓) or better (✓✓) than ZIP?	Commentary
				CMLD+DPV: 160 MW increase The CMLD+DPV model is slightly outside of uncertainty margins range.

7.4 25 August 2018 – New South Wales

7.4.1 Event overview

Table 79 Event summary – 25 August 2018 – (NSW)

Date and time		25 August 2018, 13:11[125]
Region		New South Wales
Description of the event		Both QNI lines tripped, resulting in the separation of the Queensland region from the rest of the NEM. This was followed by the separation of South Australia from the rest of the NEM and UFLS in New South Wales, Victoria, and Tasmania.
Minimum voltage recorded		0.98 pu positive sequence at Liddell (from HSM Data)
Maximum voltage recorded		1.05 pu positive sequence at Dumaresq (from HSM Data)
Frequency nadir or zenith		Nadir: 48.95 Hz
Installed capacity of DPV		Total installed capacity in South Australia: 1,760 MW (from APVI) • 67% installed under AS4777.3:2005 (from CER) • 33% installed under AS/NZS4777.2:2015 (from CER)
Prior to the event	**DPV**	500 MW, 28% capacity factor (from ASEFS2, interpolated)
	Operational demand	7,770 MW (from SCADA data)
	Underlying demand	8,270 MW (estimate from SCADA + ASEFS2)
Estimated change (post disturbance vs pre disturbance)	**DPV**	89 MW (60 – 125 MW) decrease (from Solar Analytics data)
	Operational demand	645 MW (597 – 787 MW) decrease (from SCADA data) mostly attributed to UFLS
	Underlying demand	733 MW (656 – 912 MW) decrease (from SCADA & Solar Analytics data)

7.4.2 Replication in PSS®E

Full details are provided in Section 7.1.2.

As noted in the incident report, the automatic UFLS scheme tripped 622 MW at two Tomago potlines and 93.3 MW from five feeders from various DNSP networks in New South Wales. To replicate this in PSS®E, 612 MW of Tomago load was tripped (at 5 s and 10.1 s) and 91.9 MW of load (at 10.2 s at a selection of buses associated with each DNSP) was tripped to simulate the action of the UFLS scheme.

The generation in Queensland pre-event was increased to match the observed over-frequency response in Queensland (and provide a case suitable for calibration of the over-frequency performance of the DPV and load models). This leads to a decrease in generation pre-event in New South Wales and, to a lesser degree, the rest of the NEM.

There is no DPV associated with the load buses that were tripped by the action of UFLS in this event.

7.4.3 High speed measurements

Frequency

Figure 118 shows the grid frequency in New South Wales. Prior to the disturbance, 170 MW of power was flowing from SA to VIC on the Heywood interconnector. When Heywood tripped, NSW experienced a supply deficit, resulting in a decrease in frequency to 48.96 Hz. NSW remained connected to VIC throughout the event, and VIC remained connected to TAS via the Basslink HVDC interconnector. Therefore, frequency outcomes are very similar to those for VIC (outlined in the previous section).

Figure 118 Frequency – 25 August 2018 (NSW)

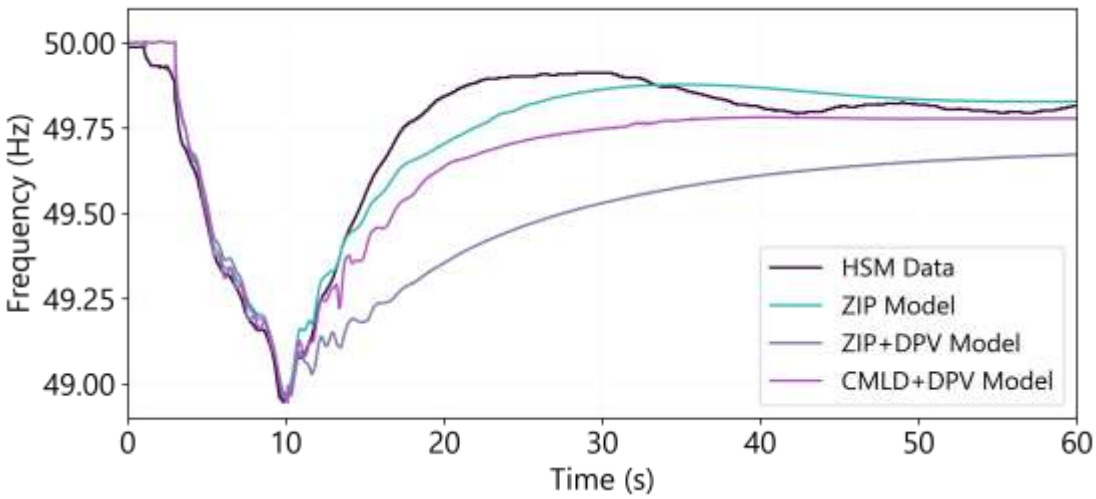

Voltage

Figure 119 shows the voltages at the 330 kV Liddell Power Station bus. Observations at this location illustrate a voltage response that reflects most of the HSM locations in the network[135].

In this disturbance, the voltage trajectory and deviation from pre-fault values is relatively well represented throughout the simulation for both the CMLD+DPV and ZIP models. The ZIP+DPV model, however, has a delayed voltage spike and recovery from ~15 s. All models are within the normal operating range for the duration of the simulation.

[135] HSM data was available at the following locations: 330 kV Bayswater, 330 kV Dumaresq, 330 kV Vales Point, 500/330 kV Eraring, 330 kV Gullen Range Wind Farm, 330 kV Jinderra, 330 kV Kangaroo Valley, 330 kV Liddell, 330 kV Munmorah, 330 kV Tomago, 330 kV Upper Tumut, 132 kV Uranquinty, 330 kV Woodlawn Wind Farm.

Figure 119 Voltage – 25 August 2018 – 330 kV Liddell Power Station G1 Feeder

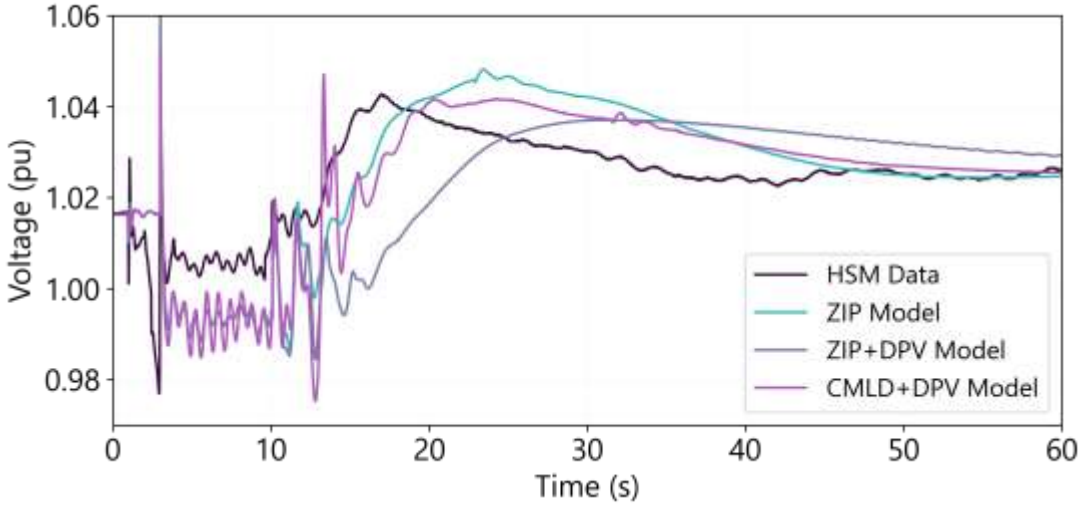

Figure 120 shows the voltages at the 500 kV Eraring Power Station bus in the vicinity of the Newcastle metropolitan region. Observations at this location illustrate a voltage response that differs from most of the HSM data.

In this disturbance, the voltages at Eraring in the initial period prior to the SA separation are overestimated by the CMLD+DPV and ZIP only models but well represented by the ZIP+DPV model. The source of the discrepancies between the models is unclear, but reactive power is damped for the ZIP+DPV model following the QNI trip, while both the ZIP and CMLD+DPV models show reactive power spikes (see Figure 122).

All models show a reasonable match for voltages at Eraring following the Heywood interconnector trip and UFLS load disconnection in NSW (at ~10 s) and a good match during steady-state (after 60 s).

Figure 120 Voltage – 25 August 2018 – 500 kV Eraring Power Station bus (NSW)

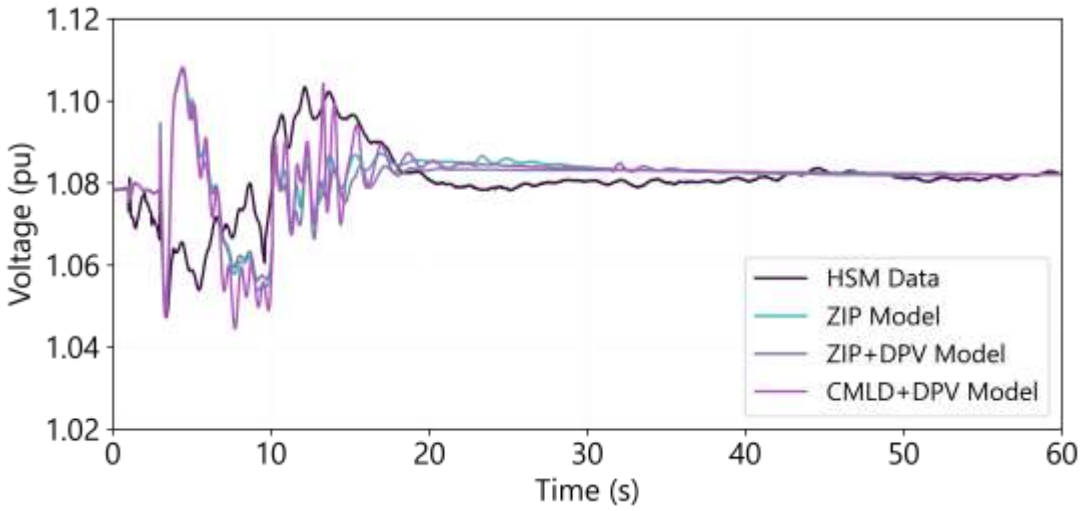

Active and reactive power flow

Figure 121 shows the active and reactive power measurements at Liddell Power Station (typical of most HSM locations).

At Liddell, all models somewhat overestimate the amplitude of the peak active power flows during QNI and Heywood interconnector trips. The trajectory of the reactive power measured on this feeder is relatively well represented by all models, although peak min/max reactive power flows are overestimated.

Steady-state active and reactive power is reasonably well represented by all models (when measured at 60s).

Figure 121 Active/reactive power – 25 August 2018 (NSW) – 330/22 kV Liddell Power Station G2 Feeder

Active power **Reactive power**

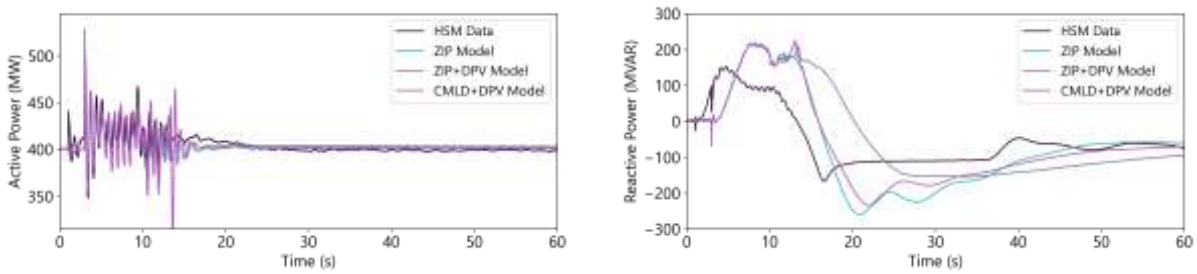

Figure 122 shows the active and reactive power measurements at the 500/23 kV Eraring Generator 3 Feeder. Observations at this location represent an outlier (not representative of most locations).

At Eraring, all models somewhat underestimate peak active power flows during QNI and Heywood interconnector trips. The trajectory of the reactive power measured on this feeder is relatively well represented by all models. The ZIP and CMLD+DPV models overestimate the peak min/max reactive flows after the QLD separation (at 3 s) and underestimate after the SA separation (at 9 s).

Steady-state active and reactive power is reasonably well represented by all models (when measured at 60 s).

Figure 122 Active/reactive power – 25 August 2018 (NSW) – 500/23 kV Eraring Generator 3 Feeder

Active power **Reactive power**

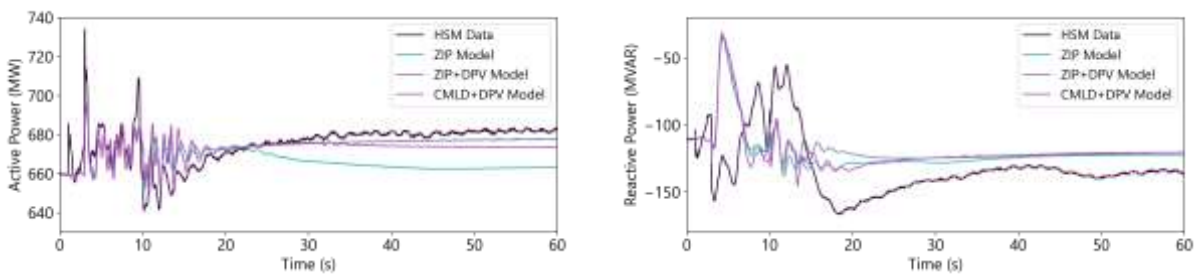

7.4.4 DPV measurements

Figure 123 shows the total measured DPV generation in New South Wales (initial value estimated from ASEFS2, and the change post disturbance estimated from Solar Analytics datasets) compared with the performance of the CMLD+DPV model and the ZIP+DPV model.

Figure 123 DPV measurement (Solar Analytics) – 25 August 2018 (NSW)

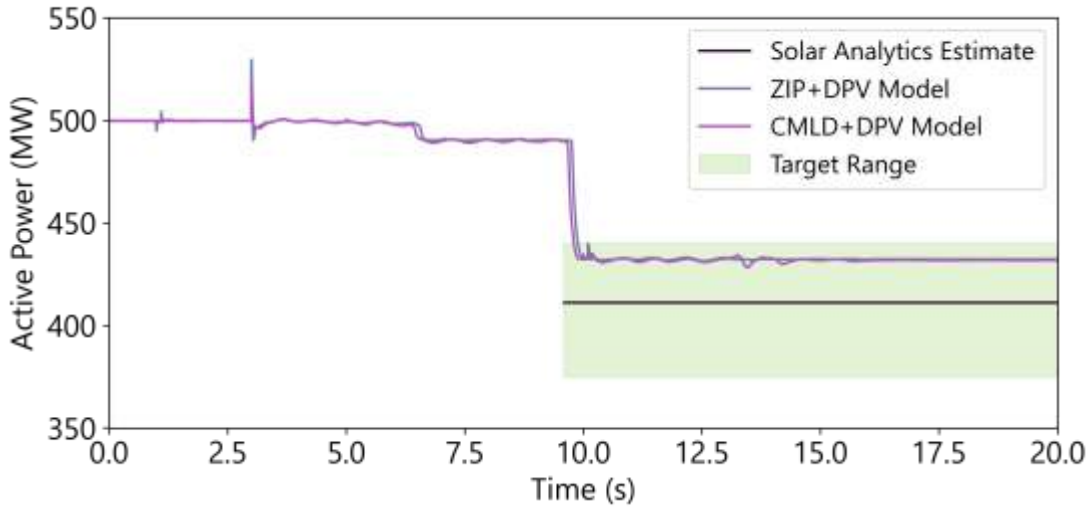

In the simulation of this event, the DPV response can be summarised as follows:

- A small amount of DPV disconnection occurs at ~6 s in response to the first under-frequency trip band (49.6 Hz with a 1.9 s delay).
- There is a larger amount of further DPV disconnection at ~9 s on the next four under-frequency trip bands (one at 49.01 Hz and three at 49 Hz) as frequency reaches the nadir.

These behaviours are consistent with the model's design, aiming to replicate the available evidence on DPV behaviour in frequency disturbances based on manufacturer surveys and field observations[126].

In this event, the CMLD+DPV model somewhat underestimates the observed 89 MW DPV disconnection, although it is within the uncertainty margin. There was no DPV curtailment for this event as under-frequency droop is not required for DPV inverters compliant with the AS/NZS4777.2:2015 standard.

Table 80 summarises estimates of the proportion of inverters that demonstrated disconnection versus curtailment. The DPV model represents these behaviours within the uncertainty margin, although it slightly underestimates total DPV disconnection.

Table 80 Summary of distributed PV behaviour – 25 August 2018 (NSW)

	Actuals (estimated)	CMLD+DPV prediction
DPV loss	89 MW (60 – 125 MW) decrease	68 MW decrease (underestimates by 23% but within range)

7.4.5 Load measurements

Figure 124 shows the active power responses of each of the load components in the CMLD model, in aggregate across the region. The Motor A and power electronics components are minimally affected by the disturbance. Motor B, C and D demonstrate a load relief response to the under-frequency, and Motors B and C also demonstrate response to the voltage dynamics. The most significant contributor to the CMLD response is from the static load model component, which does not have any frequency dependence, and is responding based on the voltage profile (shown in Figure 120). There is very minimal load disconnection in this event (<1MW) because voltage trip settings are not reached at most buses.

Figure 124 Active power responses of the CMLD load components – 25 August 2018 (NSW)

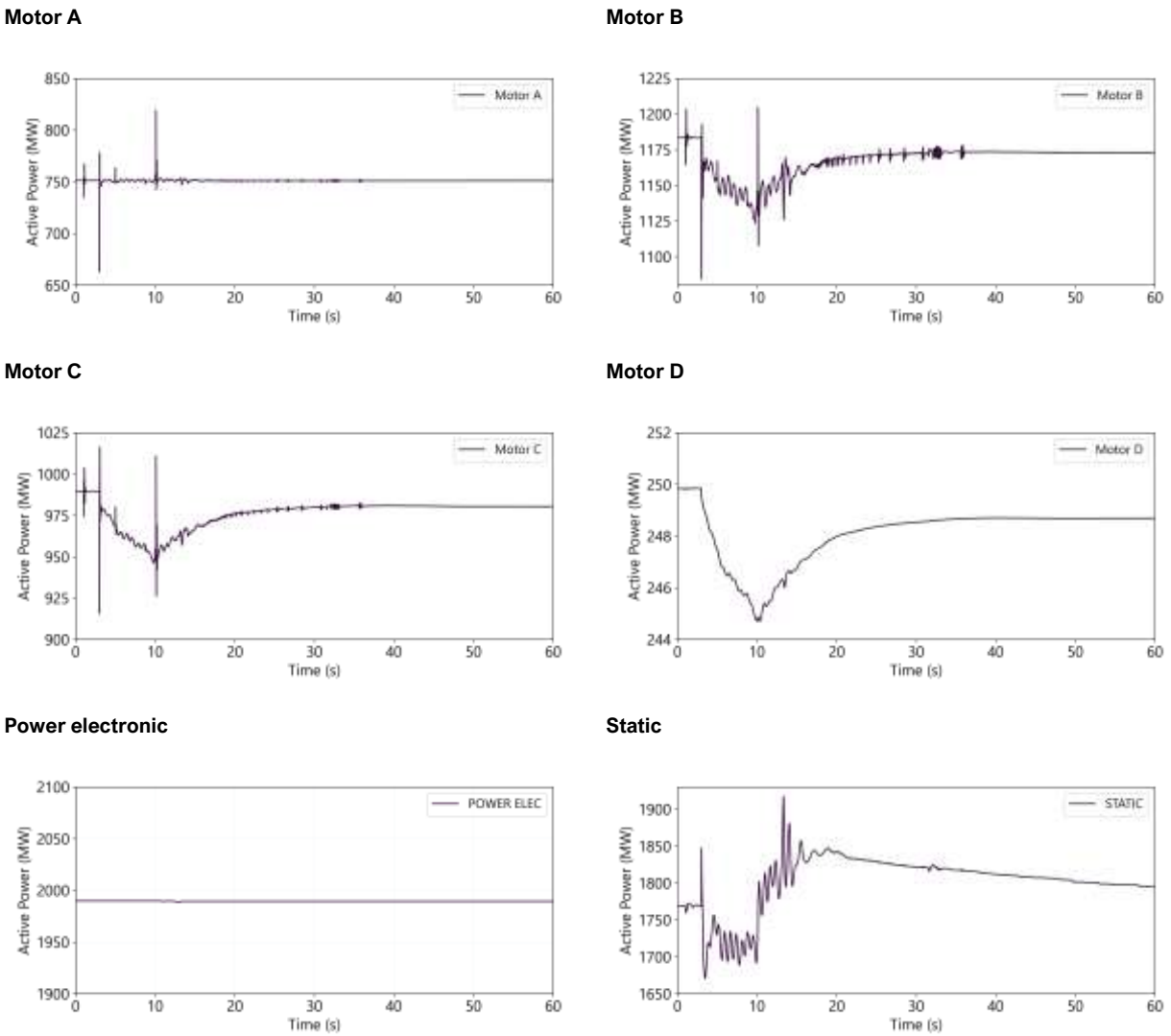

7.4.6 SCADA measurements

Figure 125 shows the total operational demand in New South Wales (from SCADA) compared with the performance of the various models. The CMLD+DPV model was tuned to match the load change measured at 72 s

post-disturbance (represented by the green dashed line in Figure 125), but it is acknowledged that there are significant inaccuracies in the SCADA measurement.

Figure 125 Operational demand measurements (SCADA) – 25 August 2018 (NSW)

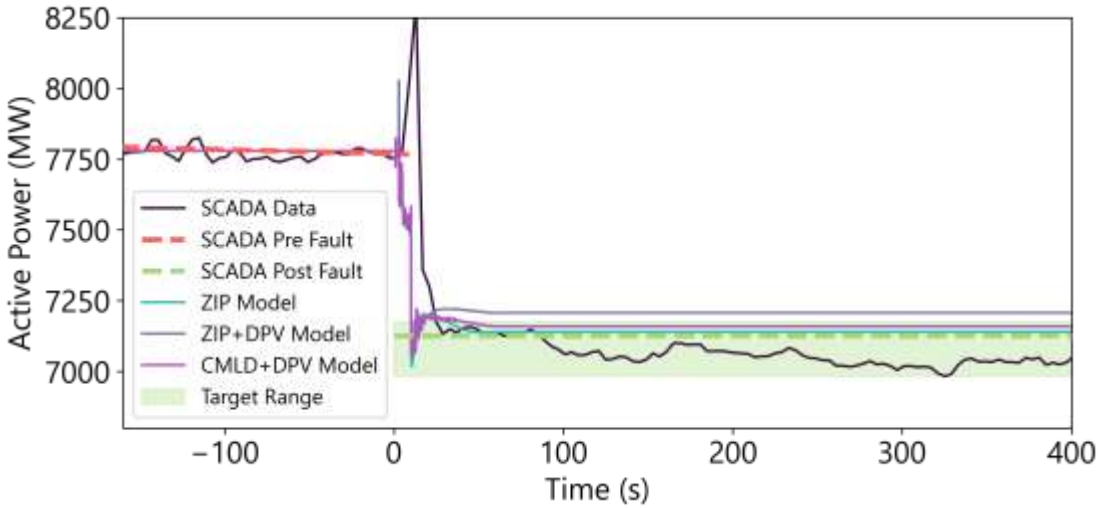

As shown in Figure 125, all models predict the total change in operational demand observed in the SCADA, since most of this is related to the UFLS trip (represented identically in all models). **Table 81** shows a comparison of the small changes in load related to the load models alone, without the UFLS trip.

Note that the CMLD model predicts a small increase in underlying load for this under-frequency event. The reduction in load due to the load relief response of the motor models is offset by a larger increase in load related to the voltage dependency of the static load component. In comparison, the ZIP+DPV model predicts a much larger increase in underlying load than the CMLD+DPV model, since the voltage dependency of the static load is not offset by the load relief in the motor model components.

It is possible to tune the CMLD model to reduce the degree of voltage dependency of the static load model (by adjusting the pfrq parameter). This was tested in sensitivity studies, and it was found that it did not improve results overall. Future revisions could explore other avenues to make the load model more representative of HSM data during frequency disturbances.

Table 81 Summary of change in demand and distributed PV – 25 August 2018 (NSW)

	Including UFLS		UFLS trip (MW)		Excluding UFLS		
	Actuals (estimated)	CMLD+DPV prediction	Actuals	CMLD+DPV	Actuals (estimated)	CMLD+DPV prediction	ZIP+DPV prediction
Change in distributed PV generation (estimated from Solar Analytics sample)	89 MW (60 – 125 MW) decrease	68 MW decrease (within range)	N/A	N/A	89 MW (60 – 125 MW) decrease	68 MW decrease (underestimates by 24% but within range)	68 MW decrease
Change in operational demand	645 MW (597 – 787 MW) decrease	620 MW decrease	715	704	70 MW (-118 – 72 MW) increase	84 MW increase	131 MW increase

	Including UFLS		UFLS trip (MW)		Excluding UFLS		
(estimated from SCADA, 60s post disturbance)		(within range)				(overestimates by 20% and outside of range)	
Change in underlying demand (estimated from SCADA & Solar Analytics)	733 MW (656 – 912 MW) decrease	688 MW decrease (within range)	715	704	18 MW decrease (197 MW decrease – 59 MW increase)	16 MW increase (accurately estimates minimal change in underlying demand)	63 MW increase

7.4.7 Assessment of model performance

Table 82 provides a summary of the performance of the CMLD+DPV models.

Table 82 Assessment of model performance – 25 August 2018 (NSW)

Quantity	Characteristic	CMLD + DPV estimates	CMLD+DPV model equal (✓) or better (✓✓) than ZIP?	Commentary
Frequency	During dynamic state	Fair match	✓	CMLD+DPV trajectory aligned with HSM, but the recovery rate is slower than observed.
	Steady-state post disturbance	Good match	✓	CMLD+DPV aligned with HSM.
Voltages	During dynamic state	Fair match	✓	CMLD+DPV trajectory somewhat misaligned with HSM (similar to ZIP model)
	Steady-state post disturbance	Good match	✓	CMLD+DPV aligned with HSM
Active power	During dynamic state	Good match	✓	CMLD+DPV aligned with HSM
	Steady-state post disturbance	Good match	✓✓	CMLD+DPV aligned with HSM
Reactive power	During dynamic state	Fair match	✓	CMLD+DPV has a comparable trajectory to the HSM, but peak flows are overestimated after the separation of QLD-NEM
	Steady-state post disturbance	Good match	✓	CMLD+DPV aligned with HSM
DPV	DPV total	Good match	✓✓	Estimated actuals: 89 MW decrease DPV: 68 MW decrease The DPV model underestimates DPV reduction by 24%.
CMLD	Underlying load change	Good match	✓✓	Estimated actuals (ex. UFLS): 18 MW decrease (72 s post disturbance) CMLD: 16 MW increase The CMLD accurately estimates a minimal change in load.
Operational demand	Net load change	Fair match	✓✓	SCADA (ex. UFLS): 70 MW increase (72s post disturbance) CMLD+DPV: 84 MW increase The CMLD+DPV model slightly overestimates net load change and is marginally outside of range.

.

7.5 16 November 2019 – South Australia

7.5.1 Event overview

Table 83 Event summary – 16 November 2019

Date and time		16 November 2019, 18:06[136]
Region		South Australia, Victoria[137]
Description of the event		The following two lines opened due to malfunction of a communication multiplexer: • Heywood – APD – Mortlake 500 kV line • Heywood – APD – Tarrone 500 kV line This resulted in South Australia separating from the rest of the NEM and interruption of 467 MW of load at APD. At the time of separation, the flows on the Heywood interconnector were 307 MW (Victoria to South Australia). Murray link was out of service on a forced outage.
Minimum voltage recorded		1.02 pu positive sequence at Pelican Point (from HSM Data)
Maximum voltage recorded		1.15 pu positive sequence at South East (from HSM Data)
Frequency nadir or zenith		Zenith: 50.83 Hz
Installed capacity of DPV		Total installed capacity in South Australia: 1,182 MW (from APVI) • 59% installed under AS4777.3:2005 (from ASEFS) • 41% installed under AS/NZS4777.2:2015 (from ASEFS)
Prior to the event	**DPV**	195 MW, 17% capacity factor (from ASEFS2, interpolated)
	Operational demand	1,274 MW (from SCADA data)
	Underlying demand	1,469 MW (estimate from SCADA + ASEFS2)
Estimated change (post disturbance vs pre disturbance)	**DPV**	36 MW (24 – 47 MW) decrease (from Solar Analytics data)
	Operational demand	14 MW (0 – 29 MW) increase (from SCADA data)
	Underlying demand	22 MW decrease (47 MW decrease to 5 MW increase) (from SCADA & Solar Analytics data)

7.5.2 Replication in PSS®E

The following element changes were made in PSS®E to replicate this event:

Table 84 Simulation event summary – 16 November 2019

Time (s)	Events simulated	Comments
0.0	Start simulation	-
1.0	Trip 500 kV Heywood Terminal Station (PSS®E bus 35342) to APD (PSS®E bus 35583) line 2 (HYTS-APD 2).	Due to non-convergence issues in PSS®E for this event, Heywood interconnector exports were reduced to 165 MW before performing

[136] AEMO. Final Report – South Australia and Victoria Separation Event on 16 November 2019, November 2020. Available at https://aemo.com.au/-/media/files/electricity/nem/market_notices_and_events/power_system_incident_reports/2019/final-report-sa-and-victoria-separation-event-16-november-2019.pdf.

[137] There was no significant voltage and frequency deviation in Victoria, so analysis was limited to the South Australian region.

Time (s)	Events simulated	Comments
	Trip 500 kV Heywood Terminal Station (PSS®E bus 35342) to Mortlake (PSS®E bus 35490) line (HYTS-MOPS). Trip 500 kV Heywood Terminal Station (PSS®E bus 35343) to APD (PSS®E bus 35584) line 1 (HYTS-APD 1). Trip 500 kV Heywood Terminal Station (PSS®E bus 35343) to Tarrone Terminal Station (PSS®E bus 35791) line (HYTS-TRTS). Trip 220 kV APD (PSS®E bus 30580) to Portland Wind Farm (PSS®E bus 32590) line. Trip 22 kV Cape Nelson North Portland Wind Farm bus (PSS®E bus 30593) Trip 700 V Cape Nelson South Portland Wind Farm bus (PSS®E bus 30595). Trip 700 V Cape Bridgewater Portland Wind Farm bus (PSS®E bus 30596). Trip 22 kV Cape Sir William Grant Portland Wind Farm bus (PSS®E bus 30599).	the simulation to enable the case to converge. As the intention is to validate the behaviour of CMLD and DPV models and the associated dynamics at a given frequency and voltage excursion, these changes should not impact validation studies. Trips at Portland are modelling artifacts required in PSS®E for the case to converge, as a dynamic simulation will not converge if an island is created with machines connected to that island. Note, Alcoa/Portland load was islanded because of the event[138].
60	End simulation	-

7.5.3 High speed measurements

Frequency

Figure 126 shows the grid frequency in South Australia. Immediately prior to the disturbance, South Australia was exporting approximately 307 MW to Victoria via the Heywood interconnector, with Murraylink interconnector out of service. As noted above, Heywood interconnector exports were reduced to 165 MW before performing the simulation to enable the case to converge.

As shown in **Figure 126**, the frequency response of all models following the SA-VIC separation shows a somewhat higher frequency zenith compared with observations. The overshoot is most severe for the ZIP model (greater than 51 Hz, not shown, tuned to match the frequency response of the HSM data) because the DPV reduction is not represented. The excessive frequency recovery time observed for all models may be explained by the known misrepresentation of generator governor controls in PSS®E (supported by the nature and timing of the observed mismatch when governors start to respond).

The CMLD+DPV model provides a reasonably accurate representation of the steady-state frequency following the event (for 40 s to 60s after the event). The ZIP/ZIP+DPV models show a comparable steady-state response (as shown in **Figure 126**). In the actual event, frequency oscillated between 50.5 Hz and 50.7 Hz for ~6 minutes after the separation before a gradual decline to 49.8 Hz over the next ~20 minutes (not shown or simulated).

[138] AEMO. Preliminary Report – South Australia and Victoria Separation Event on 16 November 2019, December 2019. Available at https://aemo.com.au/-/media/files/electricity/nem/market_notices_and_events/power_system_incident_reports/2019/preliminary-incident-report---16-november-2019---sa---vic-separation.pdf.

Figure 126 Frequency – 16 November 2019 – 275 kV Pelican Point Switching Station

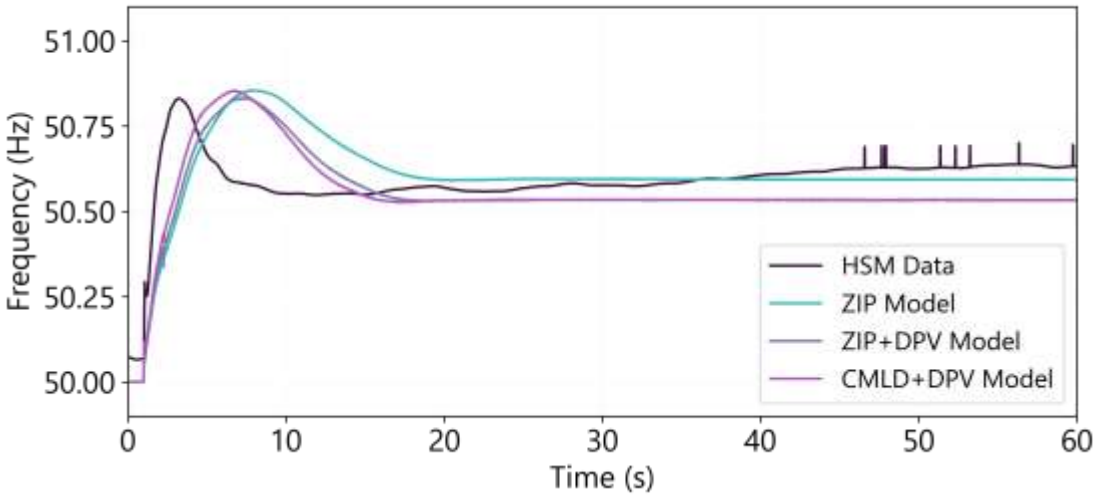

Voltage

Figure 127 shows the voltages at the 275 kV Pelican Point Switching Station (PPSS) in the vicinity of the Adelaide metro area. Observations at PPSS were found to be illustrative of the voltage response at all locations with HSM data available[139].

In this disturbance, all models underestimate peak voltages, but show a similar voltage recovery profile to the HSM. This is likely due to the reduction in Heywood interconnector flows to allow the PSS®E case to converge.

The recovery to post fault levels is slightly depressed for all models. The steady-state voltage after the disturbance (measured at 40 s) is comparable with observations.

[139] HSM data was available at the following locations: 275 kV Davenport, 275 kV Para, 275 kV Pelican Point, 275 kV Robertstown (P & Q only), 275 kV South East, 275 kV Tailem Bend, 275 kV Torrens Island.

Figure 127 Voltage – Pelican Point Switching Station – 16 November 2019 (SA)

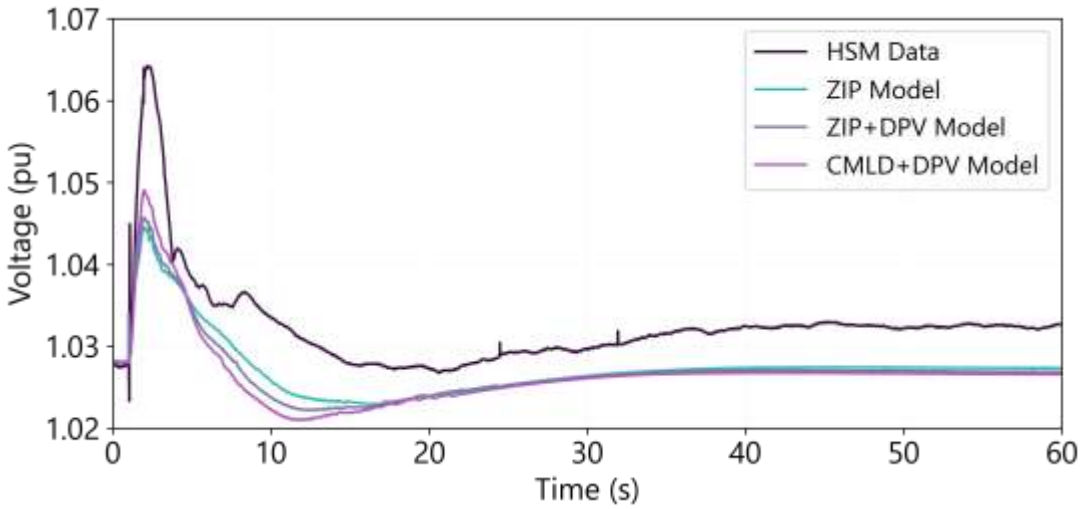

Active and reactive power flow

Figure 128 shows the active and reactive power measurements at the 275 kV Pelican Point GT12 feeder near the Adelaide metropolitan area. Observations at this location are illustrative of typical measurements recorded in this event.

For all models, active power is reasonably well represented during the initial 5 s on this feeder and most locations, although from 5 s onwards the active power exceeds observations. This overestimation is likely linked to the frequency zenith overestimation, related to inaccuracies in the PSS®E generator governors. All models also somewhat mismatch the steady-state active power (also likely related to the misrepresentation of the PSS®E generator governors droop response).

The trajectory of the reactive power measured on this feeder is reasonably well represented by all models, although the minimum/ maximum peak reactive flows are slightly underestimated and delayed in the dynamic period. Steady-state reactive power is reasonably well represented by all models.

Figure 128 Active/reactive power – 16 November 2019 (SA) – 275 kV Pelican Point GT12 Feeder

Active power

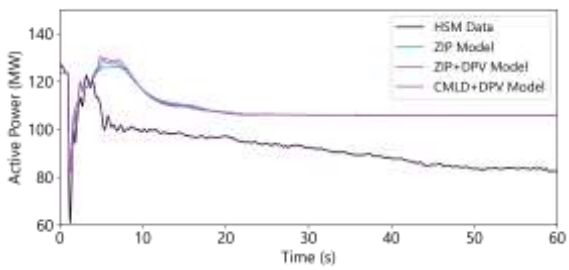

Reactive power

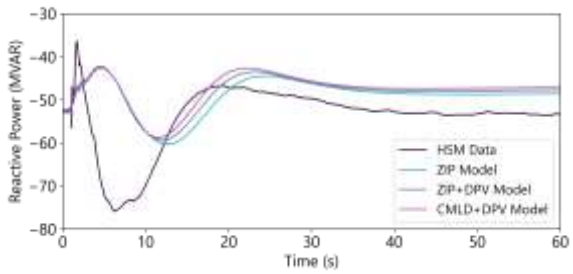

7.5.4 DPV measurements

Figure 129 shows the total measured DPV generation in South Australia (initial value estimated from ASEFS2, and the change post disturbance estimated from Solar Analytics datasets) compared with the performance of the CMLD+DPV model and the ZIP+DPV model.

Figure 129 DPV measurements (Solar Analytics) – South Australia Total – 16 November 2019

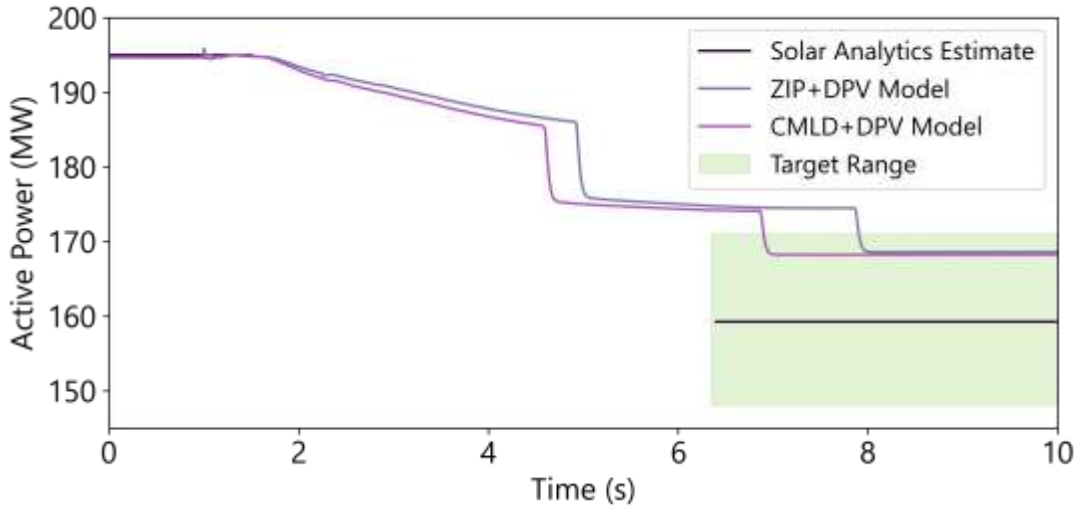

In the simulation of this event, the DPV response can be summarised as follows:

- DPV curtailment occurs at ~1.5 s to 7 s in response to the over-frequency (as required under AS/NZS4777.2:2015).
- A small amount of DPV disconnection occurs at ~5 s in response to the over-frequency exceeding the first DPV trip band at 50.5 Hz.
- There is a small amount of further DPV disconnection at ~6 s as frequency reaches the second trip band at 50.8Hz.

These behaviours are consistent with the model's design, aiming to replicate the available evidence on DPV behaviour in frequency disturbances based on manufacturer surveys and field observations[126].

The Solar Analytics dataset is only available at a 60 s resolution, so it cannot be plotted to compare model performance at the timescales shown in **Figure 129**. However, **Table 85** summarises estimates from the Solar Analytics dataset of the proportion of inverters that demonstrated disconnection versus curtailment. The DPV model represents these behaviours within the uncertainty margin.

Table 85 Summary of distributed PV behaviour – 16 November 2019 (SA)

	Actuals (estimated)	CMLD+DPV prediction
DPV curtailment	9 MW (7 – 10 MW) decrease	10 MW decrease (accurately estimates minimal curtailment)
DPV disconnection	27 MW (18 – 37 MW) decrease	17 MW decrease (underestimates by 37%, but within range)

	Actuals (estimated)	CMLD+DPV prediction
DPV total	36 MW (24 – 47 MW) decrease	26 MW decrease (underestimates by 28% but within range)

7.5.5 Load measurements

Figure 130 shows the active power responses of each of the load components in the CMLD model, in aggregate across the region. Motor A and power electronics loads are relatively unaffected, while Motor B, C and D show some increase in response to the over-frequency. The static load component initially increases in response to the over-voltage experienced at most buses (shown in **Figure 127**), then decreases to slightly below pre-event levels. The load model predicts minimal load disconnection in this event since the voltage trip thresholds for the various load model components were not reached at most buses.

Figure 130 Active power responses of the CMLD load components – 16 November 2019 (SA)

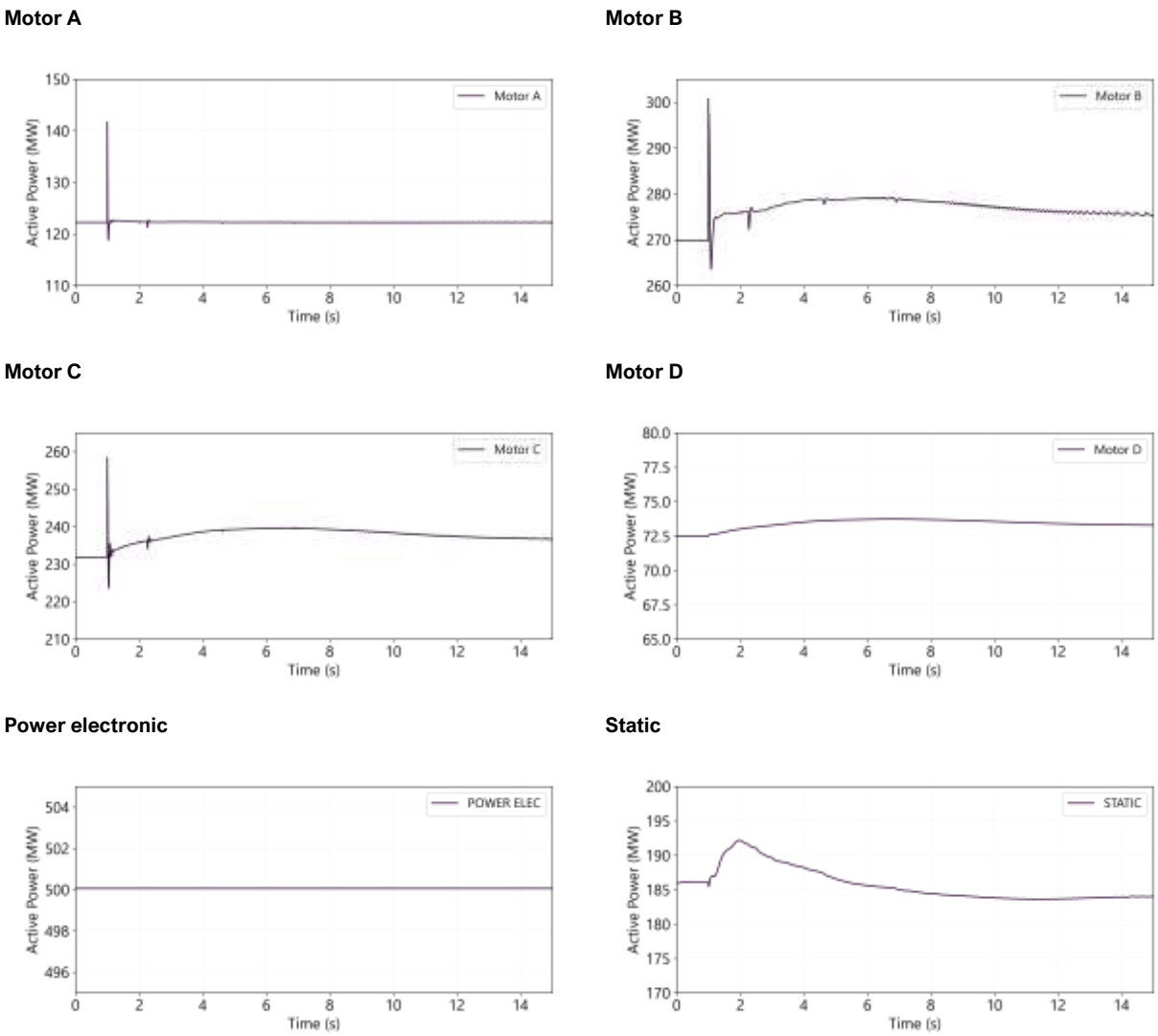

7.5.6 SCADA measurements

Figure 131 shows the total operational demand in South Australia (from SCADA) compared with the performance of the various models. In this event, the post disturbance operational demand suddenly increased by ~14 MW, then stayed relatively consistent over the subsequent minutes. The CMLD+DPV model was tuned to match the average load change measured at 64 s post-disturbance (represented by the green dashed line in **Figure 131**).

Figure 131 Operational demand measurements (SCADA) – 16 November 2019

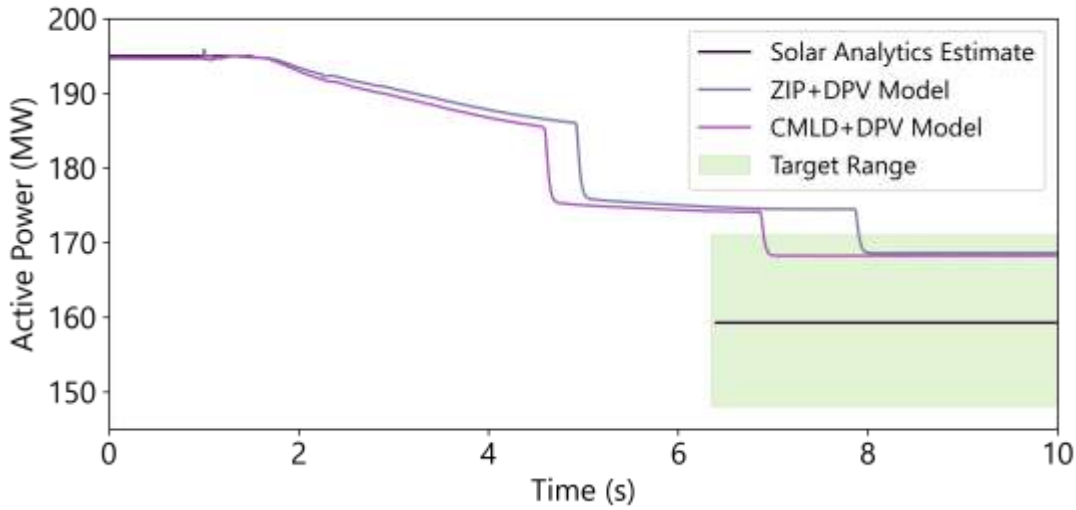

As shown in Figure 131, the CMLD+DPV model somewhat overpredicts the estimated net 14 MW increase in operational demand. The CMLD model predicts 11 MW of total underlying load increase, compounded by 26 MW of DPV disconnection predicted by the DPV model, leading to a total net increase in operational demand of 37 MW. The comparison with estimated actuals is shown in **Table 86**.

Table 86 Summary of change in demand and distributed PV – 16 November 2019

	Actuals (estimated)	CMLD+DPV prediction
Change in DPV generation (estimated from Solar Analytics sample)	36 MW (24 – 47 MW) decrease	26 MW decrease (underestimates by 28% but within range)
Change in underlying demand (estimated from SCADA & Solar Analytics)	22 MW decrease (47 MW decrease – 5 MW increase)	11 MW increase (accurately estimates minimal change in underlying demand but out of range)
Change in operational demand (estimated from SCADA, 60s post disturbance)	14 MW (0 – 29 MW) increase	37 MW increase (accurately estimates minimal change in operational demand, but outside of range)

When the ZIP model alone is applied, the estimated DPV decrease in this event is not captured, and the observed increase in operational demand is underestimated.

7.5.7 Assessment of model performance

Table 87 provides a summary of the performance of the CMLD+DPV models.

Table 87 Assessment of model performance – 16 November 2019

Quantity	Characteristic	CMLD + DPV estimates	CMLD+DPV model equal (✓) or better (✓✓) than ZIP?	Commentary
Frequency	During dynamic state	Fair match	✓✓	All models overshoot observations during over-frequency, likely due to misrepresentation of generator governors.
	Post disturbance	Good match	✓✓	CMLD+DPV aligned with HSM
Voltage	During dynamic state	Good match	✓	CMLD+DPV aligned with HSM, slightly underestimates temporary over-voltage
	Steady-state post disturbance	Good match	✓	CMLD+DPV aligned with HSM
Active power	During dynamic state	Fair match	✓	CMLD+DPV peak active power flows are overestimated, likely due to misrepresentation of generator governors.
	Steady-state post disturbance	Fair match	✓	CMLD+DPV steady-state active power flows are overestimated, likely due to misrepresentation of generator governors.
Reactive power	During dynamic state	Fair match	✓	CMLD+DPV steady-state reactive power flows are slightly underestimated, likely due to misrepresentation of temporary overvoltage.
	Steady-state post disturbance	Fair match	✓	CMLD+DPV slightly underestimates steady-state reactive power flows.
DPV	DPV curtailment	Good match	✓✓	Estimated actuals: 9 MW decrease DPV: 10 MW decrease The DPV model accurately estimates minimal DPV curtailment and is within the uncertainty range.
	DPV disconnection	Good match	✓✓	Estimated actuals: 27 MW decrease DPV: 17 MW decrease The DPV model accurately estimates minimal DPV disconnection and is within the uncertainty range.
	DPV total	Good match	✓✓	Estimated actuals: 36 MW decrease DPV: 26 MW decrease The DPV model accurately estimates minimal DPV reduction and is within the uncertainty range.
Load	Underlying load change	Good match	✓	Estimated actuals: 22 MW decrease (64 s post disturbance) CMLD: 11 MW increase CMLD accurately estimates minimal underlying load change but is outside the uncertainty range.
Operational demand	Net load change	Good match	✓✓	SCADA: 14 MW increase (64 s post disturbance) CMLD+DPV: 37 MW increase The CMLD+DPV model accurately estimates minimal net load change and is within the uncertainty range.

7.6 31 January 2020 – South Australia

7.6.1 Event overview

Table 88 Event summary – 31 January 2020 – South Australia

Date and time		31 January 2020, 13:24[140]
Description of the event		This event resulted in the non-credible loss of both the Moorabool – Mortlake (MLTS-MOPS) and the Moorabool – Haunted Gully (MLTS-HGTS) – Tarrone (HGTS-TRTS) 500 kV transmission lines, causing a separation of the Victoria and South Australia regions. Immediately after the incident, the Mortlake Power Station (MOPS) generating units and the APD aluminium smelter remained connected to the South Australia region but disconnected from the rest of Victoria. At the same time, both potlines at APD tripped, resulting in loss of load.
Region		South Australia
Minimum voltage recorded		0.88 pu positive sequence at South East (from HSM data)
Maximum voltage recorded		1.11 pu positive sequence at South East (from HSM data)
Frequency nadir or zenith		Zenith: 51.12 Hz
Installed capacity of distributed PV		Total installed capacity in South Australia: 1,169 MW (from APVI) • 55% installed under AS4777.3:2005 (from ASEFS) • 45% installed under AS/NZS4777.2:2015 (from ASEFS)
Prior to the event	**Distributed PV**	475 MW, 38% capacity factor (from ASEFS2, interpolated)
	Operational demand	2,655 MW, (from SCADA data)
	Underlying demand	3,130 MW (estimated from SCADA + ASEFS2)
Estimated change (post disturbance vs pre disturbance)	**Distributed PV**	113 MW (81 – 153 MW) decrease (from Solar Analytics data)
	Operational demand	280 MW (114 – 334 MW) increase (from SCADA data)
	Underlying demand	167 MW increase (39 MW decrease to 253 MW increase) (from SCADA & Solar Analytics data)

7.6.2 Replication in PSS®E

The following element changes were made in PSS®E to replicate this event.

Table 89 Simulation event summary – 31 January 2020

Time (s)	Region	Events simulated	Comments
0.0		Start simulation	
5.0	VIC	Apply 3P fault on the 500 kV Haunted Gully bus (PSS®E bus 10964)	
5.08	VIC	Clear 3P fault on the 500 kV Haunted Gully bus (PSS®E bus 10964) Trip 500 kV Haunted Gully (PSS®E bus 10964) to Moorabool (PSS®E bus 35480) line	
7.62	VIC	Apply a 1PG fault on the 500 kV Mortlake Power Station bus (PSS®E bus 35490)	

[140] AEMO. Final Report – Victoria and South Australia Separation Event on 31 January 2020, November 2020. Available at https://aemo.com.au/-/media/files/electricity/nem/market_notices_and_events/power_system_incident_reports/2020/final-report-vic-sa-separation-31-jan--2020.pdf?la=en.

Time (s)	Region	Events simulated	Comments
7.7	VIC	Clear 1PG fault on the 500 kV Mortlake Power Station bus (PSS®E bus 35490)	
9.02	VIC	Apply a 1PG on the 500 kV Mortlake Power Station bus (PSS®E bus 35490)	
9.1	VIC	Clear 1PG fault on the 500 kV Mortlake Power Station bus (PSS®E bus 35490) Trip 500 kV Mortlake Power Station (PSS®E bus 35490) to Moorabool (PSS®E bus 35483) line	Separation of VIC-SA, with SA subsequently operating as an extended island which includes APD. Note, APD load tripped on UFLS for this event. APD was not tripped in the PSS®E case in order to better match the power system frequency response. The intention is to validate the DPV and load models, so it is more important to accurately reflect the frequency trajectory that occurred.
10.2	SA	Trip 1 kV Waterloo Wind Farm G1 (PSS®E bus 50061) on OFGS Trip 1 kV Waterloo Wind Farm G2 (PSS®E bus 50062) on OFGS Trip 700V The Bluff Wind Farm Generator bus (PSS®E bus 50335) on OFGS Trip 700V Hallett Hill Wind Farm Generator bus (PSS®E bus 50960) Trip 1 kV Lake Bonney Wind Farm Generator 2A (PSS®E bus 50927) on OFGS Trip 1 kV Lake Bonney Wind Farm Generator 3 (PSS®E bus 50927) on OFGS Trip 700V North Brown Hill Wind Farm Generator 1A (PSS®E bus 50091)	The Bluff, Waterloo, and Lake Bonney Wind warm tripped as frequency exceeded the generator trip settings. Cathedral Rocks, Wattle Point, Macarthur, and Starfish Hill Wind Farms were tripped or reduced output during the event. Some of these generators do not exist in the PSS®E snapshot, so North Brown Hill and Hallett Hill Wind Farms were tripped in simulation instead to account for this and match the frequency response.
10.5	SA	Trip 700V Canunda Wind Farm Generator 1 (PSS®E bus 50924) on OFGS Trip 700V Canunda Wind Farm Generator 2 (PSS®E bus 50925) on OFGS	
14.6	SA	Trip 6 kV Willogoleche Wind Farm Generator (PSS®E bus 2321)	Willogoleche Wind Farm was tripped in the simulation to account for the wind farms that were not tripped in PSS®E (above) and better match the power system frequency response.
60		End simulation	

7.6.3 High speed measurements

Frequency

Figure 132 shows the power system frequency in South Australia. Prior to the disturbance, the power flow across the Victoria – South Australia (Heywood) interconnector was ~531 MW from South Australia to Victoria. Immediately after the loss of the MLTS-MOPS and MLTS-HGTS lines, South Australia experienced a supply surplus, resulting in an increase in frequency to 51.12 Hz.

As shown in Figure 132, the frequency zenith produced by the simulations that include the DPV model (following the SA-VIC separation) is comparable to observations. In contrast, the case without the DPV model slightly overestimates the frequency zenith (not shown, tuned to match the frequency response of the HSM data). This is due to the lack of DPV disconnection and curtailment (the same large-scale generation was tripped in all cases).

Following the islanding of South Australia, the CMLD+DPV and ZIP+DPV models provide a reasonably accurate representation of the steady-state frequency following the event (measured at ~50 s). In contrast, the ZIP model overestimates the steady-state frequency considerably (exceeding 50.5Hz, not shown).

Figure 132 Frequency – 31 January 2020 – 275kV Para bus (SA)

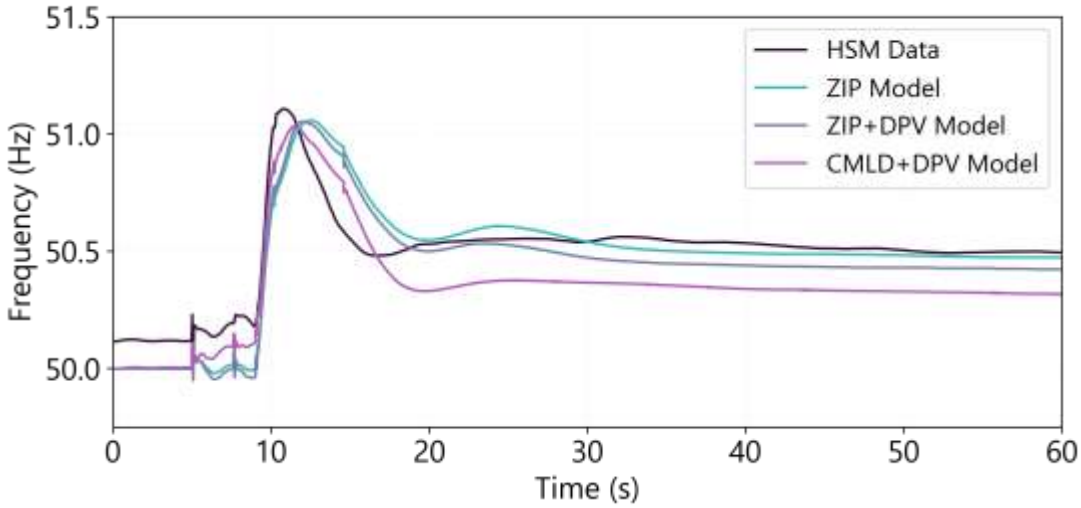

Voltage

Figure 133 shows the voltages at the 275 kV Para bus in the Adelaide metropolitan region. Observations at this location are illustrative of the voltage response at most locations in the network[141].

In this disturbance, all models show a similar voltage recovery profile to the HSM. The CMLD+DPV model exceeds the normal range (0.9 pu to 1.1 pu) for less than 60 ms (which should not result in spurious tripping of load and other network elements). For all models, voltage recovers to a slightly higher level than observed.

[141] HSM data is available at the following locations: 275 kV Davenport, 275 kV Para, 275 kV Pelican Point, 275 kV Robertstown (P & Q only), 275 kV South East, 275 kV Tailem Bend, 275 kV Torrens Island.

Figure 133 Voltage – 31 January 2020 – 275 kV Para bus (SA)

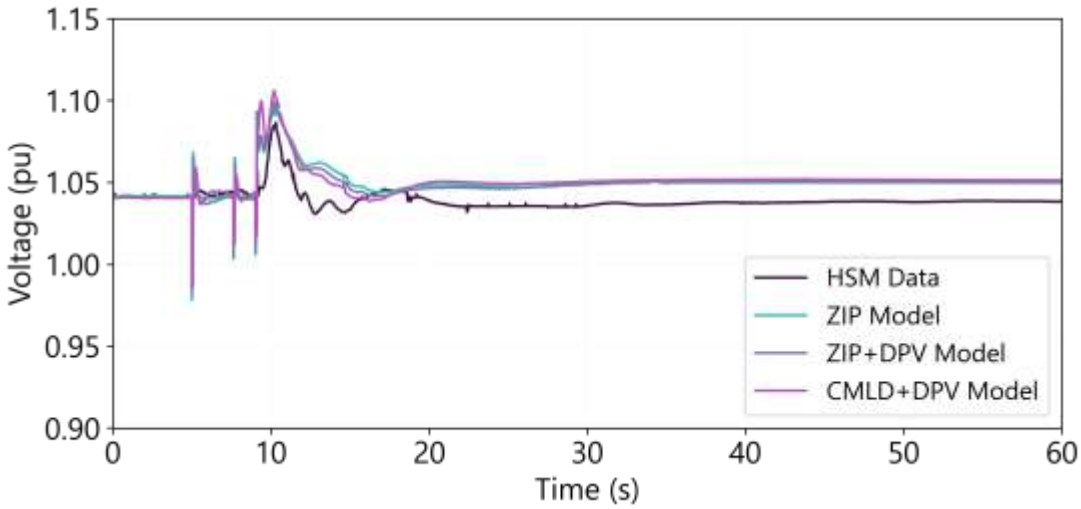

Active and reactive power flow

Figure 134 shows the active and reactive power measurements at the 275 kV Pelican Point to Lefevre feeder (in the Adelaide metropolitan area). Observations at this location are illustrative of typical measurements recorded in this event.

Active power is reasonably well represented by all models (following the VIC-SA separation from ~9 s onwards) on this feeder and most locations, although steady-state flows are somewhat underestimated.

For reactive power, the trajectory is reasonably well represented by all models, although all models underestimate the minimum/maximum peak reactive flows in the 9 s to 12 s simulation period. All models reasonably accurately represent the peak reactive power flows in the 15 s to 20 s timeframe.

Steady-state reactive power is reasonably well represented by all models (measured at 60 s, not shown), though the CMLD+DPV model shows a closer response to the HSM than the ZIP model.

Figure 134 Active/reactive power – 31 January 2020 - 275 kV Pelican Point to Lefevre Feeder

Active power

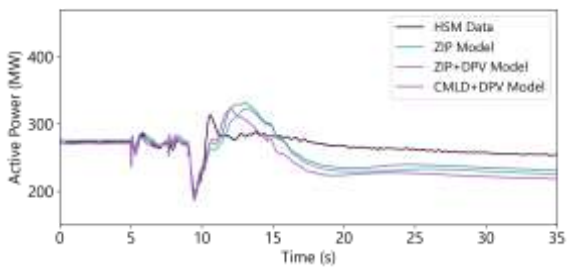

Reactive power

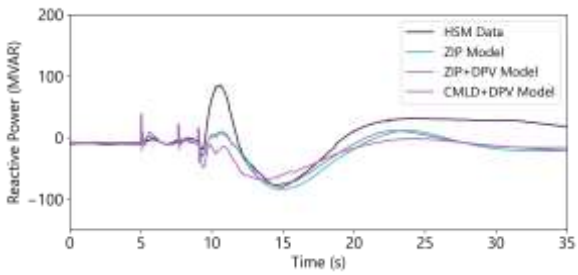

7.6.4 DPV measurements

Figure 135 shows the total measured DPV generation in South Australia (initial value estimated from ASEFS2, and the change post disturbance estimated from Solar Analytics datasets) compared with the performance of the CMLD+DPV model and the ZIP+DPV model.

Figure 135 DPV measurements (Solar Analytics) – 31 January 2020 (SA)

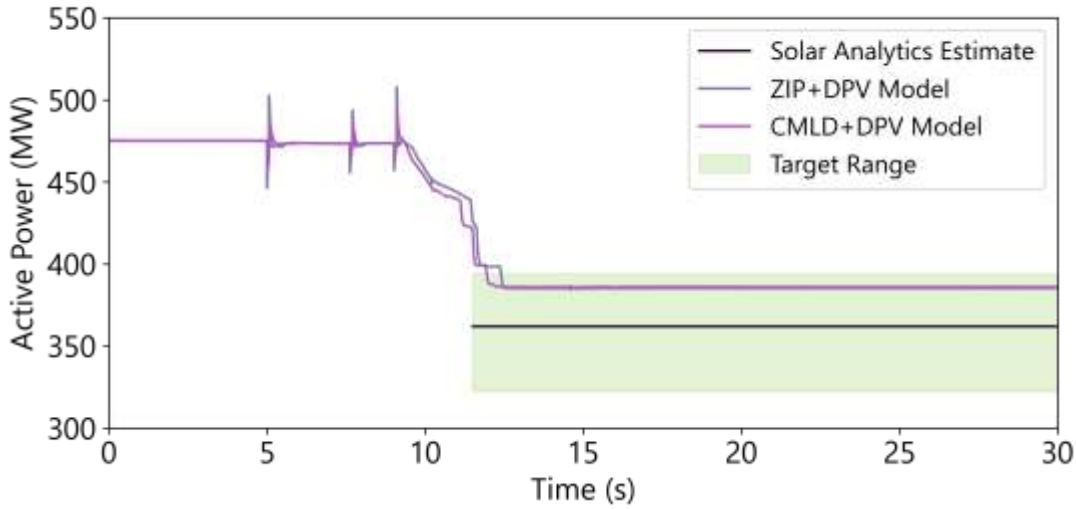

In the simulation of this event, the DPV response can be summarised as follows:

- DPV curtailment occurs at 9 s to 12 s in response to the over-frequency (as required under AS/NZS4777.2:2015).
- DPV disconnection occurs at ~11 s as frequency exceeds 50.5 Hz and 50.8 Hz (the first two over-frequency disconnection bands, which also have a 1.9s trip delay) and then again as frequency reaches the zenith (exceeding 51 Hz).

These behaviours are consistent with the model's design, aiming to replicate the available evidence on DPV behaviour in frequency disturbances based on manufacturer surveys and field observations[126].

The Solar Analytics dataset is only available at a 60 s resolution, so it cannot be plotted to compare model performance at the timescales shown in Figure 135. However, **Table 90** summarises estimates (from the Solar Analytics dataset) of the proportion of inverters that demonstrated disconnection versus curtailment. The DPV model represents these behaviours within the uncertainty margin.

Table 90 Summary of distributed PV behaviour – 31 January 2020 (SA)

	Actuals (estimated)	CMLD+DPV prediction
DPV curtailment	37 MW (29 – 43 MW) decrease	32 MW decrease (underestimates by 13%, but within range)
DPV disconnection	76 MW (52 – 109 MW) decrease	57 MW decrease (underestimates by 25% but within range)
DPV total change	113 MW (81 – 153 MW) decrease	89 MW decrease

	Actuals (estimated)	CMLD+DPV prediction
		(underestimates by 21% but within range)

7.6.5 Load measurements

Figure 136 shows the active power responses of each of the load components in the CMLD model, in aggregate across the region. Motor A remains relatively unaffected during this event, while Motors B, C and D increase somewhat in response to the over-frequency. The power electronics load shows a very small amount of disconnection, since voltages at some buses reached the under-voltage trip thresholds for this model. The static load model responds to the changes in voltages (shown in Figure 133).

Figure 136 Active power responses of the CMLD load components – 31 January 2020 (SA)

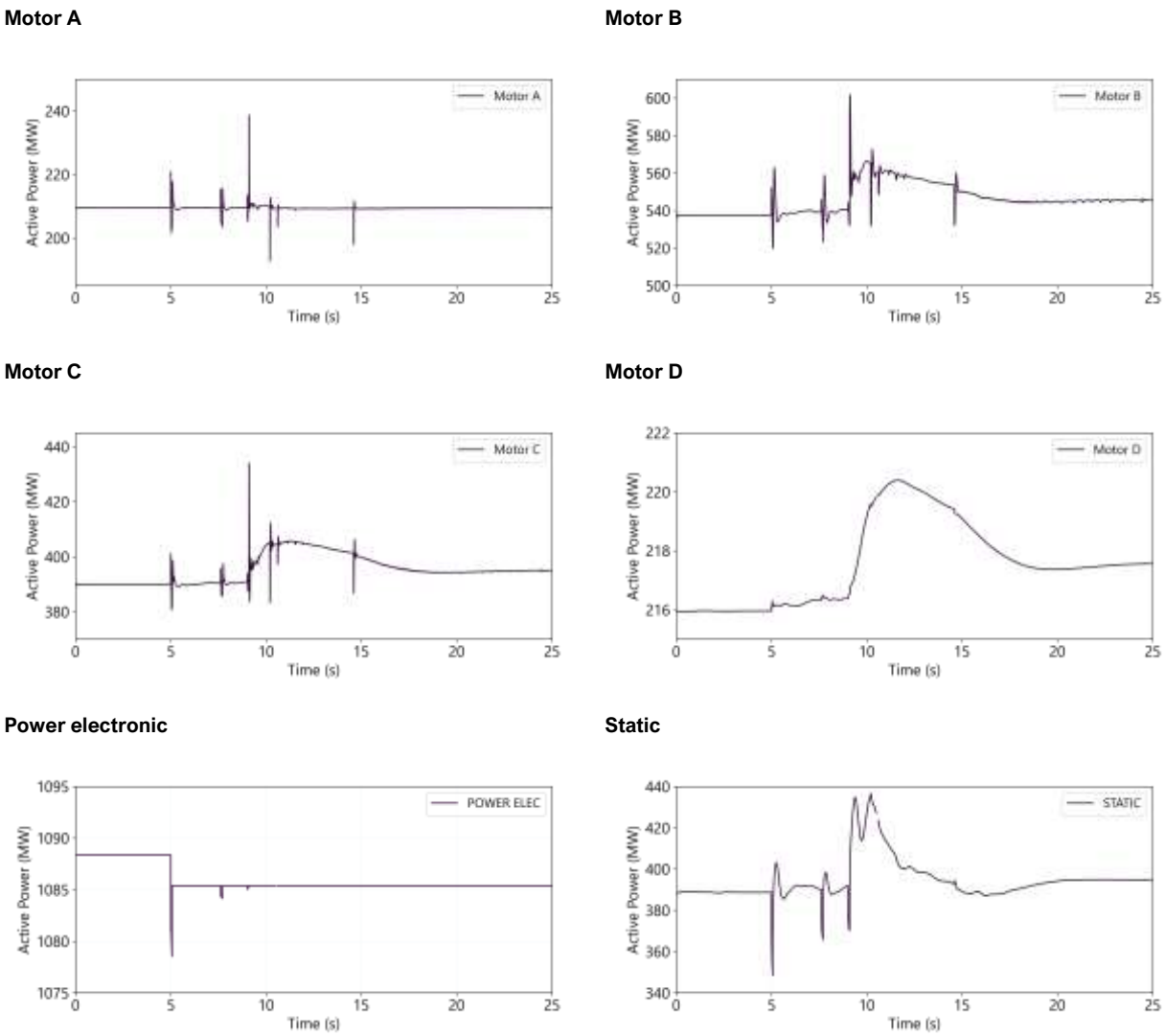

7.6.6 SCADA measurements

Figure 137 shows the total operational demand in South Australia (from SCADA) compared with the performance of the various models. In this event, it is unclear what change in operational demand really occurred in the fast timescales represented by the PSS®E model[142]. The CMLD+DPV model was therefore tuned to match the load change measured at 32 s post disturbance (represented by the green dashed line in Figure 137), with the wide error margins shown in the green shaded area.

Figure 137 Operational demand measurements (SCADA) – South Australia Total – 31 January 2020

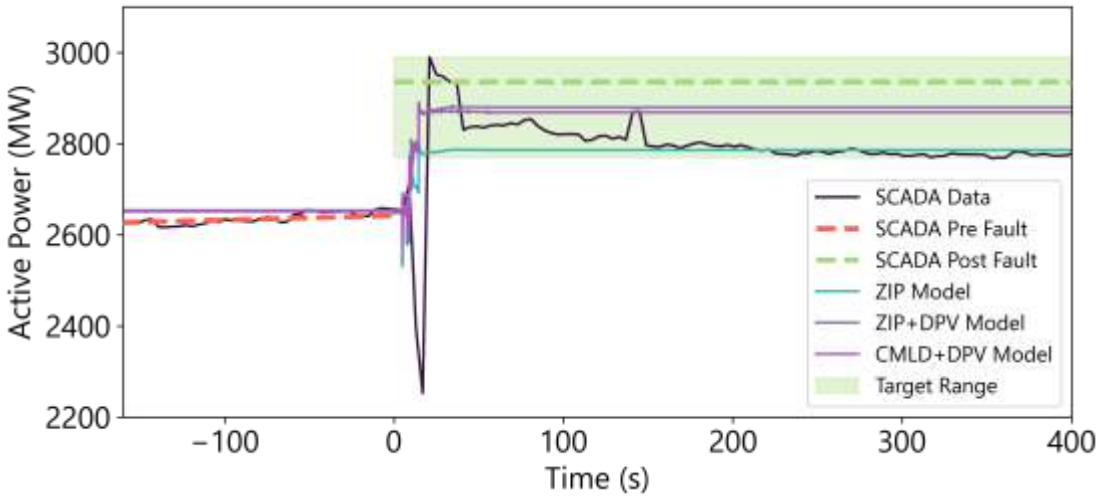

As shown in **Figure 137**, the CMLD+DPV and ZIP+DPV models somewhat underpredict the 280 MW increase in operational demand but are within the uncertainty range. The ZIP model underestimates the increase in operational demand because it does not include any representation of the change in DPV generation.

The comparison with estimated actuals is shown in **Table 91**. The CMLD model predicts an increase in underlying demand of 127 MW, which somewhat underestimates the estimated actual value of 167 MW (although acknowledging the uncertainty in this estimate is very large). This could be indicative of the load relief response to over-frequency or due to the sustained overvoltage which increases the power output of the static loads.

Table 91 Summary of change in demand and distributed PV – 31 January 2020 (SA)

	Actuals (estimated)	CMLD+DPV prediction	ZIP+DPV prediction
Change in DPV generation (estimated from Solar Analytics sample)	113 MW (81 – 153 MW) decrease	89 MW decrease (underestimates by 21% but within range)	90 MW decrease (underestimates by 20% but within range)
Change in underlying demand (estimated from SCADA & Solar Analytics)	167 MW increase (39 MW decrease to 253 MW increase)	127 MW increase (underestimates by 24% but within range)	140 MW increase (underestimates by 17% but within range)
Change in operational demand	280 MW (114 – 334 MW) increase	216 MW increase (underestimates by 23% but within range)	230 MW increase (underestimates by 18% but within range)

[142] For example, the potential for misalignment of time measurements when summing SCADA from generator terminals

	Actuals (estimated)	CMLD+DPV prediction	ZIP+DPV prediction
(estimated from SCADA, 60s post disturbance)			

7.6.7 Assessment of model performance

Table 92 provides a summary of the performance of the CMLD+DPV models.

Table 92 Assessment of model performance – 31 January 2020 (SA)

Quantity	Characteristic	CMLD + DPV estimates	CMLD+DPV model equal (✓) or better (✓✓) than ZIP?	Commentary
Frequency	During dynamic state	Good match	✓✓	CMLD+DPV aligned with HSM
	Steady-state post disturbance	Good match	✓✓	CMLD+DPV aligned with HSM
Voltage	During dynamic state	Good match	✓✓	CMLD+DPV aligned with HSM
	Steady-state post disturbance	Good match	✓	CMLD+DPV aligned with HSM
Active power	During dynamic state	Good match	✓	CMLD+DPV aligned with HSM
	Steady-state post disturbance	Fair match	✓	CMLD+DPV steady-state active power flows are underestimated.
Reactive power	During dynamic state	Fair match	✓	CMLD+DPV steady-state reactive power flows are slightly underestimated.
	Steady-state post disturbance	Fair match	✓✓	CMLD+DPV slightly underestimates steady-state reactive power flows.
DPV	DPV curtailment	Good match	✓✓	Estimated actuals: 37 MW decrease DPV: 32 MW decrease The DPV model accurately estimates DPV curtailment.
	DPV disconnection	Good match	✓✓	Estimated actuals: 76 MW decrease DPV: 57 MW decrease The DPV model underestimates DPV disconnection by 25% but within uncertainty margin.
	DPV total	Good match	✓✓	Estimated actuals: 113 MW decrease DPV: 89 MW decrease The DPV model underestimates DPV reduction by 21%.
Load	Underlying load change	Good match	✓✓	Estimated actuals: 167 MW increase (32 s post disturbance) CMLD: 127 MW increase The CMLD underestimates load disconnection by 24% when measured at 60s post disturbance, but is within range.
Operational demand	Net load change	Good match	✓	SCADA: 280 MW increase (32 s post disturbance) CMLD+DPV: 216 MW increase

Quantity	Characteristic	CMLD + DPV estimates	CMLD+DPV model equal (✓) or better (✓✓) than ZIP?	Commentary
				The CMLD+DPV model underestimates net load change by 18%, but is within range.

7.7 31 January 2020 – Victoria

7.7.1 Event overview

Table 93 Event summary – 31 January 2020

Date and time		31 January 2020, 13:24[140]
Description of the event		This event resulted in the non-credible loss of both the Moorabool – Mortlake (MLTS-MOPS) and the Moorabool – Haunted Gully (MLTS-HGTS) – Tarrone (HGTS-TRTS) 500 kV transmission lines, causing a separation of the Victoria and South Australia regions. Immediately after the incident, the Mortlake Power Station (MOPS) generating units and the APD aluminium smelter remained connected to the South Australia region but disconnected from the rest of Victoria. At the same time, both potlines at APD tripped, resulting in the loss of load.
Region		Victoria
Minimum voltage recorded		0.34 pu positive sequence at Heywood (from HSM data)
Maximum voltage recorded		1.15 pu positive sequence at Heywood (from HSM data)
Frequency nadir or zenith		Zenith: 51.20 Hz Nadir: 49.65 Hz
Installed capacity of DPV		Total installed capacity in Victoria: 2,043 MW (from APVI) • 48% installed under AS4777.3:2005 (from ASEFS • 52% installed under AS/NZS4777.2:2015 (from ASEFS)
Prior to the event	**DPV**	1,030 MW, 50% capacity factor (from ASEFS2, interpolated)
	Operational demand	8,957 MW (from SCADA data)
	Underlying demand	9,987 MW (estimate from SCADA + ASEFS2)
Estimated change (post disturbance vs pre disturbance)	**DPV**	153 MW (100 –216 MW) decrease (from Solar Analytics data)
	Operational demand	704 MW (615 –786 MW) decrease (from SCADA data)
	Underlying demand	857 MW (715 –1,002 MW) decrease (from SCADA & Solar Analytics data)

7.7.2 Replication in PSS®E

Refer to Section 7.6.2.

7.7.3 High speed measurements

Frequency

Figure 138 shows the grid frequency in Victoria. Prior to the disturbance, the power flow across the Victoria – South Australia (Heywood) interconnector was ~531 MW from South Australia to Victoria. Immediately after the

loss of the MLTS-MOPS and MLTS-HGTS lines, the areas outside of the extended South Australia island (including Victoria) fell to a minimum of 49.66 Hz, as shown in Figure 138. The frequency initially returned briefly to within the recovery band, then fell below 49.85 Hz again shortly after the separation. Frequency did not return to above 49.85 Hz until ~19 minutes following the initial disturbance.

As shown in Figure 138, all models predict the frequency trajectory reasonably well, although the CMLD+DPV models somewhat underpredict the depth of the frequency nadir.

In this event, the CMLD model predicts that underlying load reduces by ~421 MW (mostly due to disconnection of power electronic loads and Motor C loads at ~5s in response to the voltage dip experienced at many buses). This is reasonably well aligned with SCADA observations which suggest that underlying demand likely reduced by approximately 407 MW. The ZIP model does not represent this load disconnection at all.

The CMLD model somewhat over-predicts the estimated actual change in underlying load by ~4%. Compounding this, in this case the DPV model under-predicts estimated disconnection of DPV (predicting an 109 MW decrease in DPV generation, compared with estimated actuals of 153 MW, approximately a 29% error). This over-estimate of underlying load disconnection, and under-estimate of DPV disconnection, acts to alleviate the under-frequency event more than occurred in reality, and leads to the underestimation of the depth of the frequency nadir.

The ZIP model does not include any representation of load disconnection or DPV disconnection. The ZIP model predicts an underlying demand reduction of 65 MW (in response to low bus voltages), which significantly under-predicts the actual underlying load reduction of 407 MW.

The CMLD+DPV model better predicts the steady state frequency.

The voltage trip parameters for the CMLD model have been tuned to provide the best possible match to all the events modelled in this report, including the other voltage events outlined in Section 5 and 6. Further tuning in future revisions of the model may be possible to produce a better match for this event.

Figure 138 Frequency – 31 January 2020 (VIC)

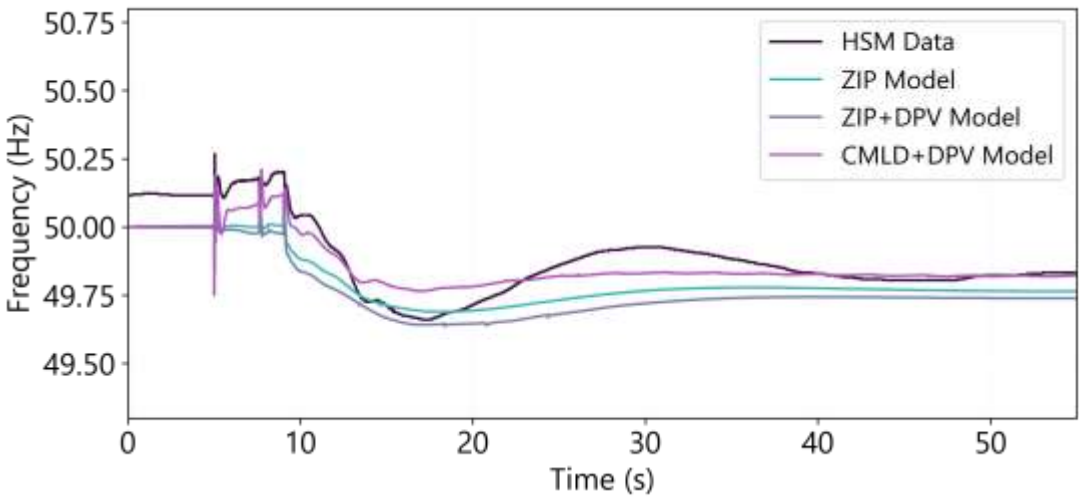

Voltage

Figure 139 shows the voltages at the 220 kV Rowville bus in the vicinity of the Melbourne metro region. Observations at this location are illustrative of the voltage response at most locations on the Victorian side of the separation[143].

In this disturbance, the CMLD+DPV model shows a slower voltage recovery profile that is similar to the HSM but shows voltage overshoot (although it remains within the normal range of 0.9pu to 1.1pu).

The steady-state voltage after the disturbance is comparable with observations for all models (measured at 60s, not shown).

Figure 139 Voltage – 31 January 2020 (VIC) – 220 kV Rowville bus

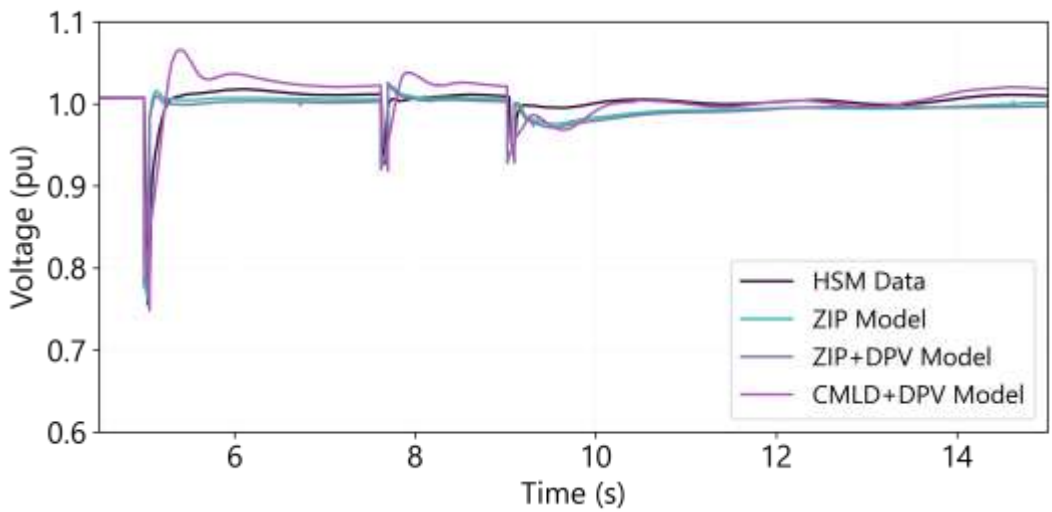

Active and reactive power flow

Figure 140 shows the active and reactive power measurements at the 500/220 kV ROTS Transformer 1 feeder (in the vicinity of the Melbourne metropolitan area). Observations at this location are illustrative of typical measurements recorded in this event.

Active power flows are somewhat underestimated by the CMLD+DPV model. This is likely related to the overestimation of load disconnection.

For reactive power flows, the trajectory measured on this feeder is accurately represented by all models, although the maximum peak reactive flows are overestimated by the CMLD+DPV model (at ~5 s) during the simulation period. As seen in **Figure 138**, this may be partially attributed to the overestimate of voltage overshoot that occurs following the HGTS-MLTS line trip. The post-fault line flows are underestimated, similar to the active power flows.

[143] HSM data is available at the following locations: 220 kV Altona, 220/66/22 kV Bendigo. 66/22 kV Brooklyn, 220 kV Cranbourne, 330 kV Dederang, 500/220 kV Hazelwood, 500/275 kV Heywood, 500 kV Loy Yang, 220 kV Mt Beauty, 330 kV Murray, 220 kV New Port, 220/66/22 kV Red Cliffs, 220 kV Rowville, 500/330 kV South Morang, 66 kV Templestowe, 220 kV Yallourn.

Steady-state active and reactive power (measured at 60s, not shown) is somewhat underestimated by the CMLD+DPV models.

Figure 140 Active/reactive power – 31 January 2020 (VIC) – 500/220 kV Rowville Transformer 1 Feeder

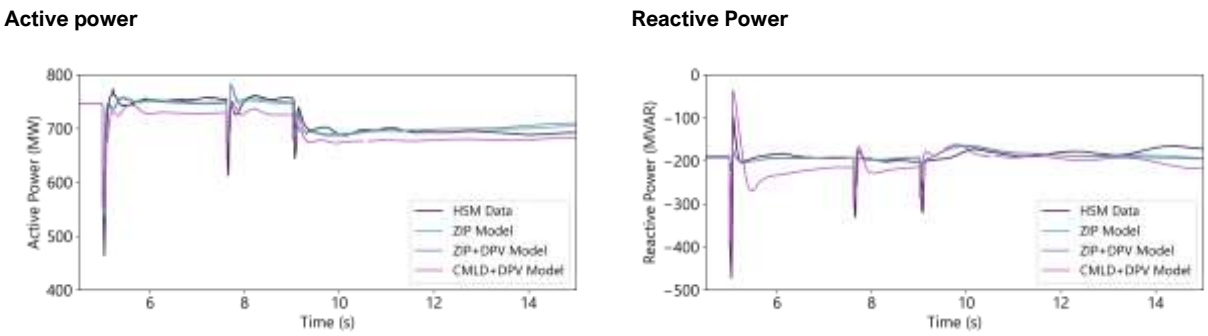

7.7.4 DPV measurements

Figure 141 shows the total measured DPV generation in Victoria (initial value estimated from ASEFS2, and the change post disturbance estimated from Solar Analytics datasets) compared with the performance of the CMLD+DPV model and the ZIP+DPV model.

Figure 141 DPV measurements (Solar Analytics) – 31 January 2020 (VIC)

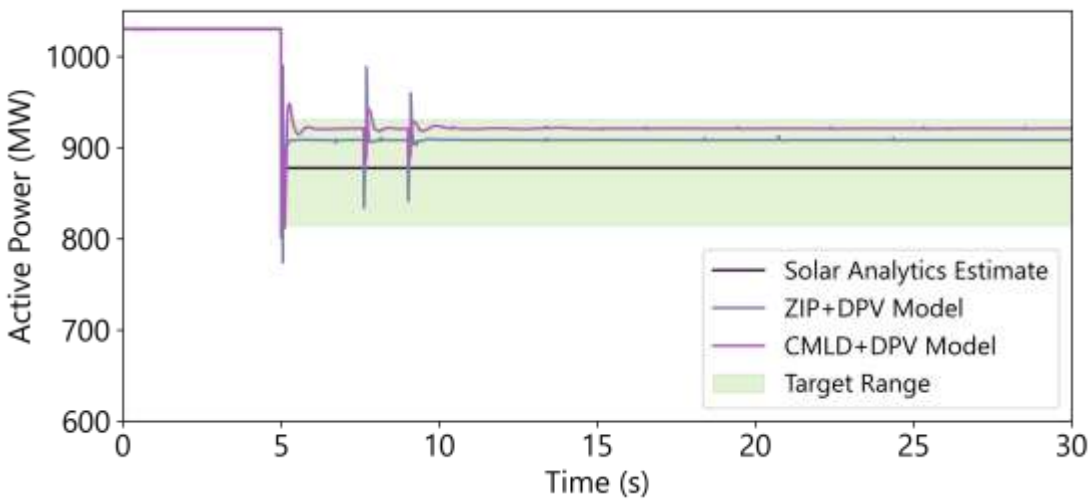

In the simulation of this event, the DPV response can be summarised as follows:

- DPV disconnection occurs at ~5 s due to the undervoltage event.
- Further DPV disconnection occurs in the ZIP+DPV case due to the lower frequency nadir falling below the first frequency tripping block 49.6 Hz)
- In this case, no DPV curtailment is observed, because frequency does not exceed 50.25Hz.

These behaviours are consistent with the model's design, aiming to replicate the available evidence on DPV behaviour during disturbances based on manufacturer surveys and field observations[144].

Table 94 summarises estimates from the Solar Analytics dataset of the proportion of inverters that demonstrated disconnection (suddenly dropping generation to close to zero and remaining close to zero for at least one minute).

Table 94 Summary of distributed PV behaviour – 31 January 2020 (VIC)

	Actuals (estimated)	CMLD+DPV prediction
DPV loss	153 MW (100 –216 MW) decrease	109 MW decrease (underestimates by 29%, within range)

7.7.5 Load measurements

Figure 142 shows the active power responses of each of the load components in the CMLD model, in aggregate across the region. The main responses are related to the disconnection of Motor C and power electronics loads, in response to the voltage dip experienced at many buses.

[144] AEMO (May 2021) Behaviour of distributed resources during power system disturbances. Available at https://aemo.com.au/-/media/files/initiatives/der/2021/capstone-report.pdf. See Section 3.

Figure 142 Active power responses of the CMLD load components – 31 January 2020 (VIC)

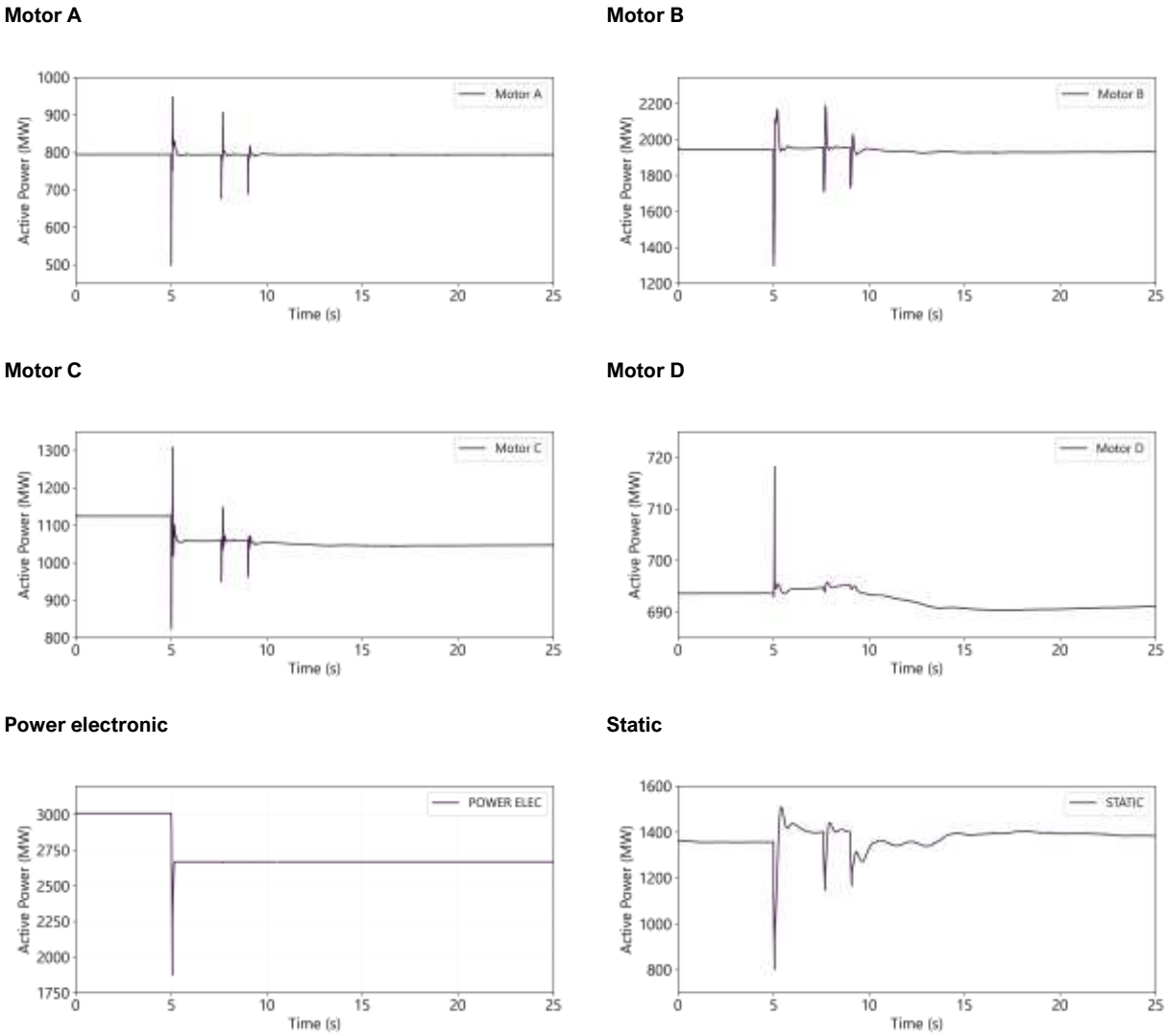

7.7.6 SCADA measurements

Figure 143 shows the total operational demand in Victoria (from SCADA) compared with the performance of the various models.

As shown in **Figure 143**, in this event, the post disturbance operational demand initially increased by ~200 MW, then declined sharply after ~20 s, followed by a relatively stable demand over the subsequent minutes. Given known inaccuracies in the SCADA data (for example, the potential for misalignment of time measurements when summing SCADA from generator terminals), it is unclear what change in operational demand really occurred in the fast timescales represented by the PSS®E model. The CMLD+DPV model was therefore tuned to match the load change measured at 64 s post disturbance (represented by the green dashed line in **Figure 143**), but it is acknowledged that there are significant inaccuracies in the SCADA measurement for this event.

Figure 143 Operational demand measurements (SCADA) – Victoria Total – 31 January 2020

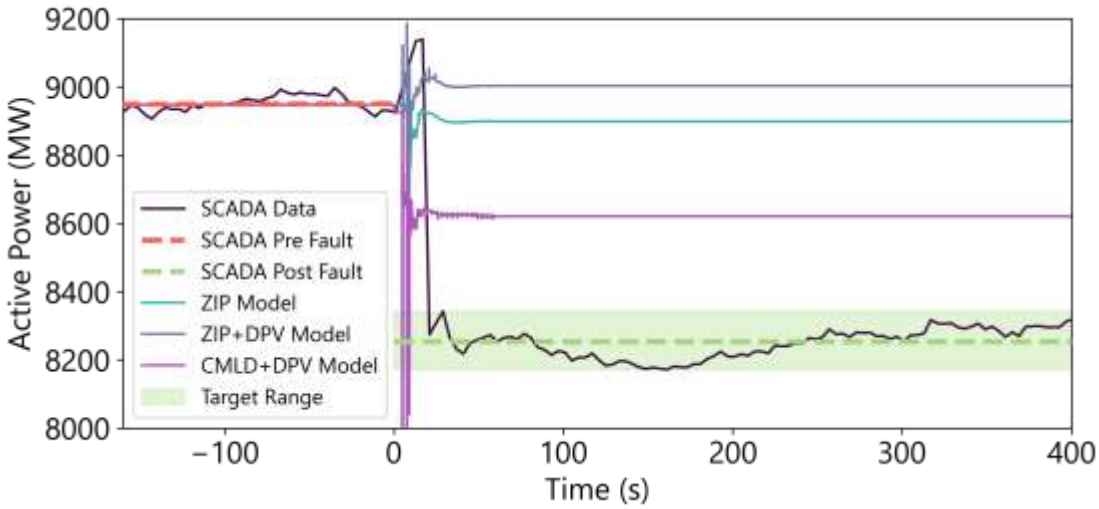

The operational demand measurement shown in Figure 143 is based on SCADA measurements which sum generation in Victoria, plus imports into Victoria (measured at the Heywood Interconnector for VIC-SA flows). In this event, the separation occurred in the Victorian network, and the Mortlake Power Station (MOPS) generating units and the APD aluminium smelter remained connected to the South Australia region but disconnected from the rest of Victoria. Both potlines at APD tripped (connected to the South Australian extended island). This trip of load at APD appeared as a reduction in operational demand in the VIC SCADA load measurement since it affects flows on the Heywood Interconnector. The observed 704 MW reduction in operational demand measured in the SCADA for VIC is therefore partly attributable to the 450 MW APD trip. The remaining reduction of 254 MW is attributable to changes in operational demand in VIC. Accounting for the estimated 153 MW reduction in DPV generation, it is then estimated that underlying load reduced by approximately 407 MW in this event. This is consistent with observations in other disturbances featuring similar voltage dips (as outlined in Section 5 and Section 6).

For comparison, the CMLD model predicts underlying demand decreasing by 421 MW. This is close to the estimated actual value of 407 MW. In contrast, the ZIP model cannot represent load disconnection behaviour, and underestimates the observed change in load considerably.

These estimates are summarised in **Table 95**.

Table 95 Summary of change in demand and distributed PV – 31 January 2020 (VIC)

	Including APD load trip		APD Load trip (MW)		Excluding APD load trip		
	Actuals	CMLD+DPV prediction	Actuals	CMLD +DPV	Actuals	CMLD+DPV prediction	ZIP+DPV prediction
Change in distributed PV generation (estimated from Solar Analytics sample)	153 MW (100 –216 MW) decrease	109 MW decrease (within range)	N/A	N/A	153 MW (100 –216 MW) decrease	109 MW decrease (within range)	121 MW decrease (within range)

	Including APD load trip		APD Load trip (MW)		Excluding APD load trip		
Change in operational demand (estimated from SCADA, 60s post disturbance)	704 MW (615 –786 MW) decrease	312 MW decrease (out of range)	450 MW (APD trip on SA side is accounted for in VIC SCADA)	0 (APD trip is on SA side, not modelled)	254 MW decrease (165 – 336 MW) decrease	312 MW decrease (within range)	56 MW increase
Change in underlying demand (estimated from SCADA & Solar Analytics)	857 MW (715 –1,002 MW) decrease	421 MW decrease (out of range)	450 MW	0	407 MW (265 MW – 552 MW) decrease	421 MW decrease (within range)	65 MW decrease

7.7.7 Assessment of model performance

Table 96 provides a summary of the performance of the CMLD+DPV models.

Table 96 Assessment of model performance – 31 January 2020 (VIC)

Quantity	Characteristic	CMLD + DPV estimates	CMLD+DPV model equal (✓) or better (✓✓) than ZIP?	Commentary
Frequency	During dynamic state	Fair match	✓	CMLD+DPV matches the overall trajectory but misrepresents zenith and nadir.
	Steady-state post disturbance	Fair match	✓✓	CMLD+DPV recovers to the normal operating range for the simulated time.
Voltages	During dynamic state	Fair match	✗	CMLD+DPV overestimates peak voltage overshoot magnitude but stays within the normal operating range in line with observations.
	Steady-state post disturbance	Good match	✓	CMLD+DPV aligned with HSM
Active power	During dynamic state	Fair match	✗	CMLD+DPV has a similar trajectory to the HSM, although it somewhat underestimates peak minimum and post-fault flows following the initial disturbance.
	Steady-state post disturbance	Good match	✓✓	CMLD+DPV trajectory aligned with HSM but underestimates steady-state flows.
Reactive power	During dynamic state	Fair match	✓	CMLD+DPV has a similar trajectory to the HSM, although it somewhat overestimates peak minimum flows and underestimates post-fault flows.
	Steady-state post disturbance	Fair match	✗	CMLD+DPV trajectory aligned with HSM slightly underestimates steady-state flows.
DPV	DPV total	Fair match	✓✓	Estimated actuals: 153 MW decrease DPV: 109 MW decrease The DPV model underestimates DPV reduction by 29%, but is within range.
Load	Underlying load change	Good match	✓✓	Estimated actuals: 407 MW decrease (64 s post disturbance) CMLD: 421 MW decrease The CMLD overestimates load disconnection by 3% when measured at 64 s post disturbance, but is within range.

Quantity	Characteristic	CMLD + DPV estimates	CMLD+DPV model equal (✓) or better (✓✓) than ZIP?	Commentary
Operational demand	Net load change	Fair match	✓✓	SCADA: 254 MW decrease (64 s post disturbance) CMLD+DPV: 312 MW decrease The CMLD+DPV model overestimates net load change by 23%, but is within range.

8 Summary of combined model performance

8.1 Performance for voltage disturbances

8.1.1 High speed dynamics – voltage disturbances

Assessment criteria

The CMLD model performance is compared against the performance of the existing ZIP load model (without DPV) as follows:

✓✓	CMLD+DPV models align with observed data *significantly better* than the ZIP model
✓	CMLD+DPV models align with observed data *at least as well* as the ZIP model
✗	CMLD+DPV models align with observed data *less well* than the ZIP model

The objective is to assess whether the CMLD+DPV model represents a general improvement over the existing ZIP load model.

The overall performance of the CMLD+DPV models is also assessed directly against the HSM data as follows:

Green	CMLD+DPV provides a *good match* to observed data
Yellow	CMLD+DPV provides a *fair match* to observed data
Red	CMLD+DPV provides a *poor match* to observed data

This second measure aims to capture cases where the CMLD+DER model may represent an improvement over the existing ZIP model but still does not provide a good match against the HSM data (and vice versa).

Model performance

Table 80 summarises the performance of the CMLD+DPV models for each of the voltage disturbances for various dynamic characteristics.

As can be seen in Table 80, for most events and most dynamic characteristics the CMLD+DPV models perform as well or better than the existing ZIP model. In most cases, CMLD+DPV is significantly better at replicating voltage recovery rates post disturbance, steady state active power post disturbance, and reactive power measurements during the dynamic state. Only a few select characteristics in a few disturbances are captured less well by CMLD+DPV than the ZIP model. In most of these cases, the CMLD+DPV still provides a fair match to the HSM. Refer to sections 5, 6 and 7 for further details on each specific case.

In several events, mismatch with HSM was observed in both the CMLD model as well as the existing ZIP model. Since this is observed for both load models, it is attributed to mismatch of the representation of the network in PSS®E or the lack of an applied smoothing constant in the simulation output data to replicate the sampling rate (20ms) of HSM data, rather than the load models themselves.

Table 97 Voltage events – comparing CMLD+DPV model performance against HSM and existing ZIP model

		Events with minimal DPV generation (CMLD)					Events with significant DPV generation (CMLD+DPV)						
		8/03/18	11/04/18	18/02/19	17/04/19	22/02/21	3/03/17	18/01/18	9/10/18	3/03/19	26/11/19	24/01/21	12/03/21
Voltages	**Voltage overshoot**	✓	X	✓	✓✓	✓✓	X	X	✓✓	✓	✓✓	✓	✓
	Voltage recovery rate	X	✓✓	✓	✓✓	✓✓	✓✓	✓✓	✓	✓	✓✓	✓✓	✓✓
	Steady state post disturbance	✓	✓	✓	✓	✓	✓	✓✓	✓	✓	✓	✓	✓
Active power	**During dynamic state**	✓	✓	✓	✓	✓✓	✓	✓✓	✓✓	✓	✓	✓	✓
	Steady state post disturbance	✓✓	✓✓	✓	✓✓	✓✓	✓	✓✓	✓	✓	✓	✓✓	✓✓
Reactive power	**During dynamic state**	✓✓	✓✓	✓	✓	✓✓	-	✓✓	✓✓	✓	✓✓	✓	✓
	Steady state post disturbance	✓	✓	✓	✓	✓✓	-	✓✓	✓	✓	✓	✓✓	✓

8.1.2 DPV loss in voltage disturbances

Table 98 summarises the performance of the DPV model in representing total DPV loss in a region following voltage disturbances. Colour coding illustrates the accuracy of the model as follows:

Green	CMLD+DPV is *accurate*, predicting loss to within ±15%
Yellow	CMLD+DPV is less accurate, but remains *within (or ±10% outside) the uncertainty range*
Red	CMLD+DPV estimates loss *outside the predicted range*

The DPV model reproduces observed DPV loss following voltage disturbances very accurately in four out of seven cases, including two cases where the model accurately predicts minimal DPV loss. Of the remaining cases:

- In three cases (18/01/2018, 12/03/2021, and 26/11/2019), the DPV model underestimates DPV loss by 25%, overestimates by 33%, and underestimates by 21%, respectively.
- In all cases, the DPV loss estimate in PSS®E is considered to adequately represent DPV loss as it is within the uncertainty range of the field measurements available.

In general, these validation studies indicate that the DPV model provides a reasonably accurate representation of DPV loss following voltage disturbances, although it may over or under-estimate the DPV loss by up to ±33%. In cases where minimal DPV loss is expected, this is accurately represented by the model.

The DPV model represents a considerable improvement over the existing models (ZIP model with DPV represented as negative load), since the existing ZIP model approach cannot replicate any DPV loss.

A large proportion of the uncertainty in the model DPV loss estimates is related to uncertainty in the original field measurements used to calibrate the model, which is considerable. This means that the potential for further improvement in the DPV model's ability to accurately represent DPV loss following voltage disturbances is limited by the accuracy of the estimates of DPV loss in field events. AEMO has established a work program collaborating

with UNSW Sydney and other partners to develop improved datasets and tools for estimating DPV loss in disturbances, which will provide further potential for improving the DPV model performance over time[145]. The latest version of AS/NZS4777.2:2020 (applicable from December 2021) aims to standardise DPV tripping and curtailment behaviour. This may ease the difficulty of tuning the DPV model in future as more inverters are installed under this standard.

Table 98 DPV model performance for voltage disturbances – events with significant DPV

Event	State	Actual DPV Loss (MW)*	DPV model estimate of DPV loss (MW)	DPV model percentage of observed (central estimate)	DPV model difference to central estimate (MW)
3/03/2017	SA	130 (43 – 253)	151	113% Within observed range	+15 MW
18/01/2018	VIC	123 (57 – 218)	92	75% Within observed range	-35 MW
9/10/2018	QLD	2 (1 – 3)	2	Accurately estimates minimal loss	-1 MW
03/03/2019	VIC	6 (3 – 19)	0	Accurately estimates minimal loss	-6 MW
26/11/2019	QLD	299 (218 – 418)	237	79% Marginally below observed range	-83 MW
24/01/2021	SA	113 (68 – 135)	104	90% Within observed range	-16 MW
12/03/2021	SA	72 (49 – 103)	98	133% Within observed range	+23 MW

*Actual DPV loss values are estimated from Solar Analytics sample datasets[146]. Ranges shown are for a 95% confidence interval, based on the Solar Analytics sample size compared with the installed population size. Ranges are smaller for more recent events due to the larger sample size available.

8.1.3 Load loss in voltage disturbances

This section summarises the performance of the CMLD model in representing load loss following voltage disturbances. The colour scheme is the same as that in Section 8.1.2.

Table 99 shows performance of the CMLD model for disturbances with minimal DPV generation. Events with significant DPV generation are summarised in **Table 100**. In Table 100, the overall performance of the CMLD+DPV model is assessed against the SCADA measurements (net load change), as well as against the estimate of load change alone (excluding changes in DPV).

In eight out of 12 cases the CMLD model accurately predicts load loss, within ±15% of the central estimate. In three cases (03/03/2017, 09/10/2018 and 24/01/2021), the CMLD model predicts load loss within ±20% and within or just outside of the uncertainty range. In one case, the CMLD model is clearly outside of the uncertainty range.

[145] UNSW Sydney, Project MATCH – Monitoring and Analysis Toolbox for Compliance in a High DER future, http://www.ceem.unsw.edu.au/project-match, and Australian Government – Australian Renewable Energy Agency (ARENA) – Project MATCH, https://arena.gov.au/projects/project-match/.

[146] AEMO (May 2021) Behaviour of distributed resources during power system disturbances. See Appendix. Available: https://aemo.com.au/-/media/files/initiatives/der/2021/capstone-report.pdf.

When considering the net load change, the CMLD (for night-time cases) and CMLD+DPV (day-time cases) is reasonably accurate (within ±15%) in eight out of twelve cases. In two cases, the models are within ±20% of the actuals estimates. In two cases, the models are less than the observed range.

In all cases, the CMLD model represents a considerable improvement over the existing ZIP model, which cannot replicate load loss.

Table 99 CMLD performance for load loss for voltage events with minimal DPV generation

Event	State	Projected underlying load change (MW)*	CMLD model loss (MW)	CMLD model % of observed (central estimate)	CMLD model difference to central estimate (MW)
8/03/2018	VIC	243 (155 – 300)	254	105% Within observed range	+11 MW
11/04/2018	SA	144 (100 – 144)	151	105% Within observed range	+7 MW
18/02/2019	VIC	100 (72 – 111)	98	98% Within observed range	-2 MW
17/04/2019	SA	127 (110 – 132)	111	88% Within observed range	-16 MW
22/02/2021	QLD	533 (418 – 584)	485	91% Within observed range	-48 MW

* Actual change in net load is estimated from four second SCADA data, which has known inaccuracies. Ranges are estimated from the range of SCADA estimates observed in the relevant 1-2 minutes before and after the event.

Table 100 CMLD performance for load loss for voltage events with significant DPV generation

		Performance of CMLD + DPV combined				Performance of CMLD alone			
Event	State	Actual operational demand change (MW)*	CMLD+DPV model loss	CMLD+DPV % of observed (central estimate)	CMLD+DPV model difference to central estimate (MW)	Underlying Demand Change (SCADA + Solar) (MW)	CMLD model loss (MW)	CMLD percentage of observed (central estimate)	CMLD model difference to central estimate (MW)
3/03/2017	SA	280 (269 – 428)	185	66% Less than observed range	-95 MW	412 (312 – 681)	336	81% Within observed range	-76 MW
18/01/2018	VIC	506 (450 – 598)	560	111% Within observed range	+54 MW	629 (507 – 815)	652	104% Within observed range	+23 MW
9/10/2018	QLD	190 (173 – 238)	154	81% Marginally less than observed range	-36 MW	192 (173 – 241)	156	82% Marginally less than observed range	-36 MW
03/03/2019	VIC	-11 (-23 – 8)	-1	Accurately estimates minimal loss	+10 MW	-5 (-20 – 27)	-1	Accurately estimates minimal loss	+4 MW
26/11/2019	QLD	330 (213 – 330)	369	112% Marginally above observed range	+39 MW	629 (431 – 748)	607	96% Within observed range	-22 MW
24/01/2021	SA	225 (211 – 280)	175	78% Less than observed range	-50 MW	340 (279 – 415)	279	82% Within observed range	-61 MW

		Performance of CMLD + DPV combined				Performance of CMLD alone			
12/03/2021	SA	96 (42 – 96)	115	120% Above observed range	+19 MW	170 (91 – 199)	213	125% Above observed range	+43 MW

* Actual change in net load + DPV is estimated from four second SCADA data, which has known inaccuracies. Ranges are estimated from the range of SCADA estimates observed in the relevant 1-2 minutes before and after the event.

One of the main limitations of the CMLD model is the ability to represent the load characteristics in the minutes following a voltage disturbance. Several events in the validation studies show load behaviour in this slower period which are not well represented by the CMLD model and could have implications for power system studies. Possible improvements can be considered in future model revisions.

The limited measurements available from field disturbances also limits the ability to accurately tune the CMLD model. This model development process has relied heavily on four second SCADA data which has known inaccuracies. High speed measurements from a larger number of network locations with large quantities of load in a radial network configuration would significantly assist future revisions of the model.

8.1.4 Estimating total contingency sizes for voltage disturbances

Figure 144 and **Figure 145** show pictorial representations of the model performance in representing load and DPV loss for each of the 12 historical voltage disturbances, both in percentage terms and absolute MW terms. For many power system security studies, one of the most important factors will be the net difference between the DPV and load loss estimates, which produces the net total contingency size that impacts the power system.

Figure 144 Model performance for load/DPV loss across voltage disturbances

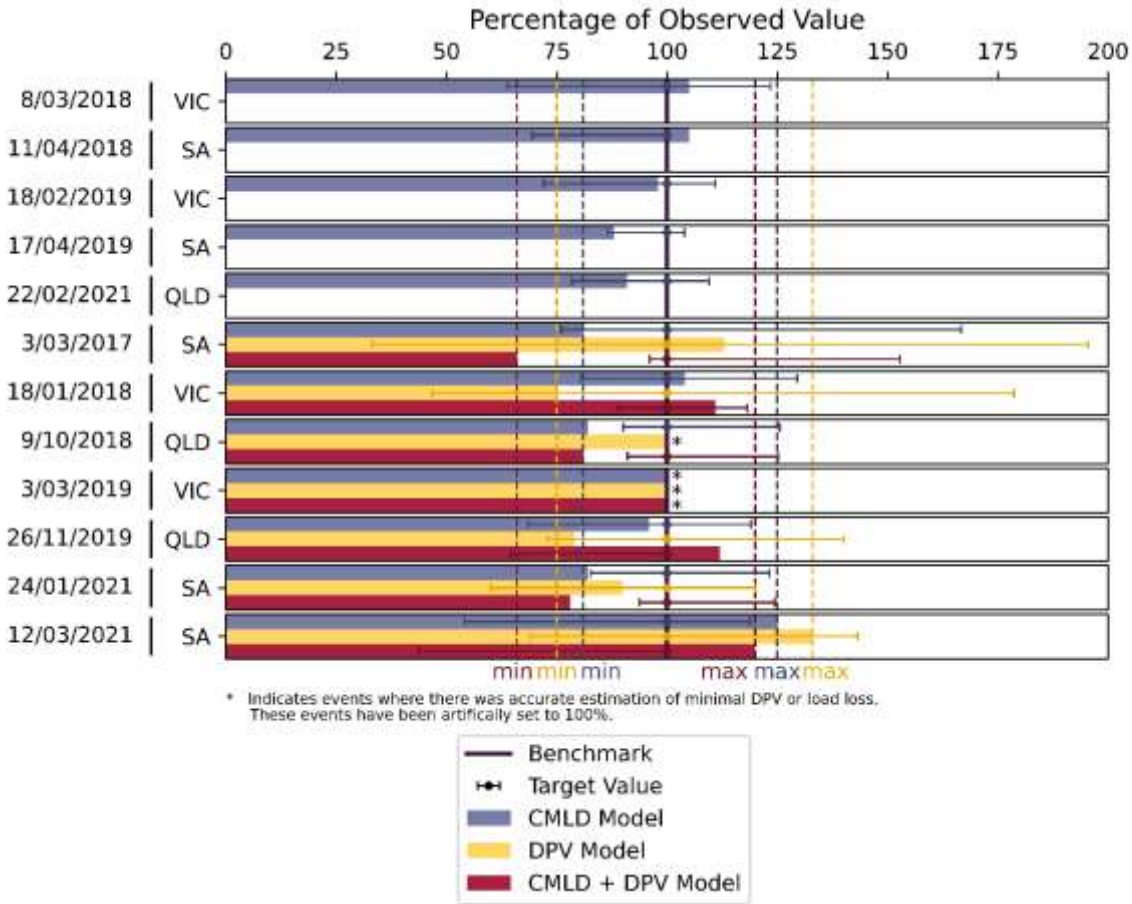

In Figure 144, the target value is 100% of the observed value, and the degree to which the models under- or over-estimate the target value is indicated. The night-time cases (CMLD only) are shown at the top, and the daytime cases (CMLD+DPV) are shown at the bottom. Blue bars indicate the load change predicted by the CMLD model, yellow bars indicate the DPV change predicted by the DPV model, and the red bars indicate the total net contingency size predicted by both models combined. Dashed lines indicate the minimum and maximum outliers for each model, across all cases.

Both the CMLD and DPV models have been tuned to produce minimal bias across the set of validation cases, such that errors fall equally above and below the target values. This is intended to produce models that are as close as possible to the central estimate.

Figure 145 provides a slightly different representation, indicating the accuracy of the models in representing load and DPV loss in absolute MW terms. The target values are indicated with dots, with error bars indicating the uncertainty in the actuals estimates. In most cases, the models predict load and DPV loss to within the uncertainty in the actuals estimates. The models are effective at distinguishing between cases with significant load/DPV loss, and those with minimal load/DPV loss.

Figure 145 Model performance for load/DPV loss across voltage disturbances

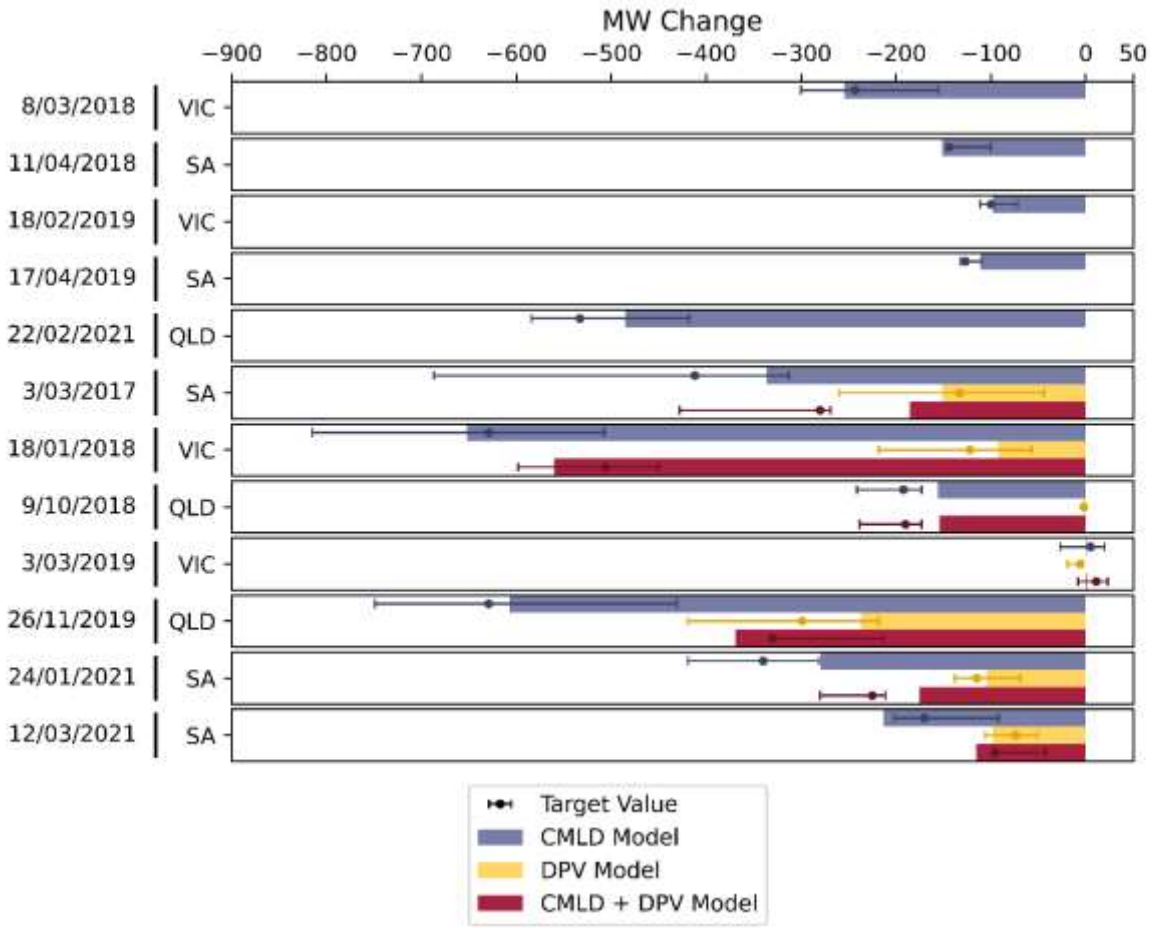

In some cases, the CMLD and DPV models show errors in the same direction (both over-predict or under-predict DPV and load loss simultaneously), for example, as seen for 24/01/2021. This will tend to lead to a reduction in overall error in the predicted total contingency size (the errors offset each other to some degree). In other cases, the CMLD and DPV models show errors in opposing directions (one model over-predicts load/DPV loss, while the other model under-predicts) (for example, 3 March 2017). In these cases, the errors sum. This indicates that although the CMLD and DPV models represent a significant improvement from the existing ZIP model approach, they do demonstrate uncertainty (in both directions from the central estimate), which should be accounted for in power system studies, and in any actions taken based on those studies.

These models may over-represent or under-represent risks, and it is not possible to determine which direction the error applies for any particular study. The models have been tuned to provide the best possible central estimate of observed behaviours. AEMO expects that appropriate engineering judgement be used in the application of these models.

Table 101 shows the estimated error in the DPV and load loss estimates for the CMLD and DPV models, based on the widest range of observed error across the validation studies. The errors observed from the validation cases with the combined models are also shown. This suggests that for any dynamic voltage disturbance studies

performed using the CMLD+DPV models, a possible uncertainty in the net contingency size of approximately ±30% (-34% / +20%) of the total contingency size should be assumed.

Table 101 Error observed for CMLD and DPV models in voltage disturbances

	CMLD (% of total load loss in a region)	DPV (% of total DPV loss in a region)	CMLD+DPV (% of total load + DPV loss in a region)
Error range	-19% / +25%	-25% / +33%	-34% / +20%

8.2 Performance for frequency disturbances

8.2.1 High speed dynamics – frequency disturbances

Table 102 summarises the performance of the CMLD+DPV models for each of the frequency disturbances for various dynamic characteristics. Model performance assessment criteria are as indicated in Section 8.1.1.

Table 102 Dynamic behaviour for frequency events – comparing CMLD+DPV vs existing ZIP model and HSM

		25/08/2018				16/11/2019	31/01/2020	
		SA	QLD	VIC	NSW	SA	SA	VIC
Frequency	During dynamic state	✓✓	✓	✓	✓	✓✓	✓✓	✓
	Steady-state post disturbance	✓	X	✓	✓	✓✓	✓✓	✓✓
Voltages	*During dynamic state*	✓	✓	✓	✓	✓	✓✓	X
	Steady-state post disturbance	✓	✓	✓	✓	✓	✓	✓
Active power	*During dynamic state*	✓	✓	✓	✓	✓	✓	X
	Steady state post disturbance	✓	✓✓	✓	✓✓	✓	✓	✓✓
Reactive power	*During dynamic state*	✓	✓	✓	✓	✓	✓	X
	Steady state post disturbance	✓	✓	✓	✓	✓	✓✓	✓

The CMLD+DPV models perform as well or better than the existing ZIP model in almost all cases and provide a fair or good representation of the HSM data in most cases. For 25/08/2018 QLD, the CMLD+DPV model doesn't represent steady state frequency as well as the existing ZIP model, but it is only misrepresented by 0.15Hz (The HSM indicates a steady state frequency of 50.7 Hz which is well reproduced by the ZIP model, while the CMLD+DPV model settles at 50.55 Hz).

8.2.2 DPV change in frequency disturbances

Table 103 summarises the performance of the DPV model in representing DPV loss in frequency disturbances. Colour coding illustrates the accuracy of the model as follows:

Green	CMLD+DPV is very accurate, predicting loss to within ±25 MW
Yellow	CMLD+DPV is less accurate, but remains within the uncertainty range, or within ±10 MW of the bounds of the uncertainty range

Red	CMLD+DPV estimates loss >10 MW outside the predicted range

In six out of seven frequency disturbances, the DPV loss is accurately estimated (within ±25 MW). In one disturbance (31/01/2020 VIC), the DPV loss is less accurate and just outside the uncertainty range.

Table 103 DPV model performance for DPV loss in under-frequency disturbances

Event	State	Disturbance Type	Actual DPV loss (MW)*	DPV model estimate of DPV loss (MW)	DPV model percentage of observed (central estimate)	DPV model difference to central estimate
25/08/2018	VIC	Under-frequency	123 (48 – 238)	139	113% Within range	+16 MW
	NSW	Under-frequency	89 (60 – 125)	68	76% Within range	-21 MW
31/01/2020	VIC	Under-frequency	153 (100 – 216)	109	71% Within range	-44 MW
25/08/2018	SA	Under/Over-frequency	71 (38 – 122)	55	77% Within range	-16 MW
	QLD	Over-frequency	143 (90-230)	137	96% Within range	-6 MW
16/11/2019	SA	Over-frequency	36 (24-47)	26	72% Within range	-8 MW
31/01/2020	SA	Over-frequency	113 (81-153)	89	79% Within range	-24 MW

* Actual DPV loss values are estimated from Solar Analytics sample datasets[147]. Ranges shown are for a 95% confidence interval, based on the Solar Analytics sample size compared with the installed population size. Ranges are smaller for more recent events due to the larger sample size available.

Table 104 summarises the performance of the DPV model in representing DPV disconnection versus controlled curtailment in over-frequency disturbances (a breakdown is not provided for under-frequency disturbances because controlled curtailment behaviour is not observed during under-frequency events). In three of the four over-frequency disturbances where DPV curtailment was observed, the curtailment is accurately estimated by the DPV model. In the fourth case (25/08/2018 QLD) DPV curtailment is underestimated, just outside the uncertainty range.

[147] AEMO (May 2021) Behaviour of distributed resources during power system disturbances, https://aemo.com.au/-/media/files/initiatives/der/2021/capstone-report.pdf.

Table 104 DPV model performance for DPV curtailment and disconnection in over-frequency disturbances

Event	State	Disturbance type	DPV disconnection				DPV controlled curtailment			
			Actual DPV disconnection (MW)*	DPV model estimate of DPV disconnection (MW)	DPV model percentage of observed (central estimate)	DPV model difference to central estimate	Actual DPV curtailment (MW)	DPV model estimate of curtailment (MW)	DPV model percentage of observed (central estimate)	DPV model difference to central estimate
25/08/2018	SA	Under/Over-frequency	64 (31 – 112)	46	72% Within range	-18 MW	8 (6 – 9)	9	Accurately estimates minimal loss	+1 MW
	QLD	Over-frequency	90 (43 – 169)	99	110% Within range	+9 MW	54 (47 – 60)	38	72% Outside of range	-16 MW
16/11/2019	SA	Over-frequency	27 (18 – 37)	17	63% Within range	-10 MW	9 (7-10)	10	Accurately estimates minimal loss	+1 MW
31/01/2020	SA	Over-frequency	76 (52 – 109)	57	75% Within range	-19 MW	37 (29 – 43)	32	87% Within range	-5 MW

* Actual DPV loss values are estimated from Solar Analytics sample datasets[148]. Ranges shown are for a 95% confidence interval, based on the Solar Analytics sample size compared with the installed population size. Ranges are smaller for more recent events due to the larger sample size available.

8.2.3 Load change in frequency disturbances

Table 105 and **Table 106** summarises the performance of the CMLD load model in estimating the change in load for under-frequency and over-frequency disturbances, respectively. Change in load due to UFLS trip has been excluded to focus on the performance of the CMLD model alone. Colour coding illustrates the accuracy of the model as outlined in Section 0 above.

In all cases, the CMLD model reproduces estimated actual load change to within the uncertainty margin in the actuals estimates.

The final column indicates the performance of the CMLD model in reproducing the estimated actual change in load, compared with the performance of the ZIP model, with assessment criteria as indicated in Section 0. In all cases, the CMLD model provides as good or better representation of the change in load during frequency disturbances, compared with the existing ZIP model.

[148] AEMO (May 2021) Behaviour of distributed resources during power system disturbances, https://aemo.com.au/-/media/files/initiatives/der/2021/capstone-report.pdf.

Table 105 CMLD model performance for underlying load behaviour in under-frequency disturbances (excluding UFLS trip)

Event	State	Disturbance type	CMLD load change				
			Actual underlying load change – excluding UFLS trip (MW)	CMLD model estimate (MW)	CMLD percentage of observed (central estimate)	CMLD model difference to central estimate	Comparison to ZIP model
25/08/2018	VIC	Under-frequency	70 (-91 to 245)	-22	Accurately estimates minimal load change	-92 MW	✓✓
	NSW	Under-frequency	18 (-59 to 197)	-16	Accurately estimates minimal load change	-34 MW	✓✓
31/01/2020	VIC	Under-frequency	407 (265 to 552)	421	103% Within range	+14 MW	✓✓

Table 106 CMLD model performance for underlying load behaviour in over-frequency disturbances (excluding UFLS trip)

Event	State	Disturbance type	CMLD load change				
			Actual underlying load change – excluding UFLS trip (MW)	CMLD model estimate (MW)	CMLD percentage of observed (central estimate)	CMLD model difference to central estimate	Comparison to ZIP model
25/08/2018	SA	Under/Over-frequency	-2 (-97 to 113)	-7	Accurately estimates minimal load change	+5 MW	✓✓
	QLD	Over-frequency	-53 MW (-117 to 152)	-73	138% Within range	-20 MW	✓✓
16/11/2019	SA	Over-frequency	22 (-5 to 47)	-11	Accurately estimates minimal load change	-33 MW	✓
31/01/2020	SA	Over-frequency	-167 (-255 to 35)	-127	76% Within range	+40 MW	✓

8.2.4 Estimating total contingency sizes for frequency disturbances

Table 107 and **Table 108** indicates the combined model performance for under-frequency and over-frequency disturbances, respectively. Colour coding illustrates the accuracy of the model as shown in 0.

For under-frequency disturbances, in one out of three cases, the model predicts net load change within the observed range. In one case (25/08/2018 VIC) the model predicts net load change just outside of the observed range. In this case, the error from the CMLD model (-92 MW) compounds with the error from the DPV model (-16 MW), resulting in a relatively large error (~-107 MW) for the net contingency size.

For over-frequency disturbances, in three out of four cases the CMLD+DPV models accurately estimates net load change to within the uncertainty margin in the actuals data. In one case (25/08/2018 QLD) the model predicts net load change just outside of the observed range.

Table 107 CMLD and DPV model performance for under-frequency disturbances (excluding UFLS trip)

Event	State	Disturbance type	Actual operational demand change (MW) – excluding UFLS trip	CMLD+DPV model estimate (MW)	CMLD+DPV percentage of observed (central estimate)	CMLD+DPV difference to central estimate (MW)
25/08/2018	VIC	Under-frequency	-53 (-139 to 7)	-160	300% Marginally outside of range	-107 MW
	NSW	Under-frequency	-70 (-118 to 72)	-84	117% Within observed range	-14 MW
31/01/2020	VIC	Under-frequency	254 (165 to 336)	312	123% Within observed range	+58 MW

Table 108 CMLD and DPV model performance for over-frequency disturbances (excluding UFLS trip)

Event	State	Disturbance type	Actual operational demand change (MW) – excluding UFLS trip	CMLD+DPV model estimate (MW)	CMLD+DPV percentage of observed (central estimate)	CMLD+DPV difference to central estimate (MW)
25/08/2018	SA	Under/Over-frequency	-74 (-135 to -8)	-61	87% Within observed range	+13 MW
	QLD	Over-frequency	-196 (-206 to -77)	-211	107% Marginally outside of range	-15 MW
16/11/2019	SA	Over-frequency	-14 (-29 to 0)	-37	Accurately estimates minimal loss	-23 MW
31/01/2020	SA	Over-frequency	-280 (-334 to -114)	-216	77% Within observed range	+64 MW

Table 109 shows the estimated error observed from the validation cases with the combined models.

Table 109 Error range observed for CMLD+DPV in frequency disturbances (excluding UFLS trip)

Quantity	CMLD (MW error per region)	DPV (MW error per region)	CMLD+DPV (MW error per region)
Under-frequency	-92 / +14	-44 / +16	-107 / +58
Over-frequency	-33 / +40	-24 / -6	-23 / +64

Figure 146 shows a pictorial representation of the model performance in representing load and DPV change for the historical frequency disturbances. In almost all cases, DPV and load change, and the total net contingency size, are predicted to within the uncertainty range of the actuals estimates. The direction of the change is also well predicted by the models in each case. The models distinguish well between cases with very large changes in load and DPV (such as 31/01/2020 SA and 31/01/2020 VIC) and cases with very small changes in load and DPV (such as 16/11/2019 SA and 25/08/2018 SA).

Figure 146 Model performance for load/DPV change for frequency disturbances (actual MW change)

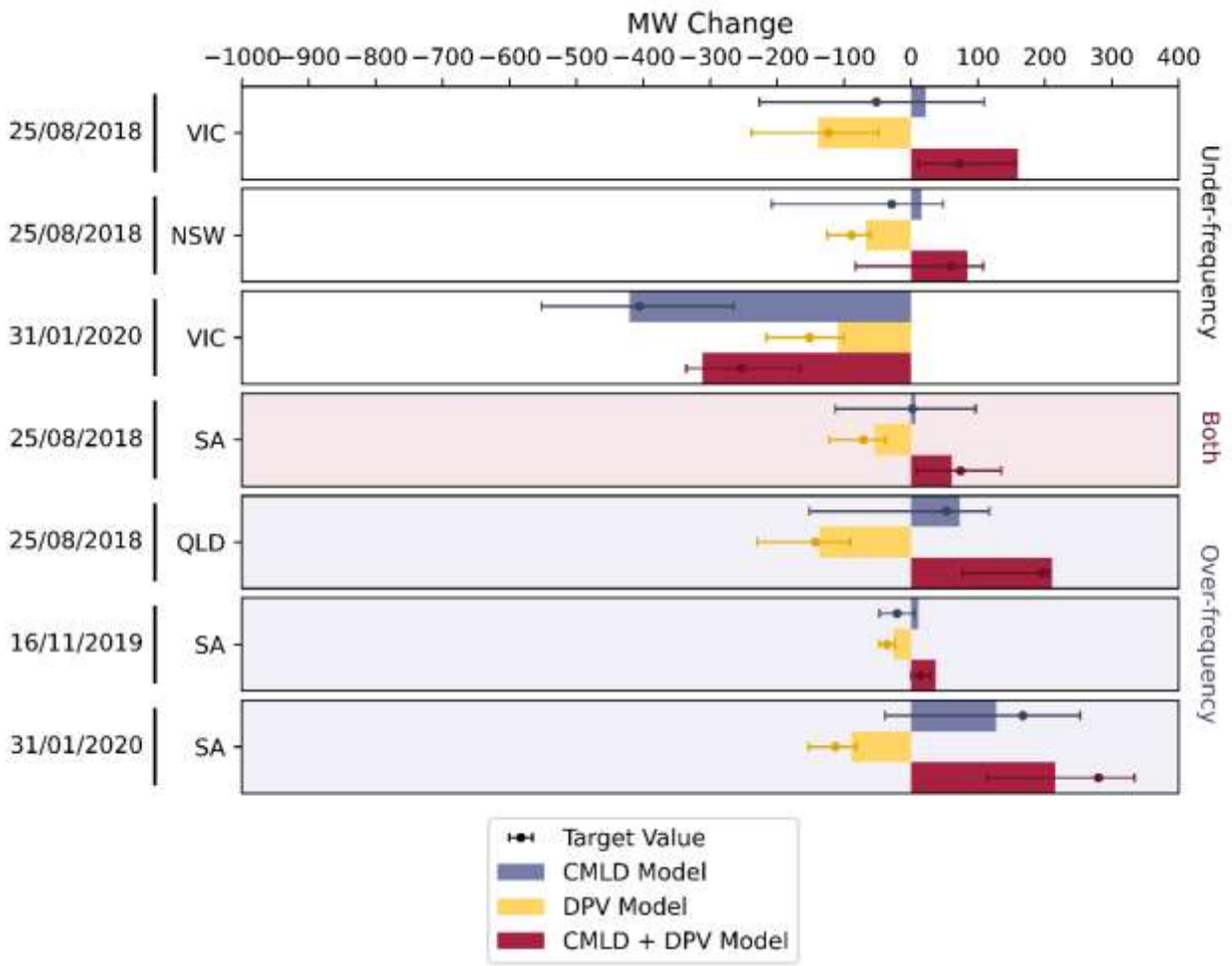

The frequency validation studies show that the CMLD and DPV models represent a significant improvement from the existing ZIP model approach. However, they do demonstrate some uncertainty (in both directions from the central estimate), which should be accounted for in power system studies and in any actions taken based on those studies.

These models may over-represent or under-represent risks, and it is not possible to determine which direction the error applies for any particular study. The models have been tuned to provide the best possible central estimate of observed behaviours. AEMO expects that appropriate engineering judgement be used in the application of these models.

9 Further improvements to load and DER models

The development of the models presented in this report represents only the first step in continuing improvement in the DER and load models utilised by AEMO, NSPs, and others. As the power system evolves, constant updates and improvements to these models are required. New data sources and evidence will also continue to become available, allowing further improvements.

This section therefore provides a summary of the further work that would improve the performance, validation and use of the load and DPV models, to inform future work in this area. Improvements are outlined in these broad categories:

- Development of suitable DPV and load models in other platforms utilised by AEMO, including PSCAD and PowerFactory.
- Avenues for future improvement to the DPV model.
- Avenues for future improvement to the CMLD model.
- Representation of under frequency load shedding and other control schemes.
- Improvements to the model validation process.
- Improvements to the deployment of models.
- Development of suitable models for other types of DER as they become prominent, such as distributed batteries, electric vehicles, and others.

9.1 EMT model development (underway)

In bench testing, UNSW observed that some DPV inverters disconnect in response to phase angle jumps[149]. It is challenging to develop an accurate PSS®E representation of the response of DPV to sub-cycle phenomena such as grid voltage phase-angle jumps because the PSS®E software applies steady-state phasor-analysis of positive sequence voltage components only. EMT modelling software, however, has the ability to replicate voltage phase-angle jump behaviour.

This report focuses on the development and validation of models in PSS®E since these models are used extensively by AEMO and other stakeholders. AEMO has also engaged Manitoba Hydro International (MHI) to implement and validate the CMLD and DPV model parameters in MHI's PSCAD software package.

The EMT models, where possible (except where fundamental differences between RMS and EMT simulation do not allow), will use the same parameters and provide the same or extended capability compared with the RMS models implemented in PSS®E. The PSCAD DPV model, in addition to the features described in this document,

[149] UNSW (February 2022), Addressing Barriers to Efficient Renewable Integration, http://pvinverters.ee.unsw.edu.au/.

will also include fractional 4 stage voltage phase-angle jump tripping. This will enable the disconnection of DPV on voltage phase-angle jump to be represented.

AEMO is also developing and validating CMLD and DPV models in the DIgSILENT PowerFactory RMS platform, applying the PSS®E model parameters as a starting point. These models will be used in the South-West Interconnected System (SWIS) and adopt SWIS specific parameters, where evidence indicates behaviour is different from the NEM.

9.2 Future improvements to the DPV model

Table 110 outlines various pathways identified for continuing improvement to the DPV model.

Table 110 Pathways for continuing improvement to the DPV model

Area	Improvements	Priority
Utilise improved datasets as they become available	**Bench testing:** AEMO is continuing collaboration with UNSW Sydney and University of Wollongong on bench testing of inverters and loads. This includes exploring a wider number of inverters, testing of 3 phase inverters, testing of battery energy storage system (BESS) inverters, testing of inverters accredited against newer standards (such as AS/NZS4777.2:2020), and testing of various load types. As further insights become available from this process, they can be incorporated into the model parameters.	High
	PMU rollout: One of the most significant factors that has limited the ability to accurately tune the DPV model is the lack of availability of high-speed measurement (HSM) data at a wide range of locations, particularly at transmission buses with radial loads and high levels of DPV. This has meant estimates of active power changes need to be based on four second SCADA data, which introduces significant inaccuracies. Installing further HSM devices at a wide range of radial load transmission buses will significantly improve the ability to calibrate these models. A rollout of PMU devices is underway at present across the NEM; as data becomes available from these devices this will be applied to improve validation of future versions of these models.	High
	New disturbances: As new power system disturbances occur, these provide new opportunities to validate these models. For example, the trip of multiple generators and lines in Queensland and associated under-frequency load shedding[150] on 25 May 2021 provides a strong candidate for model calibration, but the incident analysis was not completed in time to include in this validation round. Representation of this event will require development of new PSS®E models, including an accurate representation of under frequency load shedding (UFLS) with DPV considered. This, and other disturbances that occur, can be included in future validation rounds.	High
	Project MATCH: AEMO is collaborating with UNSW Sydney, Solar Analytics, and other collaborators on Project MATCH, which aims to improve the data sources and tools available for assessing DER behaviour in disturbances. This will reduce uncertainty in the estimates of DER behaviour that underpin model validation.	High
	CER Audits: The Clean Energy Regulator is auditing DPV installations[151]. This provides ongoing insights on DPV installation compliance, which can affect the dynamic response of the DPV model. As insights become available, they can be incorporated into model parameter tuning.	High
	DPV installed capacities: The installed capacity of DPV at each PSS®E bus needs to be continually updated, based on the latest data provided by NSPs, and the DER Register. This improves the accuracy of the distribution of DPV that is mapped to a PSS®E bus and reduces the need to scale installed capacities at PSS®E buses based on older data. In particular, ~45% of QLD DPV installed capacity is clustered at 6 transmission buses. The DPV model results in QLD might be improved by distributing DPV across the sub-transmission network represented in PSS®E associated with these buses.	High

[150] AEMO (June 2021) Preliminary Report: Trip of multiple generators and lines in Queensland and associated under-frequency load shedding on 25 May 2021, https://aemo.com.au/-/media/files/electricity/nem/market_notices_and_events/power_system_incident_reports/2021/preliminary-report--trip-of-multiple-generators-and-lines-in-queensland-and-associated-underfrequenc.pdf?la=en.

[151] CER. Small-scale Renewable Energy Scheme inspections (webpage with access to reports and inspection updates), December 2020, http://www.cleanenergyregulator.gov.au/RET/Scheme-participants-and-industry/Agents-and-installers/Small-scale-Renewable-Energy-Scheme-inspections#Inspections-updates.

Area	Improvements	Priority
	DER Register: The DER register dataset is being improved to reduce errors and inaccuracies. As this dataset is improved, it could allow more accurate estimation of the proportions of 2005, 2015, and 2020 standard inverters.	Moderate
Implement representation of new standards as they become mandatory	**AS/NZS4777.2:2020:** From 18 December 2021, all new inverters in Australia and New Zealand will need to be certified to AS/NZS 4777.2:2020. New requirements have been introduced for the power quality response modes and passive anti-islanding settings of inverters. This includes updates to sustained operation limits for both voltage and frequency variations, changes to passive anti-islanding limits for voltage and frequency, and changes to the volt-var and volt-watt response modes. These changes are expected to significantly change DPV inverter behaviour, which needs to be accurately reflected in the DPV model. This will be updated on the basis of evidence from inverter bench testing and field measurements in disturbances, as this evidence becomes available from December 2021 onwards.	High
Bespoke models for new types of DER	**BESS model:** The model presented in this report has been designed to represent DPV only and has not been calibrated to represent other types of DER, such as distributed battery energy storage (BESS). Australian BESS installations are forecast to reach 5.6 GW by 2036–37[152]. A version of the model will be required to represent distributed BESS as they become a major component of the power system. This could apply the same DPV model with an updated parameter set.	Moderate
	Other types of DER: It may also be necessary to develop bespoke models for electric vehicles and other types of DER as they become prominent.	Low
	Specific manufacturers: It may be beneficial to develop bespoke model parameters for products from specific manufacturers, where evidence indicates they behave differently to typical products, and represent significant market share.	Moderate
	Utility-scale DER: It may be beneficial to develop independent models for selected PVNSG (PV Non-Scheduled Generation, 100 kW to 30 MW) embedded in the distribution network. This is consistent with the latest recommendations from NERC[153].	Low
DPV model improvement	**Integrating the DER model into the CMLD model:** New models available in PSS®E (e.g. CMLDBLGU2) have the DPV model connected at the same location at the load components in the CMLD model. This approach may lead to a more sensible dynamic response of the DPV behaviour and has the potential to reduce simulation times.	High
	Volt-var representation: The volt-var behaviour specified in AS/NZS4777.2:2015/2020 is not represented in the present model. Future revisions could consider the best way to implement this functionality.	Moderate
	Refinement of over/under-voltage tripping logic: The DERAEMO1 model currently utilises the vrfrac logic from the DER_A model with flexible voltage tripping reference setpoints. There are limitations to this approach. As a significant element of the model, this warrants further refinement in future revisions.	Moderate
	Inverter replacements: The present model does not account for replacement of older inverters, which may demonstrate improved behaviours consistent with more recent standards.	Low

9.3 Future improvements to the CMLD model

Table 111 outlines pathways for ongoing improvements to load models:

Table 111 Pathways for continuing improvement to load models

Area	Improvements	Priority
Large industrial loads	**Bespoke models for large industrial loads:** Large industrial loads can have significant influence over power system behaviour. For large industrial customers, it is possible to survey the loads present, and develop bespoke models for the site, accurately representing the motors and power electronic loads and their protection settings. Some NSPs are already undertaking this process. Bespoke models can be implemented where	High

[152] AEMO (May 2021) Behaviour of distributed resources during power system disturbances, https://aemo.com.au/-/media/files/initiatives/der/2021/capstone-report.pdf.

[153] NERC. March 2021. Reliability Guideline: Model Verification of Aggregate DER Models used in Planning Studies, https://www.nerc.com/comm/RSTC_Reliability_Guidelines/Reliability_Guideline%20_DER_Model_Verification_of_Aggregate_DER_Models_used_in_Planning_Studies.pdf.

Area	Improvements	Priority
	available, in place of the aggregate CMLD model applied for those sites in this model version.	
	Industrial motor parameters: The inertia, transient and sub-transient reactance's for large industrial loads is considerably different to motors used in residential and light-commercial applications. It may be possible to tailor those parameters to be more representative of large industrial motor applications and assess the effect this has on the accuracy of the dynamic response seen at a faulted industrial bus.	Low
	Large data centre loads: Data centres represent up to 4% of Australia total energy consumption[154]. It may be beneficial to include data centre loads as independent large industrial loads to better represent the commercial end-use load mix.	Low
High Speed Measurements	**PMU rollout:** One of the most significant factors that has limited the ability to accurately tune the CMLD model is the lack of availability of high-speed measurement (HSM) data at a wide range of locations, particularly at transmission buses with radial loads. This has meant estimates of active power changes need to be based on four second SCADA data, which introduces significant inaccuracies. Installing further HSM devices at a wide range of radial load transmission buses will significantly improve the ability to calibrate these models. A rollout of PMU devices is underway at present across the NEM; as data becomes available from these devices this will be applied to improve validation of future versions of these models.	High
Load composition	**Residential load composition:** The Australian government has recently updated the (2014) residential baseline study. The 2023 study provides updated residential load composition estimates, taking account the changes since 2014. It provides daily load profile data to give a more recent indication of how end-use load mix changes seasonally, weekday/weekend, and by time of day. There is potential to improve the residential end use load composition by updating this dataset. During these updates, there is also provision to investigate the benefits of having two different load compositions; one for rural and one for urban residential loads. This would involve determining rural load Rules of Association (RoA), identifying the rural PSS®E buses and applying separate RoA to these buses.	High
	Commercial load composition: Delta Q was commissioned by AEMO to estimate commercial load composition, which has informed this model. The report[155] indicated that there is a lack of load profile data from some commercial and industrial sectors including petroleum refining, iron and steel. There is also a lack of load profile data for increasingly energy intensive end-use loads such as electric vehicles and data centres. There may be potential to gather increased data for these sectors. VFD's are becoming increasingly prevalent in commercial and industrial end-use loads. Future revisions of the CMLD may include an increasing end-use load mix of Power Electronic and VFD load types over time, with a decreasing mix of motor load (Motor A, Motor B, and Motor C). Finally, the dataset containing the fraction of residential and commercial load in the CMLD parameters spreadsheet was last updated in 2019, and should be updated to the latest version in future revisions.	Low
	Industrial load composition: The inertia constant of industrial loads for Motors A, B, and C are set relatively low for industrial motor loads. Increasing inertia constants based on a set of aggregated survey data may improve dynamic simulation results.	Low
	Rules of Association: NSP's and NERC[156] have suggested that motors (especially motor B) are increasingly being replaced with VFDs when they are at the end of their life. To represent this, in consultation with NSPs, the Rules of Association were adjusted to represent this increased VFD adoption. Further insights on the changing end-use load mix can be incorporated in future revisions.	Moderate
	Simplified load composition calculations: Due to the granularity of the data sources used to estimated load composition, it has been observed that the relevant load fractions	High

[154] Energy Rating (2013), Data Centres page, https://www.energyrating.gov.au/products/data-centres#:~:text=controlled%20temperature%20environment.-,Data%20centres%20are%20high%20energy%20users%20with%20significant%20scope%20for,2.1%25%20of%20national%20consumption).

[155] Delta Q. AEMO Commercial Load Model, April 2020, https://aemo.com.au/-/media/files/initiatives/der/2020/2020-06-26-deltaq-final-report-aemo-commercial-load-model-user-guide-revb.pdf?la=en.

[156] NERC. December 2016. Technical Reference Document: Dynamic Load Modelling, https://www.nerc.com/comm/PC/LoadModelingTaskForceDL/Dynamic%20Load%20Modeling%20Tech%20Ref%202016-11-14%20-%20FINAL.PDF.

Area	Improvements	Priority
	do not vary by a large amount. Future work could look at the implications of using averaged load composition for different times of day, week, or season.	
	Improved dynamic response during disturbances: There are some validation cases that exhibit voltage overshoot or reactive power overshoot behaviour immediately following a disturbance. Identifying and adjusting the model parameters that cause this behaviour may improve the CMLD model response during the dynamic stage of fault recovery.	Low
	Update the underlying Large Industrial Load (LIL) dataset. The CMLD parameters workbook has data from 2019 for electricity generated by LILs (in GWh) over the course of one year. This is an input used to determine the RoA (fraction of each load type) for the CMLD model. This data set can be further improved by: • Using the latest data from AEMO's forecasting portal. • Removing the LIL's generation that was explicitly modelled from the yearly GWh data which makes up the remaining LIL's in the general CMLD. • Removing the LIL's (Boyne Island, Bell Bay, APD, Tomago) that are modelled as ZIP loads from the yearly GWh data.	High
Incorporating international best practice developments	**Variable frequency drive (VFD) motor model:** WECC are currently developing a positive sequence variable frequency drive (VFD) motor model to be included in the existing CMLD architecture[157]. Currently VFDs are modelled as power electronic loads. However, this model is algebraic and does not capture the complete transient behaviour of VFDs. Once the VFD model has been integrated, it will be possible to split power electronic loads into VFDs and other electronic loads, and then assign the VFD portion to the new VFD model.	Moderate
Distribution network	**Distribution network representation:** The CMLD model includes an equivalent representation of the distribution network. For this model version, average feeder impedance (Rfdr, Xfdr), transformer impedance (Xxf) and on-load tap changer parameters have been estimated with advice from select DNSPs. This approach can be improved with further advice from DNSPs for their specific networks, such as: • Determining average transformer impedance, on-load tap changer time delay and step-size settings for a given transformer size • Understanding transmission and distribution loss limits to determine the resistive component (Rfdr) of the feeder impedance • Determining a typical feeder X/R ratio to determine the reactive component (Xfdr) of the feeder impedance. X/R is currently set to 1.	Moderate
User written models	**Static load tripping:** In the CMLD at present, static load components (constant current, constant impedance) do not have tripping parameters. There are known to be specific loads that do have constant impedance loads with protection devices that will trip in response to disturbances, such as metal manufacturing plant machinery, and residential electric hot water load in Queensland. Incorporating this will require development of a user written model.	Low

9.4 Under frequency load shedding

In addition to the DPV model itself, proper incorporation of DPV into PSS®E models will also require expansion of broader features of the model. For example, DPV is often connected to feeders that are tripped by under frequency load shedding (UFLS). UFLS relays are not yet explicitly represented in the PSS®E models typically used by AEMO and NSPs. This is important for accurate representation of power system behaviour in response to non-credible contingencies, where frequency can fall below 49Hz and UFLS is expected to activate. Studies of this type are becoming increasingly important for delivery of AEMO's responsibilities, such as the Power System

[157] D. Ramasubramanian, P. Mitra and A. Gaikwad. 2018. VFD Model Development, https://www.wecc.biz/Administrative/VFD%20Modeling-%20Ramasubramanian.pdf.

Frequency Risk Review (PSFRR), review of the adequacy of UFLS, and studies to support the justification of protected events to the Reliability Panel.

AEMO has now developed and validated a detailed representation of the UFLS in South Australia, incorporating explicit UFLS relays into the model at each PSS®E bus to represent the proportion of load and DPV that will be tripped by the relay, at each frequency stage. Similar models are required for other NEM regions. Development and validation of these models is a considerable exercise.

Similar model updates are required to represent other types of control schemes that involve load shedding of residential and commercial feeders, such as the SIPS (System Integrity Protection Scheme).

9.5 Future improvements to general PSS®E models

This model validation process highlighted several areas where general improvements to PSS®E models of the NEM are required:

- Improvements are required for governor models for scheduled and semi-scheduled generators in PSS®E. This will facilitate improved calibration of models to accurately represent frequency disturbances.
- In some locations, investigation is required into specific network elements, such as the Rowville SVC (Static Var Compensator). Depending on the SVC manufacturer, more comprehensive disturbance data may be available.

9.6 Model deployment process

At present, these models are in a “pilot” phase. They are intended to be distributed to NSPs and other stakeholders with the scripts and spreadsheets necessary to generate input parameters and assess model performance. To improve this model deployment process in future, AEMO is working towards making the PSS®E dynamics file (with DPV and CMLD models) available through the OPDMS (Operations and Planning Data Management System).

AEMO is also exploring the integration of the models with the AEMO Energy Management System (EMS) so that the load model parameters can be directly updated based on the snapshot date and time. This removes the need for the user to manually generate the load model parameters based on a given date and time. The existing (manual) process is outlined in the CMLD and DPV Model User Guide.

9.7 Addressing peak reactive/active power representations

Several validation cases included in this report show that the CMLD model underestimates peak active and reactive power immediately post fault, as illustrated in the example below in **Figure 147**. Other cases show overestimation of peaks in active/reactive power. Possible causes of these effects are outlined below.

Figure 147 Active/Reactive Power – 18 January 2018 – 66kV Cranbourne Terminal Station (CBTS) Transformer B1 Feeder

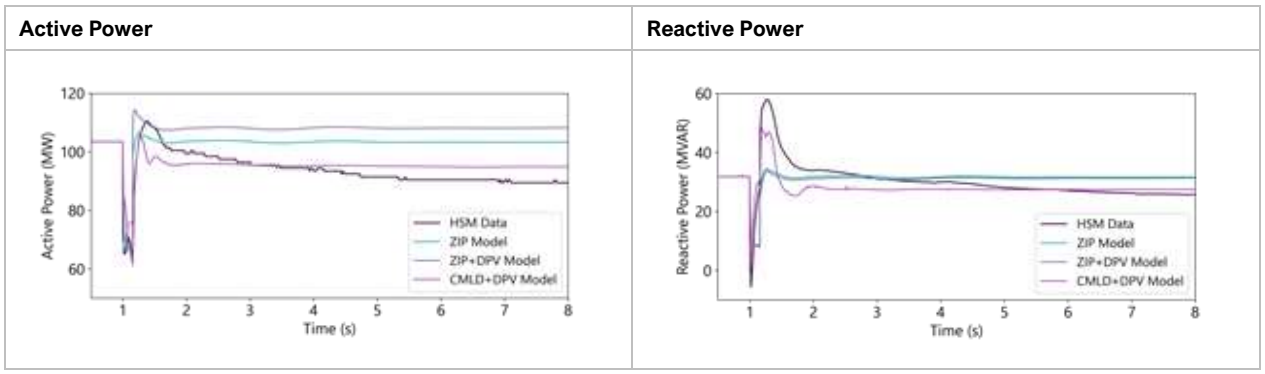

9.7.1 Under-estimating peaks: Variable frequency drive model

One possible contributing factor to the underestimation of active/reactive power peaks post disturbance may be the inability of the power electronic logic block in the CMLD model to capture the complete VFD response during voltage disturbances.

As shown in lab tests[158], during voltage disturbances, VFDs demonstrate:

1. Reverse biasing of drive diodes during a voltage sag, and
2. Inrush drawn immediately following a voltage disturbance and during voltage recovery.

AEMO has applied the power electronics model in the CMLD model to represent VFDs, because this model can replicate the reverse biasing of drive diodes during a voltage sag. The diodes at the front end of the drive get reversely biased, causing the current drawn by the drive to drop until the internal capacitor discharges into the end load and the diode becomes forward biased again. This results in the active and reactive power dropping and rising back.

However, when the voltage recovers after the sag, for VFDs the partially discharged capacitor now draws an inrush causing the active and reactive power to rise first and then slowly go down to the steady-state value. This behaviour is not represented by the power electronics model in the present CMLD model and may explain the underestimation of peak active and reactive power flows observed in many cases when applying the CMLD model.

To test the plausibility of underestimation of VFDs post fault in-rush current as the cause for misalignment of the CMLD model with the active/reactive power observations, the results for Cranbourne in the 18 January 2018 case were explored (as illustrated in **Figure 147**). Cranbourne is a mixed residential and commercial area[159] with VFD heavy[160,161] commercial end-use load users, including Cranbourne Golf Club, the Amstel Golf Club, the Ranfurlie Golf Club, an indoor swimming pool and over 20 schools.

[158] EPRI (2017). Technical Update on Load Modelling (3002010754), https://www.epri.com/research/products/3002010754.

[159] Geographical view of the area shown https://goo.gl/maps/mUt2RuqMv4hVanip7.

[160] More detailed information on the implementation of VFDs at golf courses can be found at https://www.gcsaa.org/uploadedfiles/environment/resources/energy-conservation/golf-course-energy-use-part-2-pump-stations.pdf.

[161] In most cases, VFDs are deployed in commercial HVAC systems such as those found in schools to control the speed of blower fans, pumps, or compressors. The main purpose of a cooling tower is removing the heat from a water circuit, which may be used in turn for process cooling or for a chiller plant.

In this case, the PSS®E snapshot estimates 361 MW of underlying demand in Cranbourne (103MW / 32MVar seen at the CBTS Transformer B1 feeder), of which the power electronics load component is 34% or 122MW of the total load (35MW/ 11MVar seen at the feeder). The HSM shows a voltage sag of 0.62pu, and according to the power electronics block logic in the CMLD model, the amount of power electronic load that is exposed to the fault is calculated as follows:

$$P_{seen} = 35 * 0.62pu = \sim 22MW$$
$$Q_{seen} = 11 * 0.62pu = \sim 7MVar$$

The misrepresentation of VFDs is a known shortfall of the CMLD model and improving this representation is a focus of international working groups[162]. From the draft specification for the VFD model proposed by EPRI[153], the limiters that work to limit the inrush current causing the active and reactive power to rise upon voltage recovery following a fault would be calculated as:

$$Pmax_internal = Pmax * P0 * Mul$$
$$Qmax_internal = Qmax * Q0 * Mul$$

Where:

$Pmax = Qmax = 1.1pu = Maximum\ value\ of\ active/reactive\ power\ (pu)$
$P0 = Steady\ state\ load\ active\ power\ (pu)$
$Mul = Multiplier\ value\ from\ partial\ trip\ characteristic$

Therefore, the following values can be estimated for the representation of the VFDs at this location in this disturbance:

$$Pmax = 1.1 * 22 = \sim 24\ MW$$
$$Qmax = 1.1 * 7 = \sim 7.5MVar$$

Assuming 50% of power electronic load in the area is VFD load, this represents a peak active, reactive power spike of ~12 MW and ~4 MVar higher than pre-fault conditions. In this disturbance at this location, the CMLD+DPV model underestimated active and reactive peak power flows by ~7 MW and 9 MVar, respectively. This suggests that implementation of the VFD model may better represent the dynamic response from VFD loads.

AEMO will explore implementing the latest VFD model representation once it is available in PSS®E.

9.7.2 Over-estimating peaks: HSM sampling rates

One possible explanation for the apparent over-estimation of peak active/reactive power may be that the HSM (PMU) data has a low (20ms) sampling rate. While this sampling rate may be sufficient to monitor very slow transients and steady state phenomena, it does not capture transient or fault events well, because in such cases, the waveform is not sinusoidal and changes amplitude, phase angle and frequency over a very short time interval. It is well established that PMU measurement accuracy suffers during faults[163] and may explain why the PSS®E results often show larger peak values for active and reactive power waveforms compared to the HSM data.

[162] EPRI. Technical Guide on Composite Load Modelling, August 2020, https://www.wecc.org/Administrative/Mitra%20-%20Technical%20Guide%20on%20Composite%20Load%20Modeling.pdf.

[163] See, for instance, Z. Huang, J. Hauer & K. Martin, "Evaluation of PMU Dynamic Performance in Both Lab Environments and under Field Operating Conditions," Proceedings of 2007 IEEE Power Engineering Society General Meeting; T. Becejac & P. Dehghanian, "PMU Multilevel End-to-End Testing to Assess Synchrophasor Measurements During Faults," IEEE Power & Energy Technology Systems Journal, March

To illustrate this, **Figure 148** compares the CMLD model results with and without a smoothing constant to the HSM[164] data, for two historic disturbances. The smoothing constant is intended to represent how the PSS®E results may appear if a low sampling rate (comparable to the HSM data) were applied. The smoothing constant applied for the PSS®E results is a simple 20 ms moving average, made up of the previous five, 4 ms data points.

The effects of smoothing on a typical reactive power profile are illustrated in Figure 148. The following observations can be made:

- Peak reactive power flows are more representative of HSM data for the CMLD smoothed results than the CMLD model (not smoothed). As above, the average of the data points is less severe than a single deep data point (for example at t = 1s)
- The trajectory of peak reactive power flows better represents the HSM data for the CMLD smoothed results than the CMLD model. This is because the one or two data points that represent the peaks are damped by the smoothing constant.

Figure 148 Comparison of PSS®E CMLD model results with/without smoothing constant – Reactive Power on Torrens A to Northfield line (11 April 2018)

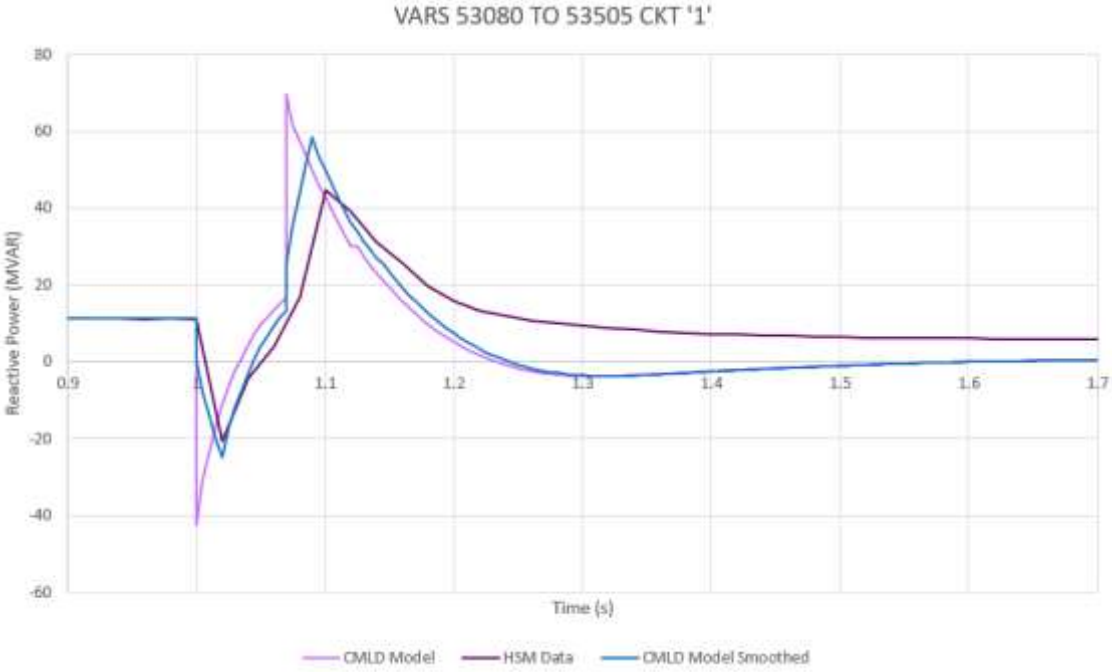

Overall, this analysis suggests that at least some of the mismatch between HSM data and PSS®E outcomes illustrated in this report (specifically during transient period) may be due to the low sampling rate of the HSM data. This could be addressed in future if high speed datasets with higher sampling rates become available.

2019; and N. Perera, R. Midence et al., "Applicability of Synchrophasor Based Frequency Data for Protection and Control Applications," IEEE, 72d Conference for Protective Relay Engineers, 2019.

[164] The HSM's that AEMO has access to at the transmission level are Phasor Measurement Units (PMU's) with 20ms sampling rates. PMU's perform extensive waveform filtering and data processing to create synchrophasors. This distorts the resulting data relative to the source waveform.

A1. DPV model parameters

Legend
Voltage control parameters
Frequency control parameters
Frequency tripping parameters
Voltage tripping parameters
RoCoF tripping parameters

Region	Date DNSP volt-VAR + EVRT requirements adopted
NSW	1/12/2018
VIC	1/12/2019
QLD	1/12/2019
SA	1/12/2017 + 28/09/2021
TAS	1/01/2021

AS4777.2 : 2015 inverters can be further subdivided into volt-var and non volt-var enabled. In South Australia, it is also possible to divide the 2015 standard into those with enhanced voltage ride through (EVDRT) enabled, and those without this enabled. The parameters for these categories are not meaningfully different to the 2015 compliant inverters, so have been excluded from the table below for the sake of simplicity.

Table 112 DPV model parameters for each inverter standard including DNSP volt-VAR requirements

			AS4777.3 : 2005 Inverters					AS4777.2 : 2015 Inverters					AS4777.2 : 2020 Inverters					
Parameter	Name	Description	NSW	VIC	QLD	SA	TAS	NSW	VIC	QLD	SA	TAS	NSW	VIC	QLD	SA	TAS	Details
M	PfFlag	reactive power control mode: • 1 : constant power factor mode • 0 : constant Q control mode	1	1	1	1	1	1	1	1	1	1	1	1	1	1	1	Based on the AS 4777.2(2005 and 2015) standard.
M+1	FreqFlag	flag to enable/disable frequency droop control: • 1 : frequency control enabled • 0 : frequency control disabled	0	0	0	0	0	1	1	1	1	1	1	1	1	1	1	1 : frequency control enabled. Over-frequency curtailment enabled for AS 4777.2 2015 standards.
M+2	PQFlag	priority for current limit • 1 : P priority • 0 : Q priority	1	1	1	1	1	1	1	1	1	1	1	1	1	1	1	According to NERC's recommended parameters, if volt-var is disabled, flag should be set to P Priority
M+3	GenFlag	mode of operation, sets real power absorption limit: • 1 : unit is a generator • 0 : unit is a storage device (Note 6)	1	1	1	1	1	1	1	1	1	1	1	1	1	1	1	Default for DPV model (as it is a generator)
M+4	VtripFlag	flag to enable/disable voltage trip logic: • 1 : enable • 0 : disable	1	1	1	1	1	1	1	1	1	1	1	1	1	1	1	Default from PEACE consulting report.
M+5	FtripFlag	flag to enable/disable frequency trip logic: • 1 : enable • 0 : disable	1	1	1	1	1	1	1	1	1	1	1	1	1	1	1	Determined by surveying manufacturer settings and bench testing.
J	Trv	(s) voltage measurement transducer time constant	0.02	0.02	0.02	0.02	0.02	0.02	0.02	0.02	0.02	0.02	0.02	0.02	0.02	0.02	0.02	Shortest typically allowed time constant according to US Standards and PEACE consulting report.
J+1	Trf	(s) frequency measurement transducer time constant	0.02	0.02	0.02	0.02	0.02	0.02	0.02	0.02	0.02	0.02	0.02	0.02	0.02	0.02	0.02	Shortest typically allowed time constant according to US Standards and PEACE consulting report.
J+2	dbd1	(pu) lower voltage deadband (<= 0)	-1	-1	-1	-1	-1	-1	-1	-1	-1	-1	-0.043	-0.043	-0.043	-0.043	-0.043	Weighted average as a proportion of installed volt-VAR enabled capacity. For dates < volt-VAR enabled, use 2005 standard (-1). Calculated per individual DNSP requirements.
J+3	dbd2	(pu) upper voltage deadband (> 0)	1	1	1	1	1	1	1	1	1	1	0.043	0.043	0.043	0.043	0.043	Weighted average as a proportion of installed volt-VAR enabled capacity. For dates < volt-VAR enabled, use 2005 standard (1). Calculated per individual DNSP requirements
J+4	Trocof	(s) RoCoF Filter time constant	0.02	0.02	0.02	0.02	0.02	0.02	0.02	0.02	0.02	0.02	0.02	0.02	0.02	0.02	0.02	Default value for time constant applied for the DPV model.
J+5	Vref	(pu) user specified voltage set-point	1	1	1	1	1	1	1	1	1	1	1	1	1	1	1	Default is 1 for symmetric deadband at 240V.
J+6	Tp	(s) power measurement transducer time constant	0.02	0.02	0.02	0.02	0.02	0.02	0.02	0.02	0.02	0.02	0.02	0.02	0.02	0.02	0.02	Typical minimum for large scale stability studies.
J+7	Tiq	(s) Q-control time constant	0.02	0.02	0.02	0.02	0.02	0.02	0.02	0.02	0.02	0.02	0.02	0.02	0.02	0.02	0.02	Typical minimum for large scale stability studies. Emulates delay in controls.
J+8	Ddn	(pu) reciprocal of droop for over-frequency conditions (< 0)	0.0	0.0	0.0	0.0	0.0	10.0	10.0	10.0	10.0	10.0	28.6	28.6	28.6	28.6	28.6	Weighted average as a proportion of installed capacity i.e. (0 * 2005 standard) + (10 * 2015 standard) + (10 * EVRT (for SA)) + (10 * volt-VAR enabled) + (10 * 2020 standard).
J+9	Dup	(pu) reciprocal of droop for under-frequency conditions (> 0)	0	0	0	0	0	0	0	0	0	0	0	0	0	0	0	Determined with the AS4777.2-2015 Standards. Not enabled.
J+10	fdbd1	(pu) deadband for frequency control, lower threshold (<= 0)	-1	-1	-1	-1	-1	-0.005	-0.005	-0.005	-0.005	-0.005	-0.005	-0.005	-0.005	-0.005	-0.005	Determined with the AS4777.2-2015 Standards. Only responds for AS4777.2-2015 inverters when frequency >50.25 Hz
J+11	fdbd2	(pu) deadband for frequency control, upper threshold (>= 0)	1	1	1	1	1	1	1	1	1	1	1	1	1	1	1	Determined with the AS4777.2-2015 Standard. Does not respond to under-frequency.
J+12	femax	(pu) freq. error upper limit	99	99	99	99	99	99	99	99	99	99	99	99	99	99	99	Neglected. Typically for PI control per PEACE consulting report.
J+13	femin	(pu) freq. error lower limit	-99	-99	-99	-99	-99	-99	-99	-99	-99	-99	-99	-99	-99	-99	-99	Neglected. Typically for PI control per PEACE consulting report.
J+14	Pmax	(pu) max. power limit	1	1	1	1	1	1	1	1	1	1	1	1	1	1	1	Set to default per PEACE consulting (1 pu = rated power). Note: if under-frequency response is ever enabled it is very important to set this value to the maximum available incident solar energy at the time being simulated.
J+15	Pmin	(pu) min. power limit	0	0	0	0	0	0	0	0	0	0	0	0	0	0	0	Default minimum power and per PEACE consulting report.
J+16	dPmax	(pu/s) power reference maximum ramp rate (> 0)	99	99	99	99	99	0	0	0	0	0	0	0	0	0	0	From AS/NZS4777.2:2015. dpMax set to zero such that the inverter will never ramp back up following an over-frequency curtailment response.
J+17	dPmin	(pu/s) Power reference minimum ramp rate (< 0)	-99	-99	-99	-99	-99	-99	-99	-99	-99	-99	-99	-99	-99	-99	-99	Setting a large negative value to allow P to drop very fast. Default per PEACE consulting report.
J+18	Tpord	(s) Power filter time constant	0.02	0.02	0.02	0.02	0.02	0.02	0.02	0.02	0.02	0.02	0.02	0.02	0.02	0.02	0.02	Default minimum time constant and in line with other time constants in the model.
J+19	Kpg	(pu) PI controller proportional gain	0	0	0	0	0	0	0	0	0	0	0	0	0	0	0	Neglect – No PI control per PEACE consulting report.
J+20	Kig	(pu) PI controller integral gain	10	10	10	10	10	10	10	10	10	10	10	10	10	10	10	Gain = 1/Kig so affects proportional droop with 0.1s time lag (time constant)

J+21	Imax	(pu) maximum converter current	1.19	1.19	1.19	1.19	1.19	1.20	1.20	1.20	1.20	1.20	1.20	1.20	1.20	1.20	1.20	Weighted average as a proportion of installed capacity. This is relatively constant as shown and does not necessarily require a time constant. Added as data was available.
J+22	vl0	(pu) first breakpoint for low voltage cut-out	0.75	0.75	0.75	0.75	0.75	0.50	0.50	0.50	0.50	0.50	0.50	0.50	0.50	0.50	0.50	Weighted average as a proportion of installed capacity for each region. Determined with the AS4777.2-2015 standards and tuned to the observed DPV disconnection. Refer to section 2.3.5.
J+23	vl1	(pu) second breakpoint for low voltage cut-out (vl1 >vl0)	0.90	0.90	0.90	0.90	0.90	0.90	0.90	0.90	0.90	0.90	0.90	0.90	0.90	0.90	0.90	Determined by UNSW voltage sag benchmark testing. Refer to section 2.3.5.
J+24	vh0	(pu) first breakpoint for high voltage cut-out	1.18	1.18	1.18	1.18	1.18	1.18	1.18	1.18	1.18	1.18	1.21	1.21	1.21	1.21	1.21	Weighted average as a proportion of installed capacity for each region. Determined by UNSW benchmark test voltage ramp test and tuned with validation cases.
J+25	vh1	(pu) second breakpoint for high voltage cut-out (vh1< vh0)	1.13	1.13	1.13	1.13	1.13	1.13	1.13	1.13	1.13	1.13	1.19	1.19	1.19	1.19	1.19	Weighted average as a proportion of installed capacity for each region. Refer to section 2.3.4.
J+26	tvl0	(s) low voltage cut-out timer corresponding to voltage vl0	1.58	1.58	1.58	1.58	1.58	1.77	1.77	1.77	1.77	1.77	1.77	1.77	1.77	1.77	1.77	Weighted average as a proportion of installed capacity for each region. Determined by UNSW benchmark test voltage ramp 230V to 160V. Refer to section 2.3.4.
J+27	tvl1	(s) low voltage cut-out timer corresponding to voltage vl1	0.027	0.027	0.027	0.027	0.027	0.037	0.037	0.037	0.037	0.037	0.037	0.037	0.037	0.037	0.037	Weighted average as a proportion of installed capacity for each region. Determined by UNSW benchmark test voltage notch 230V to 50V 0.1s. Refer to section 2.3.4.
J+28	tvh0	(s) high voltage cut-out timer corresponding to voltage vh0	0.88	0.88	0.88	0.88	0.88	0.16	0.16	0.16	0.16	0.16	0.16	0.16	0.16	0.16	0.16	Weighted average as a proportion of installed capacity for each region. Determined by UNSW benchmark test voltage notch 230V to 270V 7s. Refer to section 2.3.4.
J+29	tvh1	(s) high voltage cut-out timer corresponding to voltage vh1	1.94	1.94	1.94	1.94	1.94	1.87	1.87	1.87	1.87	1.87	1.87	1.87	1.87	1.87	1.87	Weighted average as a proportion of installed capacity for each region. Determined by UNSW benchmark test voltage step 230V to 260V. Refer to section 2.3.4.
J+30	vrfrac	fraction of devices that recovers after voltage comes back within vl1 < V < vh1 (0 <= Vrfrac <= 1)	0.625	0.625	0.625	0.625	0.625	0.713	0.713	0.713	0.713	0.713	1.00	1.00	1.00	1.00	1.00	Weighted average as a proportion of installed capacity for each region. Informed by UNSW voltage sag benchmark tests and tuned. Refer to section 2.3.5.
J+31	Kqv1	(pu) proportional voltage control gain for reactive power reduction	0.00	0.00	0.00	0.00	0.00	0.00	0.00	0.00	0.00	0.00	0.00	0.00	0.00	0.00	0.00	Weighted average as a proportion of installed capacity for each region. For dates < volt-VAR enabled, use 2005 standard (0). Calculated per DNSP requirements. Refer to section 2.3.8.
J+32	Kqv2	(pu) proportional voltage control gain for reactive power increase	0.00	0.00	0.00	0.00	0.00	0.00	0.00	0.00	0.00	0.00	0.00	0.00	0.00	0.00	0.00	Weighted average as a proportion of installed capacity for each region. For dates < volt-VAR enabled, use 2005 standard (0). Calculated per DNSP requirements. Refer to section 2.3.8.
J+33	-	reserved	0	0	0	0	0	0	0	0	0	0	0	0	0	0	0	Reserved parameter.
J+34	-	reserved	0	0	0	0	0	0	0	0	0	0	0	0	0	0	0	Reserved parameter.
J+35	Tg	(s) current control time constant (represents behaviour of inner control loops)	0.02	0.02	0.02	0.02	0.02	0.02	0.02	0.02	0.02	0.02	0.02	0.02	0.02	0.02	0.02	Typical minimum for large scale stability studies and in line with other time constants in DPV model.
J+36	rrpwr	(pu/s) ramp rate for real power increase following a fault	10	10	10	10	10	10	10	10	10	10	10	10	10	10	10	Default from PEACE consulting report[165].
J+37	Tv	(s) time constant on the output of the multiplier	0.02	0.02	0.02	0.02	0.02	0.02	0.02	0.02	0.02	0.02	0.02	0.02	0.02	0.02	0.02	Typical minimum for large scale stability studies and in line with other time constants in DPV model.
J+38	Vpr	(pu) voltage below which frequency tripping is disabled	0.90	0.90	0.90	0.90	0.90	0.90	0.90	0.90	0.90	0.90	0.90	0.90	0.90	0.90	0.90	Reasonable value to avoid known frequency tripping calculation issues.
J+39	Iqh1	(pu) upper limit on reactive current injection Iqinj	0	0	0	0	0	0	0	0	0	0	0.44	0.44	0.44	0.44	0.44	Weighted average as a proportion of installed capacity for each region. For dates < volt-VAR enabled, use 2005 standard (0). Calculated per DNSP requirements. Refer to section 2.3.3.
J+40	Iql1	(pu) lower limit on reactive current injection Iqinj	0	0	0	0	0	0	0	0	0	0	-0.60	-0.60	-0.60	-0.60	-0.60	Weighted average as a proportion of installed capacity for each region. For dates < volt-VAR enabled, use 2005 standard (0). Calculated per DNSP requirements. Refer to section 2.3.3.
J+41	fl1	(Hz) low frequency trip limit 1	49.60	49.60	49.60	49.60	49.60	49.60	49.60	49.60	49.60	49.60	-	-	-	-	-	Determined from validation studies and frequency survey results[166].
J+42	fl2	(Hz) low frequency trip limit 2	49.01	49.01	49.01	49.01	49.01	49.01	49.01	49.01	49.01	49.01	-	-	-	-	-	Determined from frequency survey results.
J+43	fl3	(Hz) low frequency trip limit 3	49.00	49.00	49.00	49.00	49.00	49.00	49.00	49.00	49.00	49.00	-	-	-	-	-	Determined from frequency survey results.
J+44	fl4	(Hz) low frequency trip limit 4	49.00	49.00	49.00	49.00	49.00	49.00	49.00	49.00	49.00	49.00	-	-	-	-	-	Determined from frequency survey results.
J+45	fl5	(Hz) low frequency trip limit 5	49.00	49.00	49.00	49.00	49.00	49.00	49.00	49.00	49.00	49.00	-	-	-	-	-	Determined from frequency survey results.
J+46	fl6	(Hz) low frequency trip limit 6	48.52	48.52	48.52	48.52	48.52	48.52	48.52	48.52	48.52	48.52	-	-	-	-	-	Determined from frequency survey results.
J+47	fl7	(Hz) low frequency trip limit 7	47.60	47.60	47.60	47.60	47.60	47.60	47.60	47.60	47.60	47.60	-	-	-	-	-	Determined from frequency survey results.
J+48	fl8	(Hz) low frequency trip limit 8	47.55	47.55	47.55	47.55	47.55	47.55	47.55	47.55	47.55	47.55	-	-	-	-	-	Determined from frequency survey results.
J+49	fl9	(Hz) low frequency trip limit 9	47.50	47.50	47.50	47.50	47.50	47.50	47.50	47.50	47.50	47.50	-	-	-	-	-	Determined from frequency survey results.
J+50	fl10	(Hz) low frequency trip limit 10	47.10	47.10	47.10	47.10	47.10	47.10	47.10	47.10	47.10	47.10	-	-	-	-	-	Determined from frequency survey results.
J+51	fl11	(Hz) low frequency trip limit 11	47.00	47.00	47.00	47.00	47.00	47.00	47.00	47.00	47.00	47.00	-	-	-	-	-	Determined from frequency survey results.
J+52	fl12	(Hz) low frequency trip limit 12	47.00	47.00	47.00	47.00	47.00	47.00	47.00	47.00	47.00	47.00	-	-	-	-	-	Requirement for anti-islanding protection as per AS 4777.2-2015.
J+53	fl13	(Hz) low frequency trip limit 13	47.00	47.00	47.00	47.00	47.00	47.00	47.00	47.00	47.00	47.00	47.00	47.00	47.00	47.00	47.00	Requirement for anti-islanding protection as per AS 4777.2-2015.
J+54	tfl1	(s) pick-up time for low frequency trip 1	1.90	1.90	1.90	1.90	1.90	1.90	1.90	1.90	1.90	1.90	-	-	-	-	-	Determined from frequency survey results.
J+55	tfl2	(s) pick-up time for low frequency trip 2	0.18	0.18	0.18	0.18	0.18	0.18	0.18	0.18	0.18	0.18	-	-	-	-	-	Determined from frequency survey results.
J+56	tfl3	(s) pick-up time for low frequency trip 3	0.06	0.06	0.06	0.06	0.06	0.06	0.06	0.06	0.06	0.06	-	-	-	-	-	Determined from frequency survey results.
J+57	tfl4	(s) pick-up time for low frequency trip 4	1.96	1.96	1.96	1.96	1.96	1.96	1.96	1.96	1.96	1.96	-	-	-	-	-	Determined from frequency survey results.
J+58	tfl5	(s) pick-up time for low frequency trip 5	2.00	2.00	2.00	2.00	2.00	2.00	2.00	2.00	2.00	2.00	-	-	-	-	-	Determined from frequency survey results.
J+59	tfl6	(s) pick-up time for low frequency trip 6	2.00	2.00	2.00	2.00	2.00	2.00	2.00	2.00	2.00	2.00	-	-	-	-	-	Determined from frequency survey results.
J+60	tfl7	(s) pick-up time for low frequency trip 7	1.80	1.80	1.80	1.80	1.80	1.80	1.80	1.80	1.80	1.80	-	-	-	-	-	Determined from frequency survey results.

[165] PEACE® Consulting. 2019. Developing Dynamic Load Models for the Australian Eastern Interconnected System, https://aemo.com.au/-/media/files/initiatives/der/2020/aemo-load-modeling-062819-final.pdf?la=en.

[166] AEMO. Technical Integration of Distributed Energy Resources, April 2019, https://aemo.com.au/-/media/files/electricity/nem/der/2019/operations/technical-integration-of-der-report.pdf.

J+61	tfl8	(s) pick-up time for low frequency trip 8	0.20	0.20	0.20	0.20	0.20	0.20	0.20	0.20	0.20	0.20	-	-	-	-	-	Determined from frequency survey results.
J+62	tfl9	(s) pick-up time for low frequency trip 9	1.80	1.80	1.80	1.80	1.80	1.80	1.80	1.80	1.80	1.80	-	-	-	-	-	Determined from frequency survey results.
J+63	tfl10	(s) pick-up time for low frequency trip 10	1.80	1.80	1.80	1.80	1.80	1.80	1.80	1.80	1.80	1.80	-	-	-	-	-	Determined from frequency survey results.
J+64	tfl11	(s) pick-up time for low frequency trip 11	1.60	1.60	1.60	1.60	1.60	1.60	1.60	1.60	1.60	1.60	-	-	-	-	-	Determined from frequency survey results.
J+65	tfl12	(s) pick-up time for low frequency trip 12	0.10	0.10	0.10	0.10	0.10	0.10	0.10	0.10	0.10	0.10	-	-	-	-	-	Determined from frequency survey results.
J+66	tfl13	(s) pick-up time for low frequency trip 13	0.00	0.00	0.00	0.00	0.00	1.65	1.65	1.65	1.65	1.65	1.65	1.65	1.65	1.65	1.65	Determined from frequency survey results.
J+67	frac_fl1	fraction for low frequency trip 1	2.00%	2.00%	2.00%	2.00%	2.00%	1.00%	1.00%	1.00%	1.00%	1.00%	0%	0%	0%	0%	0%	Determined from tuning and weighted average as a proportion of installed capacity for each region.
J+68	frac_fl2	fraction for low frequency trip 2	1.89%	4.05%	2.06%	1.40%	0.73%	1.00%	2.10%	1.10%	0.75%	0.38%	0%	0%	0%	0%	0%	Weighted average as a proportion of installed capacity for each region. Determined from frequency survey results.
J+69	frac_fl3	fraction for low frequency trip 3	12.43%	13.08%	8.94%	9.28%	16.09%	6.56%	6.80%	4.78%	4.99%	8.44%	0%	0%	0%	0%	0%	Weighted average as a proportion of installed capacity for each region. Determined from frequency survey results.
J+70	frac_fl4	fraction for low frequency trip 4	3.78%	8.09%	3.31%	2.45%	3.47%	2.00%	4.20%	1.77%	1.32%	1.82%	0%	0%	0%	0%	0%	Weighted average as a proportion of installed capacity for each region. Determined from frequency survey results.
J+71	frac_fl5	fraction for low frequency trip 5	0.09%	0.28%	0.09%	0.26%	0.00%	0.05%	0.15%	0.05%	0.14%	0.00%	0%	0%	0%	0%	0%	Weighted average as a proportion of installed capacity for each region. Determined from frequency survey results.
J+72	frac_fl6	fraction for low frequency trip 6	1.30%	0.50%	0.80%	0.90%	0.70%	0.65%	0.25%	0.40%	0.45%	0.35%	0%	0%	0%	0%	0%	Weighted average as a proportion of installed capacity for each region. Determined from frequency survey results.
J+73	frac_fl7	fraction for low frequency trip 7	8.20%	3.40%	1.90%	3.20%	1.00%	4.10%	1.70%	0.95%	1.60%	0.50%	0%	0%	0%	0%	0%	Weighted average as a proportion of installed capacity for each region. Determined from frequency survey results.
J+74	frac_fl8	fraction for low frequency trip 8	2.90%	2.20%	2.40%	4.10%	2.00%	1.45%	1.10%	1.20%	2.05%	1.00%	0%	0%	0%	0%	0%	Weighted average as a proportion of installed capacity for each region. Determined from frequency survey results.
J+75	frac_fl9	fraction for low frequency trip 9	8.10%	5.20%	10.50%	4.40%	7.60%	4.05%	2.60%	5.25%	2.20%	3.80%	0%	0%	0%	0%	0%	Weighted average as a proportion of installed capacity for each region. Determined from frequency survey results.
J+76	frac_fl10	fraction for low frequency trip 10	9.20%	9.20%	18.80%	7.70%	21.90%	4.60%	4.60%	9.40%	3.85%	10.95%	0%	0%	0%	0%	0%	Weighted average as a proportion of installed capacity for each region. Determined from frequency survey results.
J+77	frac_fl11	fraction for low frequency trip 11	1.40%	1.80%	0.80%	0.80%	0.10%	0.70%	0.90%	0.40%	0.40%	0.05%	0%	0%	0%	0%	0%	Weighted average as a proportion of installed capacity for each region. Determined from frequency survey results.
J+78	frac_fl12	fraction for low frequency trip 12	48.70%	50.20%	48.40%	63.50%	44.40%	24.35%	25.10%	24.20%	31.75%	22.20%	0%	0%	0%	0%	0%	Weighted average as a proportion of installed capacity for each region. Determined from frequency survey results.
J+79	frac_fl13	fraction for low frequency trip 13	0.00%	0.00%	0.00%	0.00%	0.00%	49.50%	49.50%	49.50%	49.50%	49.50%	100%	100%	100%	100%	100%	Weighted average as a proportion of installed capacity for each region. Determined from frequency survey results.
J+80	fh1	(Hz) high frequency trip limit 1	50.50	50.50	50.50	50.50	50.50	50.5	50.5	50.5	50.5	50.5	-	-	-	-	-	Determined from validation studies and frequency survey results[167].
J+81	fh2	(Hz) high frequency trip limit 2	50.80	50.80	50.80	50.80	50.80	50.8	50.8	50.8	50.8	50.8	-	-	-	-	-	Determined from validation studies and frequency survey results[168].
J+82	fh3	(Hz) high frequency trip limit 3	51	51	51	51	51	51	51	51	51	51	-	-	-	-	-	Determined from frequency survey results.
J+83	fh4	(Hz) high frequency trip limit 4	51	51	51	51	51	51	51	51	51	51	-	-	-	-	-	Determined from frequency survey results.
J+84	fh5	(Hz) high frequency trip limit 5	51	51	51	51	51	51	51	51	51	51	-	-	-	-	-	Determined from frequency survey results.
J+85	fh6	(Hz) high frequency trip limit 6	51.58	51.58	51.58	51.58	51.58	51.58	51.58	51.58	51.58	51.58	-	-	-	-	-	Determined from frequency survey results.
J+86	fh7	(Hz) high frequency trip limit 7	51.90	51.90	51.90	51.90	51.90	51.9	51.9	51.9	51.9	51.9	-	-	-	-	-	Determined from frequency survey results.
J+87	fh8	(Hz) high frequency trip limit 8	52	52	52	52	52	52	52	52	52	52	52	52	52	52	52	Determined from frequency survey results.
J+88	fh9	(Hz) high frequency trip limit 9	52	52	52	52	52	52	52	52	52	52	-	-	-	-	-	Determined from frequency survey results.
J+89	fh10	(Hz) high frequency trip limit 10	52.45	52.45	52.45	52.45	52.45	52.45	52.45	52.45	52.45	52.45	-	-	-	-	-	Determined from frequency survey results.
J+90	fh11	(Hz) high frequency trip limit 11	52.90	52.90	52.90	52.90	52.90	52.9	52.9	52.9	52.9	52.9	-	-	-	-	-	Determined from frequency survey results.
J+91	fh12	(Hz) high frequency trip limit 12	53	53	53	53	53	53	53	53	53	53	-	-	-	-	-	Requirement for anti-islanding protection per AS 4777.2-2015. Refer to section 2.3.8.
J+92	fh13	(Hz) high frequency trip limit 13	53	53	53	53	53	53	53	53	53	53	-	-	-	-	-	Requirement for anti-islanding protection per AS 4777.2-2015. Refer to section 2.3.8.
J+93	tfh1	(s) pick-up time for high frequency trip 1	1.9	1.9	1.9	1.9	1.9	1.9	1.9	1.9	1.9	1.9	-	-	-	-	-	Determined from frequency survey results.
J+94	tfh2	(s) pick-up time for high frequency trip 2	1.9	1.9	1.9	1.9	1.9	1.9	1.9	1.9	1.9	1.9	-	-	-	-	-	Determined from frequency survey results.
J+95	tfh3	(s) pick-up time for high frequency trip 3	0.06	0.06	0.06	0.06	0.06	0.06	0.06	0.06	0.06	0.06	-	-	-	-	-	Determined from frequency survey results.
J+96	tfh4	(s) pick-up time for high frequency trip 4	1.96	1.96	1.96	1.96	1.96	1.96	1.96	1.96	1.96	1.96	-	-	-	-	-	Determined from frequency survey results.
J+97	tfh5	(s) pick-up time for high frequency trip 5	2	2	2	2	2	2	2	2	2	2	-	-	-	-	-	Determined from frequency survey results.
J+98	tfh6	(s) pick-up time for high frequency trip 6	2	2	2	2	2	2	2	2	2	2	-	-	-	-	-	Determined from frequency survey results.
J+99	tfh7	(s) pick-up time for high frequency trip 7	1.8	1.8	1.8	1.8	1.8	1.8	1.8	1.8	1.8	1.8	-	-	-	-	-	Determined from frequency survey results.
J+100	tfh8	(s) pick-up time for high frequency trip 8	1.6	1.6	1.6	1.6	1.6	1.6	1.6	1.6	1.6	1.6	-	-	-	-	-	Determined from frequency survey results.
J+101	tfh9	(s) pick-up time for high frequency trip 9	1.8	1.8	1.8	1.8	1.8	1.8	1.8	1.8	1.8	1.8	0.15	0.15	0.15	0.15	0.15	Determined from frequency survey results.
J+102	tfh10	(s) pick-up time for high frequency trip 10	0.2	0.2	0.2	0.2	0.2	0.2	0.2	0.2	0.2	0.2	-	-	-	-	-	Determined from frequency survey results.
J+103	tfh11	(s) pick-up time for high frequency trip 11	1.8	1.8	1.8	1.8	1.8	1.8	1.8	1.8	1.8	1.8	-	-	-	-	-	Determined from frequency survey results.
J+104	tfh12	(s) pick-up time for high frequency trip 12	0.1	0.1	0.1	0.1	0.1	0.1	0.1	0.1	0.1	0.1	-	-	-	-	-	Determined from frequency survey results.
J+105	tfh13	(s) pick-up time for high frequency trip 13	0	0	0	0	0	0.15	0.15	0.15	0.15	0.15	-	-	-	-	-	Determined from frequency survey results.
J+106	frac_fh1	fraction for high frequency trip 1	7.00%	7.00%	7.00%	7.00%	7.00%	3.50%	3.50%	3.50%	3.50%	3.50%	0%	0%	0%	0%	0%	Weighted average as a proportion of installed capacity for each region. Determined from validation studies.

[167] AEMO. Technical Integration of Distributed Energy Resources, April 2019, https://aemo.com.au/-/media/files/electricity/nem/der/2019/operations/technical-integration-of-der-report.pdf.

[168] AEMO. Technical Integration of Distributed Energy Resources, April 2019, https://aemo.com.au/-/media/files/electricity/nem/der/2019/operations/technical-integration-of-der-report.pdf.

J+107	frac_fh2	fraction for high frequency trip 2	5.00%	5.00%	5.00%	5.00%	5.00%	1.00%	1.00%	1.00%	1.00%	1.00%	0%	0%	0%	0%	0%	Weighted average as a proportion of installed capacity for each region. Determined from validation studies.
J+108	frac_fh3	fraction for high frequency trip 3	6.25%	9.45%	3.19%	2.63%	8.47%	5.99%	7.01%	4.31%	4.22%	7.32%	0%	0%	0%	0%	0%	Weighted average as a proportion of installed capacity for each region. Determined from frequency survey results.
J+109	frac_fh4	fraction for high frequency trip 4	1.90%	5.85%	1.18%	0.69%	1.83%	1.82%	4.34%	1.60%	1.11%	1.58%	0%	0%	0%	0%	0%	Weighted average as a proportion of installed capacity for each region. Determined from frequency survey results.
J+110	frac_fh5	fraction for high frequency trip 5	0.05%	0.20%	0.03%	0.07%	0.00%	0.04%	0.15%	0.04%	0.12%	0.00%	0%	0%	0%	0%	0%	Weighted average as a proportion of installed capacity for each region. Determined from frequency survey results.
J+111	frac_fh6	fraction for high frequency trip 6	1.30%	0.50%	0.80%	0.90%	0.70%	0.65%	0.25%	0.40%	0.45%	0.35%	0%	0%	0%	0%	0%	Weighted average as a proportion of installed capacity for each region. Determined from frequency survey results.
J+112	frac_fh7	fraction for high frequency trip 7	8.20%	3.40%	1.90%	3.20%	1.00%	4.10%	1.70%	0.95%	1.60%	0.50%	0%	0%	0%	0%	0%	Weighted average as a proportion of installed capacity for each region. Determined from frequency survey results.
J+113	frac_fh8	fraction for high frequency trip 8	1.40%	1.80%	2.40%	4.10%	0.10%	0.70%	0.90%	1.20%	2.05%	0.05%	0%	0%	0%	0%	0%	Weighted average as a proportion of installed capacity for each region. Determined from frequency survey results.
J+114	frac_fh9	fraction for high frequency trip 9	8.10%	5.20%	10.50%	4.40%	7.60%	4.05%	2.60%	5.25%	2.20%	3.80%	100%	100%	100%	100%	100%	Weighted average as a proportion of installed capacity for each region. Determined from frequency survey results.
J+115	frac_fh10	fraction for high frequency trip 10	2.90%	2.20%	18.80%	7.70%	2.00%	1.45%	1.10%	9.40%	3.85%	1.00%	0%	0%	0%	0%	0%	Weighted average as a proportion of installed capacity for each region. Determined from frequency survey results.
J+116	frac_fh11	fraction for high frequency trip 11	9.20%	9.20%	0.80%	0.80%	21.90%	4.60%	4.60%	0.40%	0.40%	10.95%	0%	0%	0%	0%	0%	Weighted average as a proportion of installed capacity for each region. Determined from frequency survey results.
J+117	frac_fh12	fraction for high frequency trip 12	48.70%	50.20%	48.40%	63.50%	44.40%	24.35%	25.10%	24.20%	31.75%	22.20%	0%	0%	0%	0%	0%	Weighted average as a proportion of installed capacity for each region. Determined from frequency survey results.
J+118	frac_fh13	fraction for high frequency trip 13	0.00%	0.00%	0.00%	0.00%	0.00%	47.75%	47.75%	47.75%	47.75%	47.75%	0%	0%	0%	0%	0%	Weighted average as a proportion of installed capacity for each region. Determined from frequency survey results.
J+119	RoCoF_1	(pu/s) RoCoF trip limit 1	0.008	0.008	0.008	0.008	0.008	0.008	0.008	0.008	0.008	0.008	0.008	0.008	0.008	0.008	0.008	Determined with UNSW benchmark test frequency ramp (0.4Hz/s). Refer to section 2.3.3.
J+120	RoCoF_2	(pu/s) RoCoF trip limit 2	0.02	0.02	0.02	0.02	0.02	0.02	0.02	0.02	0.02	0.02	0.02	0.02	0.02	0.02	0.02	Determined with UNSW benchmark test frequency ramp (1Hz/s). Refer to section 2.3.3.
J+121	RoCoF_3	(pu/s) RoCoF trip limit 3	0.08	0.08	0.08	0.08	0.08	0.08	0.08	0.08	0.08	0.08	0.08	0.08	0.08	0.08	0.08	Determined with UNSW benchmark test frequency ramp (4Hz/s). Refer to section 2.3.3.
J+122	tRoCoF_1	(s) pick up time for RoCoF trip 1	1.41	1.41	1.41	1.41	1.41	1.41	1.41	1.41	1.41	1.41	-	-	-	-	-	Determined with UNSW benchmark test frequency ramp (0.4Hz/s).
J+123	tRoCoF_2	(s) pick up time for RoCoF trip 2	0.83	0.83	0.83	0.83	0.83	0.83	0.83	0.83	0.83	0.83	-	-	-	-	-	Determined with UNSW benchmark test frequency ramp (1Hz/s).
J+124	tRoCoF_3	(s) pick up time for RoCoF trip 3	0.29	0.29	0.29	0.29	0.29	0.29	0.29	0.29	0.29	0.29	-	-	-	-	-	Determined with UNSW benchmark test frequency ramp (4Hz/s).
J+125	frac_RoCOF_1	fraction for RoCoF trip 1	0.04	0.04	0.04	0.04	0.04	0.04	0.04	0.04	0.04	0.04	0.000	0.000	0.000	0.000	0.000	Weighted average as a proportion of installed capacity for each region. Determined with UNSW benchmark test frequency ramp (0.4Hz/s).
J+126	frac_RoCOF_2	fraction for RoCoF trip 2	0.04	0.05	0.10	0.04	0.07	0.04	0.05	0.10	0.04	0.07	0.000	0.000	0.000	0.000	0.000	Weighted average as a proportion of installed capacity for each region. Determined with UNSW benchmark test frequency ramp (1Hz/s).
J+127	frac_RoCOF_3	fraction for RoCoF trip 3	0.00	0.00	0.00	0.00	0.00	0.00	0.00	0.00	0.00	0.00	0.000	0.000	0.000	0.000	0.000	Weighted average as a proportion of installed capacity for each region. Determined with UNSW benchmark test frequency ramp (4Hz/s).

A2. CMLD Model Parameters

This is a sample set of CMLD parameters for the CMLDZNU2 model from the PSS®E model library. Comments have been added where more context may be required, or the parameter differs from that suggested in the NERC and PEACE® documentation[169,170].

Legend			
Distribution network components	Power Electronic load parameters	Motor A parameters	Motor C parameters
Composition of the load	Static load parameters	Motor B parameters	Motor D parameters

Table 113 Sample parameters for NSW load connected at the HV bus in PSS®E with commentary

PSS®E Parameter	Description	Value	Comment/ Approach
ZONE	Load zone number	29	Regional load type identifier i.e. 29: NSW load connected at the HV bus in PSS®E
LIB_MOD	Model type	'USRLOD'	-
ID	Machine identifier	*	-
NAME_MOD	Model name	'CMLDZNU2'	-
IC	User model type code	12	-
IT	Model assignment type: zone (3)	3	-
unknown3	unknown3	2	-
ICONs	Number of ICONs	133	-
CONs	Number of CONs	27	-
STATEs	Number of STATEs	146	-

PSS®E Parameter	Description	Value	Comment/ Approach
VARs	Number of VARs	48	-
unknown1	unknown 1	0	-
unknown2	unknown 2	0	-
J	Load base for xfr & feeder- MVA or calculated if <= 0	-0.8	Default value from PEACE consulting report. If negative, MVA base = Load MW/Value Specified.
J+1	Substation compensation B- pu on load base	0	Default value from PEACE consulting report and NERC documentation. Assumed no shunt compensation at bus.
J+2	Rfdr - Feeder resistance- pu on load base	0.04	Default value from PEACE consulting report and NERC documentation. 4% impedance on load MVA base. 1:1 distribution feeder impedance X:R ratio. Note, Rfdr is load type specific i.e. 4% for LV and HV CMLD general loads in PSS®E, 0% for auxiliary connections, and 1% for industrial loads.
J+3	Xfdr - Feeder reactance- pu on load base	0.04	
J+4	Fb - Not used- Fb = 0.0	0.75	Default value from PEACE consulting report. Shunt compensation.
J+5	Xxf - Transformer reactance- pu on load base	0.08	Default value from PEACE consulting report and NERC documentation. Transformer impedance on load MVA base. Appropriate for an aggregate model. Note, Xxf is load type specific i.e. 3% for LV, 8% for HV, and 6% for auxiliary loads.
J+6	Tfixhs - High side fixed transformer tap	1	Default values from PEACE consulting report and NERC documentation. Assumed 1:1 HV:LV transformer turns ratio.
J+7	Tfixls - Low side fixed transformer tap	1	
J+8	LTC - LTC flag (1=active- 0=inactive)	1	Default value from NERC documentation. Transformer on-load tap changer enabled
J+9	Tmin - LTC min tap (on low side)	0.9	Based on default parameters in PEACE consulting report and NERC documentation[169] 32 steps +/- 0.1 tap +/- 1.2% voltage operation bounds
J+10	Tmax - LTC max tap (on low side)	1.1	
J+11	Step - LTC Tstep (on low side)	0.00625	
J+12	Vmin - Min value of V target range on xfr low side	1	
J+13	Vmax - Max value of V target range on xfr low side	1.02	
J+14	TD - LTC control time delay- s	30	Default value from PEACE consulting report and NERC documentation. OLTC delay before first tap move.
J+15	TC - LTC tap adjustment time delay- s	5	Default value from PEACE consulting report NERC documentation. OLTC delay between tap moves.

[169] NERC. 2016. Technical Reference Document: Dynamic Load Modelling, https://www.nerc.com/comm/PC/LoadModelingTaskForceDL/Dynamic%20Load%20Modeling%20Tech%20Ref%202016-11-14%20-%20FINAL.PDF.

[169] PEACE® Consulting. 2019. Developing Dynamic Load Models for the Australian Eastern Interconnected System, https://aemo.com.au/-/media/files/initiatives/der/2020/aemo-load-modeling-062819-final.pdf?la=en.

PSS®E Parameter	Description	Value	Comment/ Approach
J+16	Rcmp - xfr compensating R- pu on load base	0	Default values from NERC documentation. Resistance and reactance compensation for LTC. i.e. 0: not considered
J+17	Xcmp - xfr compensating X- pu on load base	0	
J+18	FmA - Composite load motor A fraction	-	These parameters are dependent on the regional load composition calculated from the CMLD parameters spreadsheet. AEMO has developed composition parameters that vary by load type (industry), season, day (weekday, weekend), time, and date. Refer to Section **3.3** for further details.
J+19	FmB - Composite load motor B fraction	-	
J+20	FmC - Composite load motor C fraction	-	
J+21	FmD - Composite load motor D fraction	-	
J+22	Fel - Composite load electronic fraction	-	
J+23	PFel - Electronic load power factor	1	Default value from NERC documentation. Assumed power electronic load at unity power factor.
J+24	Vd1 - Voltage electronic loads start to drop	0.85	Electronic load starts tripping at 0.85 pu voltage and all electronic load is tripped by 0.5 pu voltage. Parameters selected based on tuning, to achieve more accurate load disconnection estimates.
J+25	Vd2 - Voltage all electronic load has dropped	0.5	
J+26	PFs - Static load power factor	1	Assumed unity power factor (i.e. lighting). Default parameter from PEACE consulting report.
J+27	P1e - First exponent for static load P	1	P=P0*(P1c*V/V0P1e + P2c*V/V0P2e + P3) * (1 + Pfrq * Df) Polynomial fit for static load based on default parameters from PEACE® Consulting[170] P1c is calculated as the fraction of constant current / total static load fraction P2C is calculated as the fraction of constant impedance/ total static load fraction *This is a sample value which changes by region, time, and date.
J+28	P1c - First coeff for static load P	0.22*	
J+29	P2e - Second exponent for static load P	2	
J+30	P2c - Second coeff for static load P	0.78*	
J+31	Pfrq - Frequency sensitivity for static P	0	Default value from PEACE consulting report and NERC documentation. Assume real power not frequency dependent.
J+32	Q1e - First exponent for static load Q	1	Q=Q0*(Q1c*V/V0Q1e + Q2c*V/V0Q2e + Q3) * (1 + Qfrq * Df) Polynomial fit for static load based on default parameters from PEACE® Consulting. Q1c is calculated as the fraction of constant current / total static load fraction Q2C is calculated as the fraction of constant impedance/ total static load fraction *This is a sample value which changes by region, time, and date.
J+33	Q1c - First coeff for static load Q	0.22*	
J+34	Q2e - Second exponent for static load Q	2	
J+35	Q2c - Second coeff for static load Q	0.78*	
J+36	Qfrq - Frequency sensitivity for static load Q	-1	Default value from PEACE consulting report and NERC documentation. Assume Q inversely frequency dependent.

[170] PEACE® Consulting. 2019. Developing Dynamic Load Models for the Australian Eastern Interconnected System. Available at: https://aemo.com.au/-/media/files/initiatives/der/2020/aemo-load-modeling-062819-final.pdf?la=en

PSS®E Parameter	Description	Value	Comment/ Approach
J+37	Mtyp - Motor A phase- always 3	3	-
J+38	LF - Motor A real power to power base ratio	0.75	Load MVA = MW/MVA Rating
J+39	Ra - Motor A stator resistance- pu on motor base	0.02	Value taken from EPRI Technical Guide on Composite Load Modelling.
J+40	X - Motor A synchronous reactance- pu	1.8	These are 'generic' motor parameters for this type of load, based on NERC documentation which is derived from laboratory testing.
J+41	X' - Motor A transient reactance- pu	0.12	
J+42	X" - Motor A sub transient reactance- pu	0.104	
J+43	To' - Motor A transient open circuit time constant- s	0.095	
J+44	To" - Motor A sub transient open cir time constant- s	0.0021	
J+45	H - Motor A inertia constant	0.1	Motor A is modelled as small low inertia motors.
J+46	etrq - Motor A exp for variation of torque with speed	0	Default value from NERC documentation. Load torque exponent for speed.
J+47	Vtr1 - Motor A 1st under-voltage trip voltage- pu	0.75	Assumed performance of these motors based on tuning and validation studies (from validation studies): Represents higher performance motors – large commercial building chillers/air handlers First trip level at about 0.75 pu voltage, trip delay time 60 ms. Note, the CMLD is an aggregate model, so trip time delays may not be representative of the expected motor protection relay settings. 10% of Motor A have this type of protection These motors stay disconnected and require manual reconnection
J+48	Ttr1 - Motor A 1st under-voltage trip delay- s	0.06	
J+49	Ftr1 - Motor A 1st under-voltage trip fraction	0.1	
J+50	Vrc1 - Motor A 1st under-voltage reclose voltage- pu	0.8	
J+51	Trc1 - Motor A 1st under-voltage reclose delay- s	99999	
J+52	Vtr2 - Motor A 2nd under-voltage trip voltage- pu	0.62	Assumed performance of these motors (from validation studies): Represents majority of 'brute' motors – standard design, rugged, automated Contactor tripping levels - 0.62 pu voltage, trip delay time 21 ms. Note, the CMLD is an aggregate model, so trip time delays may not be representative of the expected motor protection relay settings. 20% of Motor A have this type of protection Contactors reclose at 0.70 pu within 100 ms. Note: Vtr1A & Vtr2A should not equal 1; always keep some fraction online for numerical purposes with the model.
J+53	Ttr2 - Motor A 2nd under-voltage trip delay- s	0.021	
J+54	Ftr2 - Motor A 2nd under-voltage trip fraction	0.2	
J+55	Vrc2 - Motor A 2nd under-voltage reclose voltage- pu	0.7	
J+56	Trc2 - Motor A 2nd under-voltage reclose delay- s	0.1	
J+57	Mtyp - Motor B phase- always 3	3	-
J+58	LF - Motor B real power to power base ratio	0.75	Default value from NERC documentation. Load MVA = MW/MVA Rating
J+59	Ra - Motor B stator resistance- pu on motor base	0.03	These are 'generic' motor parameters for this type of load, based on NERC documentation which is derived from laboratory testing.
J+60	X - Motor B synchronous reactance- pu	1.8	

PSS®E Parameter	Description	Value	Comment/ Approach
J+61	X' - Motor B transient reactance- pu	0.19	
J+62	X" - Motor B sub-transient reactance- pu	0.14	
J+63	To' - Motor B transient open circuit time constant- s	0.2	
J+64	To" - Motor B sub-transient open circuit time constant- s	0.0026	
J+65	H - Motor B inertia constant	0.5	Default value from NERC documentation. Motor B is modelled as larger higher inertia motors.
J+66	etrq - Motor B torque speed exponent	2	Default value from NERC documentation. Load torque exponent for speed.
J+67	Vtr1 - Motor B 1st under-voltage trip voltage- pu	0.7	Assumed performance of these motors: All fans assumed to only have contactor tripping – no controls-based protection; therefore Two sets of tripping levels representing diversity of motor load Level 1 (from validation studies) Trip at 0.7 pu voltage, trip delay time 20 ms. Note, the CMLD is an aggregate model, so trip time delays may not be representative of the expected motor protection relay settings. 10% of these motors have this type of protection Auto-reconnect – 0.75 pu voltage within 50 ms
J+68	Ttr1 - Motor B 1st under-voltage trip delay- s	0.02	
J+69	Ftr1 - Motor B 1st under-voltage trip fraction	0.1	
J+70	Vrc1 - Motor B 1st under-voltage reclose voltage- pu	0.75	
J+71	Trc1 - Motor B 1st under-voltage reclose delay- s	0.05	
J+72	Vtr2 - Motor B 2nd under-voltage trip voltage- pu	0.45	Level 2 (from validation studies) Trip level at 0.45 pu voltage, trip delay time 21 ms. Note, the CMLD is an aggregate model, so trip time delays may not be representative of the expected motor protection relay settings. 20% of these motors have this type of protection Auto-reconnect – 0.6 pu voltage within 50 ms
J+73	Ttr2 - Motor B 2nd under-voltage trip delay- s	0.021	
J+74	Ftr2 - Motor B 2nd under-voltage trip fraction	0.2	
J+75	Vrc2 - Motor B 2nd under-voltage reclose voltage- pu	0.6	
J+76	Trc2 - Motor B 2nd under-voltage reclose delay- s	0.05	
J+77	Mtyp - Motor C phase- always 3	3	-
J+78	LF - Motor C real power to power base ratio	0.75	Load MVA = MW/MVA Rating
J+79	Ra - Motor C stator resistance- pu on motor base	0.03	These are 'generic' motor parameters for this type of load, based on WECC documentation which is derived from laboratory testing.
J+80	X - Motor C synchronous reactance- pu	1.8	
J+81	X' - Motor C transient reactance- pu	0.19	
J+82	X" - Motor C sub transient reactance- pu	0.14	
J+83	To' - Motor C transient open circuit time constant- s	0.2	

PSS®E Parameter	Description	Value	Comment/ Approach
J+84	To" - Motor C sub transient open circuit time constant- s	0.0026	
J+85	H - Motor C inertia constant	0.1	Motor C is modelled as smaller, lower inertia commercial/industrial fan and pump motor loads
J+86	etrq - Motor C torque speed exponent	2	Load torque exponent for speed.
J+87	Vtr1 - Motor C 1st under-voltage trip voltage- pu	0.8	Assumed performance of these motors based on tuning and validation studies: Level 1 (from validation studies) Trip at 0.8 pu voltage, trip delay time 30 ms. Note, the CMLD is an aggregate model, so trip time delays may not be representative of the expected motor protection relay settings. 10% fraction of motor trips These motors stay disconnected and require manual reconnection
J+88	Ttr1 - Motor C 1st under-voltage trip delay- s	0.03	
J+89	Ftr1 - Motor C 1st under-voltage trip fraction	0.1	
J+90	Vrc1 - Motor C 1st under-voltage reclose voltage- pu	0.8	
J+91	Trc1 - Motor C 1st under-voltage reclose delay- s	9999	
J+92	Vtr2 - Motor C 2nd under-voltage trip voltage- pu	0.5	Assumed performance of these motors based on tuning and validation studies: Level 2 (from validation studies) Trip at 0.5 pu voltage, trip delay time 30 ms. Note, the CMLD is an aggregate model, so trip time delays may not be representative of the expected motor protection relay settings. 20% fraction of motors trip Contactors reclose at 0.62 pu in 50 ms
J+93	Ttr2 - Motor C 2nd under-voltage trip delay- s	0.03	
J+94	Ftr2 - Motor C 2nd under-voltage trip fraction	0.2	
J+95	Vrc2 - Motor C 2nd under-voltage reclose voltage- pu	0.6	
J+96	Trc2 - Motor C 2nd under-voltage reclose delay- s	0.11	
J+97	Tstall - Motor D stall delay time- s	0.04	Due to residential air conditioner or refrigerator compressors exceedingly small inertia (on the order of 0.05 kWs/kVA), the compressors are prone to stall within a couple of cycles (0.04s) during voltage sags[171].
J+98	Trestart - Motor D restart from stall delay time- s	0.3	Induction motor restart time is relatively short. Default parameter from NERC documentation.
J+99	Tv - Motor D voltage time constant for contactors- s	0.025	Assumed generic transducer time lag. Default parameter from NERC documentation.
J+100	Tf - Motor D frequency time constant for contactors- s	0.1	Filter time constant. Default from PEACE consulting report.
J+101	CompLF - Motor D real power to motor base ratio	1	Load MVA = MW/MVA Rating
J+102	CompPF - Motor D power factor at 1.0 pu voltage	0.71	Inductive load. From the EES motor tests[172], the average refrigerator motor power factor for 1pu voltage is 0.71.

[171] A. M. Gaikwad, R. J. Bravo, D. Kosterev, S. Yang, A. Maitra, P. Pourbeik, B. Agrawal, R. Yinger, and D. Brooks. 2008. Results of residential air conditioner testing in WECC, https://ieeexplore.ieee.org/document/4596549.

[172] Energy Efficient Strategies Consulting. 2020. Stall Measurements for Refrigerators, https://aemo.com.au/-/media/files/initiatives/der/2020/2020-08-05-ees-results-of-stall-measurements-on-motor-d-and-inverter-systems.pdf?la=en.

PSS®E Parameter	Description	Value	Comment/ Approach
J+103	Vstall - Motor D stall Voltage- pu	0.49	From the EES motor tests, the average stall voltage for 1P residential and commercial refrigeration units was ~113V. Equivalent to 0.49pu.
J+104	Rstall - Motor D stall resistance- pu of motor base	0.143	From the EES motor tests, the stall power for 1P residential and commercial refrigerator compressors is shown to be ~7 times the nominal power. Therefore, stall reactance and resistance are 1/7 pu of motor base.
J+105	Xstall - Motor D stall reactance- pu of motor base	0.143	
J+106	LFadj - Adjustment to stall voltage if COMPLF /= 1.0	0	-
J+107	Kp1 - Motor D real power coeff when voltage > Vbrk	0	Default parameters from PEACE consulting report and NERC documentation.
J+108	Np1 - Motor D real power exp when voltage > Vbrk	1	
J+109	Kq1 - Motor D reactive power coeff when voltage > Vbrk	6	
J+110	Nq1 - Motor D reactive power exp when voltage>Vbrk	2	
J+111	Kp2 - Motor D real power coeff when voltage < Vbrk	12	
J+112	Np2 - Motor D real power exp when voltage < Vbrk	3.2	
J+113	Kq2 - Motor D reactive power coeff when voltage < Vbrk	11	
J+114	Nq2 - Motor D reactive power exp when voltage<Vbrk	2.5	
J+115	Vbrk - Motor D "break-down" voltage-	0.86	Vbrk is part of the polynomial fitted performance model of the single-phase induction motor. This and the other (Kp*,Np*,Kq* and Nq*) parameters of Motor D are based on an "average" fit of all the test results from the tests performed by EPRI, BPA and SCE[171]. These parameters are not changed under any circumstances in the United States of America. For example, in GE PSLFTM these parameters are hard-coded, and the user cannot change them. Siemens PTI PSS®E lets you change these parameters; however, the user must take great care since changing them inappropriately can yield non-meaningful representations.
J+116	Frst - Motor D fraction capable of restart after stall	0.1	From the EES motor tests, there are 4 compressor motors (units 22, 23, 28, 36) that can restart after a stall. There were 40 compressor units tested with valid results (units 27 & 32 blew a fuse on the variac and no valid results obtained). 4/40 = 0.1pu. From the study[171], it is shown that for scroll compressors during under-voltage conditions thermal overload may or may not operate. In most of the test cases the scroll units went into stall mode for several seconds and returned to normal operation when the line voltage increased sufficiently to restart the unit without tripping. This is presumably because of the nature of the mechanical load for scroll compressors, which allows the unit to restart if the system voltage can recover to a high level quickly enough.
J+117	Vrst - Motor D voltage for restart after stall- pu	0.95	Default from PEACE consulting report and NERC documentation. Assumed restart capability for single-phase motors.

PSS®E Parameter	Description	Value	Comment/ Approach
J+118	CmpKpf - Motor D real power frequency dependency	1	Default from PEACE consulting report.
J+119	CmpKqf - Motor D reactive power frequency dependency	-3.3	Default from PEACE consulting report.
J+120	Vc1off - Motor D voltage contactors start opening- pu	0.5	Contactor drop out: From the study[171], all the tested compressor units use standard 240 V AC contactors which trip the unit when the supply voltage drops below a certain threshold, between 40% to 50% of the rated nominal voltage of 240 V AC.
J+121	Vc2off - Motor D voltage all contactors opened- pu	0.4	
J+122	Vc1on - Motor D voltage all contactors closed - pu	0.6	Default from PEACE documentation.
J+123	Vc2on - Motor D voltage contactors start closing -pu	0.52	Compressor motor contactors have electromagnetic contactors which reclose once the voltage recovers above the drop out point.
J+124	Tth - Motor D heating time constant- s	15	Tth is the thermal time constant. Based on the various lab tests performed by NERC and WECC, they "guesstimated" that a thermal time constant of 15 seconds is reasonable for the bi-metallic plate. Note, this is an aggregate model, so there is little value in trying to fine tune this "guesstimate".
J+125	Th1t - Motor D temperature where tripping begins- pu	1.98	Assumed tripping starting at 198% temperature, with all tripped at 459% temperature. Th1t and Th2t did not come from testing. They are "guesstimates". Looking at the thermal relay block, the model is saying I^2R = heat generated, this takes Tth (time-constant) to act through the bi-metallic plate. For one single device, then it should trip. However, this is an aggregate model. So initially, when it was modelled like a single device, the whole Motor D (sometimes 10's of MWs to 100 MW at a single substation) would suddenly trip. This is unrealistic. As observed in the US at many locations, all the residential a/c do not trip at once, instead there is a gradual tripping over many seconds. So rather than having a step function, the tripping was made into a linear drop-off of Motor D, which starts at Th1t and ends at Th2t. Based on many simulations versus measurements of large FIDVR events (particularly in the South West US) these numbers were chosen.
J+126	Th2t - Motor D temperature where completely tripped	4.59	
J+127	Fuvr - Motor D fraction with under-voltage relays	0.325	Fuvr, Vtr1, Ttr1, Vtr2, Ttr2 trip Motor D, and once tripped does not come back for ~120s. For example, if you set Fuvr = 0.1, Vtr1n = 0.5, Trt1n = 0.05, Vtr2n = 0.2, Ttr2n = 0.02 (dummy values, not recommended), then once the voltage goes below 0.5 pu for 0.05 s, or below 0.2 pu for 0.02 s, then 10% of Motor D drops and never comes back. Some modern compressor units have digital thermostats, and these have an under-voltage drop out (there is no under-voltage relay on the motor), once the thermostat drops out due to under-voltage, even when the voltage recovers it will not let the a/c start up for many minutes. From the motor tests performed, 13/40 = 0.325pu units (units 6, 9, 11, 13, 15, 17, 18, 20, 24, 26, 29, 31, 33) trip before thermal overload occurs and do not recover for some time. Of the 42 compressor motors tested, units 27 & 32 blew a fuse on the variac, and no valid results were obtained.
J+128	UVtr1 - Motor D 1st under-voltage pick-up- pu	0.55	The under-voltage relay setting must be set higher than the stall characteristic to initiate a trip. This setting should also be set different to the contactor dropout and reconnect settings, as the model was shown to behave erratically when these parameters were set equal.
J+129	Ttr1 - Motor D 1st under-voltage trip delay- s	0.06	
J+130	UVtr2 - Motor D 2nd under-voltage pick-up- pu	0.1	There is no second level tripping specified.

PSS®E Parameter	Description	Value	Comment/ Approach
J+131	Ttr2 - Motor D 2nd under voltage trip delay- s	9999	
J+132	frcel - Fraction of electronic load that can reconnect	0.7	Assumed 70% of electronic load automatically reconnects upon acceptable voltage. This parameter was set based on repetitive tuning and validation testing to achieve the best overall load loss estimates. LNG frcel = 0.86, and was also set from validation studies.

A3. Validation of the DPV user written model for PSS®E

The DPV model is an in house developed (by AEMO) PSS®E user written model that can be used to represent DPV. Compared with the standard DERAU1 model available in the PSS®E model library, it has advanced over-frequency, under-frequency and RoCoF tripping functionality that can represent the broad range of disconnection mechanisms for the 2005 and 2015 standard inverters.

This appendix provides information on the DPV control block and tripping logic, and shows the summarised results from tests performed on the model including:

- Comparison of its behaviour with the DERAU1 model (original WECC DER model).
- Verification of the under and over-frequency and under and over-voltage tripping functions.

Note: in some figures, the DPV model is referred to as DERBU1.

A3.1 Active/Reactive Power Control

The active/reactive power control segment is shown in **Figure 149**, and contains two main paths. One path generates the reactive current reference (I_{qord}) and the other generates the power reference (P_{ord}).

Compared with the DER_A model, the DPV model has separate reactive power-voltage gains (K_{qv1} and K_{qv2}) to the reactive current reference path, which enables an asymmetrical voltage control response characteristic.

I_{qord} is generated from either a constant Q or constant power factor reference, which is then modified by a supplementary voltage controller if the terminal voltage falls outside of the deadband.

P_{ord} may be generated either in open-loop or closed-loop mode. In open loop mode, P_{ord} is generated from a constant power reference, in closed-loop mode P_{ord} is regulated by a closed-loop PI controller with a supplementary active power-frequency control input.

Figure 149 DPV model active/reactive power control block diagram

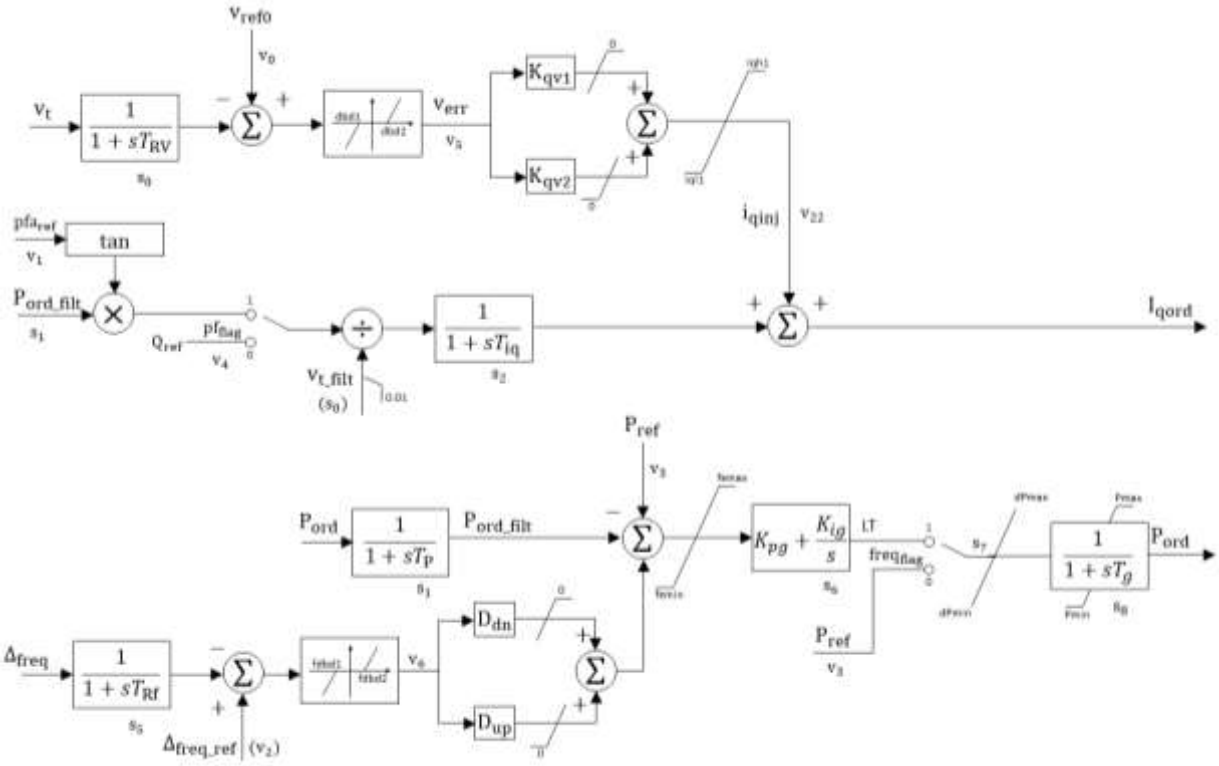

A3.2 Current/output control

The original WECC design[173] for current/output control is unchanged in the DPV model. It is shown in **Figure 150** for completeness.

The two inputs (I_{qord} and P_{ord}) are used to generate the current outputs of the DPV model, i_d and i_q. The role of the current/output control segment is to represent the simplified dynamics of inner current-control loops of inverter-based resources. This includes PQ priority mode, current limiting, and interfacing with the simulation's electrical network.

An input path is also provided for the output multiplier (mult). This is used to reduce the output current of the model. Mult is an input from the tripping logic segment and allows partial or complete reduction of the DPV output due to under-frequency, over-frequency, under-voltage, over-voltage, or RoCoF.

[173] Power and Energy, Analysis, Consulting and Education (PEACE®). Proposal for DER_A model, June 2019, https://www.wecc.org/Reliability/DER_A_Final_061919.pdf.

Figure 150 DER_A/DPV model current control block diagram

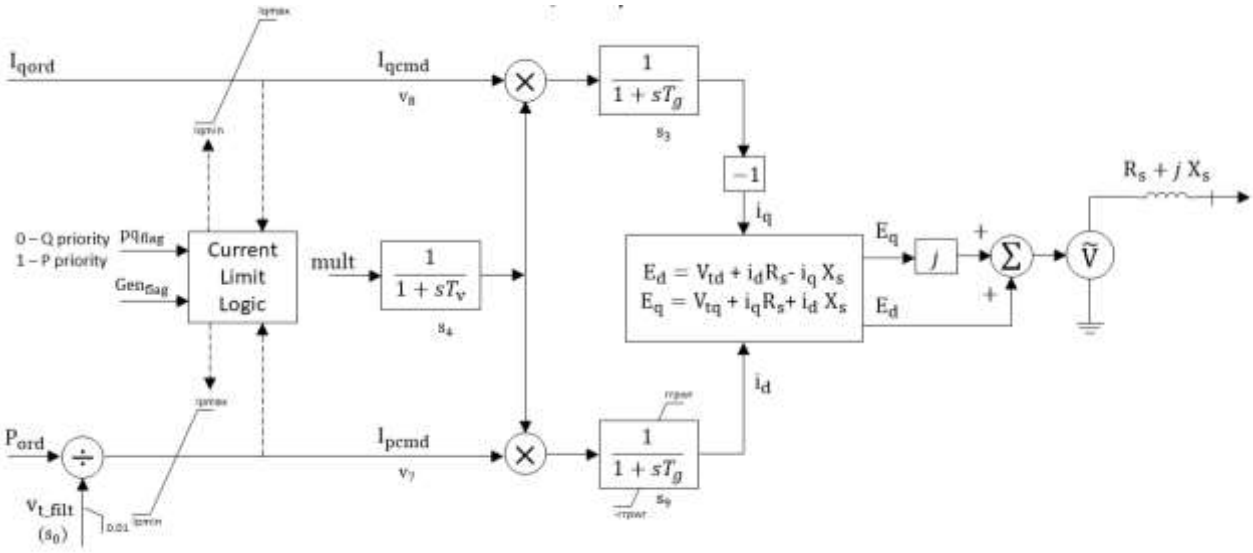

A3.3 Tripping logic

AEMO included the following additional features to the tripping logic block of the DER_A model:

- A representation of a fraction of resources tripping at low and high frequency, over 26 stages that include independent trip delay timers.
- A representation of a fraction of resources tripping at low or high RoCoF, over 3 stages that include independent trip delay timers.
- A filtered RoCoF measurement (lead-lag filter) to derive RoCoF from the terminal frequency.

From the tripping logic block diagram in **Figure 151**, there are two main inputs from the tripping logic segment, which are the filtered terminal voltage and terminal frequency[174] of the DER model.

The RoCoF is derived from the DER terminal frequency using a filtered derivative transfer function.

The three variables (filtered voltage, filtered frequency, and filtered RoCoF) are used in the aggregate under-voltage, over-voltage, under-frequency, over-frequency, and high RoCoF trip characteristics of the model.

The under-voltage/over-voltage trip function uses a piecewise linear gain to determine the reduction in DER output. In contrast, both the RoCoF and frequency tripping functions use a stepped approach with each step having an independent delay timer.

[174] The input frequency in the diagram is labelled as Δfreq_filt to reflect that it is the filtered frequency deviation from nominal frequency (50 Hz).
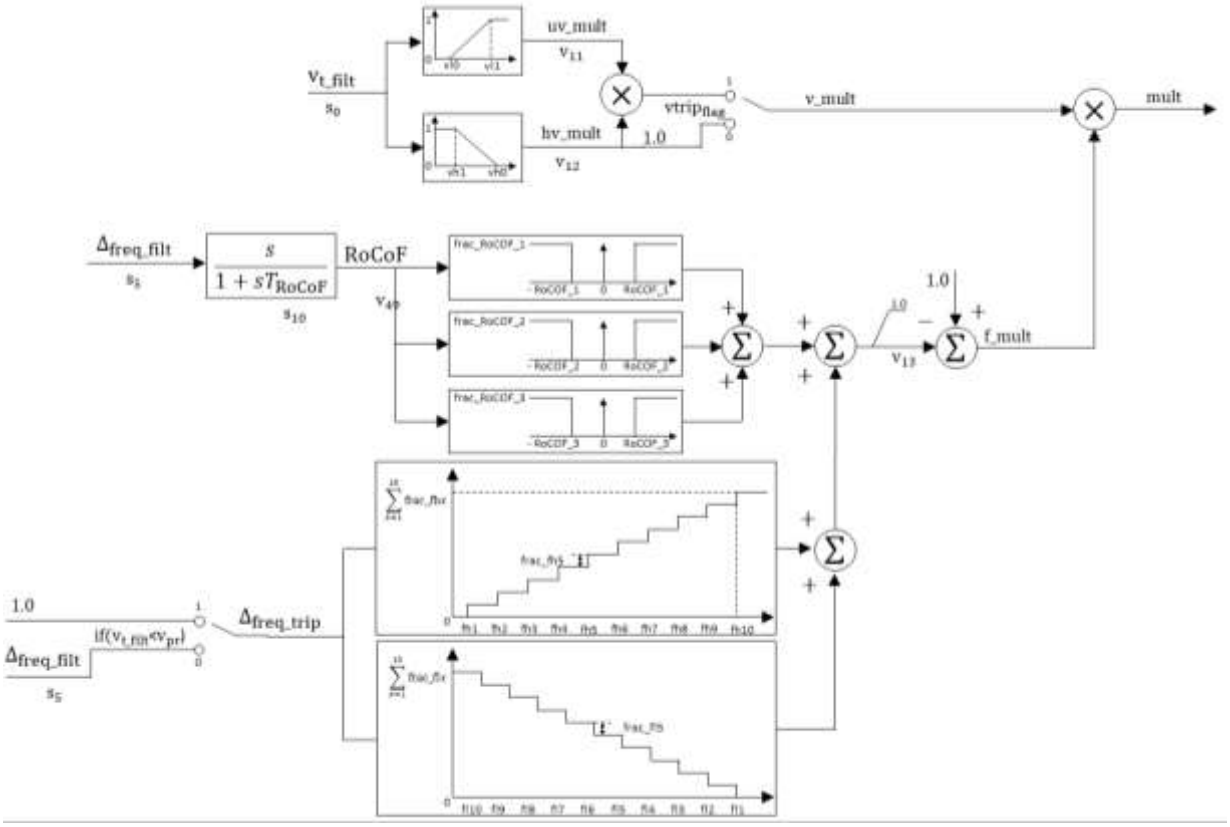
Figure 151 DPV model tripping block diagram